

Improving smart charging for electric vehicle fleets by integrating battery and prediction models

Inauguraldissertation
zur Erlangung des akademischen Grades
eines Doktors der Naturwissenschaften
der Universität Mannheim

vorgelegt von

Oliver Frendo
aus Berlin

Mannheim, 2020

Dekan: Dr. Bernd Lübcke, Universität Mannheim
Referent: Prof. Dr. Heiner Stuckenschmidt, Universität Mannheim
Korreferent: Prof. Dr. Mahnoosh Alizadeh, University of California, Santa Barbara
Tag der mündlichen Prüfung: 25. Januar 2021

Abstract

With increasing electrification of vehicle fleets there is a rising demand for the effective use of charging infrastructure. Existing charging infrastructures are limited by undersized connection lines and a lack of charging stations. Upgrades require significant financial investment, time and effort. Smart charging represents an approach to making the most of existing charging infrastructure while satisfying charging needs. Smart charging involves scheduling for electric vehicles (EVs). In other words, smart charging approaches decide which EV may charge at which charging station and at which current during which time periods. Planning flexibility is determined by the length of stay and the available electrical supply.

First, we present an approach for smart charging combining day-ahead planning with real-time planning. For day-ahead planning, we use a mixed integer programming model to compute optimal schedules while making use of information available ahead of time. We then describe a schedule guided heuristic which adapts precomputed schedules in real-time.

Second, we address uncertainty in smart charging. For example, EV departure times are an important component in prioritization but are uncertain ahead of time. We use a regression model trained on historical data to predict EV departure times. We integrate predictions directly in the smart charging heuristic used in the first approach. Experimental results show a more accurate EV departure time leads to a more accurate EV prioritization and a higher amount of delivered energy.

Third, we present two approaches which allow the smart charging heuristic to take EV charging behavior into account. In practice, EVs charge using nonlinear charge profiles where power declines towards the end of each charging process. There is thus a gap between the scheduled power and the actual charging power if nonlinear charge profiles are not taken into account. The first approach uses a traditional equivalent circuit model (ECM) to model EV charging behavior but in practice is limited by the availability of battery parameters. The second approach relies on a regression model trained on historical data to directly predict EV charging profiles. In each of the two approaches, the model of the EV's charging profile is directly integrated into the smart charging heuristic which allows the heuristic to produce more accurate charge plans. Experimental results show EVs charge significantly more energy because the charging infrastructure is used more effectively.

Finally, we present an open source package containing the smart charging heuristic and describe results from applying the heuristic in a one-year field test. Experimental results from the field test show EVs at six charging stations can be scheduled for charging when the grid connection only allows two EVs to charge concurrently. Runtime measurements demonstrate the heuristic is applicable in real time and scales to large fleet sizes.

Zusammenfassung

Mit zunehmender Elektrifizierung von Fahrzeugflotten steigt die Nachfrage nach einer effektiven Nutzung der Ladeinfrastruktur. Bestehende Ladeinfrastrukturen sind durch unterdimensionierte Anschlussleitungen und einen Mangel an Ladestationen begrenzt. Erweiterungen der Ladeinfrastruktur erfordern finanzielle Investitionen, Zeit und Aufwand. Intelligentes Laden bietet ein Ansatz, um die vorhandene Ladeinfrastruktur optimal zu nutzen und gleichzeitig den Ladebedarf zu decken. Beim intelligenten Laden geht es um die Zeitplanung für Elektrofahrzeuge. Mit anderen Worten: Intelligente Ladeansätze entscheiden, welches E-Fahrzeug an welcher Ladestation und mit welcher Leistung in welchen Zeiträumen laden darf. Die Planungsflexibilität wird durch die Aufenthaltsdauer und die verfügbare elektrische Versorgung bestimmt.

Als Erstes stellen wir einen Ansatz für intelligentes Laden vor, der Day-Ahead-Planung mit Echtzeitplanung kombiniert. Für die Day-Ahead-Planung verwenden wir ein Mixed Integer Programming Modell, um optimale Ladepläne zu berechnen und dabei die im Voraus verfügbaren Informationen zu nutzen. Anschließend beschreiben wir eine Heuristik, die vorberechnete Zeitpläne in Echtzeit anpasst.

Als Zweites gehen wir auf Unsicherheiten beim intelligenten Laden ein. Zum Beispiel sind die Abfahrtszeiten der E-Fahrzeuge eine wichtige Komponente zur Priorisierung, aber diese sind im Voraus unsicher. Wir verwenden ein auf historischen Daten trainiertes Regressionsmodell zur Vorhersage der Abfahrtszeiten. Wir integrieren die Vorhersagen direkt in die im ersten Ansatz verwendete Heuristik. Experimentelle Ergebnisse zeigen, dass eine genauere Vorhersage der Abfahrtszeit zu einer genaueren E-Fahrzeug-Priorisierung und einer höheren Menge an gelieferter Energie führt.

Als Drittes stellen wir zwei Ansätze vor, die es der Heuristik ermöglichen, das Ladeverhalten von E-Fahrzeugen zu berücksichtigen. In der Praxis laden E-Fahrzeuge mit nichtlinearen Ladeprofilen, bei denen die Leistung gegen Ende eines jeden Ladevorgangs abnimmt. Es besteht also eine Lücke zwischen der geplanten Leistung und der tatsächlichen Ladeleistung, wenn nichtlineare Ladeprofile nicht berücksichtigt werden. Der erste Ansatz verwendet ein traditionelles Ersatzschaltbild, um das EV-Ladeverhalten zu modellieren, ist aber in der Praxis durch die Verfügbarkeit von Batterieparametern begrenzt. Der zweite Ansatz stützt sich auf ein Regressionsmodell, das auf historischen Daten trainiert wurde, um Ladeprofile von E-Fahrzeugen direkt vorherzusagen. In beiden Ansätzen ist das Modell des Ladeprofils des E-Fahrzeugs direkt in die Heuristik integriert, wodurch die Heuristik genauere Ladepläne erstellen kann. Experimentelle Ergebnisse zeigen, dass E-Fahrzeuge deutlich mehr Energie laden, weil die Ladeinfrastruktur effektiver genutzt wird.

Abschließend stellen wir ein Open-Source-Paket vor, das die Heuristik enthält, und beschreiben die Ergebnisse der Anwendung der Heuristik in einem einjährigen Praxistest. Experimentelle Ergebnisse aus dem Praxistest zeigen, dass E-Fahrzeuge an sechs Ladestationen zum Laden eingeplant werden können, wenn der Netzan-schluss nur zwei E-Fahrzeuge zum gleichzeitigen Laden zulässt. Laufzeitmes-sungen zeigen, dass die Heuristik in Echtzeit anwendbar ist und auf große Flot-tengrößen skaliert.

Acknowledgements

To begin with, I would like to thank my supervisor Prof. Heiner Stuckenschmidt who supported me for the last three years and who gave me the guidance to focus on the correct topics.

This thesis would not have been possible without the collaboration of many colleagues at SAP. Most importantly, I am extremely grateful to Nadine Gaertner for being with me every step of the way, being a sounding board and for working me with on my publications. I would like to thank my manager Nemrude Verzano for making this dissertation a possibility, giving me the support to publish and to focus on academic topics and for helping to drive the open source version of the approaches presented in this work.

I would also like to thank the team working with me on the field test in the TRADE EVs project: Johannes Hoppenstedt and Markus Winkler for collaborating on the technical implementation, Steffen Wolf for the administration (and for always being a ray of sunshine) and Jerome Graf, Nico Poeringer and Luca Tallarita for helping to visualize smart charging. Finally, I would like to thank Lutz Thissen for providing guidance on the electrical engineering aspects of this work and having the patience to answer all of my questions.

On a personal level I would like to thank Nele Ecker, my friends and my family for the constant support and encouragement enabling me to reach my goals.

Table of contents

List of algorithms	ix
List of figures	xiii
List of tables	xv
1 Introduction	1
1.1 Motivation	1
1.2 Research questions and contributions	4
1.3 Publications	5
1.4 Outline	6
2 Foundations and related work	7
2.1 Scenario	8
2.2 Electric vehicle charging	10
2.2.1 Battery cells	10
2.2.2 Charging profiles	13
2.2.3 Battery packs	15
2.2.4 Battery management system (BMS)	17
2.2.5 Charging systems	18
2.2.6 Implications for charge scheduling	20
2.3 Charging infrastructure	20
2.3.1 Simultaneity factor	20
2.3.2 Load imbalance	22
2.3.3 Electrical network topology	25
2.3.4 Charging stations	26
2.4 Other factors in charge scheduling	27
2.4.1 Peak shaving	27
2.4.2 Energy markets	29
2.4.3 Implications for charge scheduling	32

2.5	Objectives and constraints	33
2.6	Related work	36
2.6.1	Objectives and methods	36
2.6.2	Scenario	37
2.6.3	Time of planning	38
2.6.4	Uncertainty	39
2.6.5	Battery models	40
2.6.6	Forecasting	42
2.6.7	Data-driven approaches	43
2.6.8	Related projects	44
3	Day-ahead and real-time charge scheduling	47
3.1	Introduction	47
3.2	Method	48
3.2.1	A MIP model for day-ahead planning	48
3.2.2	Real-time planning: Schedule guided heuristic	58
3.3	Experimental setup	62
3.3.1	Data generation	62
3.3.2	EV fleet charging simulation	63
3.3.3	Simulation parameters	63
3.3.4	Solving of MIP instances	64
3.3.5	Metrics	64
3.4	Experimental results	66
3.5	Discussion	73
3.6	Conclusion	74
4	Real-time charge scheduling with departure time prediction	76
4.1	Introduction	76
4.2	Dataset	77
4.3	Method	78
4.3.1	Regression Methods	78
4.3.2	Changes to the schedule guided heuristic	80
4.4	Experimental setup	83
4.5	Experimental results	84
4.5.1	Regression for departure time prediction	85
4.5.2	Influence of prediction accuracy on smart charging	87
4.5.3	Computation time	90
4.6	Discussion	90
4.7	Conclusion	92

5	Battery-aware charge scheduling	93
5.1	Introduction	93
5.2	Scenario	94
5.3	Method	94
5.3.1	Battery simulation	94
5.3.2	Battery pack	96
5.3.3	Charge scheduling heuristic	96
5.4	Simulation setup	102
5.4.1	EV fleet simulation	103
5.4.2	Battery simulation	103
5.5	Simulation results	105
5.6	Discussion	108
5.7	Conclusion	109
6	Data-driven charge scheduling	111
6.1	Introduction	111
6.2	Method	113
6.2.1	Data preparation	113
6.2.2	Regression methods	116
6.2.3	Integration with charge scheduling heuristic	118
6.3	Experimental setup	121
6.4	Experimental results	122
6.4.1	Regression models	123
6.4.2	Impact of integrated regression models on smart charging	125
6.5	Discussion	130
6.6	Conclusion	131
7	Open source heuristic and practical validation	132
7.1	Introduction	132
7.2	Method	133
7.2.1	Data model	133
7.2.2	Charge scheduling heuristic	134
7.2.3	Open source repository	136
7.2.4	Integration concept	139
7.3	Experimental setup	140
7.3.1	Physical charging infrastructure and field test	140
7.3.2	Open Charge Point Protocol (OCPP)	142
7.3.3	Field test assumptions	142
7.4	Experimental results	143
7.4.1	Field test of the charge scheduling heuristic	143

<i>TABLE OF CONTENTS</i>	viii
7.4.2 Runtime of the REST API	146
7.5 Discussion	147
7.6 Conclusion	148
8 Conclusion	149
8.1 Summary	149
8.2 Outlook	152
Bibliography	153
A Appendix	172
A.1 Nomenclature: MIP model	172
A.2 Nomenclature: ECM	174
A.3 Addendum: Predicting arrival SoC	175
A.4 Addendum: Predicting EV charging profiles	180
A.5 OCPP Charge Profile example	182

List of Algorithms

1	Computing optimal charge schedule value $P_{CS}(t_1, t_2)$	102
---	--	-----

List of Figures

1.1	Thesis outline	6
2.1	Constant-current, constant-voltage (CCCV) charging profile . . .	14
2.2	Constant-power, constant-voltage (CPCV) charging profile	15
2.3	Schematic representation of a battery pack	16
2.4	Schematic representation of single-phase and three-phase charging	19
2.5	Simultaneity factor	21
2.6	Diagram of power generator	22
2.7	Diagram of phase offset in a three-phase system	23
2.8	Schematic representation of a power generator	23
2.9	Hierarchical infrastructure installation	25
2.10	Charging station installation with phase rotation	26
2.11	Car park energy consumption on a week day	28
2.12	Sample historical electricity prices	30
2.13	Objectives of charge scheduling	33
2.14	Minimizing peak demand vs minimizing energy costs	35
3.1	Combination of day-ahead and real-time charge scheduling	49
3.2	Two examples for calculation of $Q'_{n,below}$ and $Q'_{n,above}$ with $SoC = 0.1$ and $SoC = 0.9$ respectively	52
3.3	Constraint: Assignment of EVs to charging stations	55
3.4	Schedule guided heuristic flowchart	60
3.5	Real-time simulation	64
3.6	Pareto fronts showing the tradeoffs between weights for energy costs (w_{costs}) and weights for fair share ($w_{fairShare}$), peak shaving ($w_{peakShaving}$) and load imbalance ($w_{loadImbalance}$) including dominated and non-dominated solutions	68
3.7	Mean final SoC subject to randomness	70
3.8	Average cost (€/MWh) subject to randomness	70

3.9	Power consumption over time as a result of different weight setting for objective function components	72
3.10	Computation time per method	73
4.1	Flowchart of the charge scheduling heuristic with integrated departure time predictions	82
4.2	EV prioritization based on predicted departure time	84
4.3	Historical availability data of a single driver	86
4.4	Trained XGBoost regression model feature importance: Historical departure time is most important followed by the arrival time.	87
4.5	Mean fraction of minimum SoC by number of EVs: Perfect information (oracle) clearly leads to the best result, showing that the best possible predictions lead to a fairer distribution.	88
4.6	Fraction of EVs adequately charged (SoC above the minimum SoC)	88
4.7	Relationship between prediction accuracy and smart charging quality for 250 EVs (correlation: -0.968)	89
4.8	Average computation time per scheduling operation	90
5.1	CPCV charging of a single EV with and without charge schedules. A more accurate battery model (ECM) leads to charge scheduling with a more effective usage of infrastructure capacity.	95
5.2	Flowchart of the charge scheduling heuristic with integrated battery model	97
5.3	Simulating future power $P(t_1)$ in CPCV ahead of time given charge schedule and initially charged energy for a single EV	98
5.4	Simulating the energy (Wh) that will be charged for a single EV in a future interval given a charge schedule	100
5.5	Open circuit voltage $V_{OC}(z(t))$ based on data for LG's E63 battery cell. Values between points are interpolated.	104
5.6	Simulation results: Mean final SoC over increasing numbers of EVs for different fleet compositions. Battery-aware scheduling, which uses an ECM as a battery model, shows consistently better performance given an initial SoC of 0.8.	106
5.7	Simulation results: Improvement in mean final SoC reached with battery-aware <i>b</i>) over simplistic <i>a</i>) charge scheduling. Battery-aware scheduling <i>b</i>) allows charging up to 8.67% more energy.	107
5.8	Average computation time per rescheduling operation of <i>a</i>) and <i>b</i>)	108
6.1	CCCV: Simulation vs observed process	112

6.2	Flowchart of the charge scheduling heuristic integrating the data-driven charge profile simulation	119
6.3	Constant current, constant voltage (CCCV) charging with and without charge plans. The charge plan specifies an upper bound for the EV's charging current.	120
6.4	EV arrival and departure time distribution	121
6.5	Observed CCCV processes and predicted power using different regression models	124
6.6	XGBoost feature importance	125
6.7	Experimental results: Mean final SoC for different EV fleet sizes	126
6.8	Power vs SoC for all data points in the dataset	127
6.9	Single simulation runs using different predictors (20 EVs)	128
6.10	Single simulation runs using different predictors (40 EVs)	128
6.11	Computation time of the charge scheduling heuristic per integrated prediction method	129
7.1	Charging stations connected to the grid with rotating phases	134
7.2	Flowchart of the charge scheduling heuristic: Program flow for creating charge plans upon arrival of an EV.	135
7.3	Screenshot: Visualization of a simple charging infrastructure with three EVs.	137
7.4	Screenshot: Visualization of individual EV charge plans	138
7.5	Screenshot: Visualization of a more complex charging infrastructure	138
7.6	Components involved in smart charging and standardized communication protocols. Arrows indicate direction of requests.	139
7.7	Sequence of requests triggered by arrival of an EV at a charging station.	140
7.8	Station exterior	141
7.9	Station interior	141
7.10	Charging infrastructure in field test operations	141
7.11	User roles and system components used in field test operations.	142
7.12	Number of charging processes per EV model	144
7.13	Two sample charging processes of a BMW i3	145
7.14	Total planned and drawn power on 2019-05-06 with four EVs connected at the same time	145
7.15	Median runtime of the REST API	146
A.1	Distribution of time between charging processes	176

LIST OF FIGURES

- A.2 Feature importance of the trained XGBoost model for predicting arrival SoC 178
- A.3 Influence of regression method and assignment approach on the fraction of minimum SoC 179
- A.4 Comparing simulated with predicted charging profiles 182

List of Tables

2.1	Overview of balancing power types	31
3.1	Objective function components for charge scheduling	50
3.2	Flexible objective function components for EV priority and timeslot ordering	61
3.3	Heterogeneous EV model data	62
3.4	Simulation parameters	65
3.5	Simulation setup: Which combinations of day-ahead and real-time planning approaches are compared?	65
3.6	Simulation results comparing various methods of combining day-ahead and real-time planning approaches (see Table 3.1). Each simulation involves 50 EVs and 25 charging stations where results in rows are averages over 20 runs.	69
3.7	Comparison of different weight settings for objective function components: w_1 to w_4 correspond to fair share, electricity costs, peak shaving and load imbalance, respectively.	71
4.1	Set of raw charging process features used for predicting EV departure time	78
4.2	Set of one-hot encoded and engineered features used for training regression models. Values for the arrival and departure time are computed across all users. The semantic description of each raw feature is shown in Table 4.1.	81
4.3	Mean absolute error (MAE) in seconds, per regression model. Models were trained on historical dataset of roughly 100.000 charging processes	85
4.4	Five most significant features (p-value < 0.001) in linear regression model (out of 58 features overall)	85

5.1	Simulation setup: The charge scheduling heuristic with the ECM is compared against the same heuristic with a simplistic battery model	103
5.2	Simulation parameters for the equivalent circuit model (ECM) and EVs	104
5.3	Overview of the three battery model operations needed for the charge scheduling heuristic	105
5.4	Sensitivity analysis of initial SoC: Simulations where EVs spend more time in the constant-voltage phase (initial SoC starting with 0.5) show an improvement when using the ECM as a battery model to reflect CPCV.	107
6.1	Dataset raw attributes	113
6.2	Sample data point in cleaned and preprocessed dataset (1.2 million data points) used for training regression models. The car model is included as a one-hot encoded feature leading to 18 individual Boolean features.	115
6.3	Car model data from manufacturers (2018 models)	116
6.4	Simulation parameters: 600 simulations total	122
6.5	Predicting charging profile power: Error metrics per prediction method	123
7.1	TRADE EVs: Experimental results overview	143
A.1	Features for predicting arrival SoC: Categorical features are one-hot encoded.	176
A.2	Strategies for assigning EVs to charging stations	177
A.3	Mean absolute error (MAE) per regression model predicting arrival SoC	178
A.4	Predicting EV charging profiles: MAE per regression model, with and without ambient temperature feature	180
A.5	Predicting EV charging profile: Sensitivity study on charging efficiency	181

Acronyms

- AC** alternating current. 1, 18, 22
- BEV** battery electric vehicle. 1, 19, 39
- BMS** battery management system. 7, 10, 13, 17, 18, 20, 41
- CCCV** constant-current, constant-voltage. x, 13, 14, 35
- CPCV** constant-power, constant-voltage. x, 14, 15, 40
- CPO** charge point operator. 2, 8, 41, 132
- DC** direct current. 18
- ECM** equivalent circuit model. i, 4, 11, 41, 95, 111, 151
- EV** electric vehicle. 1, 7
- EVSE** electric vehicle supply equipment. 26
- HEV** hybrid electric vehicle. 19
- MIP** Mixed Integer Programming. 36, 37
- ML** machine learning. 12, 41
- MPC** Model Predictive Control. 38, 39, 41
- OCPP** Open Charge Point Protocol. 8, 142
- OS** operating system. 26
- PCM** parallel-connected cell module. 17

PHEV plug-in hybrid electric vehicle. 1, 19, 42

SoC state of charge. 2, 11, 14, 50

SoH state of health. 18

V2G vehicle-to-grid. 28, 32, 38

VPP virtual power plant. 33

Chapter 1

Introduction

1.1 Motivation

The growing number of electric vehicles (EVs) poses a challenge for the existing electrical infrastructure. Undersized connection lines and a lack of charging stations raise the concern of satisfying EV charging demands. Coordinated or "smart" charging offers an approach to satisfying EV charging demands in limited charging infrastructures. Smart charging involves decision making about schedules for EVs. In other words, deciding which EV may charge at which charging station and at which current during which time periods. A charge schedule determines an EV's current over time. From a technical perspective, charge schedules are sent to charging stations. The charge schedule is implemented by charging stations by communicating to the EV the maximum allowed current at each moment in time. Scheduling flexibility in smart charging arises from the length of stay and the available electrical supply.

Scheduling is constrained by electrical engineering constraints such as three-phase charging. With regard to smart charging, a three-phase electrical infrastructure essentially consists of three conductors with alternating current (AC). Charging stations are connected to one or more phases. Similarly, EVs are able to charge on one or more phases. Plug-in hybrid electric vehicles (PHEVs) typically charge on one phase while battery electric vehicles (BEVs) are often able to charge on three phases. Smart charging must take three-phase charging into account to accurately model existing charging infrastructures.

Scheduling for three-phase charging is further complicated by the fact that phases at the charging stations may not correspond directly to phases of the grid. For example, the charging station may be installed such that the first phase of the charging station does correspond to the first phase of the grid.

The entity in control of the charging infrastructure is known as the charge point operator (CPO). In the context of smart charging, the CPO is responsible for triggering the computation of schedules and for sending schedules to charging stations.

Smart charging can be considered in different times of planning: day-ahead (offline) and real-time (online). The importance of aspects such as computation time and information availability depends on the time of planning. On the one hand, during day-ahead planning minimizing computation time is not as crucial as during real-time planning. However, there is less information available or information is less reliable. For example, the exact time of arrival and time of departure of EVs is uncertain during day-ahead planning. On the other hand, during real-time planning minimizing computation time is crucial. In this context, smart charging approaches must be flexible enough to respond to changing circumstances in real time. However, there is also more information available and information can be considered more reliable. For example, the exact state of charge can be measured on arrival and the time of departure can be estimated more accurately once the EV has arrived.

In this work we consider the scenario of employee charging at the workplace. The scenario is characterized by predictable arrival and departure times and by long stays. Furthermore, the set of EVs is assumed to be heterogeneous. In other words we take into account different EV models with varying characteristics. EV model characteristics include battery size, the number of phases used for charging and the charging power. The main requirement for the scenario is to avoid overloading the charging infrastructure while maximizing infrastructure utilization. Whether the charging infrastructure is overloaded can be quantified by the rating of electrical conductors or electrical safety devices such as fuses. In Germany, the simultaneity factor [140] is defined for determining limits in a charging infrastructure.

The goal of smart charging in the scenario of charging at the workplace is to maximize the state of charge (SoC) across the fleet. Ideally, employees should not be aware of the application of smart charging. At the end of the working period, EVs should be fully charged. If a full charge for each EV is not possible, EVs should be correctly prioritized with regard to arrival SoC and departure time. A minimum required SoC may also be used to improve EV prioritization. However, gathering a reliable value for the minimum required SoC may be difficult in practice due to issues such as inaccurate user inputs.

From the perspective of the electrical grid, smart charging is motivated by the mitigation of effects caused by uncoordinated charging. For example, load imbalance can be caused by single-phase EVs charging concurrently on the same phase. Another example commonly found in related work are peak loads caused by many EVs charging at the same time. Smart charging presents an approach to mitigating both issues. EVs can be scheduled such that load imbalance and peak loads are

minimized. However, there are gaps in the literature with respect to applying smart charging in a three-phase charging infrastructure.

In practice, applying smart charging is complicated by uncertain EV availability. In other words, it is difficult to plan ahead when the exact period in which the EV is available for charging is uncertain. EV availability can be predicted using regression models trained on historical data. For example, a regression model can be trained on historical data to estimate EV departure times. The regression model can then be used in real-time upon each EV arrival to predict its departure time.

While there is related work on predicting EV availability [59, 70, 98, 127, 172] the approach of directly integrating predictions in smart charging is unexplored. Furthermore, analyzing the relationship between prediction accuracy and smart charging quality is not covered by previous research. In other words, how does an increase in prediction accuracy affect smart charging?

Related work on smart charging positions integrating nonlinear EV charging behavior as a topic for future research [44, 168]. Charge profiles are used by EVs to control a battery's charging process. A charge profile is a nonlinear function representing battery current and voltage over time. In practice, the application of a charge profile results in a decline of charging current towards high SoC. The decline of charging current should be taken into account in smart charging approaches. Not taking into account the decline leads to a gap between the scheduled power and the actual power draw of the EV. This gap represents suboptimal infrastructure usage since infrastructure utilization is not maximized. The gap has been observed in practice [93]. There is thus a need for research on addressing the gap between scheduled power and actual power draw in smart charging.

With regard to reproducibility, the source code used for smart charging approaches in most related work is not published. Unpublished source code makes it difficult to reproduce experimental results and is a prohibitive barrier to implementing smart charging approaches in practice. In other words, there is a lack of a common code base in related work which would allow for more direct comparisons of smart charging approaches. To bridge this gap, this work presents an open source package consisting of the smart charging approaches described in this work.

Finally, in contrast to related work which typically relies on simulations we additionally validated the approaches in the open source package in a one-year field test with a real charging infrastructure. The charging infrastructure consisted of six charging stations and a deliberately undersized connection to the grid. The connection allowed for two EVs to charge concurrently. Experimental results show six EVs can be scheduled to charge throughout the day without overloading the charging infrastructure. Additionally, we show runtime measurements of the open source package to demonstrate how it may be used for real-time smart charging and that it scales to larger EV fleets.

1.2 Research questions and contributions

This section describes the main research questions addressed in this thesis. The research questions take into account literature gaps with regard to practical considerations such as uncertain EV departures and EV battery behavior.

How can EV charging be coordinated in a three-phase charging infrastructure during different times of planning? (Chapter 3)

First, we present a MIP model for making use of information that is available ahead of time. The output of the MIP model is a tentative charge plan per EV in the fleet. Second, we describe the smart charging heuristic which is used to coordinate EV charging in real-time. The heuristic is designed to adapt tentative charge plans of the MIP model but can also be used without precomputed schedules.

How can we address the uncertainty of EV availability in smart charging and quantify a solution's impact on charge schedule quality? (Chapter 4)

An important component of the heuristic for smart charging is a priority mechanism. The priority takes as input the charging urgency per EV, which is affected by the EV's departure time. We present an approach using regression models to predict each EV's departure time based on historical data in order to more accurately prioritize EVs.

How do integrated predictions of battery charge profiles affect smart charging? (Chapters 5 and 6)

In practice, EVs charge using nonlinear charge profiles. Such charge profiles lead to a decreasing power draw towards high SoC. Smart charging approaches which ignore decreasing power in practice lead to a gap between planned power and actual power draw. We present two approaches to integrate models of charge profiles in the smart charging heuristic introduced in earlier chapters in order to minimize the gap between planned and actual power. The first approach uses a traditional equivalent circuit model (ECM) to model charge profiles while the second approach relies on regression models to predict charge profiles based on historical data.

How can a charge scheduling heuristic be implemented which is open and interoperable with other systems? (Chapter 7)

Lastly, we present an open source package containing an implementation of the charge scheduling heuristic and we describe experimental results from validating the algorithm in a one-year field test.

1.3 Publications

The results described in this thesis are based on the following journal, conference and working papers:

- O. Frendo, S. Karnouskos, N. Gaertner, O. Kipouridis, K. Rehman, and N. Verzano, "Charging Strategies and Implications for Corporate Electric Vehicle Fleets," in *2018 IEEE 16th International Conference on Industrial Informatics (INDIN)*, Jul. 2018, pp. 466–471.
- O. Frendo, and N. Gaertner, "Real-Time Planning for Smart Charging of Electric Vehicle Fleets," in *Operations Research Proceedings 2018 (OR2018)*, 2018, pp. 531-537. Springer, Cham.
- O. Frendo, N. Gaertner, and H. Stuckenschmidt, "Real-Time Smart Charging Based on Precomputed Schedules," *IEEE Transactions on Smart Grid*, vol. 10, no. 6, pp. 6921–6932, 2019.
- O. Frendo, N. Gaertner, and H. Stuckenschmidt, "Improving Smart Charging Prioritization by Predicting Electric Vehicle Departure Time," *IEEE Transactions on Intelligent Transportation Systems*, pp. 1–8, 2020.
- O. Frendo, J. Graf, N. Gaertner, and H. Stuckenschmidt, "Data-driven smart charging for heterogeneous electric vehicle fleets," *Energy and AI*, vol. 1, Aug. 2020.
- O. Frendo, N. Gaertner, and H. Stuckenschmidt, "Open source algorithm for smart charging of electric vehicle fleets," Submitted to *IEEE Transactions on Industrial Informatics (under review)*, 2020.
- O. Frendo, N. Gaertner, and H. Stuckenschmidt, "Battery-aware charge scheduling," *Working paper (unpublished)*, 2020.

1.4 Outline

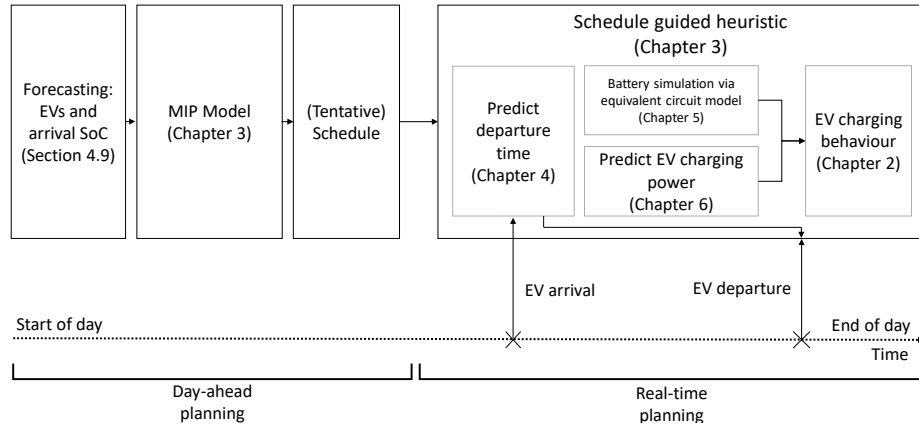


Figure 1.1: Thesis outline

Figure 1.1 shows an overview of the smart charging concepts presented in this thesis and serves as a visual outline.

Chapter 2 discusses preliminaries and the theoretical foundation. The preliminaries include the considered scenario, approaches to modelling charging infrastructures and how EVs charge in practice using nonlinear charge profiles.

Chapter 3 presents the combination of day-ahead planning and real-time planning. A mixed integer programming (MIP) model is used during day-ahead planning to compute tentative schedules. The tentative schedules are then adapted in real-time using the schedule guided heuristic.

Chapter 4 addresses uncertainty in smart charging. For example, EV departure times are uncertain but are an important component for scheduling and prioritization. An approach is presented which predicts EV departure times in order to improve prioritization during scheduling.

Chapters 5 and 6 focus on EV charging behavior and nonlinear charge profiles in more detail and present two different approaches to computing more accurate charge plans.

Chapter 7 presents the experimental results of applying the heuristic in a field test. Additionally, an open source package containing the heuristic is described.

Finally, chapter 8 concludes the thesis and contains a summary and an outlook.

Chapter 2

Foundations and related work

This chapter gives an introduction to the technical and regulatory aspects of EV charging and the implications for smart charging. The chapter is structured as follows. To begin with, section 2.1 details the EV charging scenario considered in this work. In smart charging, assumptions are usually made with regard to the time of planning (real-time vs offline planning), the location and EV availability. In this work, we consider the scenario of employee charging at the workplace. The scenario is characterized by long stays and predictable EV availability which ensures the flexibility required for smart charging.

Next, section 2.2 gives a short description of the most important components in EV charging: battery cells, charging profiles, battery packs and battery management systems (BMSs). These technical components influence EV charging behavior and how EVs respond to charge schedules in practice.

Section 2.3 explains concepts related to the charging infrastructure. This includes the simultaneity factor, load imbalance caused by single-phase charging, electrical network topology and charging stations. In smart charging, the charging infrastructure must be modelled in order to implement constraints such as the number of available charging stations and the infrastructure limit. In practice, ignoring such constraints can lead to overloading the charging infrastructure.

Section 2.4 discusses other economic and regulatory factors influencing charge schedules: Demand charges, spot energy markets and balancing energy markets. These factors usually relate to the main objective of the corresponding work on smart charging. For example, the energy price is often minimized in scenarios with long stays and short charging durations. Section 2.5 gives a description of typical objectives and constraints found in smart charging approaches.

Finally, section 2.6 concludes the chapter with an overview of related work and literature gaps in the domain of smart charging.

2.1 Scenario

Charging infrastructure and location

In this work, we consider charge scheduling in the context of employees charging at the workplace. Charging at the workplace is characterized by predictable EV availability with long stays and heterogeneous fleets. Additionally, we assume there is an entity in control of infrastructure who knows the charging infrastructure, operates charging stations and knows which EV models are in use. The entity operating the infrastructure is known as the charge point operator (CPO).

A practical application of charge scheduling requires charging stations which are able to implement schedules. The ability for charging stations to receive and communicate charge schedules is not easy to implement and requires standardized protocols such as the Open Charge Point Protocol (OCPP) version 1.6 [124].

Time of planning

Different categories of scheduling problems make differing assumptions with regard to information availability and constraints on computation time [131]. In the following, we discuss offline and online scheduling.

On the one hand, offline scheduling assumes information is known ahead of time. Schedules may thus be computed in advance. In this work, we consider offline scheduling in the form of day-ahead scheduling. As such, we assume there are less stringent requirements with regard to the computation time of scheduling. With regard to information availability in the context of charge scheduling: Some variables are difficult to acquire reliably. For example, the departure time of EVs depends strongly on its driver. However, the driver may not know in advance when he will depart.

On the other hand, online scheduling assumes less knowledge is available. In this work, we consider online scheduling as real-time scheduling. In practice, data acquisition is simpler compared to day-ahead (offline) scheduling since EVs are already connected to the infrastructure. However, the aspect of computation time is more important since a charge scheduling system must respond quickly to new information. In the context of charge scheduling, response latency translates directly to slack in the charge schedule. For example, if an EV arrives but waits for several minutes before receiving a charge scheduling, those minutes cannot be used for charging.

In this work, we discuss a combination of the two scheduling approaches in chapter 3: We use day-ahead scheduling to precompute schedules based on available knowledge. We then adapt the precomputed schedules in real-time.

EV availability

Depending on the considered charge scheduling scenario, EV availability may be

1. unpredictable: For example, a public charging infrastructure in shopping centers leads to more unpredictable stays, especially if no information about the EVs is available.
2. somewhat predictable: For example, in a private charging infrastructure for employee charging at the workplace the EV availability typically reflects business hours.
3. predictable and controlled: For example, if EVs are used for logistics as delivery vehicles with predetermined routes. Here, time constraints would likely be tighter since the EVs would be in use more leading to less standing times.

In this work, we consider the scenario of charging at the workplace and somewhat predictable EV availability. We address the involved stochastic components in chapter 4. In particular, aspects of historical data such as the EV's model, past arrivals and departures, charging locations and the typical charging duration can be used to make a prediction as to the EV's departure time. A more accurate departure time improves charge scheduling as it refines prioritization and thus reduces slack in schedules.

Depending on the considered scenario, time-dependent energy prices are considered more or less important. In the first scenario, minimizing energy prices is likely to be considerably less important compared to fully charging the EV as soon as possible. For the other two scenarios, energy prices may be taken into account depending on data reliability and each EV's length of stay.

Future developments in electric mobility may also enable hybrid approaches. For example, private charging infrastructure could be made available as public charging infrastructure outside of business hours.

Other scenarios

The methods presented in this work may be applied to other scenarios such as multi-family homes. Usually the currently installed electrical infrastructure is undersized and was originally installed primarily for low-power applications such as lighting. Thus charge scheduling presents an approach to making the most of the current electrical infrastructure.

2.2 Electric vehicle charging

This section describes components involved in battery charging from the EV's perspective based on [133]. This includes battery cells, charging profiles, battery pack topology and battery management systems (BMSs).

For a practical application of smart charging, the most important takeaway is that the EV decides how much power is drawn. Charge plans computed by smart charging only represent the maximum power draw. The EV may decide to draw less power to maximize battery life.

2.2.1 Battery cells

Battery cell variables

In this work we refer to the individual electrochemical unit as the *battery cell*. This is to avoid using the term *battery* on its own, which in the literature is used to refer to battery cells as well as battery packs (a combination of multiple battery cells). In the context of this work, the battery cell variables represent inputs and parameters required for modelling and simulating a battery cell.

Nominal cell voltage. The nominal voltage is specified by manufacturers and depends on the battery's chemical composition, among other factors. For example, the nominal voltage of Lithium-based cells is typically over 3V while lead-acid cells have a nominal voltage of 2.1V. The nominal voltage is an important factor when considering the application of the battery cell. For example, a higher voltage results in a higher power and thus a higher nominal energy capacity.

Nominal charge capacity. Cells are able to provide electrical charge to a circuit. The electrical charge is quantified by the nominal charge capacity in units of ampere-hours (Ah) or miliampere-hours (mAh). For example, a cell rated to hold 0.5 Ah is able to provide 0.5 Ampere for 1 hour.

C rate. This variable is used to describe how fast the battery cell is discharged in relation to its charge capacity. For example, a fully charged 0.5 Ah battery cell may provide 0.25A for 2 hours (a 0.5C rate) or 2A for 15 minutes (a 4C rate).

Nominal energy capacity. Not to be confused with the nominal *charge* capacity, the nominal energy capacity is measured in watt hours (Wh). It is calculated by multiplying the nominal cell voltage with the nominal charge capacity. For example, a Lithium-based cell with a nominal voltage of 3.6V and 0.5Ah has a nominal energy capacity of 1.8Wh. In comparison, a lead-acid cell with a nominal voltage of 2.1V and 0.5 Ah has a nominal energy capacity of 1.05Wh.

Energy density. In relation to EVs, the energy density of battery cells is often compared. For a given volume, a battery cell with a higher energy density will

store more energy.

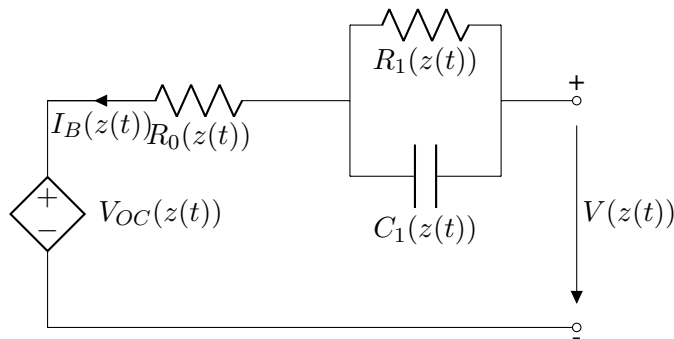
Chemistry. The influence of a battery cell's chemistry will not be discussed in detail. In this work, we focus on rechargeable Lithium-ion battery cells, a popular choice for EV applications. Other battery cell chemistries with lower nominal voltages tend to possess a lower energy density [133], making Lithium-ion battery cells a popular choice. Additionally, Lithium-ion cells possess a lower rate of self-discharge when not in use. However, Lithium-ion cells are sensitive to overcharge and require circuitry to protect against charging after 100% state of charge (SoC).

Temperature. Another important factor influencing a battery cell is its temperature. Temperatures outside the ranges recommended by the manufacturer lead to a quicker deterioration of the cell's performance. The process of battery cell deterioration is also called *aging*.

Form factor. Lastly, battery cells possess a form factor which may be cylindrical, pouch (flat, encased in a soft pouch) or prismatic (flat, encased in metal). For example, the form factor influences the amount of empty space in battery packs. In the context of EVs, energy density is usually maximized which is negatively influenced by empty space.

In the following, we outline an equivalent circuit model (ECM) to represent a single battery cell. The ECM can be used to model and simulate battery cells.

Battery cell simulation



Circuit 2.1: Battery cell equivalent circuit model (ECM)

We use equations (2.1)-(2.2) to describe the ECM [133] shown in circuit 2.1. An overview of the variables can be found in the nomenclature in section A.2. Change in the SoC $z(t)$ is expressed by differential equation (2.1). The current $I(t)$ is assumed to be negative during charging. We use $I(t)$ to define the battery's current during charging as a function of SoC.

$$\frac{dz(t)}{dt} = -\frac{\eta}{Q}I(t) \quad (2.1)$$

We use equation (2.2) to describe dependencies between components of the ECM [133]. The voltage $V(z(t))$ is held constant at a terminal voltage during the constant-voltage phase. For parameters such as charging efficiency η we use the values specified in Table 5.2 for later simulations.

$$V(t) = V_{OC}(z(t)) - I(t) * R_0(z(t)) - I_{R_1}(t) * R_1(z(t)) \quad (2.2)$$

Resistor current $I_{R_1}(t)$ is defined in equation (2.3).

$$\begin{aligned} \frac{dI_{R_1}(t)}{dt} = & -\frac{1}{R_1(z(t)) * C_1(z(t))} I_{R_1}(t) \\ & + \frac{1}{R_1(z(t)) * C_1(z(t))} I(t) \end{aligned} \quad (2.3)$$

We compute the power per battery cell via equation (2.4).

$$P_{cell}(t) = I(t) * V(t) \quad (2.4)$$

The battery cell model has the following limitations:

- we assume efficiency $\eta = const.$ whereas in practice this parameter too may be influenced by SoC and
- we do not consider battery degradation over time.

Next to ECMs, other types of battery models include physical models [133] and machine learning (ML) models [110]. Physical models are accurate but difficult to apply in real-time because they are computationally expensive [123]. The main limitation of ML models is the requirement for one historical dataset per type of battery cell.

Charging and discharging battery cells

A battery cell includes the following components [133]:

- positive electrode (or *cathode*)

- negative electrode (or *anode*)
- electrolyte
- separator

During discharge the negative electrode is oxidized and loses electrons. The positive electrode gains electrons from the external circuit. The opposite happens during charging: The negative electrode gains electrons from the external circuit while the positive electrode loses electrons.

The electrolyte and separator are ionic conductors which allow ions to move between the positive and negative electrode. The fact that they are ionic conductors but not electronic conductors means they allow the passage of ions but not electrons. If either of the elements were an electronic conductor the battery cell would short-circuit and self-discharge. The electrolyte is composed of a salt and solvent.

A battery cell also has different modes of failure. On the one hand, a battery cell ages. The age of a battery cell is not measured in terms of time passing but in the number of charging and discharging cycles. Internally, corrosion leads to increased internal resistance, reduced capacity and increased self-discharge over time. On the other hand, uncontrolled operating conditions such as applying a bad charging profile, high temperature or physical abuse can also lead to battery cell failure. Lastly, physical abuse may for example occur in automotive accidents. In this case the battery cell must not be a safety hazard. For example, it must not catch fire.

2.2.2 Charging profiles

It is beneficial to consider how batteries are charged in practice since this work's main focus lies on smart charging. Battery behavior should be taken into account or approximated in any charge scheduling approach. Otherwise, the charge scheduling approach may be difficult to apply in practice.

A *charging profile* (or *charging algorithm*, or *charging strategy*) is controlled and applied by the battery management system (BMS) and determines the amount of current applied to battery charging during the charging process [56]. The voltage of the battery cell is measured and used as a variable for the charging profile. An "optimal" charging profile is chosen and implemented by the BMS with regard to minimizing battery aging and maximizing charging speed.

The category of passive charging profiles is defined by using pre-set instructions. One of the most basic charging profiles is constant-current, constant-voltage (CCCV). It is a popular choice due to ease of implementation and simplicity [56]. CCCV consists of two discrete phases. First, the battery cell is charged with a

constant current (CC). The voltage of the battery increases with SoC, When the battery cell reaches a certain voltage (the *terminal* voltage) the constant-voltage (CV) phase begins. In the CV phase, current is decreased while voltage is kept constant. A simulation of a CCCV charging process is visualized in Figure 2.1.

Alternatively, constant-power, constant-voltage (CPCV) uses a constant-power (CP) phase followed by the same constant-voltage (CV) phase. A simulation of a sample CPCV charging process is shown in Figure 2.2.

Lastly, more sophisticated charge profiles have been proposed to minimize battery cell aging or take into account other variables such as battery cell temperature [56]. For example, five stages of constant-current are proposed by [102] to minimize battery cell aging. The choice of charging profile influences battery cell temperature, aging and charging speed. In all cases, the SoC follows a nonlinear function which is a crucial notion for charge scheduling. For example, survey paper [168] lists the assumption of linear SoC behavior as one of the main topics of future research in charge scheduling. The simplest approach to the nonlinear function found in related work such as [68, 161, 175] is to use a rough approximation and to assume the battery is only in the CC or CP phase. We present approaches to address nonlinear charge profiles in smart charging in chapters 5 and 6.

Constant-current, constant-voltage (CCCV) charging

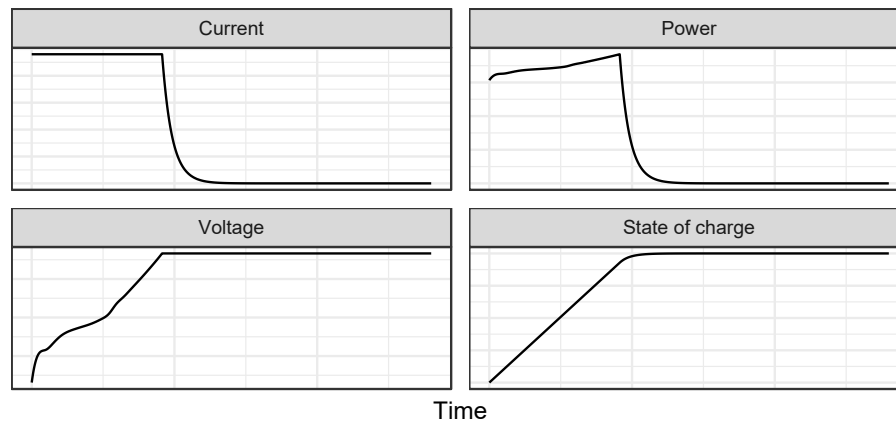


Figure 2.1: Constant-current, constant-voltage (CCCV): The charging profile begins with a constant-current phase followed by a constant-voltage phase [134]

Constant-power, constant-voltage (CPCV) charging

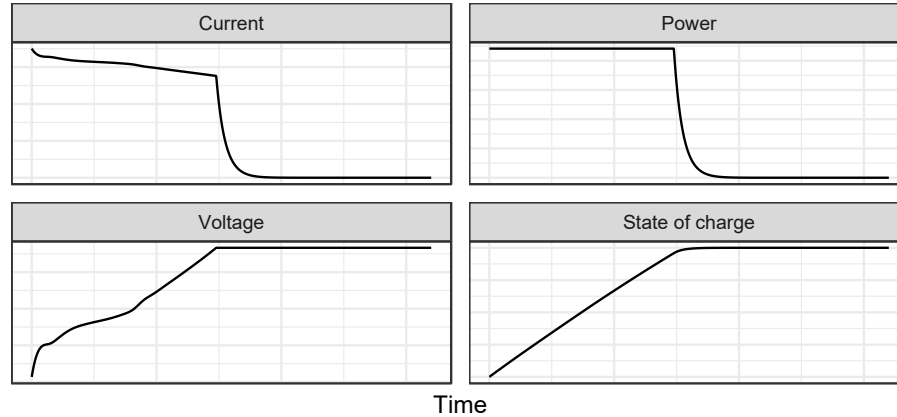


Figure 2.2: Constant-power, constant-voltage (CPCV): The charging profile begins with a constant-power phase followed by a constant-voltage phase [134]

2.2.3 Battery packs

A single battery cell does not produce enough power for an EV [134]. In practice, many small battery cells are thus combined into modules. A number of modules (specific to each EV model) make up a battery pack. A schematic representation is shown in Figure 2.3.

Reasons for using many small cells over few large cells in EVs include costs and thermal management [122]. First, existing manufacturing processes are optimized to smaller battery cells such as the 18650 form factor. Second, it is easier to keep small cells at acceptable temperatures compared to large cells.

With regard to battery pack topology there are different ways of how battery cells can be connected within a module and how modules can be connected to each other [134]. Two examples are:

- Series-connected battery cells and parallel-connected modules (SCMs): Within each module, the current is the same per cell while voltage is added. Within the battery pack, the voltage is the same per module while current is added (see Circuit 2.2).
- Parallel-connected battery cells and series-connected modules (PCMs): Within each module, the voltage is the same per cell while current is added. Within the battery pack, the current is the same per module while voltage is added (see Circuit 2.3).

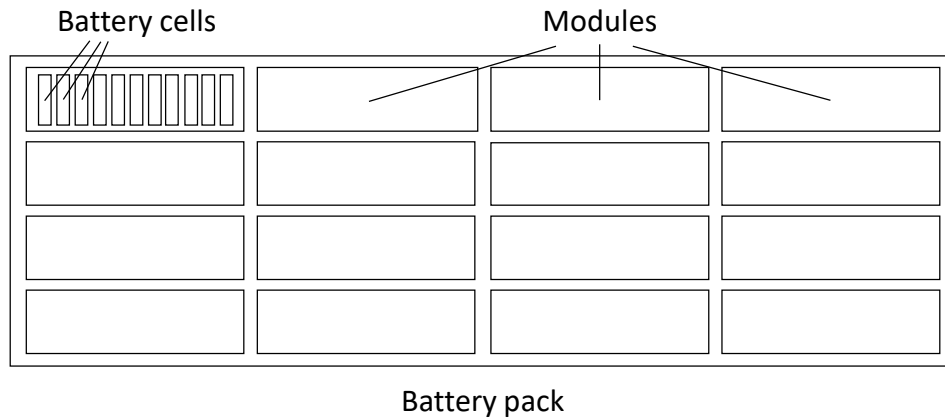
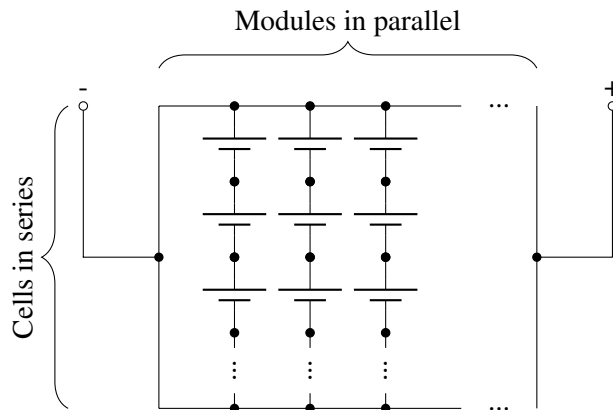


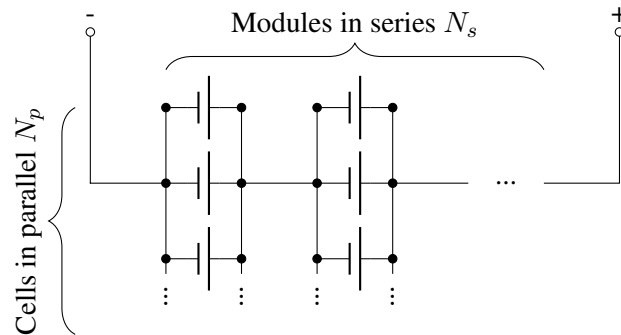
Figure 2.3: Schematic representation of a battery pack: A pack is composed of modules which consist of individual battery cells



Circuit 2.2: SCM: Battery pack composed of parallel-connected modules and series-connected cells within each module (adapted from [134])

The choice of battery pack topology is influenced by desired power output (kW), desired capacity (kWh) and safety concerns. To recap, cell voltage is determined by its chemistry. There is a limit on the current per battery cell that is determined by its construction. Thus typically battery cells are connected in parallel [134].

The number of battery cells per module is also determined by safety concerns. For example, [134] gives a 50V maximum per module, which would allow roughly 14 Lithium-ion cells with a nominal voltage of 3.6V in an SCM. The total voltage for the battery pack is typically chosen as less than 600V due to cost: Components



Circuit 2.3: PCM: Battery pack composed of N_s modules in series and N_p cells in parallel per module (adapted from [134])

for higher voltages are more expensive. There are, however, recent developments on EVs based on 800V which would also allow for faster charging [1, 43].

In this work, we use the standard $N_s N_p$ notation to describe the structure of a battery pack composed of parallel-connected cell modules (PCMs). The two variables N_s and N_p are important inputs for modelling and simulating a battery pack. For example, in chapter 5 we model a Tesla Model S with a 96s74p battery pack [96]. This means the battery pack consists of 96 modules in series with 74 battery cells in parallel per module [125]. Another example is the Renault Zoe with a 96s2p configuration.

Notably, both EV models battery packs are composed of 96 modules. The number of modules is chosen in order to reach 400V, a standard voltage for EVs [1]. To recap, the voltage of each module is added. Since cells within the module are connected in parallel, the voltage within the module stays the same. Each module would then have a voltage of 4.16V, a typical voltage for Lithium-ion battery cells. However, the battery cell used in the Renault Zoe (LG E63 [125]) is larger compared to the battery cell used in Tesla's Model S and produces a higher current. Thus fewer parallel-connected battery cells are required per module (2 instead of 74).

2.2.4 Battery management system (BMS)

A battery management system (BMS) consists of the hardware and software components required to manage a battery pack. The hardware components include the electronic circuitry to make measurements such as battery temperature and voltage. The software manages battery charging and discharging by controlling current to the battery and calculates SoC based on measurements.

There are five functional requirements for a BMS per [134]:

1. Sensing: Detect high voltages via measurements
2. Protection: Provide safety to the operator. In extreme conditions, this may require disconnecting the load from the battery pack. For example, overdischarging must be avoided for Lithium-ion battery cells because it could lead to short-circuits.
3. Interface: Must provide communication to external components in EVs
4. Performance management: Estimate SoC
5. Diagnostics: Estimate state of health (SoH)

Other goals of the BMS include maximizing battery life. From a cost perspective the BMS itself adds costs to the construction of an EV. Financially, it only makes sense to add a BMS in applications such as EVs where the cost of the battery pack itself or the cost of failure is high. Next to EVs, applications with large battery packs that require a BMS include stationary batteries for grid frequency regulation as discussed in section 2.4.2.

From the perspective of charge scheduling the BMS controls the charging process of the battery. The BMS decides on the charging profile to apply. The hardware of the EV determines whether single-phase or three-phase charging is applied. Lastly, the BMS communicates with the charging station via protocols such as IEC 68150 [141]. This communication includes how much power the EV is allowed to draw via charge plans.

2.2.5 Charging systems

This section describes how energy from the grid is used to charge the EV's battery. Today's electrical grid and transmission systems are based on alternating current (AC) [28]. However, batteries are charged with direct current (DC). The charging system is responsible for converting AC to DC.

As discussed in section 2.3.2 there are three different *phases* (for the purpose of this work, three different cables) of AC from the grid. EVs are typically designed to use single-phase or three-phase charging [45]. The number of used phases depends on the circuitry of the EV. The underlying trade-off is related to the complexity of the EV's charging circuitry: Three-phase charging is faster but also requires a more complex charging system.

To convert AC to the required DC an AC-DC converter (also named *rectifier*) is used. A schematic representation is shown in Figure 2.4.

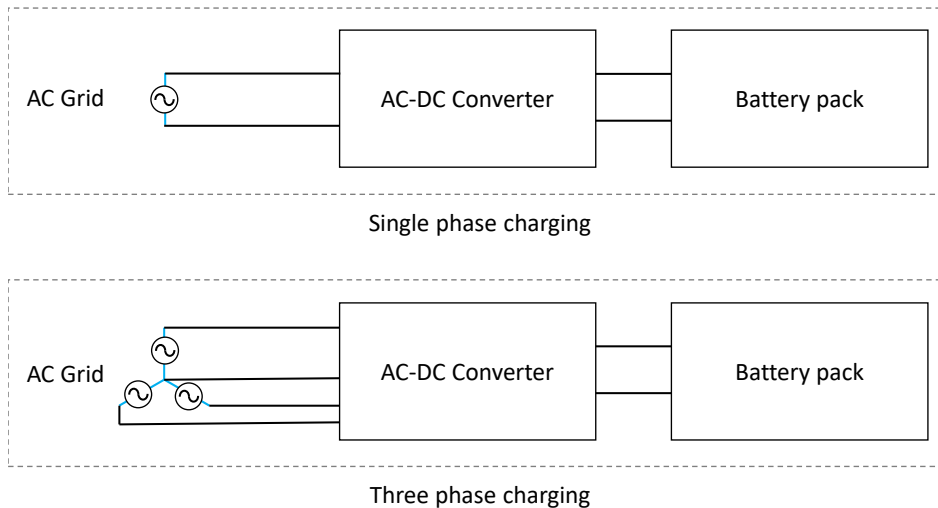


Figure 2.4: Schematic representation of single-phase (top) and three-phase (bottom) charging, adapted from [45]. In both cases, an AC-DC converter is required to convert the grid's AC to the DC required for charging batteries. The fourth line in three phase charging represents the neutral conductor.

Different types of EVs (sometimes referred to as xEV) have different requirements as to the battery pack and to the BMS [134].

- Hybrid electric vehicles (HEVs) possess a battery pack with a small amount of stored energy used to support a gasoline-based motor during certain periods such as acceleration. The electric motor is not used on its own. The battery pack is charged by the gasoline motor when power is available, for example during braking. Since HEVs do not charge using charging stations they will not be further discussed in this work.
- Plug-in hybrid electric vehicles (PHEVs) have an electric motor that can be used to drive on its own in addition to a gasoline-based motor. Compared to HEVs, the battery pack is larger and charged by plugging a cable into a charging station. EVs of this type typically charge on a single phase with 16A (3680W) or 32A (7360W).
- Battery electric vehicles (BEVs) only have an electric motor. A BEV's range relies completely on the battery pack. BEVs usually charge on a single phase or three phases at 16A (11040W) or 32A (22080W).

2.2.6 Implications for charge scheduling

The previous sections discussed battery cells, charging profiles, battery packs, battery management system (BMS) and charging systems. In practice, charging profiles in particular have a large impact on the effectiveness of smart charging. The control of the BMS supersedes any charge plans communicated by the charging station. Thus the EV's power draw P_{EV} is the minimum of the applied charge plan $P_{ChargePlan}$ and the charging profile $P_{ChargingProfile}$ in equation (2.5).

$$P_{EV} = \min\{P_{ChargingProfile}, P_{ChargePlan}\} \quad (2.5)$$

In Lithium-ion cells charging power is reduced towards high SoC to minimize battery aging. We model charge profiles for smart charging in chapters 5 and 6.

2.3 Charging infrastructure

This section describes the electrical infrastructure used for charging EVs. In smart charging, the accuracy with which the charging infrastructure is modelled determines the practicality of the approach. For example, a charge scheduling approach may model charging stations but ignore the charging infrastructure. Such a charge scheduling approach would be difficult to apply in practice since there are charging infrastructures in which stations may not be used concurrently. Limited charging infrastructures are discussed in more detail in chapter 3. This work takes into account the charging infrastructure up to the connection to the grid. In practice, the connection is represented by the transformer which converts high voltages to the 230V used in charging stations.

In the following we first describe the so-called simultaneity factor. The factor is an essential aspect of a standard for planning electrical networks and represents one of the main motivations for smart charging. Next, we explain load imbalance which results from EVs charging on a single phase and the topology of the electrical grid. Lastly, characteristics of charging stations are discussed.

2.3.1 Simultaneity factor

In Germany, the *simultaneity factor* is defined by the *DIN VDE 0100* [140] standard. In general, this factor describes the relation between the sum of consumers and the maximum power rating of an electrical network. For example, in an electrical network with a maximum power rating of 50kW and two constantly running consumers with 20kW each the simultaneity factor would be 0.8 [80]. The factor is an important indicator for planning an electrical network.

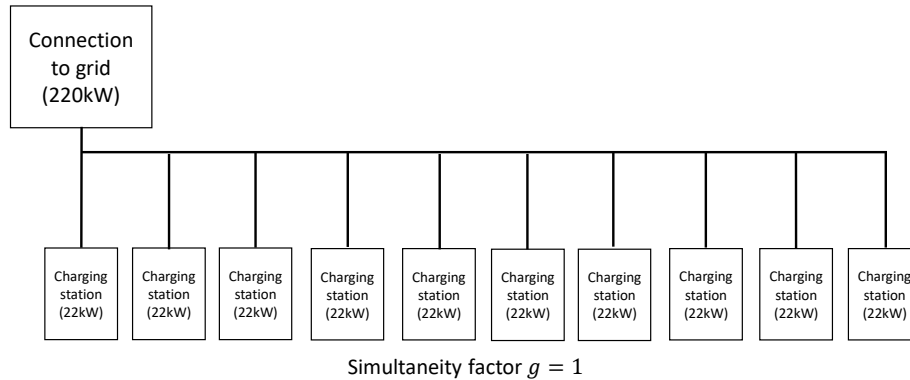


Figure 2.5: Simultaneity factor: Installing further charging stations is not permitted without an energy management system

In the context of electric mobility, DIN VDE 0100 states that the electrical infrastructure must be planned assuming a constant simultaneity factor of 1.0 per charging station unless an energy management system is applied [121].

Consequently, without an energy management system the number of charging stations is constrained by the maximum power rating of the electrical network. For example, if the maximum power rating of the network is 220kW and each charging station is able to draw 22kW then maximum number of allowed charging stations is ten. This setting is shown in Figure 2.5.

A typical AC charging station is able draw 22kW (or 32A per phase). Naive approaches to reducing the simultaneity factor include constraining each charging station to 11kW (or 16A per phase), thus doubling the number of allowed charging station but also potentially doubling the duration of charging processes.

However, if an energy management system is applied, the number of charging station is only constrained by the charging duration and the number of parking spaces. This assumes the physical charging stations themselves are not the main cost factor in a charging infrastructure. In this work we assume the main cost factor is the connection to the grid. Other cost factors in a charging infrastructure are staff costs, market access, operations and maintenance [106]. In the context of charge scheduling the energy management system would be responsible for computing and communicating schedules and ensuring that the maximum power rating of the electrical network is not exceeded.

2.3.2 Load imbalance

As described in section 2.2.5 EVs typically either charge on a single phase or on three phases of alternating current (AC). This section gives a short description of how and why three phase AC electricity is generated. To begin with, a generator generates power via electromagnetic induction by using magnets and electric coils. This produces AC [142]. However, instead of using just one electric coil, multiple coils are used that move in relation to the magnet (or vice versa). Using multiple components produces several alternating currents that are offset to each other by phase shift ϕ . A common number of phases is three, for example in Europe. A schematic diagram of a three-phase generator is shown in Figure 2.6.

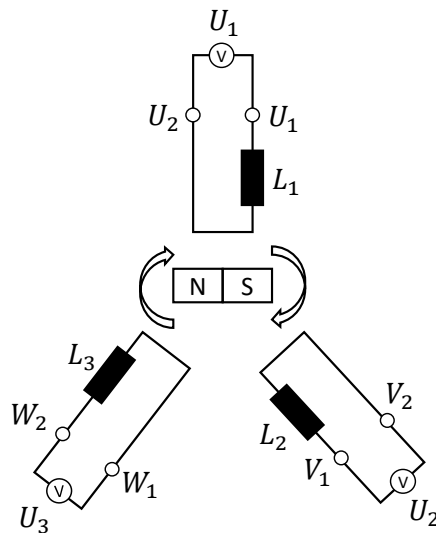


Figure 2.6: Diagram of power generator (adapted from [142])

One reason for using three phases is that power never drops below zero, producing a more constant power output compared to using fewer phases [28]. The resulting voltage in a three-phase system is shown in figure 2.7.

To implement three-phase power, a three-phase, four-wire system can be used [153]. One wire is used per phase and the fourth is the neutral conductor. A *star connection* (figure 2.8) is a possible connection between a generator and the grid.

The load imbalance is defined as the current I_N flowing through the neutral conductor. The load imbalance I_N should be minimized to protect the electrical infrastructure, in this case the power generator and transformers. For quantifying the load imbalance different methods have been proposed [153]. In three phase

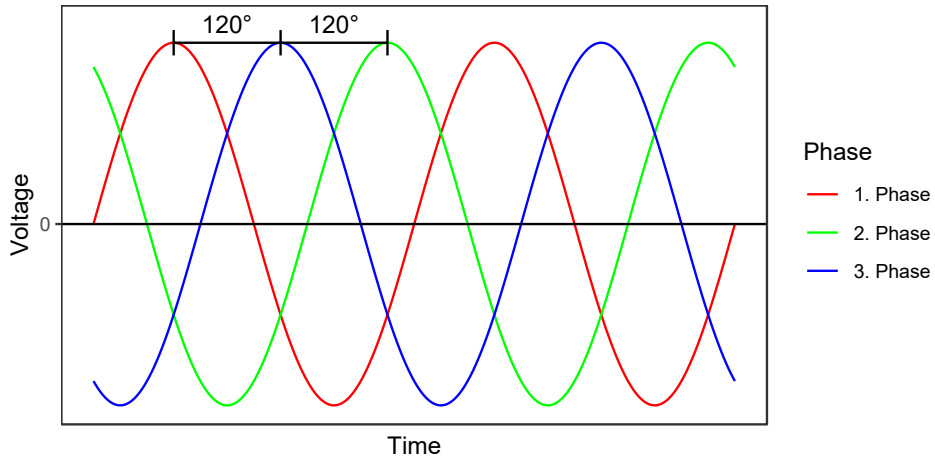


Figure 2.7: Diagram of phase offset in a three-phase system (adapted from [142])

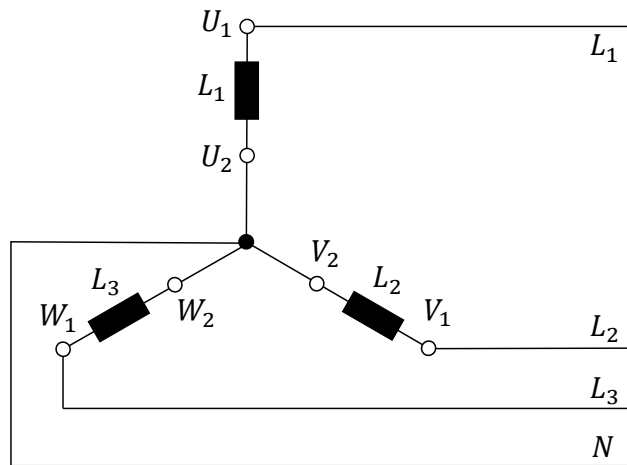


Figure 2.8: Schematic representation of a power generator connected via a *star connection* (adapted from [142]) in a three-phase, four wire system: L_1 , L_2 and L_3 as well as the neutral conductor N each represent one cable.

systems, the overall current can be expressed as the combination of three separate currents and associated phase angles, with a pairwise offset by $360^\circ/3 = 120^\circ$. Each such current I_j for one phase can be represented by a polar vector with magnitude $|I_j|$ and angle $\phi_j \in \{0^\circ, 120^\circ, 240^\circ\}$. In practice, ϕ_j is affected by resistances and components involved in the charging process.

In this work we reduce the complexity of calculations by assuming constant voltage in the network (230V) and by using a vector approximation which calculates the neutral current I_N as the sum of the three polar vectors (equation 2.6). Equation (2.7) represents the corresponding explicit form for computation where variables $|I_j|$ are replaced with the measured currents per phase. To derive equation (2.7) from equation (2.6), Pythagoras theorem is applied after a projection of the individual phase current vectors into two-dimensional Cartesian coordinates.

$$|I_N| = |I_1 + I_2 + I_3| \quad (2.6)$$

$$|I_N| = \text{sqr}t((|I_1| * \cos \phi_1 + |I_2| * \cos \phi_2 + |I_3| * \cos \phi_3)^2 + (|I_1| * \sin \phi_1 + |I_2| * \sin \phi_2 + |I_3| * \sin \phi_3)^2) \quad (2.7)$$

Equation (2.6) is nonlinear which makes it more difficult to later model and minimize using linear optimization. We later discuss a linear approximation of equation (2.6) in chapter 3 in order to use it in a linear optimization model. We then minimize load imbalance.

Minimizing load imbalance is motivated by power network operators who run AC transmission systems for long-distance transport of electrical energy. Whenever there is significant imbalance between the three phases of AC power the operators must reduce the imbalance to prevent damage to power transformers and generators. Operators require consumers to contribute towards minimizing load imbalance.

In the context of charge scheduling, load imbalance is caused in large part by EVs charging on a single phase. An EV charging on three phases does not cause load imbalance since it draws equal current per phase. In practice, the current may vary slightly from phase to phase. In this work, we assume three-phase charging draws equal current per phase.

However, single-phase charging causes load imbalance since it uses only a single phase. The phase used in a charging process cannot be changed once the process has started and is determined by the EV's and charging station's hardware.

Charge scheduling offers an opportunity to address load imbalance. First, EVs can be assigned to charging stations such that single-phase EVs do not charge on the same phase. The topic of how charging stations are connected to the grid with *phase rotation* is discussed in section 2.3.3. Second, single-phase EVs charging on different phases can then be scheduled to charge at the same time thus cancelling out each other and minimizing load imbalance.

2.3.3 Electrical network topology

We model the infrastructure per car park in a hierarchical structure as a tree of fuses. In practice both fuses and circuit breakers are used as electrical safety devices. Each node contains a fuse that may have a charging station or other nodes as children. For example, the fuse tree considered in chapter 3 has a depth of four which corresponds to a real installed infrastructure. Components of the installation are shown in Figure 2.9. A visualization of a hierarchical fuse tree is presented in chapter 7.



Figure 2.9: Hierarchical infrastructure installation: Charging stations connected to horizontal conductor bars, connected to vertical conductor bars, connected to transformer

- Charging stations (bottom left): Each charging station is able to charge one EV. Some charging station models with two plugs are able to charge two EVs concurrently. A *charging station* able to charge two electric vehicles is considered to have two *charge points*.
- Conductor bars: Conductor bars (top left and middle) are used to connect charging stations to the transformer and thus to the grid. Each cable in each conductor bar is secured by a fuse.
- Transformer (right): The transformer transforms the high voltages of the grid to lower voltages in order to supply charging stations with the 230V required by consumer devices

In the following, we assume each charging station has one charge point. Each charging station is connected via three phase alternating current (three-phase four-wire system in Germany). *Phase rotation* is used to determine which phase of

the charging station should be connected to which phase of the electrical grid. Figure 2.10 shows a sketch of a possible charging station installation where phases are rotated. The reason for the phase rotation is to allow minimizing load imbalance as discussed in the previous section. To summarize: If phases were not rotated all single-phase EVs would charge on the first phase because there would be no possibility to charge on other phases.

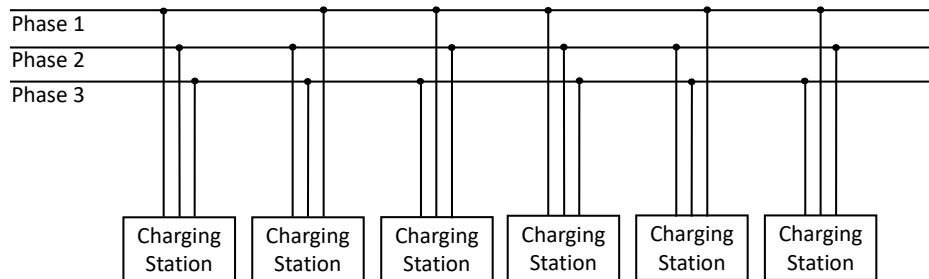


Figure 2.10: Charging station installation with phase rotation: Connection of grid phases are rotated to charging station phases to allow minimizing load imbalance for single phase EVs

2.3.4 Charging stations

A charging station, or electric vehicle supply equipment (EVSE), acts as conduit for EVs to receive energy from the electrical grid. For example, charging stations are responsible for receiving charge schedules and communicating to the EV how much power may be drawn. Charging stations include hardware as well as software components [82].

On the one hand, hardware components include a fuse to act as a safeguard against the EV drawing too much power. If the EV does draw too much power only one charging station is disabled instead of a complete conductor bar described in the previous section.

On the other hand, software components include an operating system (OS). For example, one of the charging stations we use in the practical smart charging approach in chapter 7 runs on Buildroot, a system for running Linux on embedded systems.

Other components include those designed for communication with either other charging stations or a backend server. Typical setups consist of an antenna for WiFi/cellular networks or an Ethernet connection. The Ethernet connection is more

reliable and robust but also more expensive to set up. In the practical smart charging setup discussed in chapter 7 an antenna was connected to each charging station for internet access.

In the context of charge scheduling, each charging station must be able to receive and implement charge schedules. There are proprietary as well as open protocols for communication with a backend [141]. For the practical aspects in this work, we will assume charging stations communicate with a backend via OCPP 1.6 [124].

2.4 Other factors in charge scheduling

2.4.1 Peak shaving

Types of peak shaving

Peak shaving addresses the matching and timing of supply and demand in the electrical grid [162]. A common goal of smart charging is to mitigate peak demand or shift time periods of high demand to periods of low demand. One of the benefits of a more even power demand throughout the day is a simplified energy production. Additionally, power quality is a result of how well supply and demand is matched in the electrical grid. Power quality is discussed further in the context of balancing energy in section 2.4.2.

The load factor in equation (2.8) is an example of how the effectiveness of peak shaving may be quantified [162]. A higher load factor represents a more even power demand.

$$\text{LoadFactor} = \frac{P_{avg}}{P_{Peak}} \quad (2.8)$$

Figure 2.11 visualizes the motivation behind peak shaving and the importance of the simultaneity factor. Data from a typical week day is shown from a car park with many EVs charging concurrently. There is an easily recognizable peak which can be smoothed via peak shaving.

A review on the state of the art of peak shaving [162] categorizes methods into several groups.

Traditional methods. Peaks may be mitigated from the perspective of the energy provider via gas power plants or diesel generators.

Integration of storage systems. Sizing and the optimal operation of storage systems are two commonly addressed research topics. Actual projects with large storage systems such as stationary batteries range from several hundred kW to

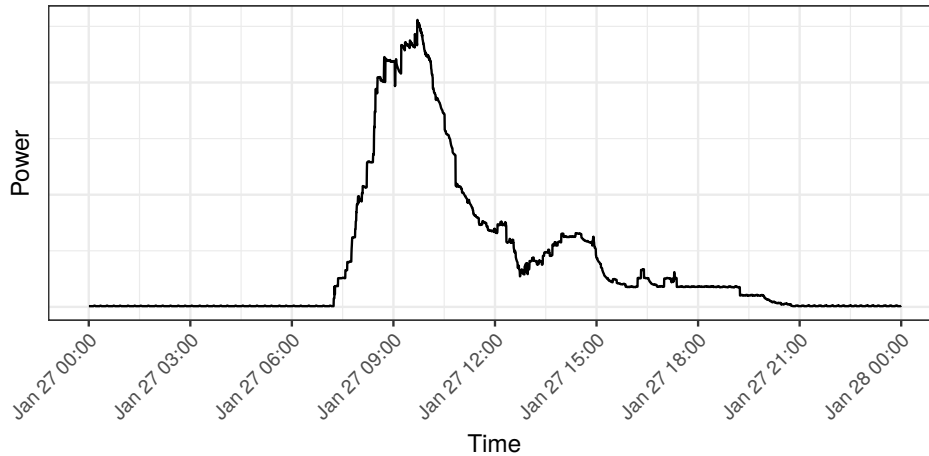


Figure 2.11: Car park energy consumption on a week day with over 100 charging stations. There is an easily recognizable peak starting at roughly 08:00 when employees typically arrive at the workplace

several MW with an energy capacity of several MWh. The goal is usually to charge the storage system when demand is low and to discharge during peak demand.

Such approaches may help reduce CO₂ emissions [86] by supporting power plants based on fossil fuels. For example, by reducing load variability periodically starting and stopping power plants can be avoided [63]. The process of starting and stopping a power plant in itself consumes fuel. Additionally, compared to other energy sources which must be physically started or stopped, batteries can be easily used to draw power or to discharge energy and react to changing demand quickly.

Demand side management. Typically, demand side management is implemented by scheduling consumers to draw power when demand is low. Consumers include controllable home appliances such as washing machines, dish washers or HVAC units [21] but also EVs. Such devices are heterogeneous in terms of power draw and scheduling constraints.

Integration of EVs. Research on the integration of EVs may assume EVs possess vehicle-to-grid (V2G) capabilities. In other words, EVs are able to discharge energy back into the grid. Research on charge scheduling such as [169] often discusses valley filling together with peak shaving. Similar to stationary storage systems, valley filling and peak shaving are implemented by charging during times when power demand in the grid is low and to discharge when demand is high. However, from a practical perspective the topic of integrating EVs for peak

shaving is different to storage system because it involves the control of many small agents vs the control of few large storage systems.

To give an idea as to the size of batteries, current BEVs possess batteries in the range of 20-100kWh. In contrast to stationary systems, the entity implementing peak shaving has little or no influence on the sizing of the individual EVs since EVs are not bought for the purpose of peak shaving. Instead, the topic of EV availability is introduced as discussed in section 2.1.

Demand charges

As explained in the previous paragraphs, peak shaving is often used as one of the main motivations for charge scheduling. The following passage explains demand charges [128] (or network charges), one of the financial motivations for peak shaving.

In the context of the electrical network, high peak demand influences the planning and sizing of infrastructure. The infrastructure must be planned according to the highest peak, otherwise it will be overloaded during peak demand. From a financial perspective, demand charges are used by energy providers to make consumers pay for generated peaks.

Depending on the country and contract, peak demand is typically recorded monthly, bi-annually or annually. In Germany, the hours of use represent the ratio of consumption to peak demand and are computed by equation (2.9). Demand charges are computed by equation (2.10) [62]. The capacity charge variable is a function of the hours of use and is set by the energy provider. This equation is designed to incentivize the consumer to mitigate peaks.

$$\text{Hours of use [h]} = \frac{\text{Consumption [kWh]}}{\text{Peak demand [kW]}} \quad (2.9)$$

$$\text{Demand charges [€]} = \text{Capacity charge [€/kW]} * \text{Peak demand [kW]} \quad (2.10)$$

Lastly, more dynamic scenarios may also be considered for charge scheduling. For example, other consumers in the infrastructure may also be taken into account. Consequently, the installed charging infrastructure is not necessarily limiting factor on its own.

2.4.2 Energy markets

Spot markets

Energy markets make use of auction mechanisms to decide energy distribution and its price [74]. Energy providers and consumers submit bids. An important aspect

of energy markets is that the electricity output and consumption must be equal. This aspect is described in more detail in the passage on balancing power.

Due to the international energy market in Europe, electricity transmission across multiple countries must be coordinated. Different exchanges offer spot markets such as the intraday and day-ahead markets in different regions. Later in this work we will later use price data from the EPEX SPOT SE which is the exchange responsible for France, Germany, Austria and Switzerland. Here, the day-ahead energy market is implemented by daily auctions at noon for electricity in units of 1MWh. Sample data is shown in figure 2.12.

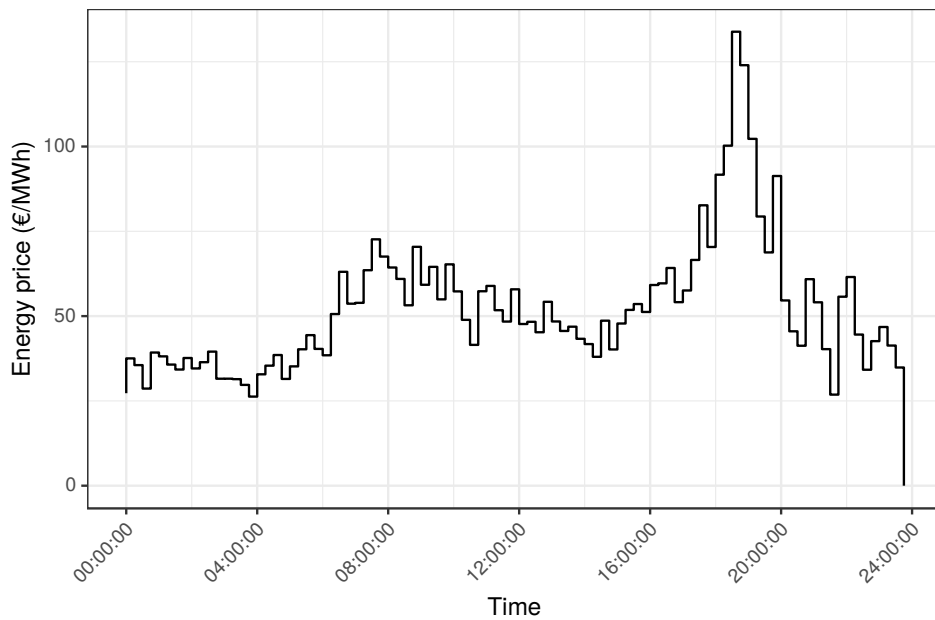


Figure 2.12: Sample historical electricity prices from the intraday market in Germany [152] on a typical weekday in October 2017 used as input for the charging simulation

Balancing power

Balancing power (or control power) can be defined as the ability to "maintain and restore the short-term active power balance in integrated electricity systems" [67]. In the electrical grid, power must be balanced between producers such as generators and consumers such as factories (or electric vehicles).

One way of measuring power balance in the electrical network is measuring the

Type	Primary	Secondary	Tertiary
Response time	30s	5 minutes	15 minutes
Minimum bid	1MW	5MW	5MW
Reserve (Germany)	600MW	2.000MW	2.500MW
Typical applications	Large stationary batteries	Hydro plants or thermal generators	Stand-by generators or consumers that are able to start quickly

Table 2.1: Overview of balancing power types [67]

frequency of the transmitted alternating current (AC). Typical AC frequencies are 50Hz as in Germany or 60Hz as in the USA. An oversupply of electricity or too much demand by electrical consumers cause frequency deviations. Mechanisms such as motors making use of electricity are built to work with a standard frequency. Frequency deviations can be harmful to such machines. One mechanism to keep electrical networks at the predefined frequency is balancing power.

Balancing power may be supplied as positive or negative power in response to current grid electricity production and consumption [154]. Positive balancing power is achieved by activating loads (or deactivating producers) while negative balancing power is implemented by activating producers (or deactivating loads). There are three types of balancing power (shown in Table 2.1). Each type of balancing power has different requirements as to how fast the response must be [67].

Similar to the energy spot markets described in the previous section, balancing power is implemented as an auction in a *balancing energy market*. Entities may submit bids to provide a certain amount of positive or negative balancing power for a certain timeslot. For example, the timeslot for secondary and tertiary power in Germany has a length of four hours. Bids are made in units of MW. Entities may be paid for making available the balancing power as well as if the balancing power is actually requested. Recently, regulatory changes were announced in Germany for submitting bids for balancing power [17]. The aim is to facilitate access to the three types of balancing power, specifically for renewable energy sources.

The goal is to replace conventional energy generation with renewable energy sources, specifically wind and photovoltaic power. For example, secondary balancing power was changed from a weekly to a daily tender and the positive/negative power offer must only be available for four hours, making it easier to submit bids.

2.4.3 Implications for charge scheduling

Peak shaving

Peak shaving is one of the main objectives addressed in chapter 3. It is one of the most intuitive objectives associated with charge scheduling as EVs are often considered as a flexible consumer.

Spot markets

A common approach in charge scheduling is to discretize time into 15 minute timeslots [168]. These 15 minute intervals correspond with the structure of the spot markets: 15 minutes for intraday and 60 minutes for day-ahead spot markets. The approaches presented in this work follow the same approach of discretizing time. A charge schedule is a set of charging assignments for an EV. Each assignment represents the EV charging at a certain power in a certain timeslot and may be based on results of the bidding process in the energy markets.

Related work considering the auction processes in energy markets for charge scheduling include [3, 12, 60, 126]. Typically, day-ahead spot markets are considered. With regard to optimization in charge scheduling, participating in day-ahead markets imposes less constraints on computation time compared to intraday markets. For example, [12] discusses the effects of charge scheduling on day-ahead energy market prices. [126] considers prosumers in general and models the bidding process together with scheduling. EVs that are able to charge as well as discharge energy can be considered prosumers. An explicit bidding strategy for day-ahead energy markets is proposed in [60] to minimize EV charging costs. Lastly, an approach combining EVs discharging energy and uncertain renewable energy sources aims to increase reliability in energy trading [3]. In this work, we approximate the auction process of the intraday market and assume a constant price in €/MWh per 15-minute interval. This approximation of the energy market is a standard approach in related work on charge scheduling [89].

Balancing power

EVs can be used as a possible source of balancing power [41], either by discharging (positive balancing power) or pausing the charging process (negative balancing power). EVs with long standing times in particular offer flexibility since EV batteries are able to respond quickly. With regard to the current state of technology, charge scheduling of EV fleets can be used to supply negative balancing power by pausing EV charging. EVs with vehicle-to-grid (V2G) capabilities are not yet

widespread. Future EV models with V2G capabilities may offer positive balancing power.

In practice, the order of magnitude required for being able to bid on balancing power with EVs alone is high. As shown in Table 2.1 the minimum bid for balancing power is 1MW which would require a minimum fleet of 45 EVs assuming a fleet of BEVs charging with 22kW. Regulatory processes to become *pre-qualified* to bid for balancing power further make it difficult to participate in the balancing energy market [67]. During the minimum four hour timeslot required for bidding, the bidder must guarantee being able to provide the balancing energy. Alternatively, EVs may be incorporated in a virtual power plant (VPP) which may take into account other resources such as renewables energy sources [113]. The complexity of scheduling in a VPP-based approach would grow corresponding to the number of resources.

Related work on contributing balancing power via smart charging includes [41, 61, 115]. For example, EVs may provide positive as well as negative balancing energy in order to balance wind power generation [41]. EVs are assumed to possess V2G capabilities and are able to discharge energy. In contrast, [61] considers the purchase of energy in day-ahead spot markets as well as offering balancing services for power generation via wind power. In other words, the forecast error of wind power is balanced. Lastly, [115] optimizes EV scheduling for day-ahead spot or balancing energy markets to maximize aggregator profits.

2.5 Objectives and constraints

This section discusses the objectives and constraints which we focus on in this work. Figure 2.13 shows an overview of the objectives discussed in this work.

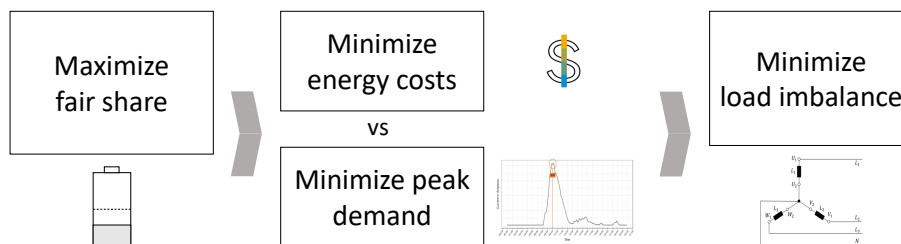


Figure 2.13: Objectives of charge scheduling

Driver satisfaction

In this work we quantify driver satisfaction [29] as maximizing the average SoC over all EVs. Ideally, EV drivers would not notice charge scheduling being applied. In other words, the EV should be fully charged upon departure.

Important factors in maximizing SoC include knowing the EV's model and EV availability. Characteristics of the EV's model include aspects discussed in section 2.2 such as single-phase or three-phase charging, the charging rate and the battery's capacity. The topic of EV availability is addressed in detail in chapter 4 where regression models are trained on historical data to predict an EV's departure time.

In the context of the private charging infrastructure discussed in section 2.1 the goal in this work is to distribute energy as fairly as possible. In other words we maximize fair share. In all of the following chapters, the objective of maximizing average SoC will be considered the most important.

Energy cost minimization

Minimizing energy costs is perhaps the most intuitive objective. EVs should charge when energy is cheap. If a V2G scenario is considered EVs should discharge when energy is expensive. From the perspective of the operator or aggregator profit maximization is also sometimes considered [115] which is more relevant for public charging infrastructures.

Depending on the chosen level of abstraction, energy spot markets can be considered directly and the charge scheduling approach participates in their auction processes as in [60, 126]. In this work, we assume a simplified energy market with a fixed energy price in €/MWh per 15-minute interval.

Peak shaving

Peak shaving is monetary in nature but directly computing costs is not as simple compared to computing energy costs. Usually charge scheduling addresses day-to-day scheduling. However, as discussed in section 2.4.1 the highest load is recorded per period (half a year or a full year). Additionally, the highest peak often depends on other consumers in the electrical network.

Lastly, the objective of peak shaving can be at odds with energy cost minimization. For example, energy cost minimization may dictate all EVs charging during an especially cheap period. However, all EVs charging concurrently would likely lead to a peak. Figure 2.14 shows an example where the two different objectives are followed with charge scheduling using the energy prices in figure 2.12.

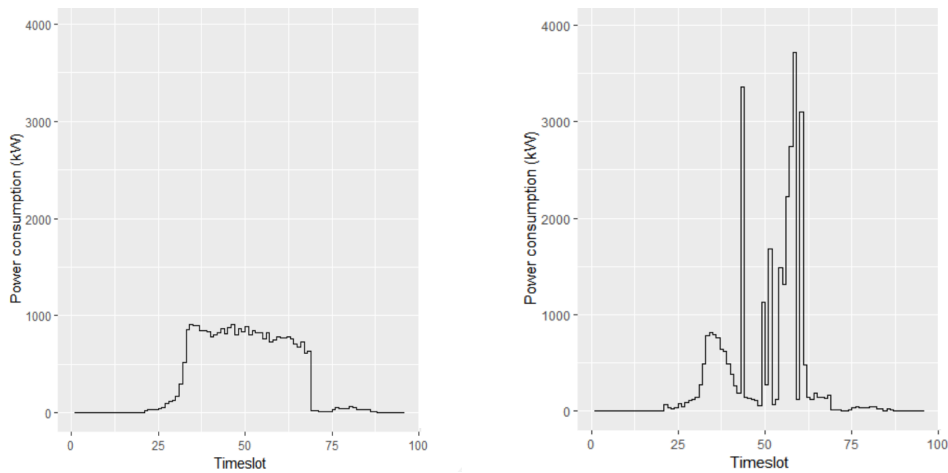


Figure 2.14: Minimizing peak demand vs minimizing energy costs: The same amount of energy is charged in both graphs. The graph on the right shows several peaks but the energy costs are roughly 10% less compared to the left graph

Load imbalance

The topic of load imbalance and how it is caused by EVs is discussed in section 2.3.2. To recap, EVs charging on a single phase can lead to load imbalance. Thus one objective of charge scheduling is to assign single-phase EVs to charging stations such that phase usage is distributed more equally in order to minimize load imbalance.

Constraints

In the following we describe hard constraints in smart charging. To recap, a charging *station* may have multiple charge *points*. Each charge *point* may only be connected to a single EV at any single point in time.

With regard to the EV itself, charge scheduling cannot cause damage to the EV's battery. This is because there is an autonomous entity, the EV's BMS, responsible for protecting the battery. If necessary, in cases such as overheating the BMS will stop or pause the charging process.

However, not correctly modelling the battery can lead to suboptimal charge schedules. For example, a common assumption is that the EV's battery can always charge at full power. Charging profiles such as constant-current, constant-voltage (CCCV) lead to power declining towards the end of the charging process at high SoC. Consequently, if we assign full power to the EV but the EV does not make

full use of the power we produce suboptimal charge plans with a gap between scheduled power and actual power draw. Such suboptimal schedules were observed during the smart charging field test in chapter 7. Taking battery behavior into account in charge scheduling is addressed in detail in chapters 5 and 6.

In contrast to the EV, charge scheduling can cause damage to components of the charging infrastructure such as blowing fuses or overloading the infrastructure. The charging infrastructure must thus be correctly modelled in any charge scheduling approach. EVs must be scheduled such that the infrastructure is not overloaded.

2.6 Related work

2.6.1 Objectives and methods

There is a large body of research on creating optimal schedules for charging EVs. Surveys such as [47, 89, 117, 168] provide a detailed overview of charge scheduling approaches. Related work on smart charging deals with different objectives such as maximizing profit [186], minimizing energy costs [36, 52, 129, 147] assigning EVs to parking spaces [158], mitigating battery aging [161], stabilizing power load [75] or maximizing driver satisfaction [2, 29, 40, 92, 146, 175]. In this work, we concentrate on maximizing state of charge (SoC), one aspect of driver satisfaction, in order to maximize fair share across a fleet of EVs.

Multi-objective charge scheduling approaches focus on the trade-off between optimizing different objectives. For example, in chapter 3 we consider the trade-off between minimizing peak demand and minimizing energy prices as discussed in section 2.5. Typical methods for addressing multi-objective problems include formulating Mixed Integer Programming (MIP) or evolutionary models. For example, [165] considers the objectives of locating and sizing of charging stations as well as minimizing power loss and voltage deviations. [11] analyzes objectives in charge scheduling from the perspective of different stakeholders such as energy providers and customers and their potentially conflicting objectives. For example, customers may want their EVs to charge as soon as possible while the energy provider may want to delay EVs charging in order to improve power quality or to maximize profits. [181] optimizes two contrasting objectives of minimizing costs and minimizing emissions and analyzes Pareto optimal solutions. Solutions are created by a nonlinear MIP model converted to a linear version. Similarly, [176] minimizes investment costs, energy losses and maximizes charging station profits but uses evolutionary algorithms (instead of a MIP) and analyzes the Pareto frontier. [75] minimizes peak demand by applying peak shaving together with valley filling and minimizes economic loss. Several variations of evolutionary algorithms are implemented and compared. [57] minimizes the two different objectives of EV

charging costs and load variance. Lastly, [150] proposes a day-ahead scheduling method based on a MIP model to hold a minimum reserve together with minimizing EV charging costs.

With regard to multiple objectives we additionally consider secondary objectives in chapter 3. We focus on the four objectives of maximizing fair share, minimizing energy prices, minimizing peak demand and minimizing load imbalance. To this end and similar to related work we also analyze pairwise Pareto fronts and Pareto optimal solutions.

Methods for smart charging include queuing theory [184], game theory [103, 138], evolutionary algorithms [75], model predictive control [36, 147] and scheduling techniques from traditional operations research such as MIP [52, 129] and a nonlinear variation [132]. We refer to [168] for a survey of smart charging from an algorithmic perspective. In this work we use a MIP together with a heuristic algorithm to compute schedules for smart charging (chapter 3). We later use other methods such as regression models (chapters 4 and 6) to improve the heuristic algorithm.

2.6.2 Scenario

Smart charging is often considered in a micro smart grid [47] such as at the workplace on company premises [53, 72, 171]. For example, [72] forecasts available curtailment power and takes into account aggregated building loads to control EV charging with the goal of minimizing peak load. Similarly, [171] optimizes usage of photovoltaic systems and EV charging to reduce energy costs. An artificial neural network is used as a regression model to forecast base load power consumption. Furthermore, [53] analyzes the impact of providing employees with incentives to charge at home as well as at the workplace. Lastly, [8] combines the control of wind power generators and EV charging for micro grid primary frequency regulation. We focus on the workplace which is characterized by EVs with routine arrivals and departures.

Smart charging approaches can be categorized into either centralized or decentralized approaches [47]. In centralized approaches, an entity such as the aggregator or system operator computes and distributes charge schedules. In decentralized approaches, charging stations may act autonomously or cooperatively with other charging stations. A typical way of modelling decentralized approaches is by using multi-agent systems. Compared to centralized approaches, decentralized approaches have a lower communication burden. However, centralized approaches allow for a more holistic view including energy prices or other additional information, allowing a more optimal use of the charging infrastructure [47]. This work focuses on centralized approaches to charge scheduling.

2.6.3 Time of planning

There is extensive literature proposing methods for *day-ahead* or *offline* planning [22, 27, 31, 34, 101, 103, 104, 116, 187, 189] while considering different objectives. To begin with, [27] considers a scenario where EVs and buildings share a common electric infrastructure such as the transformer. In scenarios with a shared infrastructure consumers which may not be as flexible as EVs must be taken into account in order to avoid overloading the infrastructure. [103] formulates a quadratic programming model using game theory to model how energy prices in the spot markets and EVs charging influence each other. [116] focuses on security aspects in smart charging and minimizes security risks such as malware spread between EVs and charging stations through vehicle-to-charging station assignment. Lastly, [104] proposes a MIP model to minimize possible congestion in a distribution network with a high penetration of EVs. Typically, such day-ahead approaches schedule EV charging well in advance and do not take into account input data collection, data reliability, computation time or the practical applicability of schedules.

Real-time planning approaches [2, 8, 14, 32, 48, 53, 65, 101, 114, 130, 146, 157, 166, 167, 179, 183] dynamically create EV schedules. The problem formulation is equivalent to coordinated EV charging. However, additional considerations such as computation time must be taken into account. A typical approach is to utilize queues based on a priority function to decide which EVs may load. Priority may be based on maximizing battery state of charge (SoC) [2], reducing load imbalance [32], reducing consumption peaks [101, 130, 183] or maximizing profit [179]. [157] considers two binary programs. First, a daily load profile is created based on a linear program. Second, the number of pauses in each EV's charging process is minimized. The EV's charging power is modelled as a discrete variable. [146] uses an EV charging queue to minimize system operating costs and maximize driver satisfaction. [166] considers a V2G scenario and schedules EVs to smooth power fluctuations by charging or discharging when needed. Additionally, spatial constraints are modelled to take into account range anxiety of EV drivers. Similarly, [65] schedules EVs to improve power quality by offering voltage support.

Hybrid approaches take into account both times of planning. For example, [146] proposes an approach for smart charging by combining an approach for predicting the number of EVs in future with a two-stage optimization model for real-time smart charging. [65] considers a V2G scenario and proposes a real-time control approach together with an hours-ahead scheduling scheme. [64] presents a two-stage approach. The first stage is a stochastic approach to renewable energies to support energy trading ahead of time. The second stage is a Model Predictive Con-

trol (MPC) strategy for EV scheduling in real-time. [105] describes a day-ahead EV scheduling approach for energy procurement. Real-time charging decisions are then made via an MPC-based approach.

In this work, we use a MIP model for day-ahead planning (chapter 3). Similar to [2, 32, 130, 179] we use a real-time heuristic based on a priority function for charge scheduling in real-time. The heuristic is designed to adapt schedules computed by the MIP model to changing circumstances in real time.

2.6.4 Uncertainty

A subset of day-ahead approaches address the problem of *uncertainty* [22, 101, 189]. Typical uncertainties in charge scheduling include EV availability for charging and energy prices. For example, [101] uses stochastic linear programming to propose a model to minimize peak demand. Instead of modelling EV availability as a stochastic variable, [189] considers deadlines as hard constraints in order to minimize energy prices. In a more deterministic charging scenario, [22] minimizes the time spent charging for battery electric vehicles (BEVs) that are used for deliveries and may only charge at predefined charging stations.

Another focus in smart charging is addressing EVs as the cause of uncertainty [5, 59, 70, 72, 73, 98, 119, 127, 172]. Uncertain factors include the time intervals in which EVs are available for charging and their SoC upon arrival. In practice, accessing EV SoC is currently uncertain due to incomplete implementations of standard protocols for vehicle-to-grid communication [72]. In this work, we assume the SoC upon arrival is known and in the following discuss only the uncertainty in EV availability. One obvious approach to avoid uncertain availability is to guarantee EVs a charging slot by reservations [5, 73] which may in practice be influenced by driver reliability or misuse.

Alternatively, uncertainty can be addressed by predicting EV arrivals and departures [59, 70, 98, 127, 172]. One approach to predicting EV availability is to first estimate and then sample from a probability distribution. For example, [98] estimates a Poisson distribution from a historical dataset. Samples are used as predictions which act as input for an optimization approach using MPC for scheduling. A more complex approach [59] predicts the first daily departure time using a time-series based forecasting technique. Their conclusions include that modelling departure time with a theoretical probability distribution alone does not yield good predictions.

A more sophisticated prediction method relies on regression models. A support vector machine (SVM) was trained in [172] using historical data to predict arrival and departure times of EVs on a university campus. Alternatively, an artificial neural network (ANN) was used in [127] to predict daily arrival time and travel

distance which in turn allows forecasting load throughout the day. An ANN was also trained on historical data including arrival time and departure time in [70] to improve grid usage by aggregators.

In chapter 4 we predict individual EV departure times within the fleet using regression models trained on historical data similar to related work [70, 127, 172]. Predictions are used as input for our charge scheduling approach. In contrast to references [70, 127, 172] we train and compare multiple regression models for EV departure time prediction.

Studies [70, 127, 172] focus on the topic of EV departure prediction. However, there is a lack of work on integrating the predicted departure time in smart charging as well as quantifying the relation between prediction accuracy and scheduling quality. In other words: By how much can smart charging be improved if a more accurate departure time prediction was used? Chapter 4 presents an approach to bridging this literature gap by training different regression models that have varying levels of accuracy and by evaluating their predictions during smart charging.

2.6.5 Battery models

Charge scheduling models can have nonlinear aspects, for example in objective functions or constraints [89]. Such models implicitly or explicitly contain a battery model, which in itself can be linear or nonlinear. The battery model determines how accurately battery charging is reflected.

The simplest battery model assumes a constant charging power. Simplifying the battery model allows considering charge scheduling models which focus on other complex aspects such as nonlinear power systems [68], minimizing costs incurred through battery aging [161] or taking into account renewable energy sources [175].

More complex battery models assume a continuous function to express decreasing power over time or over SoC. For example, a linear approximation of power as a function of SoC has been used to maximize profit at fast charging stations [88]. Similarly, an exponential function to approximate SoC as a function of time was used to create a heuristic to minimize energy costs [20]. This particular function has been used in other works such as [44] to evaluate the difference in charge scheduling between considering battery power as constant and as decreasing.

Battery models with piecewise defined functions allow a closer approximation of the two distinct phases of constant-power, constant-voltage (CPCV) charging. For example, the charge scheduling approach in [129] uses a piecewise linear function. Similarly, [159] defines a piecewise exponential function to approximate battery power as a function of time.

In battery research, a standard approach to creating battery models is to use an equivalent circuit model (ECM) [56]. The ECM can be described using differential equations and simulated with a discrete time formulation [133]. There is related work on charge scheduling that makes use of this approach, for example using MPC to minimize energy costs for smart charging [36, 66]. An ECM is used to simulate a battery charging with CPCV but the model is only used during simulation, not in the control model. Similarly, [147] uses MPC in combination with a discrete time formulation of SoC for minimizing energy costs. However, power available to charge batteries is assumed constant instead of as a function of SoC. Works using ECMs and considering charge scheduling for single battery cells or packs to maximize battery life include [100, 108, 151].

Survey [168] lists the assumption that battery charging is linear and independent of SoC as one of the main areas for future work in smart charging. However, in battery research, accurately modelling and simulating battery charging profiles such as CPCV is standard practice [133, 160]. There is a lack of cross-discipline work on charge scheduling for EV fleets which contain an accurate battery model that reflects a charging profile. This work describes an approach to bridging this gap between disciplines (chapter 5).

Next to ECMs, another type of traditional battery models are physical models [133]. Physical models are more accurate compared to ECMs but are also more expensive computationally and thus unsuitable to apply in real-time [123]. Machine learning (ML) models present a recent development to predicting battery behavior [38, 110]. We refer to a recent survey [123] for an overview of the state of the art for predicting battery behavior based on internal EV battery data such as voltage, current and battery pack configuration.

One difficulty of using a detailed battery model in smart charging for EV fleets lies in the model's parameterization. The parameterization is limited in practice by data availability on operational conditions such as temperature and state of health. Additionally, the EV's battery management system (BMS) controls the selection of the charging profile [100]. From the perspective of the charge point operator (CPO) such battery models are even more difficult to apply for heterogeneous fleets. Different EVs each require one set of model parameters.

There is a lack of related work in smart charging which takes into account EV charging behavior while also ensuring the practicality of the approach. To address the literature gap, in this work we describe an approach without knowledge of detailed battery model parameters. We use a data-driven approach with machine learning models trained on historical time series data of EV charging processes. The historical data was gathered by the CPO thus ensuring the applicability of the approach in practice.

2.6.6 Forecasting

In the domain of smart charging, forecasts can be combined with EV scheduling to improve resource utilization. Typical forecasts address uncertainties involving renewable energy sources, conventional electrical loads and charging demands of EVs [163, 164, 171, 178]. Smart charging can be supported by forecasting renewable energy sources, conventional electrical loads and charging demands of EVs [6, 10, 85, 127, 163, 164, 170, 171, 173, 182]. Forecasting is commonly implemented with a regression model trained on historical data to predict future data. Such regression models may in turn be directly used to support scheduling EV charging [163, 164, 171].

For example, EV charging serves as a controllable load in the context of renewable energy production and can be used to increase self-consumption [163] as well as to compensate forecast errors [164, 178]. Typical problems considered include increasing photovoltaic (PV) self-consumption [163] or compensating day-ahead renewable energy forecast errors by adapting EV schedules [164, 178]. Charge scheduling has been used to compensate forecast errors of a wind power plant [164] with a tradeoff between EV charging flexibility and energy cost minimization. A different approach schedules EV charging as one of multiple controllable loads to address uncertainty in renewable energy forecasts [178]. A forecast of EV velocity has been used to improve fuel economy [182].

Predicting the charging demand of a fleet of EVs without detailed battery knowledge is a well studied problem. For example, a fleet of EVs is simulated based on three different static charging profiles in [136]. EVs are assumed to arrive according to a probability distribution of arrival and departure times. An artificial neural network (ANN) is used in [127] to predict daily arrival time and travel distance to allow forecasting load. Data on traffic patterns is used to forecast power demand of a fleet of EVs [9]. Lastly, [42] uses a support vector machine (SVM) to predict building power load while taking into account an EV fleet.

More granular approaches predict the charging demand of individual EVs. GPS data from 76 (conventional) vehicles is used in [10] to simulate plug-in hybrid electric vehicle (PHEV) charging processes. A constant battery size (24kWh) and charging rate (3.7kW) is assumed. Similarly, an ANN is used in [120] to predict individual charging profiles. The ANN is trained on data generated by a stochastic random process. In contrast to considering charge profiles, there is also work on predicting individual EV energy consumption during driving [177, 188]. However, we focus on EV charging profiles. In chapter 6 we use regression models trained on real data to predict individual charging profiles while taking into account EV specific characteristics.

An obvious approach to predicting EV charge profiles would be to use tradi-

tional time series models for forecasting. Traditional time series models for forecasting univariate time series include *Auto Regressive Moving Average* (ARMA) and *Auto Regressive Integrated Moving Average* (ARIMA) [19]. For example, [6] uses an ARIMA model for forecasting the load demand of a parking lot. A fleet of heterogeneous EVs is considered with a discrete set of constant charging rates. Forecasts are then used in day-ahead scheduling. Furthermore, [58] uses an ARMA model to predict PV generation. The ARMA model is combined with an EV scheduling approach. Lastly, charging process time series from 20 real charging stations are divided into fragments which are clustered using the Euclidean distance measure in [109]. Future energy consumption for a given fragment is predicted using the most similar existing fragment via k-nearest neighbours.

In this work, time series forecasting would be of interest for predicting individual EV charge profiles. However, the integration of time series forecasting with real-time smart charging is conceptually problematic because charge plans influence the course of each time series. Instead of time series forecasting we predict individual EV power in relation to SoC.

2.6.7 Data-driven approaches

Related work on data-driven approaches in the context of electric mobility typically makes use of private datasets consisting of aggregated information on charging processes. For example, the statistics of 400.000 charging processes in the Netherlands are described in [51]. A dataset consisting of 21.918 charging processes in 2012-2013 from 255 different charging stations in the UK is analyzed in [174]. The dataset is combined with weather data to characterize the load demand of a fleet of EVs. Similarly, 8.929 processes from 2014-2016 are analyzed in [33]. Compared to other work in this category, the timestamp of reaching full SoC is included. The popularity of EV charging infrastructure is predicted in [156] based on geographic information system (GIS) data. A large dataset of 500.000 charging processes and 2.000 charging stations in the USA from 2013 is used to estimate the benefits of smart charging in [76]. Charging profiles are considered as static profiles depending on temperature in [177]. The profiles are computed based on 8.300 EVs in 2011-2013. Lastly, [97] uses GPS and trip meter data of 490 PEV taxis in 2013 to simulate charging profiles. In [97], a single EV model (75kWh) is modelled to charge using constant-power at 22kW up to 80% SoC even though a two-stage charging profile is mentioned.

In this work and in contrast to the references above we use a historical dataset which includes charging process data over time. The data-driven approaches above each use a dataset which includes only aggregated attributes such as energy (Wh), average power (W) or maximum power (W) and lack the accompanying time-series

of power over time. Due to the more granular dataset used in this work we are able to take into account arbitrary charging profiles.

Public historical datasets in the domain of electric mobility lack the required granularity and diversity required for training machine learning models to predict charging profiles. Basic datasets include charging station locations for use in navigation such as [71].

Charging process data is available in datasets such as [111] and typically includes information such as the total energy charged (Wh) and the duration of the process. Time series data (power over time) is not included.

More granular charging process data includes the accompanying time series. For example, [119] provides a dataset which contains simulated time series of charging currents for homogeneous EVs based on household energy consumption from 2009. A large dataset containing 4 million charging processes from 8.300 EVs in 2011-2013 is analyzed in [149,177]. The data includes 6 different car models such as the Nissan Leaf and the Toyota Prius. However, the dataset includes a limited number of sample charging process time series (19) without SoC and is therefore not suitable for training machine learning models. A more comprehensive dataset is discussed in [94]. The data is a result of applying a smart charging approach [93] in a real charging infrastructure. The dataset contains over 30.000 charging processes and time series with charge schedules and the resulting charging current. However, the dataset does not include SoC over time and the EV's model. In this work, we make use of a charging process dataset containing EV models and the accompanying time series data (chapter 6).

2.6.8 Related projects

In the following, we first discuss related open source smart charging projects.

The Adaptive Charging Network (ACN) portal used in [94] is an open source project¹ containing an interface to a dataset of EV charging processes. The EV charging processes are controlled by a smart charging algorithm. However, the source code of the actual algorithm used to gather the dataset is not published.

EVLlib² is a library for the management and the simulation of EV charging events [77]. A simple queue-based algorithm is provided for smart charging. However, EVLib is missing many of the electrical engineering constraints found in practice, namely complex charging infrastructures with hierarchical levels of fuses and the three phases of the electrical grid.

The goal in [37] is to minimize peak consumption and CO_2 emissions³. A

¹<https://github.com/zach401/acnportal>

²<https://github.com/skarapost/EVLlib>

³<https://github.com/bukhsh/Smart-EV-Charging>

heuristic for valley filling is used to schedule EVs to charge during times of low energy consumption in the grid. Next, [91] contains a simulation for EVs and implements different algorithms such as voltage management or time-of-use (TOU) scheduling⁴. Other examples include a constraint modelling approach⁵ as well as genetic optimization and EV prioritization⁶ for smart charging.

Chapter 7 presents an open source package containing a charge scheduling heuristic for EV fleets. The charge scheduling heuristic is a heuristic approach with the goal of maximizing SoC across the fleet. In contrast to the open source projects described above, we present a well documented open source package designed to be usable out of the box.

Note that the term *smart charging* is not always well defined and is used to refer to different concepts depending on context. For example, the smart charging approach in [4] simulates EV charging demand based on changing inputs such as renewable energy production⁷. Furthermore, [99] maintains a system for price optimization for a single EV. A semantic web approach⁸ to describing smart charging inputs and outputs is published in [95]. SmartEVSE⁹ maintains open source firmware for the charging station to allow communication with the EV and the charging current to be controlled [155]. In this work, we refer to smart charging as scheduling a fleet of EVs for charging while pursuing one or more optimization objectives.

Next, we discuss related research projects.

To begin with, *Integration of renewable energies and e-mobility* (IRENE) [148] included practical experiments such as integrating a 150 kWh battery into an existing electrical system to improve power quality. Similar to the physical experimental setup in chapter 7, power draw was monitored as a safeguard against scheduling errors or EVs drawing more than scheduled. Key outcomes include the necessity of real-time measurements to control the smart grid.

Next, *green eMotion* [46] integrated developments from research on a smart grid for the European market for electromobility. The project involved data collection and analysis across European countries with a focus on user acceptance.

iZEUS [144] created a platform for electric mobility services including routing and reservations of EVs. The platform includes decentralized energy management, fleet management and the management of interoperable charging infrastructure.

MeRegioMobil [78] used battery storage systems in vehicles in existing electri-

⁴<https://github.com/regeork/smart-charging>

⁵<https://github.com/SheperoMah/ElectricVehiclesSmartCharging>

⁶<https://github.com/jdong28/SmartChargerAlgorithm>

⁷<https://github.com/mjulian55/SmartCharge>

⁸<https://github.com/thSMARTenergy/CNR-SmartChargingProvider>

⁹<https://github.com/SmartEVSE/smartevse>

cal networks such as a smart home in order to use surplus energy from renewable energy sources. From a technical perspective, a draft version of ISO 15118 was used to control smart charging [118].

NOBEL [79] created concepts for a set of decentralized energy services such as monitoring and trading in a smart grid neighborhood. So-called "prosumers" are entities capable of consuming as well as producing energy. Similar to the charge scheduling in chapter 7 [79] proposes a concept for an energy optimization service to produce load profiles with a set of constraints and multiple objectives.

Open ECOSPhERE [49] focused on the integration of EVs and renewable energies. The main goals were to improve the sustainability and reliability of electric mobility through services such as the ability to reserve charging stations. Similarly, in *TRADE EVs* a system of reservations via OCPP was also trialed.

Smarthouse/SmartGrid [87] proposes the infrastructure for energy monitoring and the local control of energy in a smart house in combination with a smart grid infrastructure. A decentralized system consisting of multiple consumers and producers is created.

Chapter 7 includes the discussion of a one-year field test. The physical experimental setup for the field test was a component of the research project *TRADE EVs* which lies in the German government funding program ELEKTRO POWER II [18]. The overall goals in the program are to reduce costs across the supply chain of EVs, to integrate EVs in existing energy systems and to make recommendations with regard to norms and standards. The analyzed norms and standards include inductive charging systems or enabling bidirectional charging to implement vehicle-to-grid (V2G). The project *TRADE EVs* focused on validation of a smart charging approach with a physical experimental setup in the context of external energy systems such as energy markets.

In conclusion, the source code used for most related work on smart charging is not published. Unpublished source code makes it difficult to reproduce experimental results and is a prohibitive barrier for CPOs to implementing smart charging approaches in practice. In this work, we present an open source package for smart charging EV fleets. In contrast to related work which typically relies on simulations we additionally validated our approach in a one-year field test with a real charging infrastructure.

Chapter 3

Day-ahead and real-time charge scheduling

3.1 Introduction

As described in section 2.1 charge scheduling approaches are considered in different contexts with regard to the time of planning. To recap, in day-ahead (or offline) planning we schedule EVs in advance while in real-time (or online) planning we schedule EVs as they arrive.

In practice, day-ahead planning requires some type of data collection. Most importantly data collection includes EV availability: Which EV will be available to charge when? In our scenario, EV availability is not known in advance. The EV drivers themselves often do not know exactly when they will depart the workplace. In this chapter we assume we know EV availability. This assumption is later relaxed: We discuss how finding a value for each EV's departure time may be implemented in chapter 4. We assume the charging infrastructure is not modified regularly and that changes are known.

In contrast to day-ahead planning, real-time planning deals with a different set of constraints. Data such as EV models and SoC is available. However, computation time becomes more relevant, especially when considering how often to reoptimize. In a practical setting, latency to send charge schedules to charging stations must also be taken into account.

In day-ahead as well as real-time planning we take into account electrical engineering constraints. One of the most important constraints not taken into account in related work is a phase-wise power assignment. As described in section 2.2.5, EVs typically charge only on the first phase or on all three phases. A scheduling system not taking into account such electrical engineering constraints require additional

post processing to be usable in practice.

In this chapter, the following research question is discussed:

How can EV charging be coordinated in a three-phase charging infrastructure during different times of planning?

In the following we present an approach to real-time smart charging by combining day-ahead planning with real-time coordination. The approach and results in this chapter are based on [52]. The main contributions in the following chapter are:

- We consider electrical engineering constraints of the installed infrastructure such as phase-wise power assignment directly in a MIP model,
- we adapt charging schedules in real-time based on a queue with a priority function and
- we combine four objective function components: maximize fair share (comparable to social welfare), minimize energy costs, minimize peak demand and minimize load imbalance.

This chapter is structured as follows. First, the MIP model for day-ahead planning and the schedule guided heuristic for real-time planning are described in section 3.2. The experimental setup using simulation for evaluation is introduced in section 3.3. Results and the overall approach are discussed in sections 3.4 and 3.5. Section 3.6 concludes the chapter.

3.2 Method

This section describes the methods proposed in [52]. First, we use a MIP model for day-ahead planning. We do not use it in real-time because of high computation time. Second, we adapt precomputed schedules from the MIP model in real-time using a schedule guided heuristic. The overall process of combining day-ahead and real-time planning is shown in figure 3.1.

3.2.1 A MIP model for day-ahead planning

Smart charging can be seen as a multiple-machine, partially preemptive scheduling problem with due dates and flexible processing times. Scheduling problems are often addressed using linear programming (LP) or mixed integer linear programming (MIP) [135]. We require binary or integers variables to model the problem

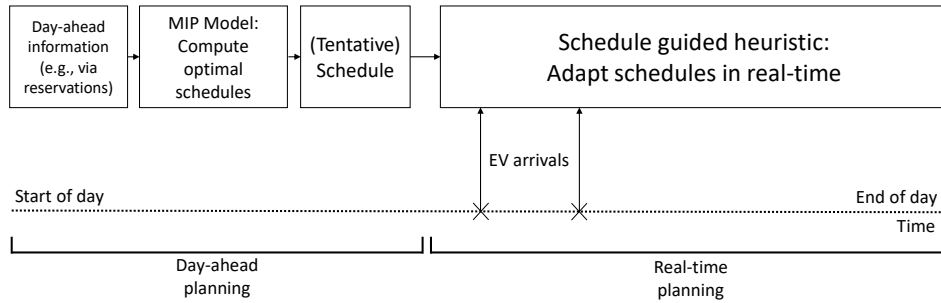


Figure 3.1: Combination of day-ahead and real-time charge scheduling

and thus in the following describe a MIP for smart charging. For example, an intuitive binary variable is to model the fact that only one EV may be assigned to each charging station. This results in a set of combinatorial binary variables consisting of all possible assignments of an EV to a charging station.

The MIP model described in this chapter resembles the charge scheduling problem [31] with N EVs, where each EV n represents a charging job which is to be scheduled on one of i charging stations, during k timeslots. The exact number of cars, charging stations and fuse sizes are variable parameters for later simulations.

In contrast to related work we regard electrical engineering constraints such as phase-wise power assignment. Resulting schedules can thus be directly applied without post processing thus avoiding loss of optimality.

In the charge scheduling problem EVs with their individual charging needs compete for limited resources expressed as power line capacities restricted by installed fuses. In the following MIP model we use an objective function that is a weighted linear combination of the four components described in section 2.5 and Table 3.1.

In contrast to related work on the charge scheduling problem [26, 31, 34, 143] this work adds flexibility of the optimization goals via the weighted objective function. In business contexts where the installed charging infrastructure tends to be the limiting factor the fair share between EVs can be weighted highest. In this work, we use fair share to decide which EVs should be prioritized. The goal is that each EV should receive at least a minimum state of charge (b'_n) before any EV is charged to full SoC.

Furthermore, this work considers detailed electrical engineering constraints in order to compute a feasible solution which can be directly applied in real life. Engineering constraints include the multi-level, hierarchical fuse trees discussed in section 2.3. Additionally, the model reflects car model dependent charging behavior, including for example whether charging processes may be suspended, are

Component	Description
Maximize fair share	Maximize fraction of minimum SoC and capture inequalities between individual EVs' final states of charge
Minimize energy costs	Minimize charging price (in €/Mwh) per 15-minute timeslot according to intraday market prices
Minimize peak demand	Minimize peak demand which represents the system usage fees and are determined by the highest consumption peak
Minimize load imbalance	Minimize impact of single-phase EVs and capture unbalanced electricity consumption between the three phases

Table 3.1: Objective function components for charge scheduling

delayable and allow variable current. Not being able to suspend charging means if the current is set to 0A during a charging process, the EV will not resume charging even if the permissible current is increased again later on. Non-delayable EVs require a current greater than 0A immediately after the start of the charging process. EVs that do not allow variable current require the same current throughout the charging process.

The engineering point of view also adds the phase dimension where fuse limits per phase and phase rotations in the installed charging stations are considered. Overall the engineering details increase the set of constraints significantly.

An overview of the variables can be found in the nomenclature in section A.1. In the MIP model the main decision variables are assignment variables $X_{i,n}$ between charging station i and car n and the current $I_{i,j,k}$ at station i during timeslot k per phase j . In this work we discretize time into intervals k of 15 minutes length corresponding to intraday market timeslots.

Binary auxiliary variables are used with the big-M [83] modelling method ($M = 10^5$) to express relationships such as phase ratios, delayable and suspendable charging and the capability to increase or decrease charging power over time. The big-M method is typically implemented by one or more constraints to control binary variables. Such modelling techniques avoid nonlinearity and thus significant complexity in the MIP model.

Objective function. The objective function (3.1) of the MIP model is the cost minimization of a weighted combination of penalty costs for fair share z_1 (3.2), electricity costs z_2 (3.3) and penalty costs for peak shaving z_3 (3.4) and load im-

balance z_4 (3.5) with weights $w_1 - w_4$. Section 3.4 contains a discussion of how weights are chosen. Furthermore, each objective function component z_1 - z_4 is normalized by coefficients c'_1 - c'_4 that cancel out the unit of measure and scale the individual components to interval $[0, 1]$. Table 3.1 shows an overview of the objective function components.

$$\min : z = w_1 * z_1 + w_2 * z_2 + w_3 * z_3 + w_4 * z_4 \quad (3.1)$$

$$z_1 = c'_1 * \sum_n (Q'_{n,below} + c * Q'_{n,above}) \quad (3.2)$$

$$z_2 = c'_2 * \sum_i \sum_j \sum_k 0.25 * c_k * I_{i,j,k} \quad (3.3)$$

$$z_3 = c'_3 * \sum_k (E_k^+ + E_k^-) \quad (3.4)$$

$$z_4 = c'_4 * \sum_k ((D_{k,1,2}^+ + D_{k,1,2}^-) + (D_{k,2,3}^+ + D_{k,2,3}^-) + (D_{k,1,3}^+ + D_{k,1,3}^-)) \quad (3.5)$$

Objective function fair share component. For the calculation of fair share penalty costs in (3.2) the utility variable $Q'_{n,below}$ represents the fraction of the minimum SoC that car n lacks. $Q'_{n,above}$ is the equivalent to express the SoC gap between the minimum SoC and the full SoC. Weight $c = 0.1$ is chosen in (3.2) to express that it is considered 10 times as important to fill EVs to their minimum SoC compared to full SoC. Figure 3.2 illustrates the computation of $Q'_{n,below}$ and $Q'_{n,above}$ for two examples with different states of charge.

For the formal computation of $Q'_{n,below}$ and $Q'_{n,above}$ further utility variables $Q_{i,k,n}$ and $U_{k,n}$ are introduced with lower and upper bounds as follows. $Q_{i,k,n}$ (in ampere hours) aggregates the previously charged currents $I_{i,j,k}$ (3.6)-(3.9). The coefficients in the aggregation (3.6)-(3.7) include charging efficiency w_n and EV availability $d_{k,n}$ as well as the scalar 0.25 to convert the momentary current to electric charge during 15-minute timeslots. The big-M method ($M = 10^5$) is applied to ensure the aggregation is applied only when EV n is assigned to station i ($X_{i,n} = 0$) and that $Q_{i,k,n} = 0$ otherwise.

$$Q_{i,k',n} \geq \sum_j \sum_{k < k'} 0.25 * w_n * d_{k,n} * I_{i,j,k} - M * (1 - X_{i,n}) \quad (3.6)$$

$$Q_{i,k',n} \leq \sum_j \sum_{k < k'} 0.25 * w_n * d_{k,n} * I_{i,j,k} + M * (1 - X_{i,n}) \quad (3.7)$$

$$Q_{i,k,n} \leq M * X_{i,n} \quad (3.8)$$

$$Q_{i,k,n} \geq -M * X_{i,n} \quad (3.9)$$

The binary utility variables $U_{k,n}$ and $U'_{k,n}$ as defined in (3.10)-(3.13) rely on $Q_{i,k,n}$ and express whether car n needs further charging at timeslot k to reach its full SoC and its minimum SoC respectively. Constraints (3.10)-(3.11) enforce that $U_{k,n} = 0$ if and only if the EV has reached its full SoC. Similarly, (3.12)-(3.13) enforce that $U'_{k,n} = 0$ if and only if the EV has reached its minimum SoC.

$$U_{k,n} \geq \frac{b_n - (\sum_i Q_{i,k,n} + b''_n)}{b_n} \quad (3.10)$$

$$U_{k,n} \leq \frac{b_n - (\sum_i Q_{i,k,n} + b''_n)}{b_n} + 0.9 \quad (3.11)$$

$$U'_{k,n} \geq \frac{b'_n - (\sum_i Q_{i,k,n} + b''_n)}{b'_n} \quad (3.12)$$

$$M * U'_{k,n} \leq \frac{b'_n - (\sum_i Q_{i,k,n} + b''_n)}{b'_n} + M \quad (3.13)$$

Finally, the fair share utility variables $Q'_{n,below}$ and $Q'_{n,above}$ rely on utility variables $Q_{i,k,n}$ and $U'_{k,n}$ to express the fractions of SoC that are missing with respect to reaching the minimum SoC (3.14) and the full SoC (3.15) respectively. When an EV has not even reached its minimum SoC ($U'_{k,n} = 1$) then (3.16) forces $Q'_{n,above}$ to value 1.

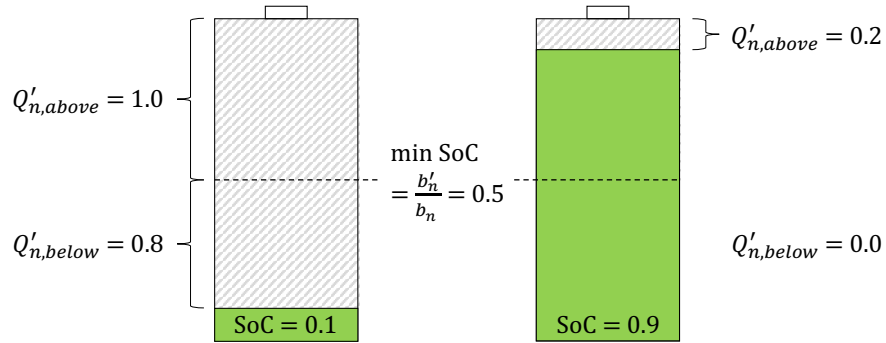


Figure 3.2: Two examples for calculation of $Q'_{n,below}$ and $Q'_{n,above}$ with $SoC = 0.1$ and $SoC = 0.9$ respectively

$$Q'_{n,below} \geq 1 - \left(\frac{\sum_i Q_{i,k,n} + b'_n}{b'_n} + M * (1 - U'_{k,n}) \right) \quad (3.14)$$

$$Q'_{n,above} \geq 1 - \left(\frac{\sum_i Q_{i,k,n} + b''_n - b'_n}{b_n - b'_n} + M * U'_{k,n} \right) \quad (3.15)$$

$$Q'_{n,above} \geq 1 - M * (1 - U'_{k,n}) \quad (3.16)$$

Normalizing coefficient c'_1 (3.17) is an upper bound for z_1 which assumes all N EVs are fully discharged.

$$c'_1 = \frac{1}{(1 + c) * N} \quad (3.17)$$

Objective function energy cost component. The minimization of direct energy costs is expressed by z_2 in (3.3). A fixed energy price c_k is assumed for each timeslot k . The charging current during the timeslot is converted into an electric charge value by multiplying it with the fixed timeslot duration of 15 minutes or 0.25 hours.

Normalizing coefficient c'_2 (3.18) is an upper bound for z_2 which assumes all charging needs are satisfied using the most expensive energy price. Its unit is $[\frac{1}{\text{€}}]$.

$$c'_2 = \sum_n \frac{w_n}{(b''_n - b_n) * 230V * \max_k c_k} \quad (3.18)$$

Objective function peak shaving component. For the minimization of peak shaving we utilize the relationship that power peaks are caused by a change of total charging currents between adjacent timeslots. For this purpose, we introduce z_3 in (3.4) as penalty costs for changing currents.

Peaks can be indicated by either increasing or by decreasing currents between timeslots. The absolute value of the difference is captured by using non-negative utility variables E^+ and E^- as defined in (3.19). This construct is a linear modelling technique and minimizing both E^+ and E^- in the objective function guarantees one of the two variables to be positive (or 0) and the other 0.

$$E_k^+ - E_k^- = \sum_{i,j} (I_{i,j,k} - I_{i,j,k+1}) \quad (3.19)$$

Normalizing coefficient c'_3 (3.20) is an upper bound for z_3 which assumes each EV alternately charges with full current $f_{j,n}$ and 0A. Its unit is $[\frac{1}{A}]$.

$$c'_3 = \frac{1}{\sum_j \sum_n a_{j,n} * f_{j,n} * (\sum_k d_{k,n})} \quad (3.20)$$

Objective function load imbalance component. The load imbalance z_4 in (3.5) is captured by the pairwise difference between each of the three phases. $PhaseMap(i, j)$ is an auxiliary index mapper function which converts the installed phase rotations back to the externally connected phases. For example, for the rightmost charging station in figure 2.10 $PhaseMap(i, 1) = 3$ and $PhaseMap(i, 2) = 1$.

Utility variables $D_{k,i,i'}^+$ and $D_{k,i,i'}^-$ as defined in (3.21)-(3.23) are used to model with linear variables the absolute value of difference of total current between each pair of phases. In other words, (3.21)-(3.23) define a linearized measure of the load imbalance by approximating (3.51). The linear approximation effectively implements $|I_{i,1,k} - I_{i,2,k}| + |I_{i,2,k} - I_{i,3,k}| + |I_{i,1,k} - I_{i,3,k}|$ in the objective function.

$$\begin{aligned} D_{k,1,2}^+ - D_{k,1,2}^- &= \sum_i I_{i,PhaseMap(i,1),k} \\ &\quad - \sum_i I_{i,PhaseMap(i,2),k} \end{aligned} \quad (3.21)$$

$$\begin{aligned} D_{k,2,3}^+ - D_{k,2,3}^- &= \sum_i I_{i,PhaseMap(i,2),k} \\ &\quad - \sum_i I_{i,PhaseMap(i,3),k} \end{aligned} \quad (3.22)$$

$$\begin{aligned} D_{k,1,3}^+ - D_{k,1,3}^- &= \sum_i I_{i,PhaseMap(i,1),k} \\ &\quad - \sum_i I_{i,PhaseMap(i,3),k} \end{aligned} \quad (3.23)$$

Normalizing coefficient c'_4 (3.24) is an upper bound for z_4 which assumes each EV that does not charge on 3 phases charges with full current over all timeslots. The factor 2 stems from the linear approximation of the load imbalance. Its unit is $[\frac{1}{A}]$.

$$c'_4 = \frac{1}{\sum_n 2 * f_{1,n} * (\sum_k d_{k,n})} \quad (3.24)$$

Constraints. The following paragraph details the constraints of the MIP model. To recap $X_{i,n}$ is the binary decision variable whether EV n is assigned to station i and $I_{i,j,k}$ the current for station i on phase j during timeslot k . Various business and technical parameters affect the model and are assumed to be fixed and known. These parameters include the energy price time series, charging needs, EV availability and current limits per fuse. Depending on the model, EVs charge on one or more phases with a car model dependent ratio between the currents per phase.

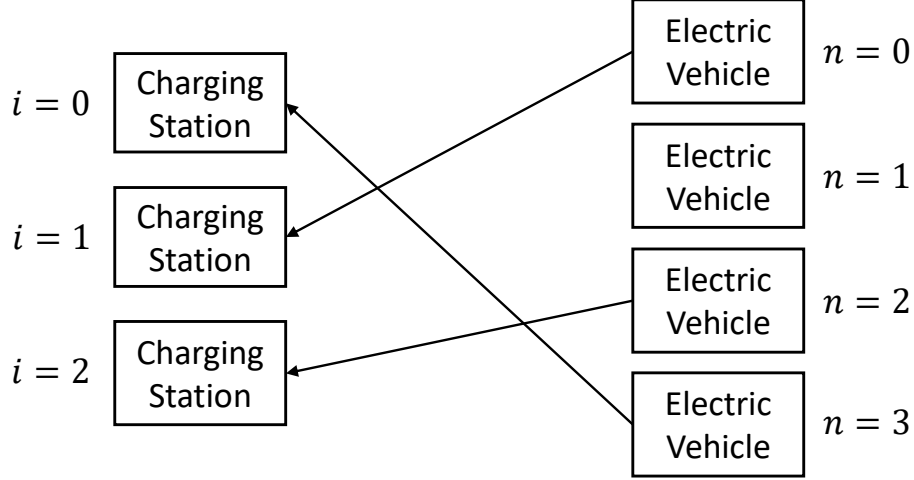


Figure 3.3: Constraint: Assignment of EV n to charging station i . In this image, binary assignment variables $X_{i,n}$ are assigned as $X_{0,3} = X_{1,0} = X_{2,2} = 1$, all other variables X are assigned 0.

Assignment constraints (3.25)-(3.28) ensure orderly assignment of EVs to charging stations. Each EV n may only be assigned to a single station i (3.25). Each station may only be used by a single EV during each timeslot k (3.26). In the given business context, some charging stations i are reserved for BEVs ($o_i'' = 1$) and/or PHEVs ($o_i''' = 1$) exclusively. For each EV n the property whether it is a BEV ($o_n = 1$) or PHEV ($o_n' = 1$) must be considered accordingly in the charging station assignment (3.27)-(3.28). Figure 3.3 shows a sample set of car assignments.

$$\sum_i X_{i,n} \leq 1 \quad (3.25)$$

$$\sum_n X_{i,n} * d_{k,n} \leq 1 \quad (3.26)$$

$$X_{i,n} \leq 1 - o_n + o_i'' \quad (3.27)$$

$$X_{i,n} \leq 1 - o_n' + o_i''' \quad (3.28)$$

Constraints regarding charged quantities (3.29)-(3.31) ensure that each EV charges at most to its capacity b_n while considering the starting capacity b_n'' . As modelled with the big-M technique the constraints (3.29) apply only when EV n is assigned to station i . The charging station assignment $X_{i,n} = 1$ together with the availability $d_{k,n}$ is also the prerequisite for a nonzero charging current $I_{i,j,k}$ in

any interval k (3.30). The same constraints ensure that in all intervals k and for all phases j the charging current cannot exceed the amount $e_{i,j}$ which the fuse at the charging station tolerates. The knapsack-type constraints (3.31) reflect the fuse tree where the sum of the current consumed by children must not overload each parent fuse $h_{l,j}$ for all phases j and the fuses l at all levels of the fuse tree.

$$\sum_{j,k} 0.25 * w_n * d_{k,n} * I_{i,j,k} \leq b_n - b_n'' + M(1 - X_{i,n}) \quad (3.29)$$

$$I_{i,j,k} \leq e_{i,j} * \sum_n (X_{i,n} * d_{k,n}) \quad (3.30)$$

$$\sum_{\text{Child } i \text{ of } h_{l,j}} I_{i,PhaseMap_{i,j,k}} \leq h_{l,j} \quad (3.31)$$

Finally, constraints (3.32)-(3.47) capture car model specific properties and behavior. Some EVs charge using only one phase. When charging on more than one phase then fixed ratios apply for the currents on the individual phases. Constraints (3.32)-(3.35) restrict the phases used and the ratios between them. For example, an EV with $a_{1,n} = 1; a_{2,n} = 1; a_{3,n} = 0$ charges equally on phases 1 and 2. In this case, (3.32), (3.33) give an upper bound and lower bound for the ratio of the first to the second phase. Similar to (3.29) each equation contains a condition modelled by big-M.

$$a_{2,n} * I_{i,1,k} - a_{1,n} * I_{i,2,k} + M * d_{k,n} * X_{i,n} \leq M \quad (3.32)$$

$$a_{2,n} * I_{i,1,k} - a_{1,n} * I_{i,2,k} - M * d_{k,n} * X_{i,n} \geq -M \quad (3.33)$$

$$a_{3,n} * I_{i,1,k} - a_{1,n} * I_{i,3,k} + M * d_{k,n} * X_{i,n} \leq M \quad (3.34)$$

$$a_{3,n} * I_{i,1,k} - a_{1,n} * I_{i,3,k} - M * d_{k,n} * X_{i,n} \geq -M \quad (3.35)$$

Cars have different capabilities regarding the flow of current and for delaying or suspending charging. To capture whether an EV tolerates currents to be changed during charging (3.36)-(3.37) define a lower and upper bound for whether EV n supports a variable current. For each interval $k + 1$ the current $I_{i,j,k+1}$ is restricted to the same value as the current $I_{i,j,k}$ of the previous interval when the EV is available ($d_{k,n} = 1$), assigned ($X_{i,n} = 1$) and not full ($U_{k+1,n} = 1$) and does not support variable charging ($t_n = 0$).

$$I_{i,j,k} \leq I_{i,j,k+1} + M * t_n + M * (1 - d_{k+1,n}) + M * (1 - X_{i,n}) + M * (1 - U_{k+1,n}) \quad (3.36)$$

$$I_{i,j,k} \geq I_{i,j,k+1} - M * t_n - M * (1 - d_{k+1,n}) - M * (1 - X_{i,n}) - M * (1 - U_{k+1,n}) \quad (3.37)$$

Constraint (3.43) captures whether for an EV the flow of current can be suspended during charging. When charging cannot be suspended ($s_n = 0$) then there must be at most one interval k where the car starts charging ($Y_{k,n} = 1$). Binary utility variables $V_{k,n}$ are introduced to reflect whether EV n is charging during interval k or not and are defined by lower bound (3.38) and upper bound (3.39). Binary utility variables $Y_{k,n}$ reflect whether the car starts charging after interval k , namely when it charges during interval $k + 1$ but not during k . $Y_{k,n}$ is defined by lower bound (3.40) and upper bounds (3.41, 3.42).

$$V_{k,n} \geq \frac{I_{i,j,k}}{M} - M * (1 - X_{i,n}) - M * (1 - d_{k,n}) \quad (3.38)$$

$$V_{k,n} \leq I_{i,j,k} + M * (1 - X_{i,n}) + M * (1 - d_{k,n}) \quad (3.39)$$

$$Y_{k,n} \geq V_{k+1,n} - V_{k,n} \quad (3.40)$$

$$Y_{k,n} \leq V_{k+1,n} \quad (3.41)$$

$$Y_{k,n} \leq (1 - V_{k+1,n}) + (1 - V_{k,n}) \quad (3.42)$$

$$\sum_k Y_{k,n} \leq 1 + M * s_n \quad (3.43)$$

Constraints (3.44), (3.45) capture whether an EV n is delayable ($r_n = 1$) or whether it requires current immediately ($r_n = 0$) at the first timeslot $min_k(n)$ where the car is available. For non-delayable EVs, being assigned to a station but not charging at all is also feasible. (3.44) restricts $V_{min_k(n),n}$ if the EV is available ($d_{k,n} = 1$) and assigned $X_{i,n} = 1$. (3.45) further forbids charging during later timeslots if the EV did not start charging in the first available timeslot. The constraint should be applied only for $k > min_k(n)$.

$$V_{min_k(n),n} \geq (1 - r_n) * \frac{\sum_{i,j,k} I_{i,j,k}}{M} - M * (1 - X_{i,n}) - M * (1 - d_{k,n}) \quad (3.44)$$

$$V_{k,n} \leq r_n * V_{min_k(n),n} \quad (3.45)$$

Each EV n has a minimum charging current $g_{j,n}$ (3.46) and maximum charging current $f_{j,n}$ (3.47). The minimum current needs to be considered only for those phases j which the EV n can charge on ($a_{j,n} = 1$) and only when the EV charges at all ($V_{k,n}$) at station i during interval k .

$$I_{i,j,k} \geq g_{j,n} * a_{j,n} * d_{k,n} - M * (1 - X_{i,n}) - M * (1 - V_{k,n}) \quad (3.46)$$

$$I_{i,j,k} \leq f_{j,n} * d_{k,n} * X_{i,n} \quad (3.47)$$

The model complexity leads to a high number of variables and constraints. For example, one real-world instance with 50 cars and 25 charging stations results in roughly 10^5 continuous variables, 10^4 binary variables and 10^6 constraints. In practice this leads to prohibitive computation times for real-time planning when making use of standard MIP solvers such as SCIP [107]. This fact motivates the introduction of heuristics to solve the online charge scheduling problem.

Assigning EVs to charging stations via heuristic (variables $X_{i,n}$)

For day-ahead planning we further combine the MIP model with an assignment heuristic. The heuristic improves computation time by avoiding the combinatorial problem of EV-to-station assignment. The assignment heuristic fixes charging station assignment variables $X_{i,n}$ in a pre-processing step before running the MIP solver. For example, in a scenario without charge scheduling and a first-in-first-out queue the assignment heuristic would assign EVs greedily based on their arrival time. In this work we assign EVs to stations greedily based on their relative state of charge.

3.2.2 Real-time planning: Schedule guided heuristic

Creating high quality schedules in advance (day-ahead) is a common approach to smart charging [26, 31, 34, 143]. However, results from day-ahead planning are difficult to apply in practice since circumstances may have changed since the time of planning. For example, drivers may arrive late or not at all. Similarly, there is previous work on scheduling in real-time [2, 130, 179, 183]. Real-time approaches typically do not utilize knowledge that may be available in advance such as planned arrivals and departures or even which EVs plan to charge.

There is little previous work on combining day-ahead knowledge and real-time scheduling. This section describes the *schedule guided heuristic* (SGH) which (optionally) takes as input day-ahead schedules and adapts them in real-time as EVs arrive and depart proposed in [52]. Compared to other approaches, SGH uses results from day-ahead planning. It offers a flexible priority function by reusing objective function components of the MIP model.

EVs are assigned to charging stations under two conditions: If they are present in the original precomputed schedule or if there are charging stations that are not

reserved. A station is reserved if there is no EV currently charging at it or if an EV originally planned is late by at least some time (in this work 15 minutes).

Lastly, creating (or adapting) schedules is implemented via a greedy filling technique. A schedule is filled by selecting timeslots for charging until the planned capacity reaches the desired capacity. This filling operation can be performed repeatedly on the same schedule with different desired capacities. Timeslots are ordered by time (as soon as possible), by cost (minimize electricity costs), by sum of planned currents (minimize peaks) or by load imbalance (minimize current differences). After a single car is assigned a schedule, all schedules must be rechecked for possible violations at the time of arrival and in the future. A violation, for example, is the sum of planned schedules at timeslot k being higher than a fuse (equivalent to restriction (8) in the MIP model). If there are any violations at k , each EV is assigned a priority. The EVs with the highest priorities may charge during k while others are rescheduled. In this context, rescheduling an EV implies recomputing its schedule while taking into account blocked timeslot k and retaining the assigned charging station. Lastly, schedules are not permanent. If a new EV arrives and causes violations during planning but has priority, other EVs are rescheduled. The schedule guided heuristic is depicted in figure 3.4.

For unplanned EVs no day-ahead knowledge is available. Specifically, we lack its departure time. In this chapter the historical median (17:15) is assumed. Chapter 4 focuses on possible approaches such as forecasting for estimating the departure time of unplanned EVs.

We use a flexible priority function with four weighted components to resolve violations (equivalent to the objective function in the MIP model). Actual (re-)scheduling is similarly flexible and one of four sorting criteria in Table 3.1 may be chosen depending on the scenario. Higher priority values indicate preferred EVs.

Equation 3.48 shows the priority per EV for the fair share objective component in which the goal is to minimize the number of EVs below their minimum SoC (SoC_{min}). To prioritize those EVs leaving soon Δt is used as the remaining time the EV is on company premises. This is where forecasting would potentially increase solution quality.

With regard to notation M is a large number, k is the 15 minute timeslot, t the continuous time in seconds, $I_{i,j,k}$ the current for charging station i on phase j during k (or for brevity $I_{n,t}$ for car n during t) and f_n the maximum current available for car n .

$$priority_1(n, t) = \begin{cases} \frac{SoC_{min} - SoC_t}{|\Delta t| * f_n + \epsilon}, & \text{if } SoC_t < SoC_{min} \\ \frac{SoC_{max} - SoC_t}{|\Delta t| * f_n + \epsilon} - M, & \text{otherwise} \end{cases} \quad (3.48)$$

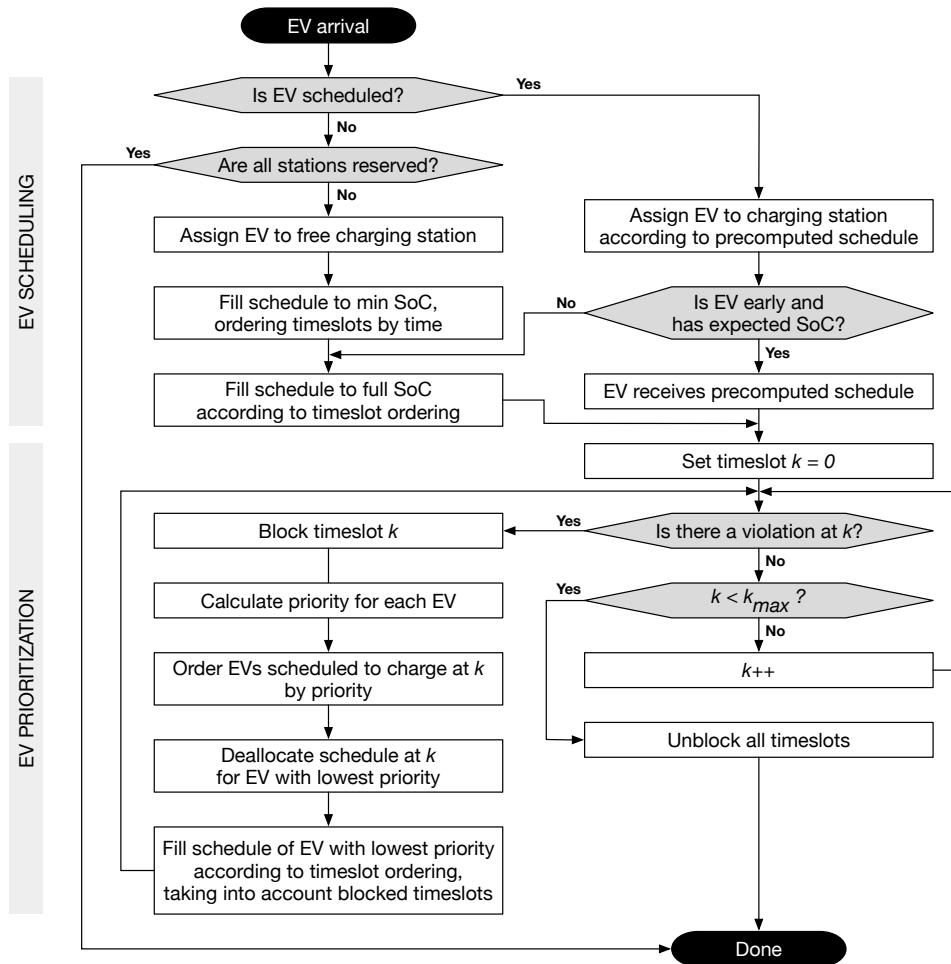


Figure 3.4: The schedule guided heuristic is executed on each EV arrival, EV departure, and periodically. Precomputed schedules are first looked up and if needed adjusted. During EV prioritization any violations, such as overloaded fuses, are resolved by rescheduling EVs with low priority.

Component	EV priority at timeslot k	Timeslot priority
Fair share	Current SoC	Order by time
Cost	Cost of schedule at k	Order by timeslot cost
Peak shaving	Schedule at k	Order by sum of schedules
Load imbalance	Effect on I_N at k	Order by I_N per timeslot

Table 3.2: Flexible objective function components for EV priority and timeslot ordering

The priority with respect to electricity costs is calculated in equation 3.49 by the average cost (€/MWh) of the EV's schedule.

$$priority_2(n, t) = -\left(\frac{1}{t_{max}} \sum_{t=1}^{t_{max}} c_t * I_{n,t}\right) \quad (3.49)$$

To minimize peak demand, the planned charging current for t in an EV's schedule determines its priority. Effectively, this would cause the EV with the highest planned current to be rescheduled.

$$priority_3(n, t) = -I_{n,t} \quad (3.50)$$

We describe we compute load imbalance in section 2.3.2. In contrast to the MIP model we are not required to use a linear approximation and may use the original equation shown in (3.51).

$$|I_N| = \text{sqrt}((|I_1| * \cos \phi_1 + |I_2| * \cos \phi_2 + |I_3| * \cos \phi_3)^2 + (|I_1| * \sin \phi_1 + |I_2| * \sin \phi_2 + |I_3| * \sin \phi_3)^2) \quad (3.51)$$

When minimizing load imbalance EV priority is calculated by the average load imbalance the EV's schedule is causing. This is calculated by (3.52) where $I_N(n, t)$ is the load imbalance at time t with car n charging and $I'_N(n, t)$ without car n charging at t . In other words, (3.52) quantifies by how much the load imbalance would change if car n were to be rescheduled. For EVs able to charge on 3 phases (3.52) returns 0, since they do not cause load imbalance among the three phases.

$$priority_4(n, t) = I'_N(n, t) - I_N(n, t) \quad (3.52)$$

Table 3.2 shows an overview of the objective function components used in the schedule guided heuristic and its equivalent in the MIP model. To summarize,

Model name	Battery size (Ah)	Number of phases
Tesla Model S85	369.565	3
Nissan Leaf 2016	130.435	1
BMW i3 2017	94.000	3
Mercedes GLC 350e	37.826	1
Renault Zoe R240	95.500	3

Table 3.3: Heterogeneous EV model data from manufacturers used as input for the charging simulation

calculating EV priorities is used to determine which EVs should be rescheduled in order to resolve violations. Once the EVs have been chosen, timeslots are ordered by one of the criteria in the third column and then each EV is planned in order to satisfy its charging needs.

3.3 Experimental setup

The testing environment for evaluation contains several components. First, a dataset is generated based on historical data (section 3.3.1). Second, the dataset is used to create a problem instance of the MIP model (section 3.2.1). The problem instance is then solved to produce precomputed schedules. Third, a real-time charging simulation (chapter 3.3.2) is run which simulates the generated dataset. The schedule guided heuristic (section 3.2.2) is used during the simulation to adapt the precomputed schedules of the MIP model.

3.3.1 Data generation

EVs. In this chapter, to capture a diverse set of EVs with different characteristics five car models are considered (see Table 3.3), battery electric vehicles (BEVs) as well as plug-in hybrids electric vehicles (PHEVs). They include popular models on the German market: Tesla Model S, Nissan Leaf, BMW i3, Mercedes GLC and Renault Zoe. In contrast to related literature, we model EVs with heterogeneous charging behavior. This affects parameters such as battery capacity, maximum charging current and whether the EV can charge on one or three phases.

Drivers. In order to create realistic simulations historical data from a German company was used to derive two discrete probability distributions for EV arrival and departure time. These are two roughly normal distributions with an average of 08:00 and 17:15 and standard deviations of 2.56 hours and 2.42 hours, respectively. Since the departure time is dependent on the arrival time, the two were

combined to form a joint probability distribution. For the simulation, to generate a tuple <arrival, departure> a value is chosen based on this discrete probability distribution.

3.3.2 EV fleet charging simulation

A Java-based charging simulation is used to evaluate the combination of day-ahead and real-time planning across many randomized variables. The simulation is discrete and event-based where each event represents an EV arrival, EV departure or a periodic recalculation. A recalculation is triggered every 15 minutes due to possible electricity price changes.

The simulation models the charging infrastructure, EVs and the energy market (assuming a fixed price per 15-minute timeslot). To recap, figure 2.12 shows the historical electricity prices on a typical weekday in 2017 from the intraday market in Germany that are used as input to calculate energy costs. Randomized variables within data generation and the simulation are reproducible using a seed. For example, each EV's model, arrival and departure time is generated randomly based on historical data as described in the previous section. An overview of the variables contained in the simulation may be found in the nomenclature in section A.1. The generation of instances of the MIP model is described in section 3.3.4.

Within the simulation loop, each time step within the simulation represents one second. For each second, events such as car arrivals are processed and EVs are updated with how much energy they were scheduled to charge with. Additionally, the simulation validates the current state at each second to ensure none of the constraints described in section 3.2.1 are broken. If any constraints are broken the simulation is aborted and the program throws an error.

The results from a simulation are written to a file. A SQLite database is used to track and manage simulation results since this work analyzes the results of many thousands of simulations. Simulation results are analyzed using R. Figure 3.5 shows an overview of the simulation.

3.3.3 Simulation parameters

Simulations show the impact of combining day-ahead and real-time planning with varying levels of randomness. Randomness defines how different the data for day-ahead planning is from the data that is used for the real-time simulation. Randomness thus represents a prediction error if the data for day-ahead planning were a result of predictions.

Values of randomness between 0 and 1 represent the proportion of EVs that do not arrive exactly as expected. For example, a value of 0 signifies no changes

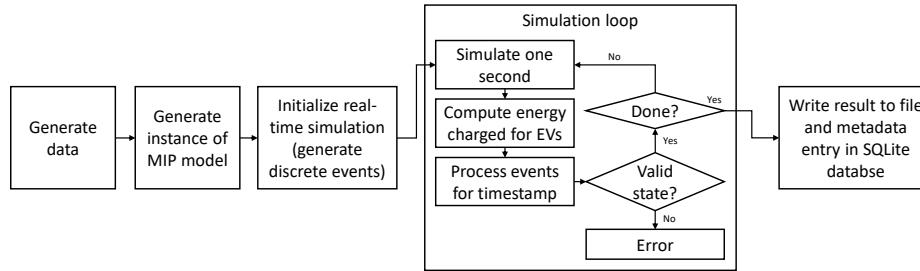


Figure 3.5: Diagram of the real-time simulation used for evaluation

(all EVs arrive exactly as expected) while a value of 1 represents a completely different set of EVs arriving. Electricity prices are also changed from day-ahead prices randomly. The size of the price change is proportional to randomness where higher randomness causes larger price changes. To remove noise, the dataset used as input for each simulation is randomly generated with each parameter setting 20 times and results are averaged.

Table 3.4 gives an overview of the most important simulation parameters which describe the simulated scenario. Table 3.5 shows which combinations of day-ahead and real-time planning methods are compared. Uncoordinated charging is included as a baseline.

3.3.4 Solving of MIP instances

Instances of the MIP model are constructed after data generation. Each instance is then saved as a file in the `.lp` format [69].

Generated MIP models are solved with SCIP v4.0.1 [107] with the relative optimality gap (`limits/gap`) set to 0.01. Experiments are run on a machine with an Intel Xeon E5-2660 v4 CPU and 128 GB RAM.

3.3.5 Metrics

A range of quality metrics analog to the objective function components are reported.

Mean min SoC. Primary objective to be maximized and average of each EV's fraction of the minimum SoC reached. If an EV is adequately or more than adequately charged, the fraction of the minimum SoC is 1.

Simulation parameter	Sample value	Description
Number of EVs	200	Set of heterogeneous EVs
Number of charging stations	100	Set of charging stations
Charge infrastructure	Figure 2.10	Configuration of charging stations and fuse sizes
Randomness	0.4	Proportion of day-ahead data changed: For example, unplanned EVs arrive and planned EVs do not arrive
Electricity prices (€/MWh)	< 27.27, ... >	Assumed fixed energy prices per 15-minute interval
Seed	8	Reproducible randomized values via seed

Table 3.4: Simulation parameters

Label	Method
a)	No day-ahead planning and uncoordinated charging: A first-come-first-serve approach acts as the baseline (similar to approach in [179])
b)	Day-ahead planning: A simple algorithm tries to follow schedules from day-ahead planning exactly. If an EV is not in the dataset for day-ahead planning, it is not scheduled. Performance will decrease in proportion to randomness.
c)	No day-ahead planning and the schedule guided heuristic: Performance of the heuristic without any day-ahead planning (investigated in [53]). EVs are assigned to charging stations on a first-come-first-serve basis since no day-ahead planning is performed.
d)	Day-ahead planning and the schedule guided heuristic: EVs are assigned to charging stations by day-ahead planning and schedules are precomputed.

Table 3.5: Simulation setup: Which combinations of day-ahead and real-time planning approaches are compared?

$$\frac{1}{N} \sum_{n=1}^N \min\left(1, \frac{SoC_{n,current}}{SoC_{n,min}}\right) \quad (3.53)$$

Mean final SoC. Objective to be maximized, average of each EVs fraction of the total SoC reached. Secondary in importance to the fraction of the minimum SoC.

$$\frac{1}{N} \sum_{n=1}^N \frac{SoC_{n,current}}{SoC_{n,min}} \quad (3.54)$$

Energy costs (€). Secondary objective, to be minimized with energy costs per timeslot c_k .

$$\sum_{i=1}^I \sum_{j=1}^3 \sum_{k=1}^K c_k * P_{i,j,k} \quad (3.55)$$

Maximum power (kW). Secondary objective, to be minimized (peak shaving).

$$\max_{k=1}^k \sum_{i=1}^I \sum_{j=1}^3 P_{i,j,k} \quad (3.56)$$

Average load imbalance (A). Secondary objective, to be minimized over K timeslots with load imbalance for a timeslot $I_{N,k}$.

$$\frac{1}{K} \sum_{k=1}^K I_{N,k} \quad (3.57)$$

Power charged (kWh). An indicator of solution quality. However, a higher number does not necessarily lead to a higher fair share. The factor 0.25h is used to transform values from the charge schedule (in kW) to energy consumption (in kWh).

$$\sum_{i=1}^I \sum_{j=1}^3 \sum_{k=1}^K 0.25h * P_{i,j,k} \quad (3.58)$$

3.4 Experimental results

The objective function contains weights w_1 to w_4 to quantify the relative importance per objective component. Fair share must be prioritized over the other three components (cost minimization, peak shaving and load imbalance minimization). Otherwise, the optimal solution would be to not charge at all. In the MIP model, each objective function component is normalized by coefficients $c'_1-c'_4$.

The MIP model objective function component weights are set to $w_1 = 10^{12}$ (fair share), $w_2 = 1$ (costs), $w_4 = 10^{-3}$ (load imbalance), $w_3 = 0$ (peak shaving). A large value for w_1 is chosen purposefully in order to guarantee that charging EVs is always the highest priority.

These weights were derived from a deterministic one-at-a-time sensitivity analysis and were found to lead to charge schedules that clearly prioritize fair share over energy costs. Load imbalance has the lowest priority and peak shaving is disregarded. Weights for the schedule guided heuristic were chosen analogously.

For the sensitivity analysis the same problem instance (25 cars, 25 charging stations) is repeatedly solved where a single weight is varied at a time while the others are held constant. Figure 3.6 visualizes pairwise Pareto fronts showing the tradeoffs between each objective function component and the average energy cost. For each pairwise comparison, the weight(s) not being considered in the tradeoff are set to 0 in order to cause fewer dominated solutions. $w_{fairShare}$ is kept at 10^{12} when not part of the comparison in order to prioritize satisfying charging needs.

Table 3.6 shows the results from simulations described in section 3.3 with the specified weights. Fair share corresponds to the mean minimum SoC (that is required for EVs to reach their destination) and thus highest values indicate preferred solutions. The other metrics are reported for completeness.

With increasing randomness (which represents the proportion of unplanned EVs) the performance of day-ahead planning in isolation *b*) predictably decreases since unplanned EVs are not scheduled. There is no benefit to using day-ahead planning with randomness 1. This represents the case when no originally planned EVs arrive. Real-time planning in isolation *c*) shows similar performance in SoC with large differences in average cost (a secondary objective) independent of randomness. The combination of day-ahead planning and the schedule guided heuristic *d*) shows the best results at an increased load imbalance. For randomness 1 the combined approach *d*) shows slightly worse performance compared to using purely the schedule guided heuristic *c*). Because cost minimization is chosen as a secondary objective over peak shaving the maximum consumption P_{max} is similar in all cases.

Figure 3.7 shows the mean final SoC subject to increasing randomness. For low randomness (below 0.4) day-ahead planning yields the best results, whether used in isolation or combined with the schedule guided heuristic. For very high proportions of unplanned EVs (above 0.9) the schedule guided heuristic by itself *c*) performs best since all charging stations are free of blocking reservations. For randomness values in between, the schedule guided heuristic combined with day-ahead planning performs *d*) slightly better than without.

Figure 3.8 shows results for the secondary objective of minimizing energy costs. The graph shows the average energy cost subject to increasing random-

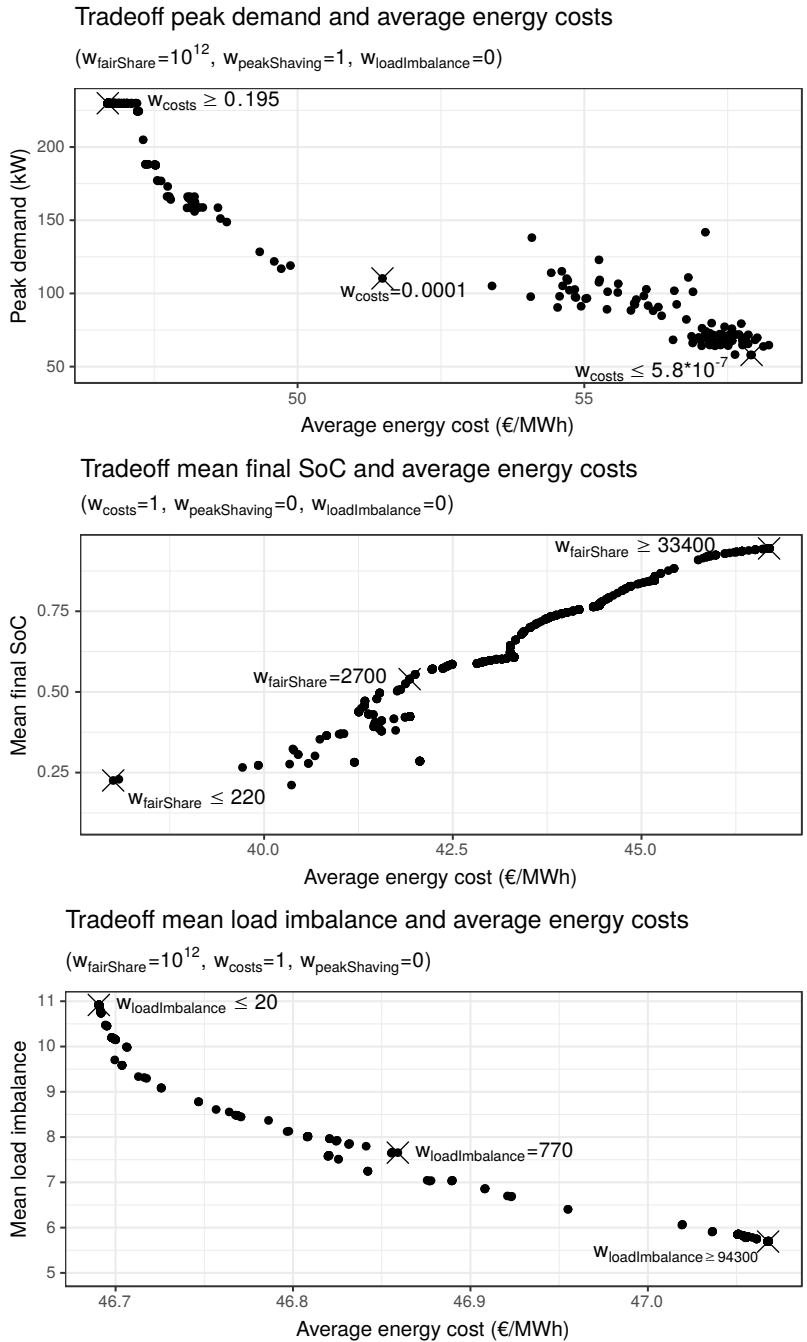


Figure 3.6: Pareto fronts showing the tradeoffs between weights for energy costs (w_{costs}) and weights for fair share ($w_{fairShare}$), peak shaving ($w_{peakShaving}$) and load imbalance ($w_{loadImbalance}$) including dominated and non-dominated solutions

Method	Power charged (kWh)	Cost ($\frac{\text{€}}{\text{MWh}}$)	Mean min SoC	Mean final SoC	P_{max} (kW)	Mean I_N (A)
Randomness = 0.00						
a)	332.2	59.44	0.84	0.69	90.47	9.406
b)	737.7	50.78	0.99	0.89	103.50	11.051
c)	526.0	52.04	0.91	0.77	93.69	12.578
d)	740.6	52.98	0.99	0.89	97.91	15.616
Randomness = 0.20						
a)	317.7	59.57	0.83	0.67	92.47	7.870
b)	574.8	50.59	0.94	0.81	96.22	12.195
c)	495.3	51.22	0.89	0.75	95.34	12.188
d)	583.0	51.06	0.92	0.80	94.64	14.694
Randomness = 0.40						
a)	325.1	59.02	0.84	0.69	92.32	7.310
b)	439.4	50.14	0.89	0.73	83.85	10.677
c)	475.7	49.12	0.90	0.75	93.40	9.704
d)	530.3	49.82	0.91	0.78	93.80	13.489
Randomness = 0.80						
a)	322.7	58.21	0.84	0.69	92.07	7.878
b)	154.0	49.16	0.80	0.58	42.26	6.040
c)	494.9	44.95	0.90	0.76	92.23	10.314
d)	498.1	45.44	0.90	0.77	93.49	11.228
Randomness = 1.00						
a)	328.5	58.21	0.85	0.71	89.31	8.644
b)	0.0		0.75	0.50	0.00	0.000
c)	475.8	42.26	0.91	0.77	93.29	11.380
d)	441.4	41.90	0.89	0.75	92.45	9.996

Table 3.6: Simulation results comparing various methods of combining day-ahead and real-time planning approaches (see Table 3.1). Each simulation involves 50 EVs and 25 charging stations where results in rows are averages over 20 runs.

ness. Here, for low randomness (below 0.4) day-ahead planning yields slightly better results compared to the other approaches. For higher values of randomness the schedule guided heuristic in isolation *c*) performs similar to the combination of both methods *d*).

Simulations in Table 3.7 show how objective function component weight settings affect scheduling. Similar scenario settings were chosen (25 cars, 25 charg-

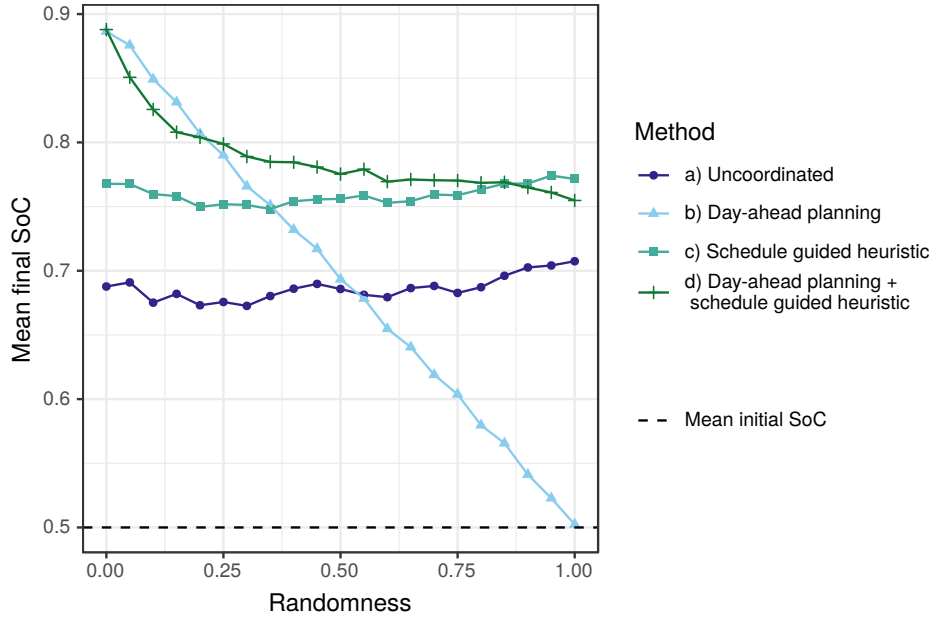


Figure 3.7: Mean final SoC subject to randomness

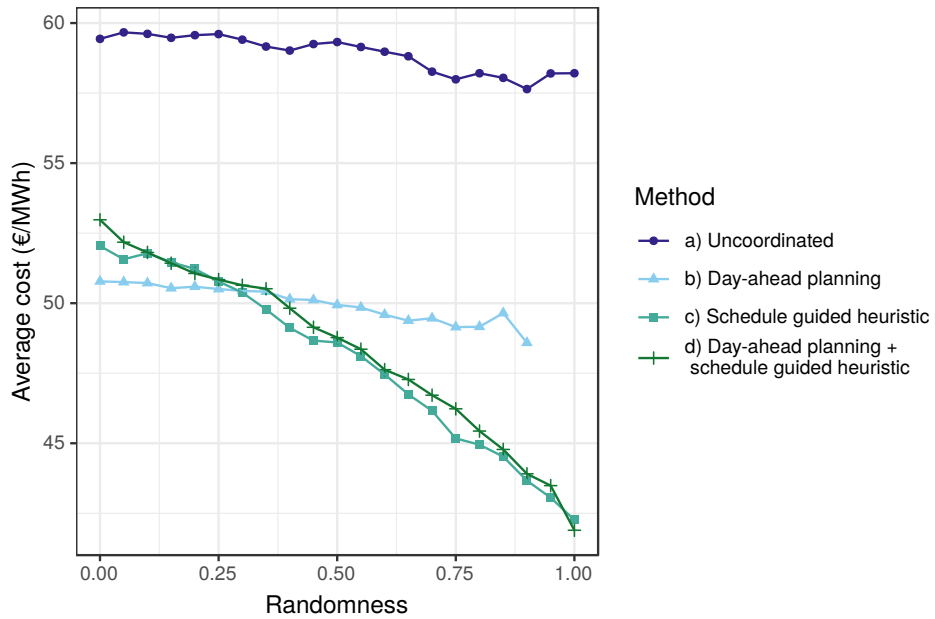


Figure 3.8: Average cost (€/MWh) subject to randomness

Method	Power charged (kWh)	Cost ($\frac{\text{€}}{\text{MWh}}$)	Mean min SoC	Mean final SoC	P_{max} (kW)	Mean I_N (A)
Uncoordinated						
a)	717.7	57.52	0.98	0.97	222.16	13.6
Cost minimization ($w_1 = 10^{12}, w_2 = 10^0, w_3 = 0, w_4 = 10^{-3}$)						
b)	697.5	46.69	0.98	0.94	229.93	10.9
Peak demand minimization ($w_1 = 10^{12}, w_2 = 0, w_3 = 10^0, w_4 = 10^{-3}$)						
b)	696.7	56.02	0.98	0.94	91.46	13.9
Load imbalance minimization ($w_1 = 10^{12}, w_2 = 0, w_3 = 10^{-3}, w_4 = 10^0$)						
b)	687.9	55.75	0.98	0.93	143.46	8.8

Table 3.7: Comparison of different weight settings for objective function components: w_1 to w_4 correspond to fair share, electricity costs, peak shaving and load imbalance, respectively.

ing stations) with no randomness. The results show the flexibility of the presented MIP model. Depending on the given scenario, the components cost, peak demand or the load imbalance can be prioritized over others. For example, weight settings for cost minimization show the lowest average cost (46.69€/MWh) while peak demand shows the lowest peak power demand during the day (91.46kW). Weights for load imbalance minimization show the lowest average load imbalance I_N .

To illustrate the weight settings in more detail, figure 3.9 shows the aggregated power consumption for table 3.7 where each value is the sum of the three phases per timeslot. Notably, there are large differences between cost and peak demand minimization (46.69€/MWh vs 56.02€/MWh, 229.93kW vs 91.46kW). Cost minimization minimizes the electricity costs in figure 2.12 while peak shaving minimizes differences between consumption per timeslot.

Figure 3.10 shows the computation time per method subject to the number of cars. The number of charging stations is held constant at 25. Uncoordinated charging is included as a benchmark. The schedule guided heuristic in isolation is faster by several orders of magnitude compared to methods involving the MIP model. The results show that using the MIP model in a real-time setting is infeasible especially since the MIP model size further increases with the number of charging stations and cars.

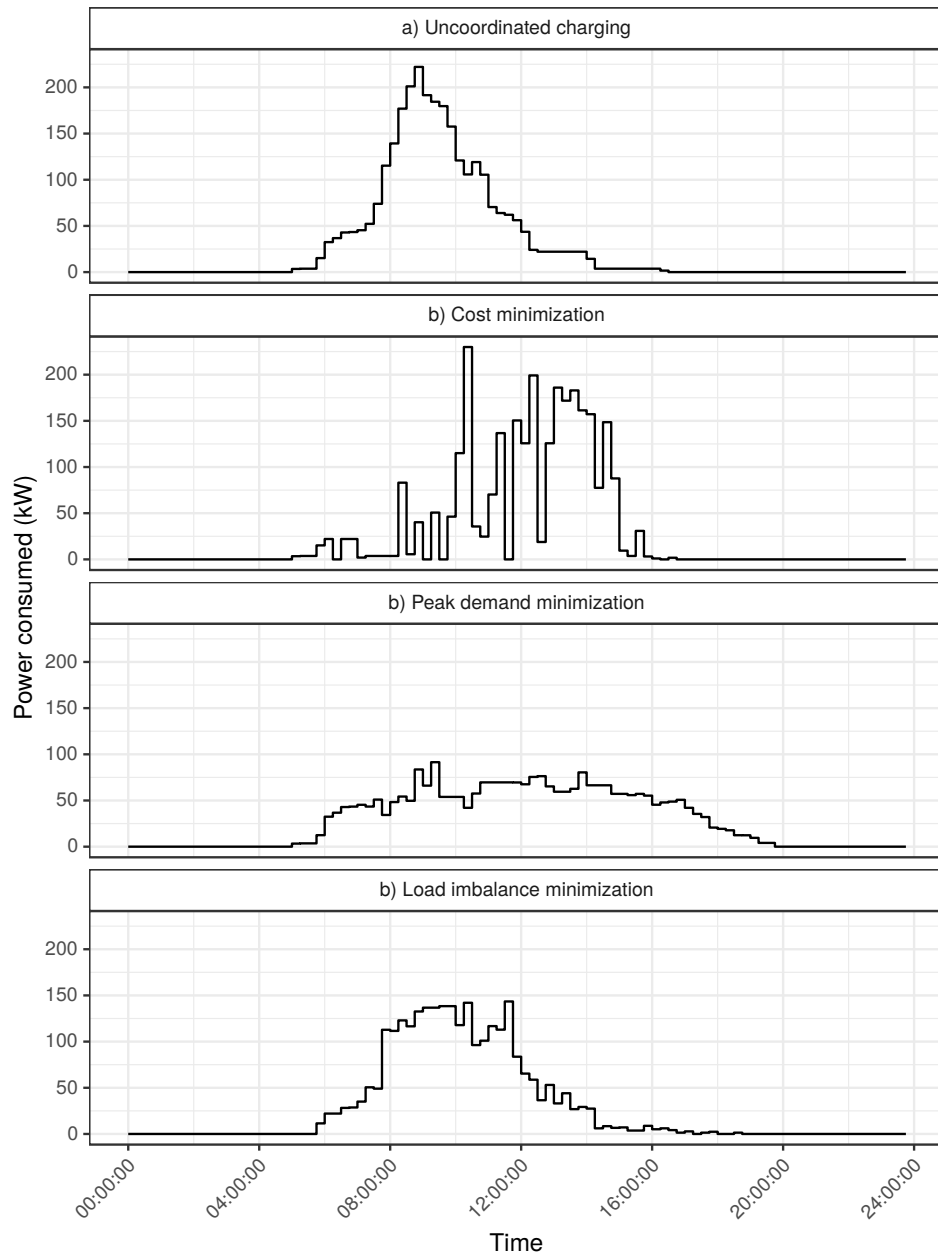


Figure 3.9: Power consumption over time as a result of different weight setting for objective function components

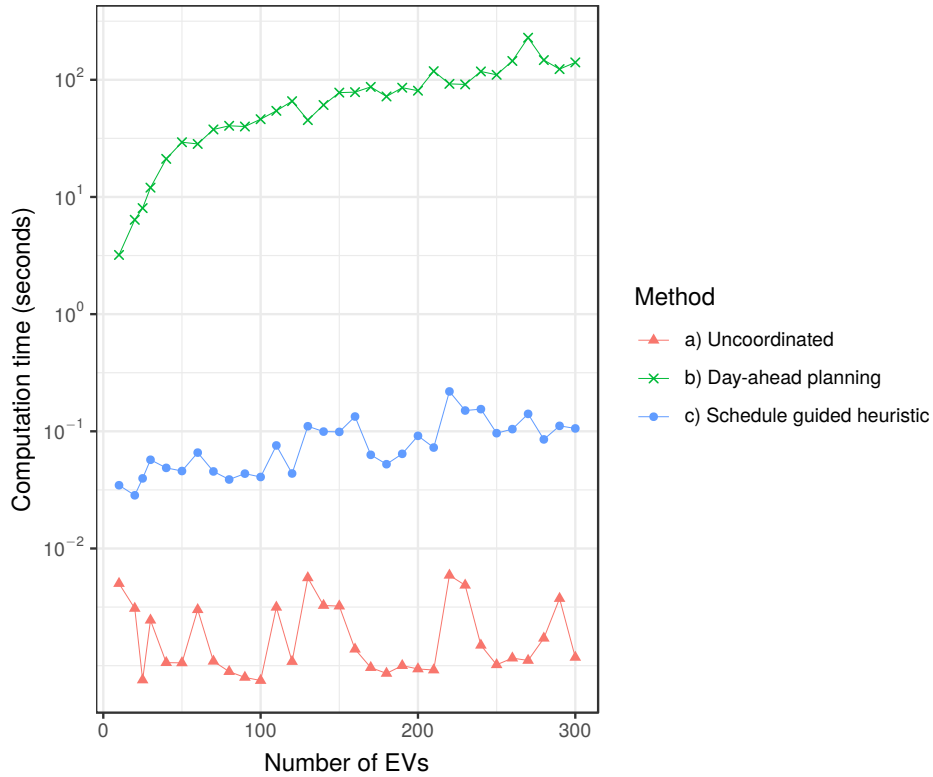


Figure 3.10: Computation time per method: The schedule guided heuristic is faster by several orders of magnitude compared to the MIP model, making it usable in real-time

3.5 Discussion

The mathematical model for smart charging used in this chapter attempts to depict electrical engineering constraints as closely as possible so that the resulting solution may be applied directly via smart charging protocols such as OCPP [81]. However, the model makes some simplifying assumptions that require further evaluation. For example, each EV's departure time is assumed to be known. This assumption is relaxed and analyzed in detail in chapter 4.

Regarding battery charging, this chapter assumes linear charging over time. In practice, EVs possess battery management systems that apply approaches such as Constant Current Constant Voltage (CCCV) to increase battery life, which leads to nonlinear behavior of the state of charge [168]. Nonlinear battery behavior is

addressed in chapters 5 and 6.

Regarding advance data availability and accuracy, both day-ahead and real-time planning in this chapter depend on parameters that reflect driver behavior and battery state. For example, the priority mechanism in the schedule guided heuristic relies strongly on EV departure times and on charging needs. Both are data which is difficult to acquire in practice. For example, the SoC is not reliably retrievable by the charging station because of limited protocol support by manufacturers [81]. In this chapter, a data generator creates randomized datasets with varying levels of randomness such that data for day-ahead planning is changed prior to the real-time simulation. The experimental results show that improved data reliability leads to better charging schedules. Data quality improvements could be achieved in practice by gathering manual user input or by using forecasting techniques.

Regarding cost calculation, the model assumes electricity purchases on the intraday market exclusively. This may or may not reflect the purchasing process of the EV fleet operator. Additional corner cases such as negative energy costs could be considered in future experiments.

Lastly, the scenario considered in this chapter is characterized by EVs that are on company premises for a long duration. Other scenarios such as a logistics center may also be considered. In this context, time constraints would likely be tighter since the EVs would be less idle leading to shorter standing times. The day-ahead planning process may be more reliable in logistics where vehicle usage is predictable.

On a technical note, advanced modelling techniques may help speed up the solution of the MIP model. One approach of interest is staged planning which involves groups of charging stations versus individual stations. Here, symmetries from the phase rotation would be exploited.

3.6 Conclusion

This chapter describes a method for combining day-ahead planning with real-time coordination of smart charging proposed in [52]. A mixed integer programming (MIP) model for day-ahead planning is presented. Precomputed schedules are used by a schedule guided heuristic for real-time planning.

The research question of how to create charging schedules for EVs with limited resources in real-time is addressed. Compared to related literature, this chapter makes use of detailed day-ahead knowledge such as EV models and arrival times.

Both the MIP model and the schedule guided heuristic provide the flexibility to choose which objective component should be prioritized based on the business context. For example, peak shaving can be prioritized in settings in which other

consumers in the local network cause spikes. Alternatively, electricity costs can be minimized in cases of widely ranging prices such as intraday markets. Lastly, in situations with large load imbalances, differences in the current per phase may be minimized.

Experimental results from simulations demonstrate how using prior knowledge in day-ahead planning improves the quality of schedules created by smart charging. However, using day-ahead planning in isolation is impractical in a real life setting due to inaccuracies that occur in real-time. These inaccuracies can be addressed by the proposed schedule guided heuristic which adapts schedules in real-time.

The next chapter focuses on improving the schedule guided heuristic in the case of unplanned EVs. Instead of using the historical median, the departure time and the available timeslots for planning are predicted via forecasting. Forecasts are then integrated in the heuristic to improve EV prioritization.

Chapter 4

Real-time charge scheduling with departure time prediction

4.1 Introduction

One of the main limitations of the chapter 3 is the assumption that each EV's exact departure time is known. Within the charge scheduling heuristic and the MIP model, EV prioritization takes into account the extent to which the EV is charged, how fast it can charge and how urgently it needs to charge. The urgency is influenced by the remaining time that an EV is available at the charging station.

Possibilities for determining an EV's departure times include collecting user input (for example, via reservations) or estimating the departure time based on historical data. This chapter focuses on estimating EV departure times based on historical data in order to accurately prioritize EVs [54].

We use regression models trained on historical data to predict EV departure times. In this chapter we use a diverse historical dataset with high geographical spread (8 cities) and many different drivers (over 1.000) over a long time period (3 years).

Compared to previous studies [127, 172, 173], we create regression models based on features with wide value ranges. Features such as location and previous driver arrivals and departures thus contain a broad set of values. As in the previous chapter we focus on the workplace which is characterized by EVs with routine arrivals and departures.

In this chapter, we consider the following research question:

How can we address the uncertainty of EV availability in smart charging and quantify a solution's impact on charge schedule quality?

We present an approach to improve the charge scheduling heuristic by incorporating predictions for individual EV departures based on historical data.

The main contributions of this chapter are:

- We predict individual EV departures using regression models trained on historical data,
- we incorporate this prediction in the charge scheduling heuristic and
- we analyze and quantify the influence of prediction accuracy on smart charging quality in simulations.

The structure of this chapter is as follows. The dataset used for training regression methods is described in section 4.2. Section 4.3 introduces the applied methods which includes both the regression methods used for predicting EV departure and the charge scheduling heuristic. After detailing the experimental setup in section 4.4 the results are presented in section 4.5. Finally, section 4.6 discusses the findings and section 4.7 concludes with an outlook.

4.2 Dataset

In this chapter we make the simplifying assumption that the fleet is homogeneous and consists of vehicles loosely based on the Tesla Model S specification. For each EV we assume a battery capacity of 85 kWh and a maximum charging power of 22 kW.

Regarding driver behavior we assume a workplace context where EVs arrive spontaneously and charge at a private charging infrastructure during working hours. Charging operations are run on a first-come-first-served basis and there is no queuing system. The scenario is characterized by uncertainty in the departure time. We assume the SoC of each EV is known even though in practice it may not be [72]. This assumption reduces the uncertainty to a single variable, namely the departure time.

We use historical data to predict EV departure time from the workplace similar to related work [59, 172]. In this chapter, we use a dataset from a large company in Germany containing roughly 100.000 charging processes ranging from years 2016 to 2019 to train regression models. While the dataset includes charging processes by a heterogeneous fleet we assume a homogeneous fleet of EVs. There is currently no smart charging system in place that would prioritize according to different EV models. As such EV arrival and departure times are independent of the EV model in this dataset. We can thus make the assumption of a homogeneous fleet without loss of generality with regard to predicting EV departure time.

Feature name	Description
Car ID	Anonymized car ID (roughly 1.000 unique cars)
has ID?	Boolean reflecting whether the charging session is associated with a car ID: Roughly 6.000 processes (6%) are not associated with an ID.
Car type	Hybrid or fully electric vehicle
Weekday	Weekday of the charging process (7 one-hot encoded features)
Charge point ID	Which charge point was used for charging (several hundred unique charge points)
Car park	Location of the charging process (12 car parks in 8 cities)
Floor	Floor of the car park
Arrival time	Start of the charging process (in seconds since midnight)
Departure time	End of the charging process (in seconds since midnight) and target feature to predict
Duration	Duration of the charging process (not used for training since the duration is not known at the beginning of the charging process)

Table 4.1: Set of raw charging process features used for predicting EV departure time in a dataset of roughly 100.000 charging processes

Table 4.1 shows relevant attributes of the dataset. Some attributes are derived from raw attributes such as the weekday from the date. We use the term *feature* to refer to an attribute of the dataset. Additional features such as part time employment of drivers would likely improve predictions but are limited by data protection regulations.

4.3 Method

4.3.1 Regression Methods

This section addresses the uncertainty in EV availability. Predictions are made with regression models trained on the large historical dataset introduced in 4.2.

We use the following methodology for incorporating historical data to improve EV scheduling. To begin with, our dataset preprocessing includes feature engineering, a common technique to improve prediction accuracy of regression models. For example, this involves adding new features based on the target feature (departure time). In this work, we add mean arrival, departure and duration while grouping

by car ID, car type, weekday, charge point, car park and floor. This process adds a further 18 features.

Another technique we use is one-hot encoding. Here, values of categorical features are converted to Boolean features. This allows using purely numerical models such as linear regression. We one-hot encode car type, weekday, car park and floor. For example, this technique converts car park from a single categorical feature with 12 unique values to 12 Boolean features. We do not make use of a one-hot encoded car ID. First, it did not lead to improvements in prediction accuracy. Next, training on IDs can lead to overfitting since it adds one feature per unique car. Lastly, using the car ID makes it difficult for trained regression models to generalize to new cars. The final dataset has 58 features as shown in Table 4.2.

We improve the charge scheduling heuristic presented in chapter 3 by refining prioritization. In chapter 3, the historical median of EV departures was used as a trivial prediction. In this chapter, we integrate real-time predictions made with the models described in this section. We improve the precision of $t_{\text{expectedDeparture}}$ in (4.3) by using regression models instead of the historical median as a prediction method. We then experimentally check the influence of its precision on the charge scheduling heuristic.

Metrics allow quantifying the performance of regression methods. In this work we use the mean absolute error (MAE), a standard metric for regression methods. Additional metrics are introduced to reflect the impact of MAE (prediction accuracy) on resulting charge schedules. We measure smart charging quality as the average fraction of minimum SoC (fair share) and the number of adequately charged EVs.

To evaluate regression methods computation time as well as prediction quality are relevant criteria. Computation time is measured during model training and during prediction (*inference*). Runtime for inference is important in real-time smart charging because of the short planning window. The process of training regression models is less time-critical and can be performed ahead of time. In the following, we list the regression methods compared in this chapter.

Oracle. In order to show room for improvement in regression methods, the oracle always makes the perfect prediction and thus has an MAE of 0.

Constant. We use the historical median across all drivers as a baseline to represent the simplest possible prediction. It also provides a point of comparison to chapter 3 where the historical median was used as a trivial predictor.

Additionally, we use midnight as a second choice of a constant to show the impact of a bad prediction and a correspondingly high MAE.

Linear model. A basic regression method uses a linear model in which we fit

the following model:

$$y = \beta_0 + \sum_{i=1}^m \beta_i * x_i + \epsilon_j \quad (4.1)$$

In (4.1) y represents the EV’s departure in seconds since midnight, x_i feature i for each of the $m = 58$ features and ϵ_j the error per data point j .

XGBoost. We use XGBoost [24], a sophisticated regression method able to exploit complex relationships in the data. More formally, XGBoost lies in the family of gradient boosted decision trees. To avoid overfitting during training, we train using 10-fold cross validation and report the MAE on each test set. We perform hyperparameter tuning based on grid search using the R package MLR [15]. For reference, the final best parameters based on the average mean absolute error on test sets during cross validation are `max_depth: 6`, `min_child_weight: 8.19`, `subsample: 0.81`, `colsample_bytree: 0.93` and `eta: 0.3`.

Artificial Neural Network. We use Keras [25] for training an Artificial Neural Network for regression. We use an architecture of two hidden layers each consisting of 128 neurons with rectified linear activation functions. Weights are regularized using L1 regularization. The final layer is a single neuron. An 80-20 train and test split was used for evaluation. Additionally introducing a combination of dropout layers and a higher number of hidden layers did not result in an improved MAE.

4.3.2 Changes to the schedule guided heuristic

In this chapter, we use the charge scheduling heuristic introduced in section 3.2.2 to schedule EVs for real-time charging without precomputed schedules. This means we omit the computation of charge schedules beforehand and treat every EV as if it were a spontaneous arrival without a reservation.

To recap, the goal of the heuristic is to maximize fair share similar to related work addressing driver satisfaction [29] or social welfare [5]. We define maximizing fair share as maximizing the average fraction of minimum SoC over all EVs. Figure 3.2 shows the concept of the fraction of minimum SoC.

We define the minimum SoC as the sufficient charge required to at least reach the next charging station. An EV that has reached its minimum SoC is considered *adequately charged*. In this work, we assume a fixed value of 0.5 (or 42.5 kWh) for each EV. In practice, the fixed value of 0.5 should be set according to the driver’s needs. The value should be chosen based on data such as commute distance but access is limited by data protection regulations. The minimum SoC is also influenced by battery size which varies in scenarios with a set of heterogeneous EVs.

Categorical features	39 features
has ID?	1 feature
Car type	3 one-hot encoded features (missing values are also included as "N/A")
Weekday	7 one-hot encoded features
Car park	12 one-hot encoded features
Floor	16 one-hot encoded features
Numerical features	19 features
Mean arrival	6 features (arrival grouped by ID, car type, charge point, car park, floor, weekday)
Mean departure	6 features (arrival grouped by ID, car type, charge point, car park, floor, weekday)
Mean duration	6 features (arrival grouped by ID, car type, charge point, car park, floor, weekday)
Arrival time	Mean: 09:17, median: 08:27, standard deviation: 169 minutes, min: 00:01, max: 23:07
Target feature	
Departure time	Mean: 16:30, median: 17:03, standard deviation: 141 minutes, min: 00:16, max: 23:59

Table 4.2: Set of one-hot encoded and engineered features used for training regression models. Values for the arrival and departure time are computed across all users. The semantic description of each raw feature is shown in Table 4.1.

The charge scheduling heuristic is outlined in figure 4.1 and works as follows. Upon each EV's arrival, its departure time is predicted. Next, the EV is temporarily scheduled so it reaches its full SoC as soon as possible: We iterate over each timeslot k and set its schedule at k to its maximum charging rate p_n .

Subsequently we check all 15-minute timeslots where the infrastructure would be overloaded by planned schedules with planning horizon k_{max} . In case of one or more violations at timeslot k we block k and calculate a priority per EV that plans to charge during k . The EVs with the lowest priority are rescheduled to a different timeslot. To reschedule an EV we first deallocate its schedule at timeslot k . For example, we set its charging rate from 10kW to 0kW. We then move the deallocated schedule value (10kW) to the next possible timeslot. The next possible timeslot is determined by which timeslots are blocked so far. After confirming there are no more remaining infrastructure violations all timeslots are unblocked as initialization for the next run of the heuristic. The timeslot length was chosen corresponding to intraday energy prices which are typically available on a 15 minute basis.

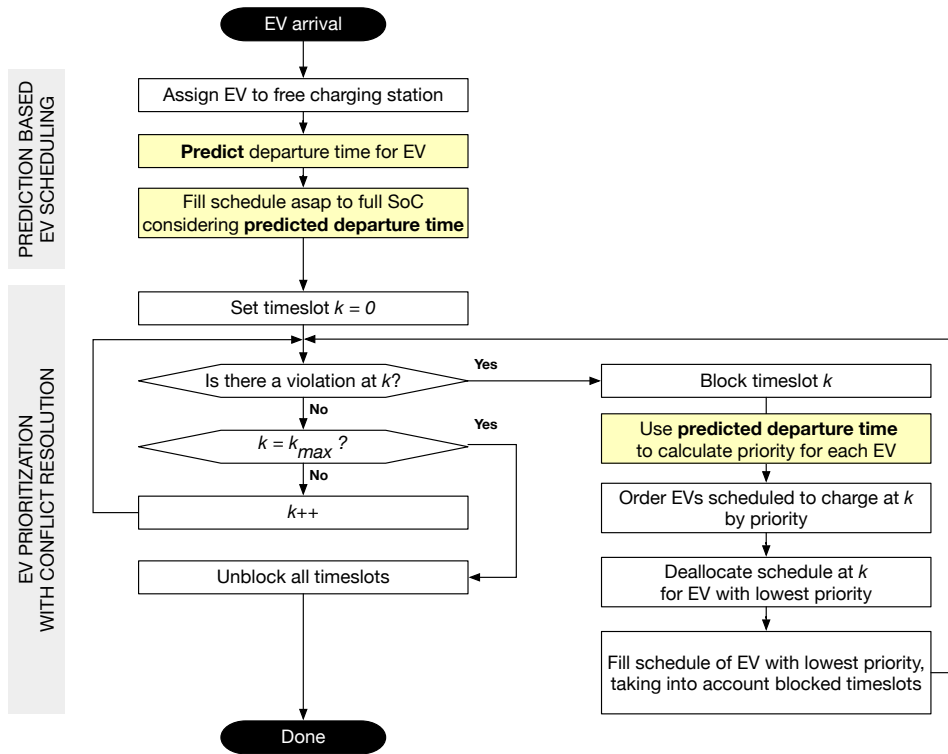


Figure 4.1: The charge scheduling heuristic is executed on each EV arrival and departure. During EV prioritization EVs with low priority are rescheduled to charge at a different timeslot. Colored fields denote components using departure prediction.

The priority mechanism which determines EVs for rescheduling pursues a fair share of SoC among EVs. The priority reflects the urgency to charge and is influenced by five variables:

p_n	The maximum power the EV n can charge at (in kW)
$b_{n,t}$	The level to which EV n is charged at time t (in kWh)
$b_{n,min}$	The minimum level to which EV n should be charged (in kWh)
$b_{n,max}$	Battery capacity of EV n (in kWh)
Δt	The remaining time until departure (in seconds)

Uncertainty arises in the remaining time until departure. In this chapter we focus on obtaining an accurate prediction based on historical data in order to correctly prioritize EVs.

EV priority for car n at time t is calculated according to equations (4.2)-(4.3). The priority mechanism depends strongly on the accuracy of the predicted departure time. That is, the more accurate $t_{\text{predictedDeparture}}$ is, the more accurately EVs can be prioritized. For example: if an EV were to be assumed to leave at 17:00, but actually leaves at 16:00 it would wrongfully receive a low priority which may lead to the EV missing out on charging opportunity. Alternatives to predicting departure time include assuming a fixed value or prompting drivers for direct input via reservations. However, assuming a fixed departure time leads to inaccurate prioritization in general. In this work, we assume we do not have direct access to drivers whose input may additionally be affected by reliability or misuse.

$$priority(n, t) = \begin{cases} \frac{b_{n,min} - b_{n,t}}{|\Delta t| * p_n + \epsilon}, & \text{if } b_{n,t} < b_{n,min} \\ \frac{b_{n,max} - b_{n,t}}{|\Delta t| * p_n + \epsilon} - M, & \text{otherwise} \end{cases} \quad (4.2)$$

$$\Delta t = t_{\text{predictedDeparture}} - t \quad (4.3)$$

The priority decreases with increasing SoC. Dividing by the predicted remaining time Δt expresses the urgency. We divide by the absolute value $|\Delta t|$ to ensure only non-negative priority values. Division leads to a high priority around the estimated point of departure. This also means an EV's priority decreases the longer it is available after its predicted departure time. We add $\epsilon = 10^{-8}$ to avoid dividing by zero when $\Delta t = 0$. With M , a large number (e.g., $M = 10^5$), we introduce the required bias to ensure that such EVs are preferred which are below their minimum SoC. The time-dependent priority curve is shown in figure 4.2.

4.4 Experimental setup

Our methodology for incorporating historical data includes the R language for the offline steps of data cleansing, feature engineering and training regression models.

Additionally, we use R before each simulation to sample from historical data. We assume a fleet of homogeneous EVs in order to avoid noise due to additional input dimensions such as battery capacity and maximum charging power. The initial SoC is set to 0.2 (or 17kWh) for each EV. The minimum SoC is set to 0.5 (or 42.5kWh). In practice, the minimum SoC would be chosen according to each drivers' needs. All other attributes such as arrival time, departure time and the others listed in Table 4.1 are sampled from the historical dataset using R. In the simulated environment, the connection to the grid is limited to 620 kW. For reference, each EV may charge up to 22 kW. Each charging station is also rated for 22 kW. This lets approximately 28 EVs charge at full power concurrently.

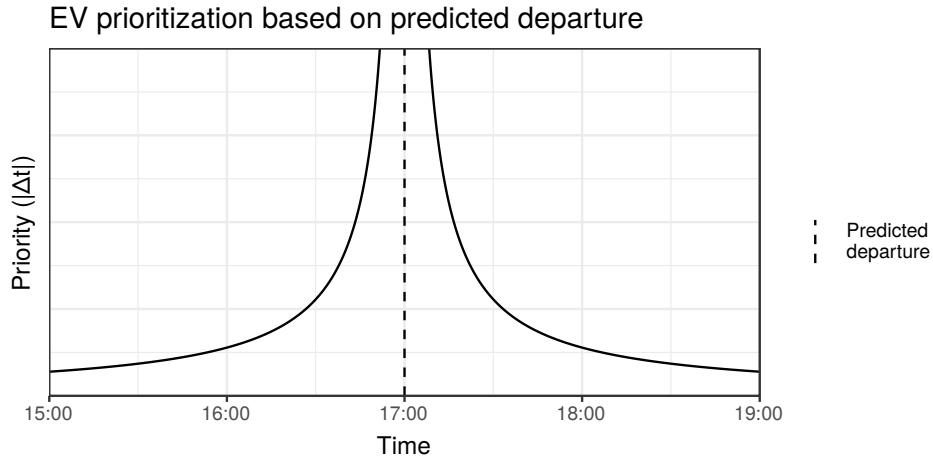


Figure 4.2: EV prioritization based on predicted departure time. In the figure, a departure time of 17:00 has been predicted

We use an extended version of the discrete event simulation described in section 3.3 to simulate real-time smart charging. EVs arrive and depart according to the data generated by R. A trained regression model is used to predict each EV’s departure. This prediction is made available to the charge scheduling heuristic. The main parameters for each simulation are the number of cars and a seed in order to ensure reproducible results especially during data generation. In each simulation, we set the number of available charging stations to be equal to the number of cars covering charging infrastructures with up to 400 stations.

Simulations are performed on a server with an Intel Xeon E5-2660 v4 CPU and 128 GB RAM.

4.5 Experimental results

To recap, we compare regression methods by the MAE (section 4.5.1). However, this does not directly translate to quality of charging schedules. We thus also observe the influence of each regression method on EV prioritization by simulating real-time smart charging. We quantify this secondary effect by the average fraction of minimum SoC as well as by the number of adequately charged EVs (section 4.5.2).

Regression Method	MAE
Constant: Midnight	59444.63
Constant: Historical median	6245.04
Linear regression	5187.79
Artificial Neural Network	5112.99
XGBoost	4911.56
Oracle	0.00

Table 4.3: Mean absolute error (MAE) in seconds, per regression model. Models were trained on historical dataset of roughly 100.000 charging processes

4.5.1 Regression for departure time prediction

Table 4.3 shows the MAE for each method. For XGBoost, we report the mean MAE on the test sets during cross validation. More complex regression models lead to slightly better results. For example, XGBoost predictions are on average 5 minutes more accurate compared to linear regression.

Figure 4.3 shows 395 charging processes of a single driver. The mean departure for this driver is 17:04, the standard deviation is 98 minutes. The fact that a single driver shows such irregular behavior demonstrates the difficulty of predicting departure time.

Other drivers show similarly irregular behavior. For comparison, the average departure time for all drivers is 16:30 and the standard deviation is 141 minutes.

With regard to potential improvements for prediction accuracy, using charging duration as the target feature instead of departure time did not improve MAE. Similarly, MAE was not improved by a different feature selection.

For example, deriving the city from the car park and adding it as an additional variable did not lead to improvements in the MAE of any of the trained regression models.

Feature name	Coefficient	t value
Intercept	-19282.782495	-14.583
Mean Duration by ID	0.965463	146.356
Arrival Timestamp	0.300236	98.038
Mean Timestamp Arrival by ID	0.699365	91.770
Week Day (Monday)	6070.829638	20.318

Table 4.4: Five most significant features (p -value < 0.001) in linear regression model (out of 58 features overall)

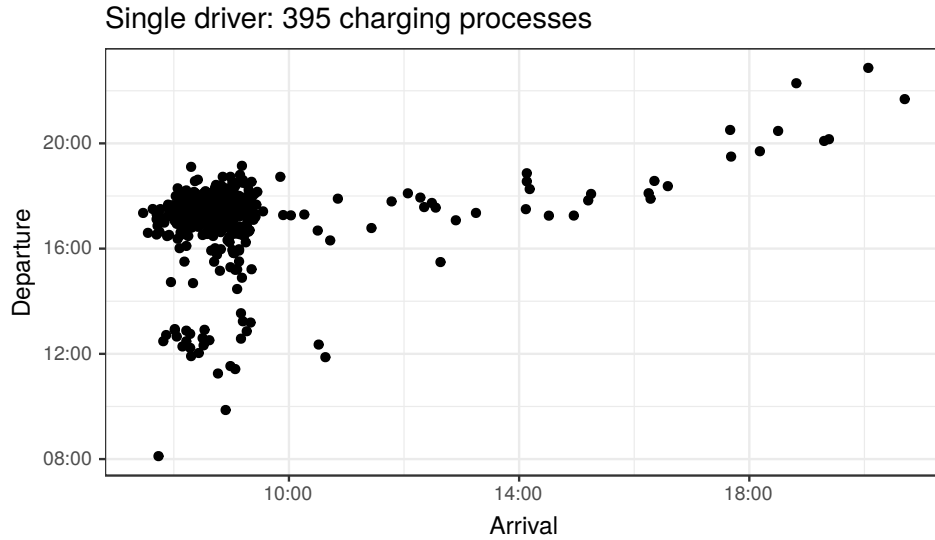


Figure 4.3: Historical data of a single driver shows irregular availability, making it difficult to predict departure time. Arrivals before 10:00 show a large spread in departure times.

Regarding feature significance the linear regression model contains 15 significant features with a p-value below 0.001. The most relevant of these 15 features according to t-value are listed in Table 4.4.

The top features overlap with the top features of XGBoost except for the departure time by ID which is eliminated in the linear regression model due to linear dependency with arrival time and duration. The p-value of the F-statistic is minimal (reported as 10^{-16}) indicating that the linear model is significantly superior to a constant model.

With regard to interpreting the significant variables in Table 4.4 the coefficients of the linear model support intuitive expectations as to which variables are important. A driver's mean historical duration (*Mean Duration by ID*) would be expected to have a major influence on the departure time. This expectation is supported by its coefficient (0.965). The driver's current arrival time (coefficient 0.699) and historical mean arrival time (coefficient 0.300) can be interpreted analogously.

Related work on predicting EV departure time [127, 172] also considers the arrival time as an important variable. The features for individual week days have coefficients ranging from roughly 4.000 (Friday) to 6.000 (Monday). One interpretation is that employees typically stay longer on a Monday compared to a Friday.

Besides MAE another approach to analyzing XGBoost regression results in

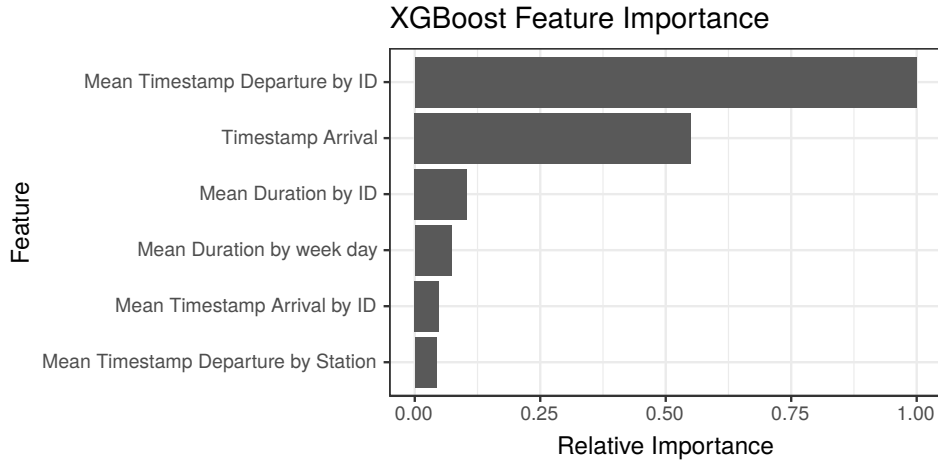


Figure 4.4: Trained XGBoost regression model feature importance: Historical departure time is most important followed by the arrival time.

particular is to visualize feature importance. In tree-based models this can be expressed as the gain per feature. In a single decision tree for a given feature, its gain expresses how well splitting on that feature improves results. XGBoost has multiple trees and thus the gain is averaged over all trees [24]. Figure 4.4 shows the feature importance for the trained model. If available, historical departure time per driver is considered most important followed by the arrival time.

4.5.2 Influence of prediction accuracy on smart charging

This section describes how the results from regression influence the charge scheduling heuristic. To recap, figure 3.2 shows the fraction of minimum SoC which we maximize for a fair share distribution. The experimental results in figure 4.5 show the average fraction of the minimum SoC depending on the number of cars by regression model. Each point represents the average result of 50 simulations with different random sets of EVs (14,000 simulations in total). Using oracle as the perfect predictor produces the highest fraction of minimum SoC for all simulations. This implies that prioritizing EVs accurately leads to an improved fair share distribution.

Regression methods show a wide spread of performance. XGBoost shows the highest mean fraction of minimum SoC followed closely by the neural network and the linear model. Using the historical median departure time of 17:03 as a predictor is slightly worse. Midnight as a predictor shows that a bad prediction

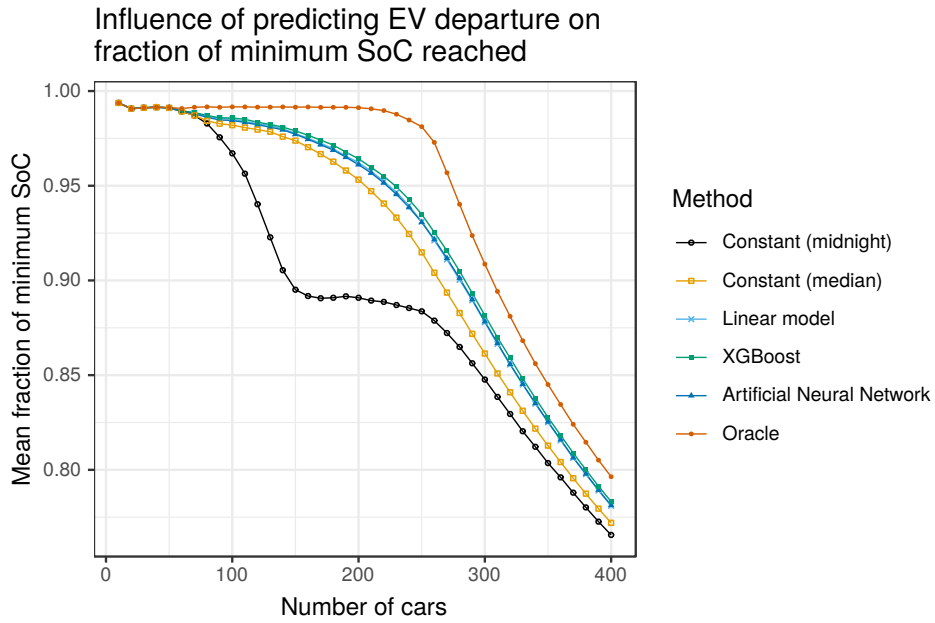


Figure 4.5: Mean fraction of minimum SoC by number of EVs: Perfect information (oracle) clearly leads to the best result, showing that the best possible predictions lead to a fairer distribution.

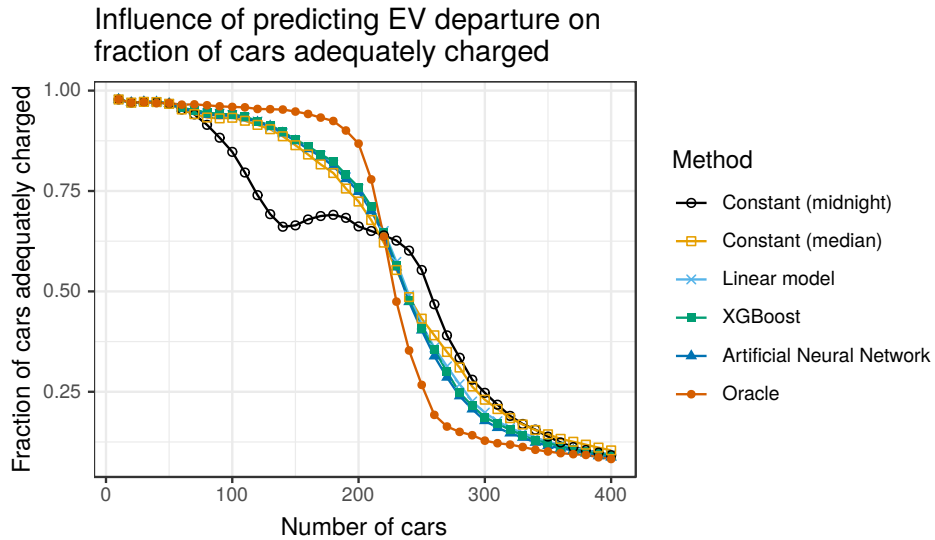


Figure 4.6: Fraction of EVs adequately charged (SoC above the minimum SoC)

leads to a lower mean fraction of minimum SoC. There is also a point at around 250 cars after which there is a strong decline for all methods even if the exact departure is known (oracle). After 250 cars, the bottleneck for sufficient charging is the connection to the grid and not inaccurate prioritization of EVs.

Figure 4.6 shows a different perspective by visualizing the fraction of adequately charged EVs (those above their minimum SoC). At first, the fraction of adequately charged EVs shows behavior similar to the fraction of minimum SoC. However, there is a turning point at around 250 cars. After the turning point, oracle seems to show worse results compared to the other prediction methods. However, this can be explained by the priority function in equation (4.2) prioritizing EVs with the lowest fraction of minimum SoC. If, instead, the priority function were to prioritize for the *highest* fraction of minimum SoC the ranking of the methods in figure 4.6 would be inverted after the turning point. Comparing figures 4.5 and 4.6 after the turning point thus shows the trade-off between fair share and the fraction of adequately charged EVs.

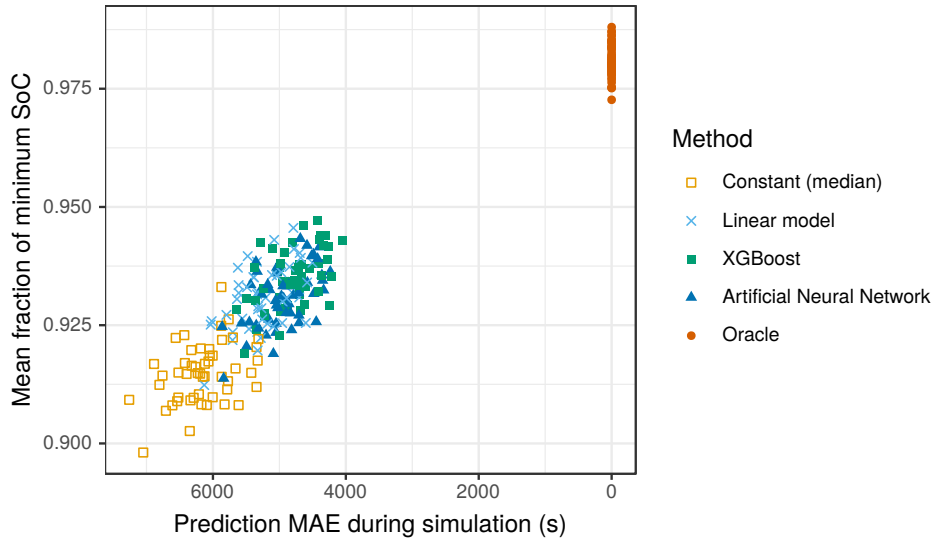


Figure 4.7: Relationship between prediction accuracy and smart charging quality for 250 EVs (correlation: -0.968)

Figure 4.7 shows and quantifies the relationship between prediction accuracy and smart charging quality for 250 cars. Each point represents the result of one simulation. In total, five methods are compared with 50 simulations each. The method where midnight is used as a predictor is omitted since it has a high MAE (> 50.000) and would distort the graph. The graph displays a clear relationship

between MAE and mean fraction of minimum SoC quantified by a correlation of -0.968 (including midnight as a predictor: -0.754). In other words, a higher prediction accuracy leads to higher smart charging quality.

4.5.3 Computation time

An important metric for the practical application of an approach designed to be used in real-time is computation time. In this context, computation time impacts how long an EV waits before receiving a schedule.

Figure 4.8 shows the average computation time per scheduling operation for each regression model. This operation includes one prediction by the regression model (for predicting the departure of the arrived EV) as well as any necessary rescheduling as shown in figure 4.1.

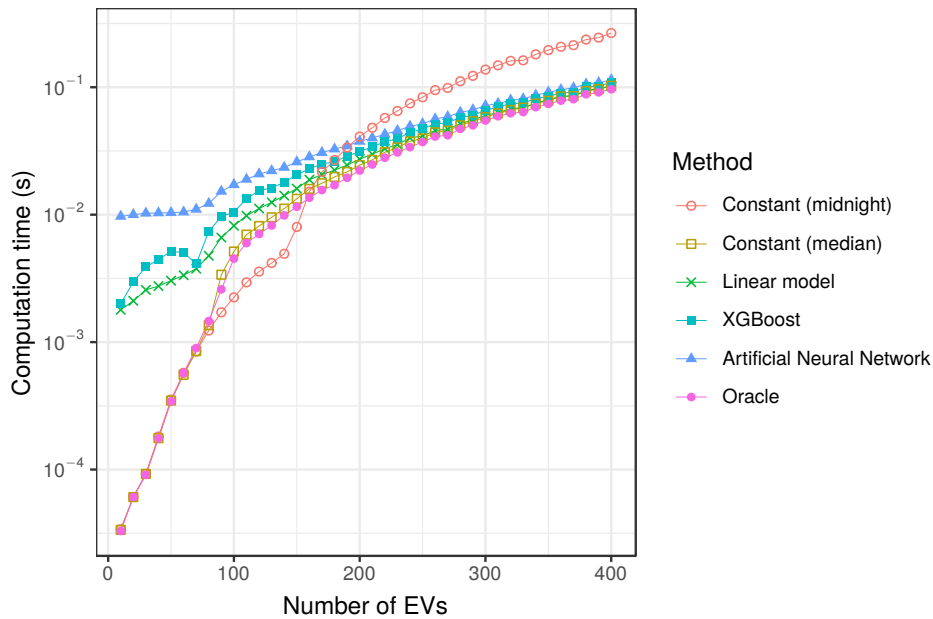


Figure 4.8: Average computation time per scheduling operation

4.6 Discussion

Regarding prediction accuracy the trained regression models show overall similar results with mean absolute errors within one standard deviation (141 minutes). Predicting departure time once (*inference*) is very fast ($<15\text{ms}$) in all of the trained

regression models. Consequently, the computation time of inference does not have an impact on choosing a regression model to use in practice. The overall computation time, which includes scheduling, is sub-second even for 400 EVs making it feasible for a real-time application.

Irregular driver behavior leads to limited predictability based solely on historical data. XGBoost, the best performing prediction method yields an MAE of 82 minutes. Incremental improvements in the regression accuracy can be achieved by refining the regression model. Refinements include increasing the number of charging processes for training and augmenting the dataset with additional features such as part-time employment of drivers.

Improving regression model accuracy would likely lead to a more accurate prioritization and thus improved EV scheduling. However, figure 4.3 illustrates how even a single driver shows irregular behavior. Thus increased regression model accuracy will not reach the perfect predictions of the oracle.

An alternative approach to predicting EV departure time is collecting direct input from users. For example, a reservation system for charging stations allows deducing EV availability. In practice this leads to new challenges including reservation misuse due to collective action problems. Such game theoretical concepts have been applied for achieving efficient reservations [185].

The approach presented in this chapter has the following limitations. First, the approach relies on the availability of a historical dataset of EV charging processes. Second, we assume we know each EV’s model, their SoC upon arrival and the required minimum SoC. If any of the variables are not known, prioritization will be inaccurate. Access to SoC upon arrival is a matter of protocol implementation [72] while the minimum SoC stays user-specific and is subject to data protection regulations. With regard to arrival SoC, experiments in section A.3 show how predictions improve smart charging prioritization if it is unavailable.

With regard to reproducibility, the accuracy of the approach depends on the quality and size of the dataset and the considered scenario. In this work, we consider a scenario with routine arrivals and departures, namely employee charging at the workplace. Predicted departure times in other scenarios containing stays with higher variance would likely be less accurate.

A possible extension to the approach in this chapter could be incorporating additional data for estimating the minimum SoC. For example, data on EV trips such as commute distance may be used as input for predicting the minimum SoC. Other useful variables would be historical energy consumption and whether the EV is charged at locations other than on company premises.

In this chapter, we assume a homogeneous fleet of EVs. A heterogeneous set of EVs differ most importantly in the maximum charging rate p_n and the battery size $b_{n,max}$. In order to apply our approach to a heterogeneous fleet variables p_n

and $b_{n,max}$ must be correspondingly set in equation (3.48). Resulting priorities are relative and unitless and are thus comparable across heterogeneous EVs.

Our prioritization mechanism considers the EV's urgency to charge. Alternative prioritization approaches include minimizing emissions from electricity generation during charging [90] or maximizing electric miles traveled [39].

4.7 Conclusion

This chapter presents an approach to improving smart charging by making use of historical data [54].

We consider the research question of how to address uncertainty of EV availability in order to improve smart charging. Furthermore, we show and quantify the relationship between prediction accuracy and quality of resulting charge schedules.

First, we predict EV departures by training regression models on historical data. In the dataset, the standard deviation for the departure time is 141 minutes. The best model was trained with a mean absolute error of 82 minutes. Next, we improve an existing heuristic for EV charge scheduling by incorporating predictions during EV prioritization. Finally, we quantify the impact of accurate EV departure predictions on smart charging in simulations. Results clearly demonstrate how a higher prediction accuracy leads to a higher mean fraction of minimum SoC.

The next chapters focus on further aspects of uncertainty in smart charging. For example, SoC shares a nonlinear relationship with the current drawn by the EV. A nonlinear smart charging model could more easily reflect this relationship with the potential for more efficient infrastructure usage. Two such nonlinear models are presented in chapter 5 and chapter 6.

Chapter 5

Battery-aware charge scheduling

5.1 Introduction

This chapter presents an approach to adapt the charge scheduling approaches presented in chapters 3 and 4 to how EVs charge in practice.

Section 2.2 describes how one aspect of EV charging in practice is the application of battery charging profiles such as *constant-power, constant-voltage* (CPCV) charging [112]. Battery management systems which implement CPCV first charge at a constant power [134]. Upon reaching a certain battery voltage the charging power is decreased while voltage is kept constant. This means the charging power follows a nonlinear function. In charge scheduling, schedules should take into account this nonlinearity to avoid slack in the allocation of power between EVs.

This chapter discusses extending the charge scheduling heuristic to be able to make use of battery models. In this chapter, we integrate a popular battery model, namely an equivalent circuit model (ECM) [133]. However, the approach is open to integrating arbitrary battery models. Compared to related work, this allows us to accurately consider battery charge profiles such as CPCV during charge scheduling. We address the following research question:

How does considering a battery model impact real-time charge scheduling for EV fleets?

The main contributions of this chapter are:

- We extend the heuristic for charge scheduling EV fleets with an integrated battery model and
- we analyze the impact on the solution quality of charge scheduling by comparing the heuristic with the ECM against the same heuristic with a simplistic battery model.

The remainder of the chapter is organized as follows. First, section 5.2 introduces the context of the charge scheduling problem we consider. The presented solution approach consists of two central components, namely the charge scheduling heuristic and the battery model which are described in section 5.3. Section 5.4 details the simulation setup for evaluation of the presented solution. Numerical results from simulations are presented together with a sensitivity analysis on the initial SoC in section 5.5. Finally, section 5.6 critically discusses the results and section 5.7 provides a conclusion and an outlook.

5.2 Scenario

Overall charging is limited by the rated capacity of the power connection to the grid. Due to the long standing times EVs can be charged to full SoC. However, timeslots in which to charge must be distributed efficiently between EVs in order to reach full SoC.

For studying the effects of battery-aware charging we define a reference scenario with several hundred EVs, the same number of charging stations and an average standing time of 9 hours. We assume a heterogeneous EV fleet with two models and different charging characteristics.

Furthermore, we assume EVs charge using CPCV and follow charge schedules as shown in figure 5.1. The charge schedule communicated by the charging station to the EV defines an upper bound for the charging power. In this chapter we use a more accurate battery model (ECM) in charge scheduling. A more accurate battery model allows charge scheduling approaches to use available infrastructure capacity more effectively and thus increases the overall energy charged by the fleet.

5.3 Method

5.3.1 Battery simulation

Related work on charge scheduling for EV fleets uses various approaches to approximate battery behaviour. Some ignore changing power altogether by assuming a constant power throughout the complete charging process [36, 52, 103, 129, 138]. Others use a continuous or piecewise defined function to express changing battery power [13, 16, 20, 44, 88, 129, 159]. This allows using models traditionally used for scheduling problems such as mixed integer linear programming, at the cost of losing accuracy when it comes to modelling the battery.

In this chapter we present a charge scheduling approach that takes into account how batteries are charged in practice with one possible battery model. This is nec-

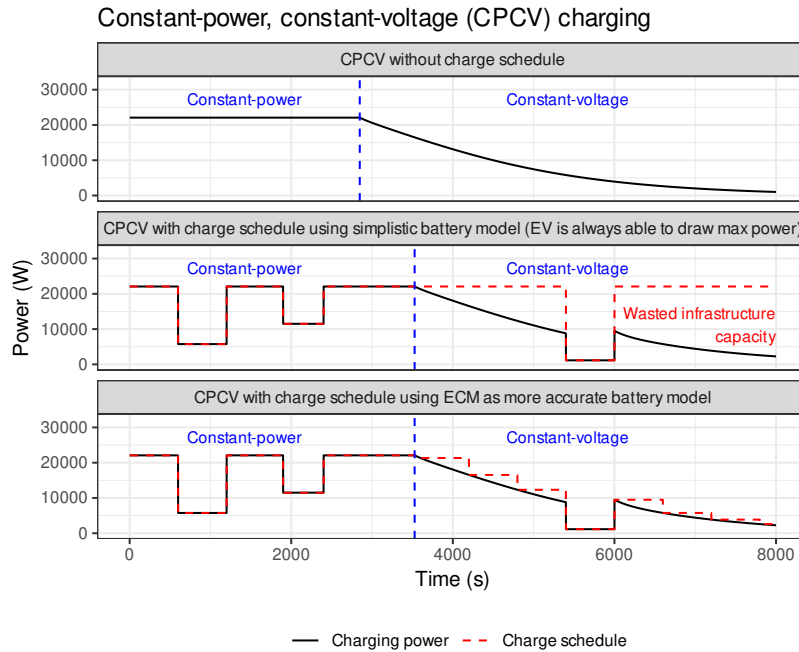


Figure 5.1: CPCV charging of a single EV with and without charge schedules. A more accurate battery model (ECM) leads to charge scheduling with a more effective usage of infrastructure capacity.

essary in order to assign schedules that avoid assigning too much power, i.e., slack, to maximize infrastructure usage. As such we require a more sophisticated battery model similar to the charge scheduling approaches in [36, 66, 147]. Crucially, the maximum current I drawn by the battery must be a function of SoC $z(t)$ since charge schedules may dynamically restrict the rate of charging for future intervals.

We use the well-established equivalent circuit model (ECM) discussed in section 2.2.1, also known as a first order RC model, as one example of describing a single battery cell. To put the ECM into context, the charge scheduling heuristic discussed in section 5.3.3 is able to deal with arbitrary ECMs or other battery models. This ECM in particular was chosen because model parameters are available for two different battery cells used in popular BEVs: LG E63 [125] in Renault’s Zoe and Panasonic NCR18650B [139] in Tesla’s Model S. Properties of the cells are described in more detail in section 5.4. Parameterizing the ECM based on real battery cells allows simulating battery behaviour in the context of real BEVs. ECMs with more components such as further RC circuits would require more parame-

ters. Even if such parameters were publicly available for cells commonly used in BEVs there is a trade-off between model accuracy and computation time. Adding components to the ECM increases accuracy but comes at a higher computational cost [133].

5.3.2 Battery pack

In this chapter we consider a traditional battery pack of parallel connected cell modules (PCMs) as discussed in section 2.2. A PCM consists of N_s modules in series and N_p cells in parallel per module.

For ease of discussion we consider battery cells to be identical. We refer to [134] for a simulation of PCMs where battery cells are not identical. We disregard resistance between battery modules.

Equation (5.1) computes the overall voltage of the battery pack with series-connected modules m .

$$V_{pack}(t) = \sum_{m=1}^{N_s} V_m(t) \quad (5.1)$$

We compute the power draw of the pack according to the standard power formula for series circuits as detailed in equation (5.2) with parallel-connected cells j .

$$P(t) = V_{pack}(z(t)) * \sum_{j=1}^{N_p} I_j(z(t)) \quad (5.2)$$

5.3.3 Charge scheduling heuristic

This section describes the heuristic we present to compute charge schedules for EV fleets. The heuristic is an extension of the schedule guided heuristic presented in section 3.2.2 and internally requires a battery model. The ECM introduced in the previous section represents one possible battery model. We discretize time into 15-minute intervals which correspond to energy market timeslots. One aspect of how we use the ECM is to distribute power evenly within each timeslot, compared to related work which integrates ECMs in model predictive control (MPC) approaches to set a power limit at the beginning of a timeslot [36, 66, 147].

An overview of the heuristic is shown in figure 5.2. We first schedule each EV in the fleet individually upon arrival. We then check each timeslot for violations: Do charge schedules lead to the grid connection being overloaded? If there are any violations, we calculate a priority per EV using equation (5.3). We then reschedule the EV(s) with the lowest priority.

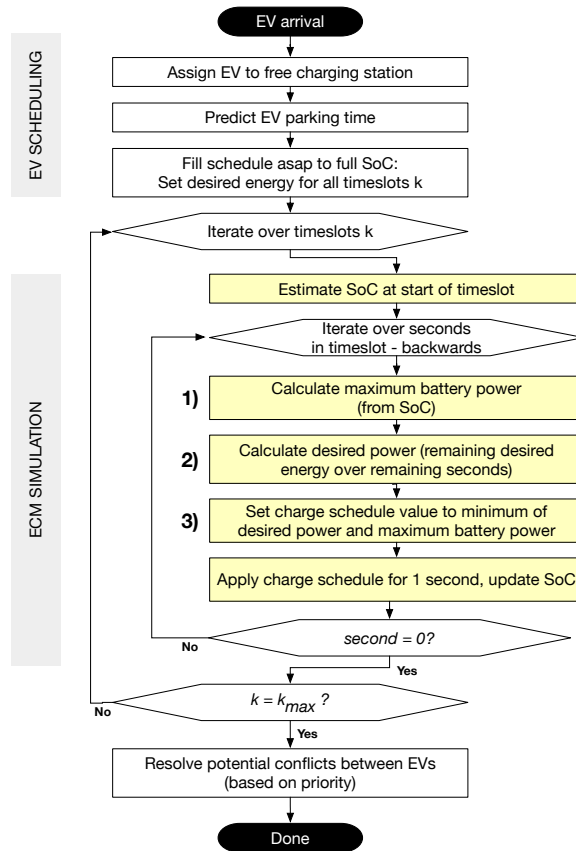


Figure 5.2: Flowchart of the charge scheduling heuristic: Yellow fields indicate operations involving a battery model. Numeric labels correspond to operations detailed in section 5.3.3.

During rescheduling we reduce an EV’s assigned power such that the sum over all EVs charging respects the infrastructure limit. We then calculate the lost energy that would have been charged in this timeslot. If possible, the lost energy will be distributed to other timeslots.

We schedule new arrivals independent of existing schedules even though this may cause violations. Scheduling is applied with this isolated perspective at first because new arrivals may have the highest priority. Equation (5.3) shows how the priority per EV is computed. The priority expresses charging urgency by including the remaining time until departure (5.4).

EVs are prioritized by how far below their minimum SoC z_{min} they are. The currently charged energy of each EV is normalized by the maximum current $I(t)$ it

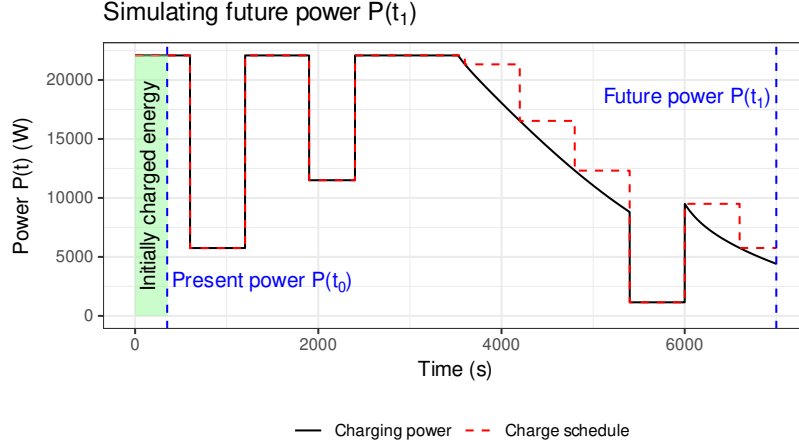


Figure 5.3: Simulating future power $P(t_1)$ in CPCV ahead of time given charge schedule and initially charged energy for a single EV

can draw which depends on output of the battery model. EVs above their minimum SoC are penalized via term M , a large number (e.g., $M = 10^5$).

The departure time $t_{\text{departure}}$ may be computed using forecasting or other methods for estimation and has been described in chapter 4. In this chapter, we assume we know the EV's departure time.

$$priority(t) = \begin{cases} \frac{Q^*(z_{min} - z(t))}{|\Delta t| * I(t) + \epsilon}, & \text{if } z(t) < z_{min} \\ \frac{Q^*(1 - z(t))}{|\Delta t| * I(t) + \epsilon} - M, & \text{otherwise} \end{cases} \quad (5.3)$$

$$\Delta t = t_{\text{departure}} - t \quad (5.4)$$

The battery model is involved in three main operations as shown in figure 5.2. An overview of the variables can be found in the nomenclature in section A.2.

1) Maximum power. We refer to $P(t)$ as the maximum power that each EV in the fleet is able to draw at any point in time t . Accurate values for $P(t)$ are required ahead of time to minimize slack in charge schedules of the fleet. In this context, slack is caused by each charge schedule that is not fully utilized by the EV. Slack represents power that cannot be assigned to other EVs, leading to an inefficient usage of charging infrastructure.

For example: Given an EV in the constant-voltage phase which can draw up to $P(z(t)) = 10kW$ and a charge schedule with $P_{CS}(t) = 15kW$ there is $5kW$ of slack. The maximum power $P(t)$ under CPCV in one simulation is shown in figure 5.3.

2) Planned capacity. Next, equation (5.5) expresses how much energy (Ah) will be charged in an interval $[t_1, t_2]$. The amount of energy is required for rescheduling EVs to ensure the planned capacity is the same in the original and the rescheduled timeslot. Figure 5.4 shows a sample interval $[t_1, t_2]$ with the area under the curve that must be computed.

$$PlannedCapacity(t_1, t_2) = \int_{t_1}^{t_2} P(t) dt \quad (5.5)$$

3) Charge schedules. Lastly, charge schedules $P_{CS}(t)$ must be computed. We use the notation $P_{CS}(t_1, t_2)$ to describe a scalar value valid for the interval $[t_1, t_2]$. The goal is to find a minimum power $P_{CS}(t_1, t_2)$ for an interval $[t_1, t_2]$ given desired energy \hat{P}_{t_1, t_2} (kWh).

Computing $P_{CS}(t_1, t_2)$ leads to charge schedules with exact amounts of energy during initial scheduling and rescheduling. We maximize energy charged (5.6) while not charging more than required (5.7) and avoiding slack (5.8).

$$\max \quad \int_{t_1}^{t_2} P(t) dt \quad (5.6)$$

$$\text{s.t.} \quad \int_{t_1}^{t_2} P(t) dt \leq \hat{P}_{t_1, t_2} \quad (5.7)$$

$$P_{CS}(t_1, t_2) \leq \min\{P_{CP}, P(t)\} \quad (5.8)$$

In the following we detail two possible implementations of the three steps described above. The first implementation *a)* assumes a simplistic battery model with constant power and operations **a.1)**, **a.2)** and **a.3)**. The second implementation *b)* uses the ECM to consider decreasing power as in CPCV with operations **b.1)**, **b.2)** and **b.3)**.

Simplistic implementation with constant battery power.

a.1) Maximum power. The maximum power P_{CP} is assumed to be always available for charging unless a charge schedule $P_{CS}(t)$ is defined during t . This is expressed by equation (5.9) where we use $P^{lin}(t)$ to refer to a linear estimation of the actual $P(t)$. This implementation thus ignores the constant-voltage phase of CPCV.

$$P^{lin}(t) = \min\{P_{CP}, P_{CS}(t)\} \quad (5.9)$$

a.2) Planned Capacity. Equation (5.10) shows how the energy that will be charged in an interval $[t_1, t_2]$ may be trivially estimated with efficiency η if battery power is constant.

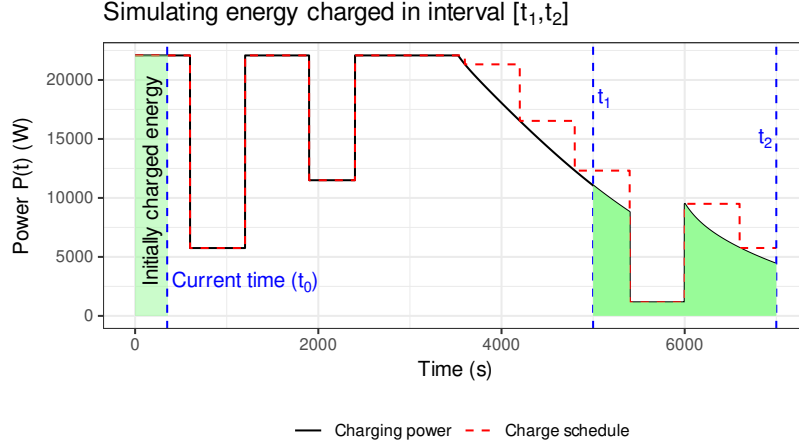


Figure 5.4: Simulating the energy (Wh) that will be charged for a single EV in a future interval given a charge schedule

$$PlannedCapacity^{lin}(t_1, t_2) = \min\{P_{CP}, P_{CS}(t_1, t_2)\} * \eta * (t_2 - t_1) \quad (5.10)$$

a.3) Charge schedules. Charge schedules for interval $[t_1, t_2]$ are computed using equation (5.11). The charge schedule strategy is to use the maximum battery power when the EV can consume it for the complete interval. Otherwise, if the desired energy \hat{P}_{t_1, t_2} can be filled in the interval the power is scaled down to spread the energy over the interval.

$$P_{CS}^{lin}(t) = \min\{P^{lin}(t), \frac{\hat{P}_{t_1, t_2}}{(t_2 - t_1) * \eta}\} \quad (5.11)$$

Implementation assuming CPCV charging. In the following we describe how we take into account CPCV charging in the charge scheduling heuristic. To begin with, we define a discrete time formulation for simulating CPCV with battery models such as this ECM. We first convert the differential equations (2.1)-(2.2) that describe the ECM in circuit 2.1 to discrete time [134]. We use the symbol k to refer to k discrete steps of the simulation. We use a step size of $\Delta t = 1s$.

We refer to the system of equations (5.12)-(5.16) as the discrete time formulation [36, 134] of the ECM in Circuit 2.1. A simulation of the ECM via the discrete time formulation with and without charge schedules is shown in figure 5.1.

Equations (5.12)-(5.14) are used to simulate the constant-power phase. A fixed voltage term $v_f[k]$ is introduced to simplify the notation. Equation (5.13) applies charge schedules $P_{CS}[k]$.

$$v_f[k] = V_{OC}(z[k]) - i_{R_1}[k] * R_1(z[k]) \quad (5.12)$$

$$p_{max}[k] = \min\{P_{CP}, P_{CS}[k]\} \quad (5.13)$$

$$i[k] = \frac{v_f[k] - \sqrt{v_f^2[k] - 4 * R_0(z[k]) * p_{max}[k]}}{2 * R_0(z[k])} \quad (5.14)$$

Equation (5.15) corresponds to equation (2.2) and is used to calculate current at step k during the constant-voltage phase.

$$v_{terminal} = V_{OC}(z[k]) - i[k] * R_0(z[k]) - i_{R_1}[k] * R_1(z[k]) \quad (5.15)$$

Lastly, equation (5.16) is used during each step to update the SoC and corresponds to equation (2.1).

$$z[k + 1] = z[k] - \frac{\eta \Delta t}{Q} i[k] \quad (5.16)$$

b.1) Maximum power. The maximum power $P(t)$ is determined ahead of time by simulating the ECM from the current time t_0 with given initial SoC $z(t_0)$ and charge schedules. Equations (5.12)-(5.16) are used to simulate the ECM. We use $P^{cont}(t)$ as an estimate of the actual $P(t)$ in equation 5.17.

The maximum power $P(t)$ in a sample simulation is shown in figure 5.3.

$$P^{cont}(t) = p[k] \quad (5.17)$$

b.2) Planned capacity. The energy that will be charged in interval $[t_1, t_2]$ is computed analog to computing the maximum power. To take into account the current SoC at t_0 we simulate from current time t_0 to the end of the interval t_2 . During the simulation, we record $P(t)$. Equation (5.18) computes the energy that was charged. The energy charged in a sample simulation is shown in the area under the curve in figure 5.4.

$$PlannedCapacity(t_1, t_2)^{cont} = \sum_{t=t_1}^{t_2} P^{cont}(t) \quad (5.18)$$

b.3) Charge schedules. We compute charge schedules by solving equation (5.16) for $i[k]$. The goal is to find a scalar value $P_{CS}(t_1, t_2)$ for a charge schedule for the

Algorithm 1 Computing optimal charge schedule value $P_{CS}(t_1, t_2)$

Initialize target SoC

$$z_1 \leftarrow z_0 + \frac{\hat{P}_{t_1, t_2}}{\hat{P}_{total}}$$

Start at end of interval

$$k \leftarrow k_2$$

$$z[k] \leftarrow z_1$$

while $k \geq k_1$ **do**

Compute maximum battery power

$$i[k] \leftarrow \text{Use equations (5.14), (5.15)}$$

$$p[k] \leftarrow v[k] * i[k]$$

Compute power to fill rest of desired energy

$$p_{desired} \leftarrow (\hat{P}_{t_1, t_2} - \hat{P}_{total} * (z_1 - z[k])) / (\eta * (k - k_1))$$

$$P_{CS}(t_1, t_2) \leftarrow \min\{p[k], p_{desired}\}$$

if $p_{desired} \leq p[k]$ **then return** $P_{CS}(t_1, t_2)$

end if

$$z[k - 1] \leftarrow z[k] + \frac{\eta * \Delta t}{Q} * i[k]$$

Simulate backwards

$$k \leftarrow k - 1$$

end while

return $P_{CS}(t_1, t_2)$

interval $[t_1, t_2]$. To recap: With the charge schedule, we maximize the energy charged (5.6) and follow the constraints in (5.7)-(5.8).

The process of computing the charge schedule $P_{CS}(t_1, t_2)$ with desired energy \hat{P}_{t_1, t_2} is shown in Algorithm 1. To recap, we consider $k = t$ with step size $\Delta t = 1s$. We initialize z_1 as the targeted SoC. This enables us to compute the maximum power $p[k_2]$ at the end of the interval. The variable $p_{desired}$ is the charging power that would lead to filling the rest of the desired energy. We simulate backwards until we need to set a lower value $p_{desired}$ compared to what the battery could handle ($p[k]$). At the same time, we avoid slack in the charge schedule assignment by restricting $P_{CS}(t_1, t_2)$ to the maximum battery power.

5.4 Simulation setup

We use simulations to quantify the impact of battery models integrated in the charge scheduling heuristic. To begin with, we simulate one day of an EV fleet charging with varying numbers of EVs (section 5.4.1). During the simulation of an EV fleet, we use the charge scheduling heuristic to compute charge schedules. In-

ternally, the charge scheduling heuristic uses the ECM to simulate CPCV charging. We describe how we parametrize the ECM in section 5.4.2.

Label	Scheduling method
a)	Simplistic charge scheduling: Charge scheduling heuristic using a simplistic constant-power battery model
b)	Battery-aware charge scheduling: Charge scheduling heuristic using a more sophisticated equivalent circuit model (ECM) to accurately reflect decreasing power during the constant-voltage phase of CPCV charging

Table 5.1: Simulation setup: The charge scheduling heuristic with the ECM is compared against the same heuristic with a simplistic battery model

5.4.1 EV fleet simulation

Simulation results are gathered from the discrete event-based simulation presented in section 3.3.2. The battery model for each EV implements equations (5.12)-(5.16). We vary the number of EVs between 100 and 200 to check whether differences are consistent across different simulation parameters. Each EV is assumed to arrive with an initial SoC of 0.8 representing a typical value for frequently recharging commuters' cars. We measure the average final SoC at the end of simulations.

We perform a detailed comparison of results for initial SoC 0.8 to compare how the two different phases (constant-power and constant-voltage) of CPCV charging impact simulation results. The switch from CP to CV charging happens at an SoC of 0.88 for the Panasonic cell and at 0.96 for the LG cell. We further perform a sensitivity analysis in section 5.5 for how initial SoC impacts simulation results.

5.4.2 Battery simulation

We use the ECM parameters in Table 5.2 based on tests of two real battery cells which are used in popular BEVs. Using two cells allows analyzing scenarios with homogeneous as well as heterogeneous fleets of EVs by of way example. Panasonic's cell NCR18650B is used in Tesla's Model S in a 96s74p configuration [96]. LG's cell E63 is used in Renault's Zoe in a 96s2p configuration [125].

For example, Figure 5.5 shows the data for the open circuit voltage $V_{OC}(z(t))$ of the LG E63 battery cell [30]. Values between points are estimated using linear interpolation. The same approach is used for the Panasonic NCR18650 data [139] and its open circuit voltage follows a similar curve.

ECM parameters are given with respect to a constant temperature of 23°C for the NCR18650B cell and 25°C for the E63 cell. In practice, ECM parameters would vary with temperature which changes during the charging process. However, for ease of discussion temperature effects are considered out of scope for this chapter.

Parameter	Renault Zoe [125]	Tesla Model S [96]
Battery cell	LG E63 [30]	Panasonic NCR18650B [139]
Cell capacity Q	65.6Ah	3.350Ah
Open circuit voltage $V_{OC}(z(t))$	See [30] or figure 5.5	See [139]
Terminal voltage $V_{terminal}$	4.166V	4.1099V
Modules in series N_s	96	96
Cells per module N_p	2	74
Constant-power P_{CP}	115W	3.108W
Efficiency η	0.85	
Initial SoC $z(t_0)$	0.8	
Minimum SoC z_{min}	0.5	

Table 5.2: Simulation parameters for the equivalent circuit model (ECM) and EVs. Other SoC dependent parameters $R_0(z(t))$, $R_1(z(t))$, $C_1(z(t))$ are also from [30, 139].

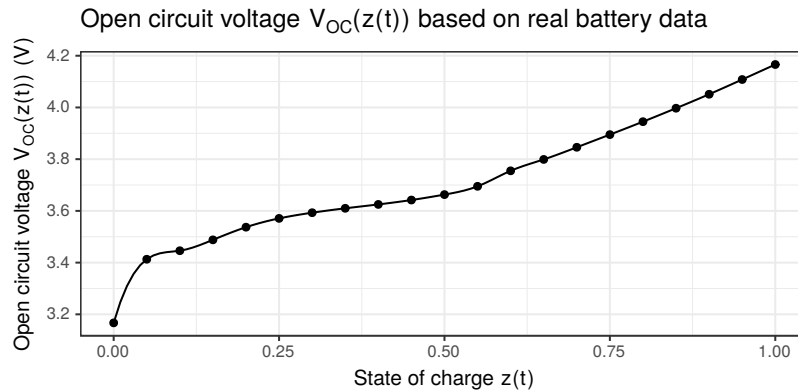


Figure 5.5: Open circuit voltage $V_{OC}(z(t))$ based on data for LG's E63 battery cell. Values between points are interpolated.

Operation	<i>a) Simplistic battery model</i>	<i>b) Equivalent circuit model</i>
1) Estimate maximum current $P(t_1)$ at time t_1	Assumes Constant-Power (5.9)	Simulate ECM until t_1 and record $P(t_1)$ (5.17)
2) Estimate planned energy in interval $[t_1, t_2]$	Trivial estimation (5.10) using linear scaling	Simulate ECM from current time until t_2 and record $P(t)$ (5.18)
3) Assign charge schedule $P_{CS}(t)$	Maximum or scaled down power (5.11)	Approach in Algorithm 1

Table 5.3: Overview of the three battery model operations needed for the charge scheduling heuristic

5.5 Simulation results

Figure 5.6 shows results for different fleet sizes and compositions. Results for the heuristic using simplistic charge scheduling *a)* and battery-aware scheduling *b)* are compared. Each graph represents a different fleet composition. The first two graphs show simulations of homogeneous fleets (Tesla Model S and Renault Zoe and their respective battery cells). The third graph shows results for heterogeneous fleets with an equal number of each car model per fleet size. To recap, the parameters shown in Table 5.2 lead to a switch from CP to CV at an SoC of 0.88 for Panasonic cell and at 0.96 for the LG cell.

Figure 5.7 shows the relative improvement in mean final SoC reached with battery-aware *b)* compared to simplistic *a)* charge scheduling. Notably, battery-aware scheduling allows charging up to 8.67% more energy consequently leading to a higher mean final SoC.

After a certain point in all graphs, the improvement curve levels off. The flattening is explained by the fact that the grid connection is the bottleneck, independent of which version of the charge scheduling heuristic is used. Scheduling with the battery-aware version of the charge scheduling heuristic *b)* shows consistently better performance compared to the simplistic version *a)* for fleets containing Tesla Model S vehicles.

The higher mean final SoC can be explained by the more accurate scheduling during the constant-voltage phase of charging. Only for the homogeneous Zoe fleet is there no significant improvement from using *b)* because the LG E63 cell used by the Zoe switches to a CV phase at a very high SoC of 0.96.

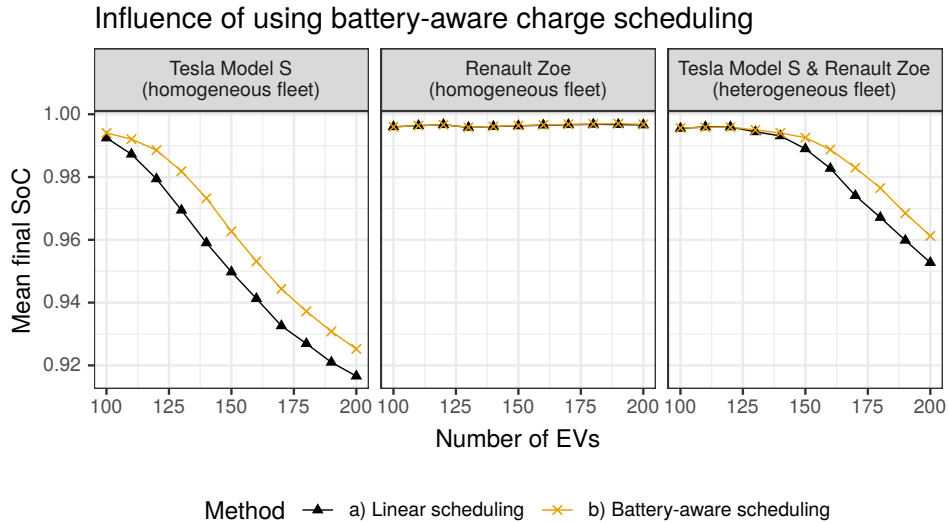


Figure 5.6: Simulation results: Mean final SoC over increasing numbers of EVs for different fleet compositions. Battery-aware scheduling, which uses an ECM as a battery model, shows consistently better performance given an initial SoC of 0.8.

Sensitivity analysis. We perform a sensitivity analysis to further analyze the impact of initial SoC on simulation results. We hold the number of cars constant at 150. We modify the initial SoC from 0.50 to 0.95 in steps of 0.05.

The results in Table 5.4 show that if EVs charge primarily in constant-power mode there is no significant impact of battery aware charge scheduling. Likewise, there is no improvement with initial SoC ranging from 0.00 to 0.50.

However, starting with an initial SoC of 0.50 there is a significant improvement in the final SoC when comparing the linear *a)* and battery-aware version *b)* of the charge scheduling heuristic. On average, EVs are charged by up to 8.67% more. For initial SoC values above 0.5, EVs charge mostly using constant-voltage charging and thus require the more accurate schedules of the battery-aware heuristic *b)*.

To put this into context: In chapter 3, we use historical data which contains more than 100.000 charging processes on company premises with a diverse set of EVs and charging behavior. For BEVs, the average charged energy is 15.1kWh. For a battery size of 40kWh (Renault Zoe) and 85kWh (Tesla Model S) this corresponds to an initial SoC of 0.62 and 0.82. The sensitivity analysis shows this value lies in the region for which the battery-aware version of the charge scheduling heuristic *b)* produces better results compared to the heuristic which uses a constant-power battery model *a)*.

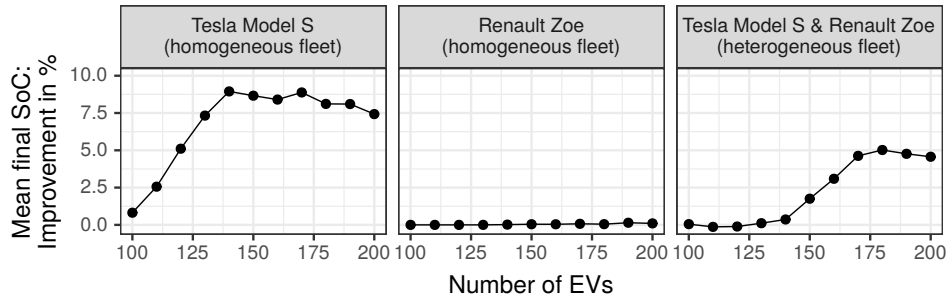


Figure 5.7: Simulation results: Improvement in mean final SoC reached with battery-aware *b*) over simplistic *a*) charge scheduling. Battery-aware scheduling *b*) allows charging up to 8.67% more energy.

Initial SoC	Mean final SoC a)	Mean final SoC b)	Relative difference
0.50	0.670	0.670	0.00%
0.55	0.719	0.720	0.59%
0.60	0.768	0.770	1.19%
0.65	0.816	0.819	1.81%
0.70	0.863	0.867	2.45%
0.75	0.908	0.915	4.43%
0.80	0.950	0.963	8.67%
0.85	0.982	0.993	8.33%
0.90	0.997	0.998	1.03%
0.95	0.999	0.999	0.00%

Table 5.4: Sensitivity analysis of initial SoC: Simulations where EVs spend more time in the constant-voltage phase (initial SoC starting with 0.5) show an improvement when using the ECM as a battery model to reflect CPCV.

A further parameter that may be varied is the target maximum SoC. Some battery management systems allow manually setting a target maximum SoC less than 100% to mitigate battery degradation. With decreasing target maximum SoC the benefit from using the ECM in method *b*) over *a*) also decreases. In this chapter we assume a target maximum SoC of 100%. This value is motivated by the underlying business scenario described in section 5.2, where we consider charging infrastructure and stations as scarce resources. Consequently, the EV may not be able to charge daily and thus requires a full charge at each charging opportunity.

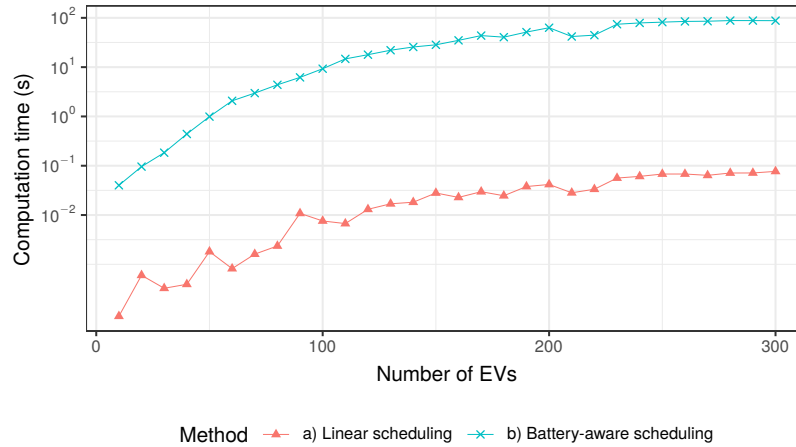


Figure 5.8: Average computation time per rescheduling operation of *a)* and *b)*

Computation time. An important aspect of the applicability of the charge scheduling heuristic is its computation time. Figure 5.8 shows the average computation time per rescheduling operation for the simulations executed for figure 5.6. In other words, how long does an EV wait, on average, until it receives a charge schedule?

Computation time for both methods increases with the number of EVs. Rescheduling as described in section 5.3.3 takes longer for higher numbers of affected EVs. Battery-aware scheduling *b)* is clearly slower as it is more computationally complex compared to the linear version *a)* of the heuristic. However, absolute values of computation time per rescheduling operation remain in the order of 90 seconds for fleets of up to 300 EVs.

5.6 Discussion

The charge scheduling heuristic combined with the ECM *b)* leads to improved charge schedules for EV fleets compared to scheduling using a simplistic battery model. Improvement is understood as a more efficient use of the charging infrastructure and thus a higher mean final SoC among EVs. The sensitivity analysis shows the highest improvement is achieved for charging processes where batteries are at least half charged initially. In practice, high initial SoC values occur in scenarios where EVs travel short distances such as the commute to the workplace.

The presented cross discipline approach combines the domains of battery modelling and charge scheduling. Results show how improvements in charge schedul-

ing gained by using the ECM over the simplistic battery are higher the longer the constant-voltage phase of the battery cell is. The duration of the constant voltage phase differs by battery cell model and is influenced by various factors including resistance R_0 . The practicality of the approach presented in this chapter depends on the public availability of model parameters of the battery cells.

This approach shows that the total power charged by an EV fleet increases when integrating an ECM in charge scheduling. The improvement achieved with an established battery model indicates further potential for improvement with more sophisticated models from battery research. This chapter encourages studying the integration of improved battery models once they become practically usable with parameters of real battery cells published in the future. More sophisticated models could include additional variables such as state of health and temperature given that a public dataset become available which includes these parameters.

Possible extensions to this approach include simulating charge profiles other than CPCV. Examples of other charge profiles include multiple stages of CP with decreasing power or rapid charge profiles [56]. The findings of this chapter still apply for these profiles as they are characterized by decreasing power compared to the constant power assumed by the simplistic battery model.

5.7 Conclusion

In practice, EVs are commonly charged using charging profiles with decreasing power. Related work on charge scheduling for EV fleets, however, often use a simplistic battery model with a linear or even constant relationship between battery power and the battery's SoC [168]. In contrast, we present a charge scheduling heuristic able to directly integrate battery models such as an ECM. Using the ECM improves the accuracy of charge schedules during the constant-voltage phase.

We address the research question of how charge scheduling is impacted by considering a more sophisticated battery model. First, we describe how CPCV charging can be modelled using an established equivalent circuit model (ECM) [133]. The ECM may be simulated by converting a set of differential equation to a discrete time formulation. Next, we describe the battery-aware charge scheduling heuristic. The heuristic uses the ECM to estimate a battery's future maximum power, to estimate the energy that will be charged in an interval and to compute charge schedules. The ECM is interchangeable and other battery models may also be integrated into the heuristic.

We use simulations to compare the charge scheduling heuristic with the integrated ECM against the same heuristic with a simplistic battery model. Simulation results with different numbers of EVs in the fleet show a consistently higher mean

final SoC by the scheduling heuristic with the integrated ECM. A sensitivity analysis on initial SoC further shows the difference is highest when EVs charge mostly in the constant-voltage phase.

The next chapter focuses on the charge scheduling heuristic with a different battery model. A data-driven approach is presented which uses regression models trained on historical data to model charging behaviour.

Chapter 6

Data-driven charge scheduling

6.1 Introduction

One of the main limitations of the battery-aware approach in chapter 5 is the availability of parameters for equivalent circuit models (ECMs). This chapter uses regression models instead of ECMs to predict battery behavior. Using regression models also makes it simpler to generalize to new EV models. In this chapter we consider heterogeneous EV fleets which consist of different EV models.

Existing approaches to smart charging such as [117] have achieved real-time charge scheduling with increasing efficiency in the assignment of scarce charging resources. However, in practice the execution of the charge schedules deviates from the theoretically planned schedules when the complex charging behavior of the EVs themselves are not reflected in the scheduling decisions [93]. Battery management systems (BMS) in EVs control the charging behavior of the battery [134]. In particular, BMS limit the power drawn during charging to protect battery health and safety. Consequently, reserved infrastructure charging capacity is wasted when batteries draw less power than planned by the central smart charging system.

As discussed in section 2.2 battery behavior during charging is determined via the BMS' implementation of *charging profiles*. Charging profiles express charging currents drawn over time. Common charging profiles include constant-current, constant-voltage (CCCV) [100]. Charging profiles represent patterns that can be observed in every charging process. Figure 6.1 shows a simulation of a CCCV process compared to a real process. The CCCV process was simulated by one of the ECMs described in chapter 5.

The approach used in chapter 5 uses ECMs to model battery behavior. Detailed parameters of an ECM as well as the battery pack composition generally equate to trade secrets of the manufacturers and are cumbersome to determine via experi-

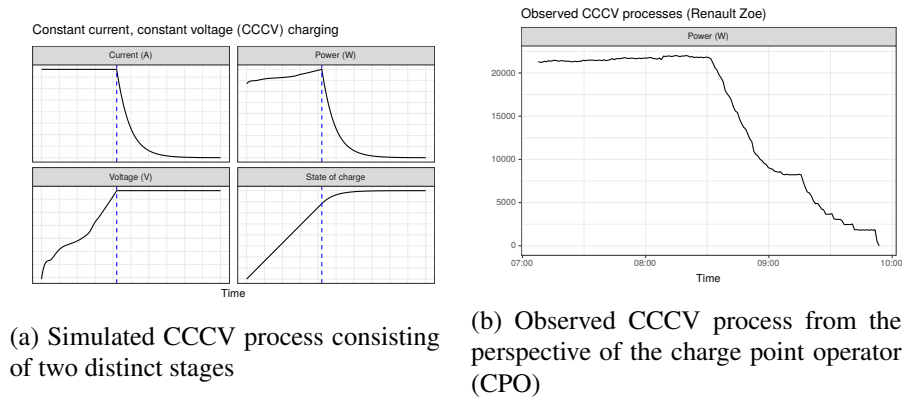


Figure 6.1: CCCV: Simulation vs observed process

mental battery measurements and reverse engineering. Modelling battery behavior with factors such as temperature and battery state of health (SoH) requires more complex ECMs and more data.

In this chapter, we use an alternative approach to modelling battery behavior. Instead of approximating battery behavior by adding more and more refining elements in an ECM we infer charge profiles from a machine learning model that has been trained on real historical data.

The ECM model requires battery parameters (resistance and capacitance) and battery inputs and outputs (voltage and current). In contrast, the model learned via machine learning only requires the car model and its state of charge. We compare different machine learning models, namely linear regression, neural networks and XGBoost. The learned battery behavior is directly incorporated in smart charging.

We thus present an integrated approach which produces charge plans for a heterogeneous set of EVs while considering their battery behavior. The approach was proposed in [55]. We address the following research question:

How do integrated predictions of battery charge profiles affect smart charging?

The main contributions of this chapter are:

- A methodology for preprocessing a dataset and training a regression model to predict battery charge profiles,
- the integration of the regression model into a charge scheduling heuristic and
- a quantification of the impact of integrated charge profile predictions on smart charging in simulations of historical data

The remainder of the chapter is organized as follows. Section 6.2 introduces the data-driven methods, including the methods for data preparation, the machine learning models and the embedding smart charging heuristic. Sections 6.3 and 6.4 describe the experimental setup and the experimental results for smart charging with an integrated prediction mechanism for battery behavior. Finally, section 6.5 discusses the applicability and limitations of the results while section 6.6 presents the conclusions of this chapter.

6.2 Method

6.2.1 Data preparation

This section discusses the methodology we use to clean and preprocess a dataset of meter values collected from charging stations in order to train regression models. We use the term *charging process* to refer to the complete session of an EV charging. We use the term *meter value* to refer to a single data point of a time series. For example, a measured power of 10kW at a charging station at 10:18 is one meter value. Each charging process is associated with one time series of power over time. In contrast to related work such as [120], we do not simulate this time series but work with real data. We use the R programming language for dataset preparation.

Attribute	Sample value
EV data (18 unique models)	
Battery capacity	41.000Wh
Maximum power	22080W
Three phase charging	True
Charging process data (10.595 processes)	
Arrival time	08:12:37
End time	17:48:01
Car model	Renault Zoe (2018)
Total power consumption	26120Wh
Meter value data (Granularity: 1 minute, 5.2 million data points)	
Timestamp	09:01:37
Power	22.080W

Table 6.1: Dataset raw attributes

Dataset structure. To begin with, we gather EV model data published by manufacturers (Table 6.3). We then combine the manufacturer’s EV model data with

the charging process data and the meter value data. Meter value data is gathered with a granularity of 1 minute. Table 6.1 shows the raw attributes of the dataset.

Dataset characteristics. The dataset consists of 10.595 uncontrolled charging processes gathered from employee charging at the workplace. The processes stem from the years 2016-2018 and from 1001 EVs charging at 338 charging stations in 8 different cities. The EV fleet is heterogeneous and is composed of 18 unique EV models, each of which has different values regarding maximum charging rate, battery capacity, three phase charging (see Table 6.3). BEVs typically charge on three phases while PHEVs usually charge on a single phase. The mean energy charged per charging processes is 7.01kWh while the mean duration is 7 hours and 17 minutes.

Dataset preprocessing. Next, we describe the steps we perform for cleaning and preprocessing the dataset. To begin with, we estimate SoC assuming a charging efficiency η of 0.85. Based on studies [7, 84, 145] on EV charging, this is an optimistic value. EV charging efficiencies computed from experimental data include values of 85% [145], between 60% and 85% [84] or between 64% and 88% [7]. In practice, charging efficiency is not constant but a function of attributes of EV charging such as heat, SoC and power. For the sake of simplicity, we assume a constant value.

We use equation (6.1) to estimate the SoC $z_{n,t}$ for EV n at t . We use the time series X of a charging process to compute the SoC as the difference between the EV's capacity Q_n (Wh) and missing relative capacity based on the previously charged energy X_t (Wh) taking into account efficiency η .

$$z_{n,t} = Q_n - \eta * \frac{X_{end} - X_t}{Q_n} \quad (6.1)$$

Data cleansing. First, we remove processes without an associated car model. Such processes can be a result of backend system tests. Next, we remove processes with negative SoC values. Negative SoC values are generated by equation (6.1) in processes where our efficiency estimate (85%) is too optimistic. We also limit processes to those with a maximum length of 24 hours. We assume longer stays contain irregular charging behavior not in the scope of charging at the workplace. Similarly, we remove processes shorter than 10 minutes.

We remove charging processes with missing data due to charging station connectivity problems. Furthermore, we remove charging processes with a flat charging profile. We assume processes with a flat charging profile were stopped before reaching full SoC and thus have no second charging profile stage. We identify such processes by analyzing whether the values of the time series are all within 95% of the maximum value of the time series. The remaining cleaned dataset consists of 10.595 charging processes.

Regarding the time series, we remove meter values after power reaches 0W for the first time. Artifacts such as remote air conditioning sometimes results in a power draw greater zero just before the end of the process. This leaves us with 1.2 million data points (from 5.2 million originally).

Feature engineering. Table 6.2 shows the preprocessed attributes of the dataset. We use the standard approach of one-hot encoding categorical features. In one-hot encoding each value of a categorical feature is converted to its own Boolean feature and the original categorical feature is removed. We one-hot encode the categorical variable EV model leading to 18 individual Boolean features. In regression models requiring only numerical features we use values of 0 and 1 for the Boolean features.

Feature name	Sample value
Input features (23 features)	
Is model BMW i3?	false
Is model Renault Zoe?	true
...	false
Is model Mercedes Benz C 350e?	false
Three phase charging?	true
Is BEV?	true
Is PHEV?	false
State of charge	0.3892
Arrival time (seconds after midnight)	29557
Target feature	
Power (W)	21358

Table 6.2: Sample data point in cleaned and preprocessed dataset (1.2 million data points) used for training regression models. The car model is included as a one-hot encoded feature leading to 18 individual Boolean features.

Car model	Type	Three phase charging	Capacity (kWh)	Max power (kW)
Audi A3 e-tron	PHEV	×	8.8	3680
BMW 225xe	PHEV	×	7.6	3680
BMW 330e	PHEV	×	12.0	3680
BMW 530e	PHEV	×	12.0	3680
BMW i3	BEV	✓	42.2	11040
Hyundai Kona 150kW	BEV	✓	64.0	11040
MINI Cooper S E Countryman	PHEV	×	7.6	3680
Mercedes Benz B250e	BEV	✓	28.0	11040
Mercedes Benz C 350e	PHEV	×	7.0	3680
Mercedes Benz E 300de	PHEV	×	13.5	7360
Mercedes Benz E 350e	PHEV	×	6.2	3680
Mercedes Benz GLC 350e	PHEV	×	13.5	7360
Mercedes Benz GLC 350e COUPE	PHEV	×	7.0	3680
Mercedes Benz GLE 500e	PHEV	×	8.8	3680
Nissan Leaf	BEV	×	62.0	6600
Renault ZOE	BEV	✓	41.0	22080
Smart ED	BEV	✓	17.6	22080
Smart fortwo ED	BEV	✓	17.6	22080
Smart fortwo EQ Cabrio	BEV	✓	17.6	22080
Tesla Model S	BEV	✓	75.0	11040
VW Golf GTE	PHEV	×	8.7	3680
VW Passat GTE	PHEV	×	9.9	3680
VW e-Golf	BEV	×	35.8	7200
Volvo V60 2,4 PHEV	PHEV	×	11.6	3680

Table 6.3: Car model data from manufacturers (2018 models)

6.2.2 Regression methods

Training regression models is a proven data-driven methodology for estimating one output feature given a set of input features. In the context of battery-aware smart charging the charging power is the feature to be predicted via a regression model. This section discusses how we train different regression models and which baseline we use to predict charging power given the EV model, SoC and arrival time from the preprocessed dataset described in Table 6.2. We train a linear regression model, an XGBoost regression model as well as a neural network.

Constant. We use a constant predictor as a baseline with the simplest possible predictions and to represent the approach in chapter 3 [52]. For the constant predictor, we use the maximum power draw per EV model according to manufacturers (see Table 6.3).

Linear regression. Linear models represent a common benchmark for regression models. We fit the model in equation (6.2) with predicted power y , 23 features x_i and error ϵ_j per data point j .

$$y = \beta_0 + \sum_{i=1}^m \beta_i * x_i + \epsilon_j \quad (6.2)$$

We also fit a second linear regression model on data where the target feature y has been logarithmically transformed to maximize prediction accuracy. The motivation for logarithmically transforming power y is that the power in the second stage of charging profiles is often modelled as an exponential decrease [44, 112]. In section 6.4 both linear regression models are evaluated independently.

Neural networks. Related work on predicting or modelling battery behavior with neural networks includes [23, 180]. Both approaches use neural networks to predict SoC taking into account battery voltage, current and temperature.

In this chapter we use Keras [25] for training neural networks. To begin with, we use the commonly applied standardization approach where each input feature has a mean value of 0 and a standard deviation of 1. The neural network consists of two hidden layers, each of which has 128 neurons with rectified linear activation functions. Weights are regularized using L1 regularization. Because we use the neural network for regression on a single target feature (power) the final layer is a single neuron. An 80-20 train and test split was used for evaluation. Additionally introducing dropout layers, a higher number of hidden layers or a different number of neurons did not result in an improved MAE.

XGBoost. Gradient boosting machines are a popular regression model for structured data. XGBoost (eXtreme Gradient Boosting) in particular has become widespread [24]. In the domain of battery technology, work such as [110] uses gradient boosted trees to predict the remaining useful life (RUL) of batteries. Similarly, [38] uses XGBoost to predict SoC. Both approaches require internal variables such as battery voltage and current. However, charge point operators do not have access to internal battery variables.

We perform hyperparameter tuning via grid search using the `mlr` package in R. To avoid overfitting, hyperparameters are tuned using 10-fold cross validation. For reference, the best parameters based on the grid search are `booster=gbtree`, `nrounds=100`, `eta=0.1`, `max_depth=9`, `min_child_weight=1`, `gamma=0`, `colsample_bytree=1` and `objective=reg:linear`.

6.2.3 Integration with charge scheduling heuristic

In this chapter we improve on the real-time charge scheduling heuristic introduced in chapter 3 [52]. The algorithm is a heuristic method which creates individual charge plans for a set of vehicles. It represents a practically oriented method with goals similar to the method proposed in [93].

The algorithm solves the decision problem of assigning charging power to EVs over time. Charging capacities are limited by fuses in the installed charging infrastructure and ultimately by the connection to the power grid. The goal of the algorithm is to maximize the average SoC over all vehicles while respecting charging capacities of the infrastructure. The output of the algorithm is one charge plan per vehicle. The charge plan is a time-series discretized into 15 minute timeslots and specifies the charging power for each time slot. From the perspective of the CPO, a charge plan specifies desired values for charging power. On a technical level, the charging station implements the charge plan as an upper bound to EV power draw. The actual power draw is controlled by the EV's BMS.

The flow of the algorithm is depicted in figure 6.2 and involves the following scheduling and prioritization steps. Each time a vehicle begins a charging process the charge scheduling heuristic is triggered and computes a charge plan. The scheduling step iterates over all timeslots and includes a timeslot in the vehicle's charge plan as long as the vehicle has a charging need. The initial charge plan is optimistic in the sense that it uses the earliest available timeslots for each vehicle.

The prioritization step deals with a conflict resolution when capacity allocations reach the limits of the infrastructure. Allocations are reassigned between vehicles and between timeslots. When reassigning charging capacities, vehicles with higher charging urgency are preferred. The charging urgency is associated with the charging priority and is related to the remaining parking time Δt and the state of charge $z(t)$ as detailed in equation 5.3. Each vehicle's departure time $t_{\text{departure}}$ is assumed to be known in advance. Vehicles are prioritized by whether and how much they are charged above their minimum required SoC z_{min} at time t .

This chapter enhances the algorithm so that it takes into account charge profiles such as CCCV when computing charge plans. The heuristic in chapter 3 creates charge plans assuming each EV is able to draw its maximum power irrespective of SoC and charge profile. Figure 6.3 depicts a sample CCCV process without a charge plan, with a charge plan as per chapter 3 and with a charge plan from this chapter. In the constant current phase of the charging profile the vehicle follows the charging plan directly. In the constant voltage phase, the current drawn follows a declining curve which is only affected by the charge plan if the charge plan current is below the CV current. When the vehicle draws less power than is reserved by the charge plan then charging capacity is wasted.

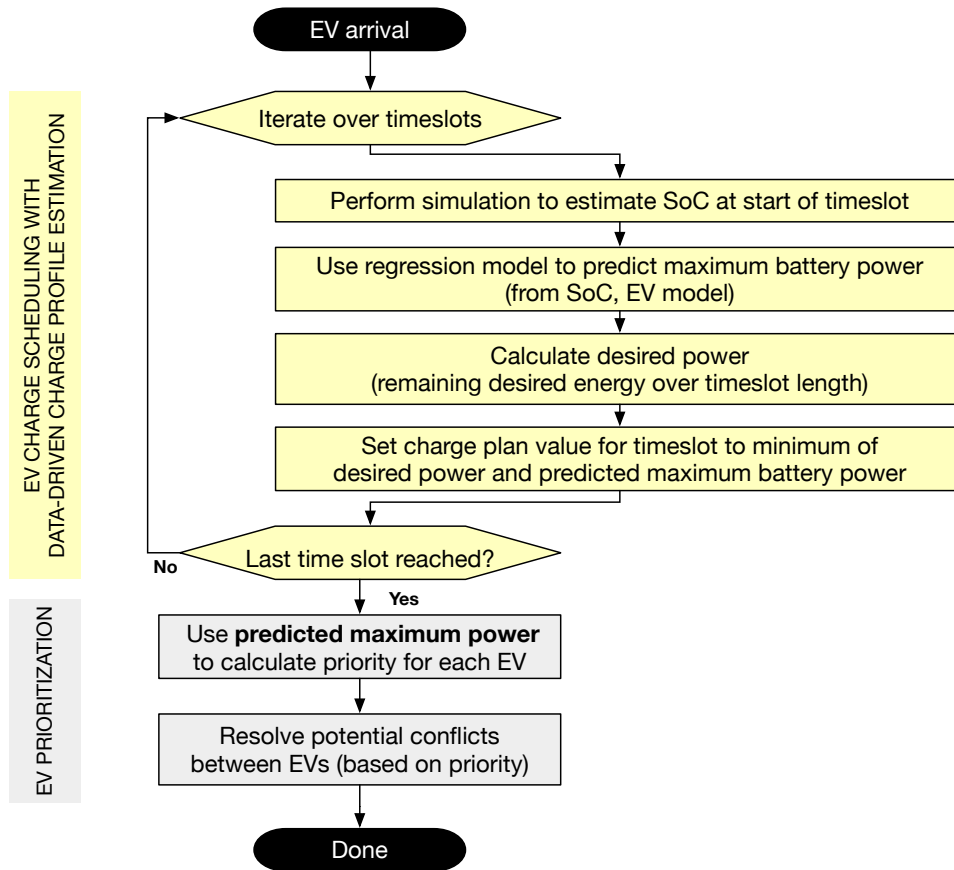


Figure 6.2: Flowchart of the charge scheduling heuristic integrating the data-driven charge profile simulation

The improvement presented in this chapter consists of reducing wasted capacity by considering the anticipated power drawn during the creation of charge plans. The approach is to introduce a data-driven charge profile simulation which integrates a regression model as introduced in section 6.2.2. The regression model is used to predict the maximum power drawn by the vehicle at any point in time based on features including the state of charge. The charge scheduling heuristic uses the estimated maximum power to reserve a more realistic charging capacity. Consequently, the resulting charge plan reflects the actual charge profile more closely as visualized in the last diagram within figure 6.3. The strength of integrating a regression model is that it allows to reflect arbitrary charge profiles and is not restricted to CCCV charging only.

Constant current, constant voltage (CCCV) charging profile

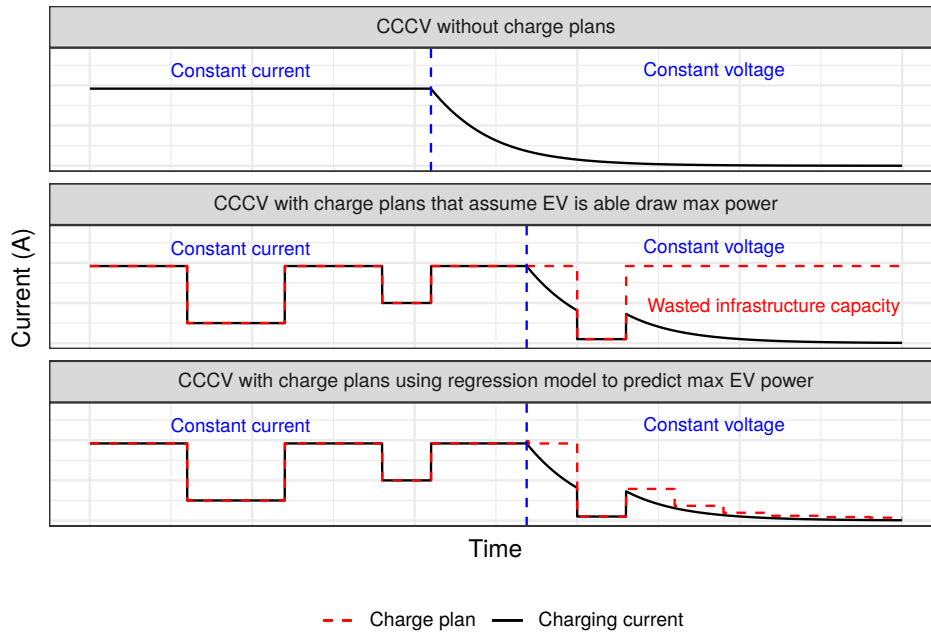


Figure 6.3: Constant current, constant voltage (CCCV) charging with and without charge plans. The charge plan specifies an upper bound for the EV’s charging current.

Regarding performance requirements of the algorithm: In a real life setting, vehicles connect and disconnect from the charging infrastructure frequently. In the scenario of workplace charging the frequency distribution of arrivals and departures is characterized by a peak of arrivals between 8 and 9 am and a peak of departures after 5 pm. In the dataset used in this chapter the median arrival is at 8:22 am while the median departure is at 5:01 pm. Figure 6.4 shows the distributions for EV arrival and departure times.

During peak arrival several new charging processes are started each minute. The fact that every connection triggers a computation of charge plans and potentially a reallocation of charging capacities motivates the need for a real-time capable algorithm. The charge scheduling heuristic is designed to perform with sub-second response times for charging infrastructures with 300 charging stations while achieving comparable smart charging quality compared to the approach involving the mixed integer linear programming model presented in chapter 3.

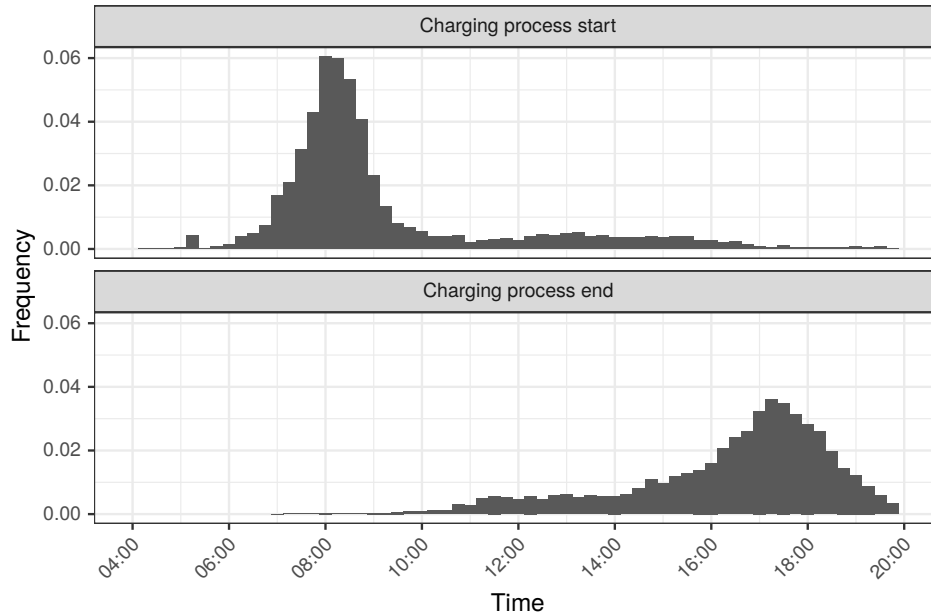


Figure 6.4: EV arrival and departure time distribution

6.3 Experimental setup

We reuse the discrete event simulation introduced in sections 3.3 and 4.4. The simulation models EVs and a three phase charging infrastructure. We trigger re-optimization on new events. Events include new EV arrivals, EVs reaching 100% SoC, EV departures and changes to the charging infrastructure. Reoptimizing includes recomputing charge plans via the algorithm as discussed in section 6.2.3

For predicting individual EV charge profiles we use a pure Java implementation¹ of XGBoost. XGBoost models are trained with the programming language R as discussed in section 6.2.2. For each simulation run we select a random historical charging process per EV and simulate the charging profile via a lookup table consisting of SoC and power draw. We use a seed when selecting the random historical charging processes to ensure reproducible results. A seed is used in pseudo-random number generators as a base value. The generator will always generate the same sequence of numbers with a given seed. In other words, the results of a simulation are reproducible with a given seed because the same historical charging processes will be selected.

¹<https://github.com/komiya-atsushi/xgboost-predictor-java> version 0.3.1

Table 6.4 shows the simulation parameters we use for simulations. The number of cars is variable and is increased for each simulation to show the impact of the infrastructure bottleneck (30kW). With a charge scheduling heuristic this infrastructure should be sufficient to fully charge roughly 40 EVs considering the main business hours of 08:00-17:00. The average energy consumption per session is 7 kWh and the infrastructure could be used for 270kWh spread out over 9 hours.

Each charging station is rated for a three phase BEV (22kW). We set the number of charging stations to allow for every EV to plug in. We use a constant charging efficiency of 0.85 as discussed in section 6.2.1. Finally, Table 6.3 shows the car model data published by manufacturers that we use.

Parameter	Values
Number of cars	{5, 10, ..., 100}
Number of charging stations	100
Charging station power rating	22kW
Charging efficiency	0.85
Infrastructure limit	30kW
Power prediction method	{Constant, XGBoost, ...}
RNG seed	{0, 1, ..., 9}

Table 6.4: Simulation parameters: 600 simulations total

6.4 Experimental results

This section discusses results from the simulations in section 6.3. First, in section 6.4.1 we analyze the performance of the different regression models by comparing error metrics. Based on the error metrics we discuss the suitability of the regression models for integration in the charge scheduling heuristic. We then show six examples of charging profiles and the accompanying predictions. Finally, we analyze feature importance in the best performing model (XGBoost).

In section 6.4.2 we directly measure the effect of the integrated regression models on smart charging by comparing charging output measured as mean final SoC. We evaluate the relevance of individual features within the model and present an ablation study to further quantify possible adverse effect when omitting features from the model. Lastly, we analyze two simulations in more detail and the influence of integrating regression models on the computation time of smart charging.

6.4.1 Regression models

Method	MAE	RelMAE
Baseline (predict maximum power)	2077.63	1.00
Linear regression	656.13	0.32
Linear regression (on log-power)	765.97	0.37
Neural Network	151.28	0.07
XGBoost (ablation study)	145.96	0.07
XGBoost	126.21	0.06

Table 6.5: Predicting charging profile power: Error metrics per prediction method

Comparison of regression models. In this chapter, we use the metrics mean absolute error (MAE) and the relative MAE (RelMAE) to quantify regression model results. The relative MAE is computed by dividing the MAE of a method with the MAE of a baseline [137]. We use the EV’s maximum power as the baseline.

Table 6.5 shows the MAE and RelMAE per regression model. To begin with, the baseline which assumes the EV will always draw its maximum power has the highest MAE (2077.63) thus motivating the use of regression models. Next, the standard linear regression model as well as the model fitted to logarithmically transformed power both perform poorly with an MAE of 656.13 and 765.97 respectively. The high MAE of both linear regression models can be explained by the intrinsic nonlinear relation between SoC and power [168].

More sophisticated regression models which are able to deal with nonlinear relations between attributes show better results. Neural networks and XGBoost show a comparable MAE of 151.28 and 126.21. However, XGBoost shows slightly better performance. As described in section 6.2.2 we report the average MAE on each test set during 10-fold cross validation. We use the best performing regression model (XGBoost) for the simulations of EV fleets in section 6.4.2.

As discussed in section 6.2.1 in this chapter we assume an efficiency value of $\eta = 0.85$. A sensitivity study on varying efficiency values can be found in section A.4. The sensitivity study shows no significant difference in prediction accuracy.

Charge profile prediction examples. In the following we discuss six examples of charging processes to visualize the inherent nonlinearity in charging profiles as well as regression model prediction accuracy. Figure 6.5 shows the six processes involving three popular EV models from the fleet. To show charging profile diversity in the dataset we present three processes with a high prediction accuracy (left column) and three processes with a low prediction accuracy (right column).

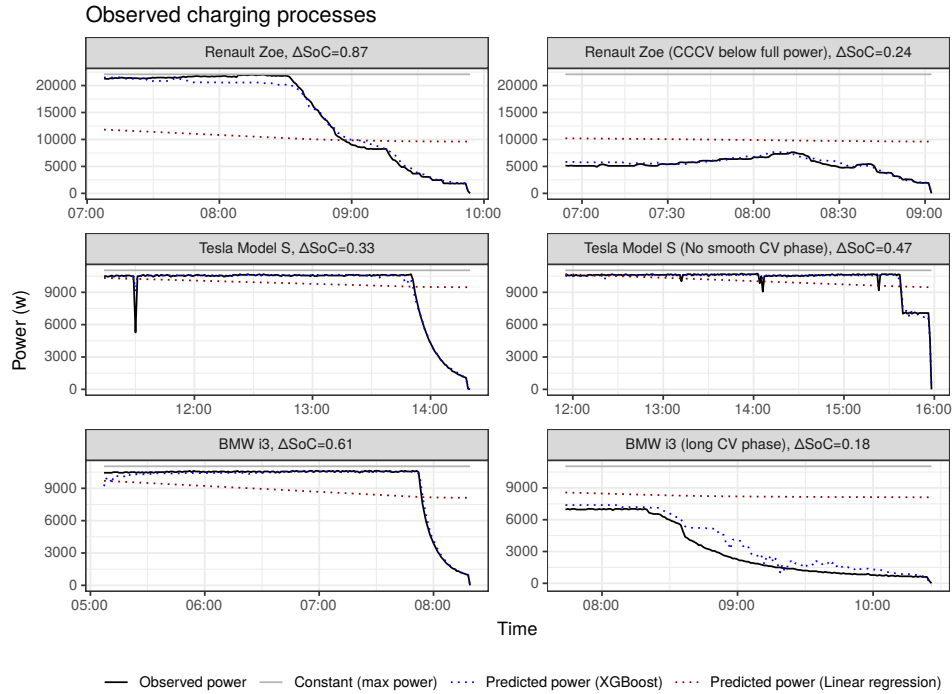


Figure 6.5: Observed CCCV processes and predicted power using different regression models

Interestingly, when observing the first stage in the charge profile of each process, the Renault Zoe appears to implement CCCV while the Tesla Model S and the BMW i3 appear to implement constant-power, constant-voltage (CPCV). We base this observation on the steady increase of power in the first stage of CCCV. In comparison, the CPCV processes show a first stage with recognizably constant power.

For each of the six charging processes we show the charge profile predictions for two regression models. XGBoost shows significantly better prediction accuracy compared to a linear regression model which corresponds to the lower MAE in Table 6.5 (126.21 vs 656.13). The diversity in such sample charging processes underscores the need for data-driven approaches to take into account processes that do not follow the expected theoretical charge profiles.

Comparisons of predicted profiles via regression model and profiles simulated via ECM are shown in section A.4. The comparisons show the predicted charging profiles are more accurate compared to the simulated profiles.

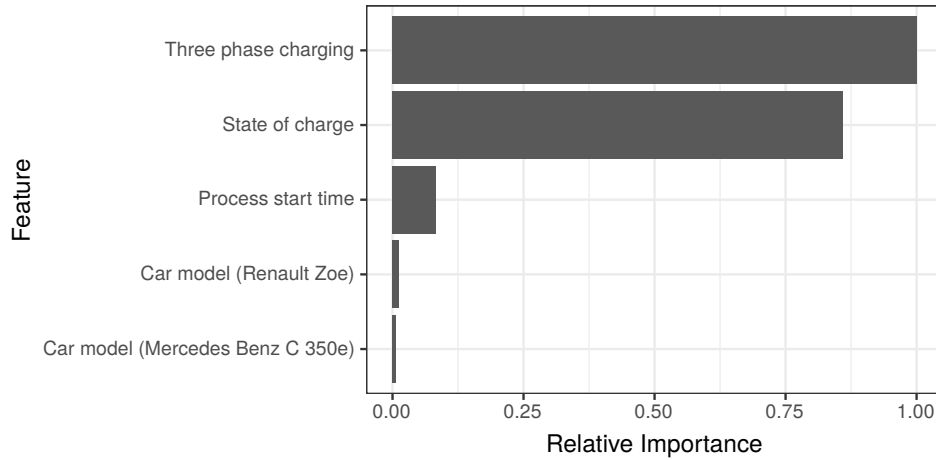


Figure 6.6: XGBoost feature importance

Feature importance. Analyzing the feature importance in trained regression models presents another approach to evaluation of regression results. For tree-based models such as XGBoost, feature importance expresses the impact on the regression when splitting on the feature.

In a single decision tree, the *gain* for a feature expresses how well splitting on that feature improves results. An XGBoost model consists of multiple trees and the gain is averaged over all trees. We refer to [24] for a more in-depth explanation of feature importance in XGBoost models.

Figure 6.6 shows the feature importance for the trained model. The most important feature is whether the EV is able to use three phases followed by the state of charge and the charging process' start time. The relative importance of *three phase charging* is explained by the fact that vehicles charging on three phases draw significantly more power than vehicles charging on only one phase, namely roughly by factor three. The fact that *state of charge* ranks high in feature importance emphasizes that the power drawn changes significantly with the SoC. In particular, the power draw decreases significantly towards high SoC.

6.4.2 Impact of integrated regression models on smart charging

Scheduling quality. Figure 6.7 shows the mean final SoC for different EV fleet sizes. The mean final SoC is the average SoC after charging computed over all EVs in the fleet. Each point in the plot is the average result of 10 simulations (600 simulations total). All methods show a decline after 35 EVs in the mean

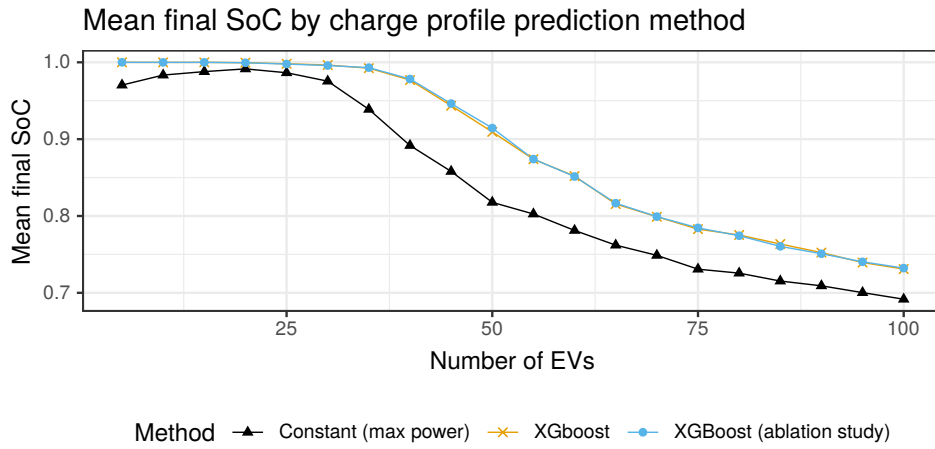


Figure 6.7: Experimental results: Mean final SoC for different EV fleet sizes

final SoC because of the infrastructure bottleneck (30kW). However, each method shows a different mean final SoC because the infrastructure is used more or less effectively. For example, the difference in SoC with 40 EVs is large. Assuming a constant battery model leads to a mean final SoC of 87%. In comparison, a mean final SoC of 96% is reached when using XGBoost as a charge profile predictor.

Ablation study. An ablation study can be used to determine the influence of certain features on ML models by retraining the models without said features. In the following we discuss whether the EV’s actual car model is necessary or whether it is sufficient to know the EV’s type (BEV/PHEV) and whether the EV is able to charge on three phases. The EV’s model may not be available to the charge point operator, for example, in scenarios where users do not authenticate.

In this chapter, we perform an ablation study assuming charging features (car type, three phase charging) are available via organisational measures. For example, parking spaces may be reserved specifically for BEVs or PHEVs and charging stations may be connected on one or three phases. The regression results in Table 6.5 show a slightly higher MAE (145.96 vs 126.21) when training the XGBoost model without the one-hot encoded car model features.

We thus conclude the car model itself is not needed. However, the EV’s charging features (BEV/PHEV, three phase charging) are needed as per the following reasoning. Figure 6.8 shows power in relation to SoC and contains all data points from the dataset. There are many different charging profiles and the typical charging levels are easily recognizable as horizontal lines (single phase 3.7kW, three phase 11kW or 22kW). Intuitively, without the car type and the three phase charg-

ing characteristic there are multiple values on the y-axis per single value on the x-axis. It is thus infeasible to find a function to accurately predict power based solely on SoC which confirms the need to include further features such as the charging features discussed above.

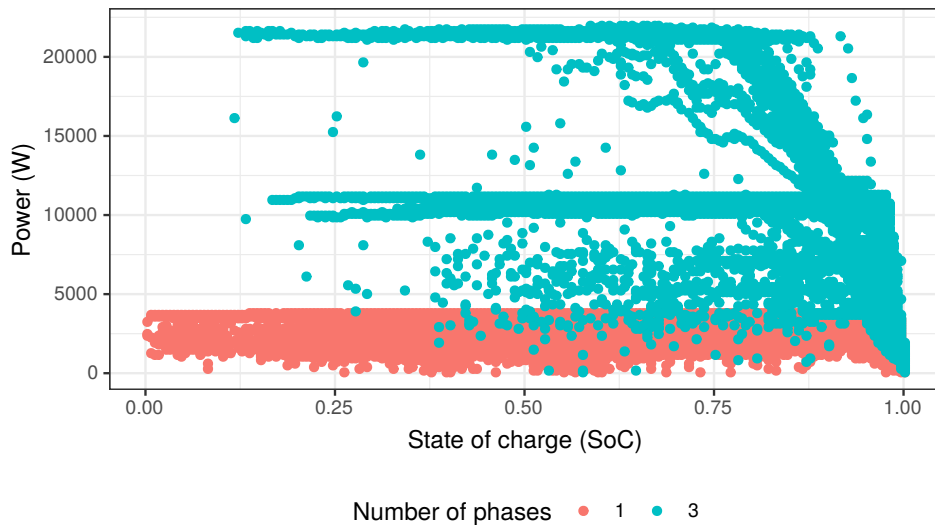


Figure 6.8: Power vs SoC for all data points in the dataset

Example simulation runs. Figure 6.9 shows the aggregated consumed power for two different simulations using different predictors. Notably, when using *Constant (max power)*, there are large differences between the actually drawn power and the aggregated charge plans. In other words, there is a gap between each EV's power and the power assigned via a charge plan. Semantically, the gap represents the difference between assuming a constant battery model and taking into account EV charge profiles. In the upper plot of figure 6.9, 196kWh was planned but only 129kWh was drawn which represents a charge plan utilization of 65.8%. In the lower plot, XGBoost more accurately predicts charge profiles leading to 144kWh planned and 136kWh drawn and a charge plan utilization of 94.4%.

Figure 6.10 shows the aggregated consumed power for two simulations with 40 EVs. With 40 EVs, the impact of a lower charge plan utilization is more pronounced and leads to 21% more energy being drawn in total (259kWh vs 213kWh) when using the more accurate prediction method (XGBoost). That is, the accuracy of the charge profile prediction impacts how effectively the infrastructure is used. Consequently, using XGBoost leads to a significantly higher mean final SoC of 98% compared to the baseline of *constant (max power)* of 90%.

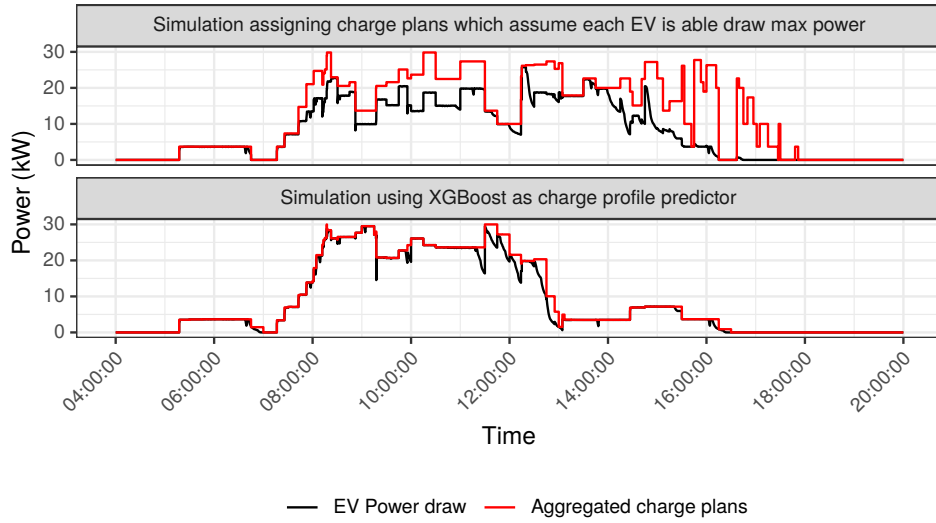


Figure 6.9: Single simulation runs using different predictors (20 EVs)

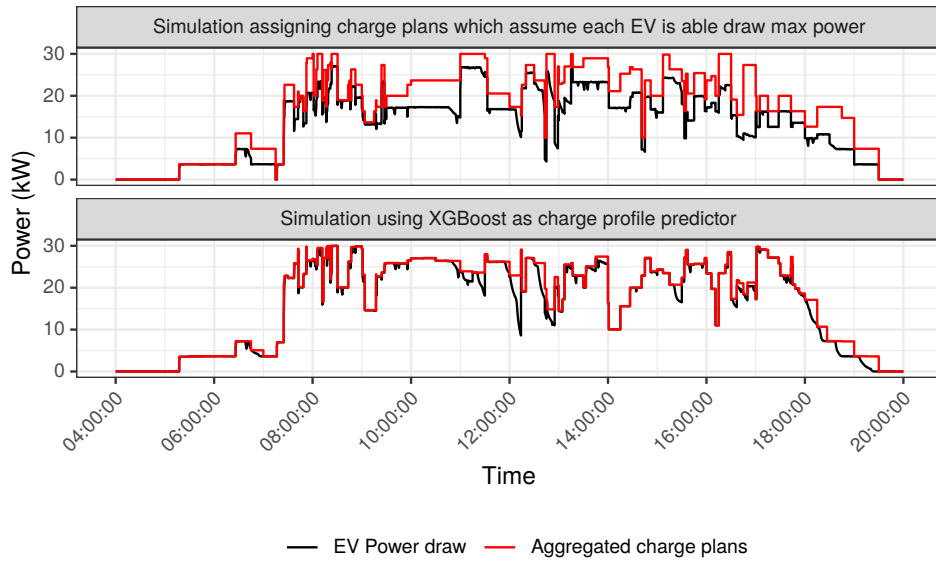


Figure 6.10: Single simulation runs using different predictors (40 EVs)

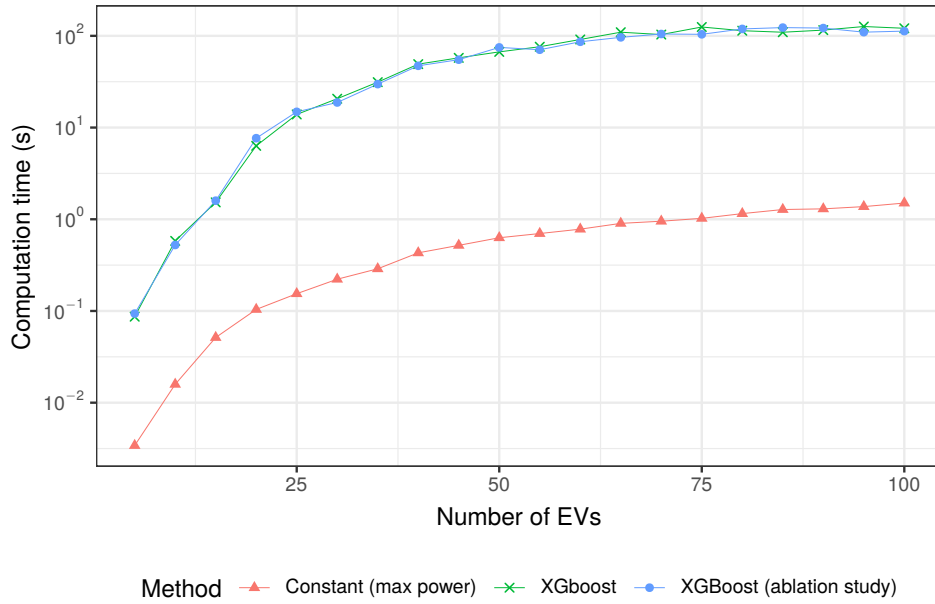


Figure 6.11: Computation time of the charge scheduling heuristic per integrated prediction method

Smart charging computation time. Figure 6.11 shows the average computation time per rescheduling operation of the charge scheduling heuristic. In other words, how long does an EV wait, on average, before receiving a charge plan? The computation time includes the time applying the regression model as well as computing charge plans.

In a real-time context, charge plans should be computed as quickly as possible in order to make the most of the EV's stay. Both methods show increasing computation time depending on the number of EVs. Using *Constant (max power)* is clearly faster. The charge scheduling heuristic performs many charge profile predictions with the integrated XGBoost model. The computation time of each XGBoost prediction is roughly 30ns and is independent of the number of EVs. The number of EVs influences how often the prediction method is used. For the charge scheduling heuristic, the overall computation time remains in the order of 100s for fleets of up to 100 EVs.

6.5 Discussion

Using a data-driven approach to reflect charging behavior in smart charging leads to improved charge plans. Here, improvement is understood as reaching a higher mean final SoC for the vehicle fleet by using the limited charging infrastructure more efficiently. The EV type (BEV versus PHEV, three phase charging) and SoC data is sufficient to train a regression model reflecting charge profiles. The smart charging approach presented in this chapter reaches an improvement of up to 21% in charging power consumed in total over an approach which does not take into account charging behavior. An ablation study showed how contrary to initial intuition, the EV's model is neither necessary nor does it produce a significant improvement in the performance of the regression model.

From a computation time perspective, the integration of the regression model is negligible with an average runtime of 30ns per prediction.

With regard to the impact of prediction accuracy: If the power prediction is too low the EV will draw less power than it is capable of. However, the charge scheduling heuristic can assign the unused infrastructure capacity to other EVs if available. If the power prediction is too high the EV will follow its normal charging profile and draw less power than specified by the charge plan. Consequently, infrastructure capacity is reserved which cannot be assigned to other EVs.

The studied scenario of workplace charging generalizes to other smart charging applications that involve EVs topping up batteries in limited charging infrastructures. Such applications include charging delivery fleets over night and topping up EV batteries at gyms, airports or retail locations. It can be argued that the main gain of integrating the regression model is leveraged when vehicles approach 100% SoC. However, it is to be expected that with an increasing number of charging opportunities frequent topping up becomes common charging behavior.

The fact that the regression model for the charge profile prediction is agnostic of EV models makes it versatile and applicable to use with any EV. Regarding continuous SoC data, the vehicles' SoC is not commonly accessible in practice due to pending implementations of the ISO15118 [141] standard in charging stations and EVs. The missing access to SoC is expected to resolve with time. We describe how we estimate SoC for historical charging processes in this chapter in section 6.2.1.

Additional features such as EV internal temperature and battery SoH may improve the accuracy of the regression models. However, such features are not reported to the charging station and thus not available to the CPO. The sensitivity study in section A.4 on charging efficiency shows no significant differences in regression model accuracy. Furthermore, we omit external temperature from the set of regression model features. The experiments in section A.4 show that retraining the regression models with external temperature as an additional feature does not

improve accuracy.

The limitations of the presented approach relate to the availability of historical data. A large enough dataset with car models and meter data from charging processes is necessary to train the regression model for predicting charge profiles. The trained model only reflects the charging behavior of the EV models included in the historical dataset. With new EV models and EVs aging over time the dataset will need to be continuously updated and the regression model will need to be re-trained. Furthermore, in this chapter we assume we know each EV's departure time. In practice, it is difficult to reliably estimate departure times. We present an approach to predict EV departure time with machine learning in chapter 4.

As far as alternative approaches to charge profile prediction are concerned, time series forecasting may at first seem to suggest itself. However, the application of charge plans influences the course of each time series making the integration of time series forecasting with real-time smart charging conceptually problematic.

6.6 Conclusion

In this chapter we present the integration of a regression model for charge profile prediction in a charge scheduling heuristic as proposed in [55]. The regression model is trained on a large historical dataset of charging processes and predicts the power drawn by the EV over the course of the charging process. A data-driven regression model is more practical to infer charge profiles than traditional battery models such as ECMs and physical models. Battery internal parameters such as current, voltage or state of health are required for such analytical models but are not publicly available. Additionally, the regression model is trained on arbitrary charge profiles and thus not restricted to a single charge profile such as CCCV.

We address the research question of how integrated EV charge profile predictions impact smart charging. We show how with our approach EVs charge up to 21% more energy and reach a 9 percentage point higher mean final SoC in a limited infrastructure. Consequently, more energy can be delivered without the need for costly and time-consuming upgrades of the charging infrastructure.

Furthermore, an ablation study shows that the EV model is not a necessary attribute for considering charge profiles in heterogeneous EV fleets. However, EV characteristics are required including the type (BEV or PHEV) and the number of the phases used for charging.

Future work includes studying the impact on smart charging of how well regression models generalize to new EV models as they enter the fleet. Progress in battery technology leads to EV models with new charge profiles not contained in the historical dataset.

Chapter 7

Open source heuristic and practical validation

7.1 Introduction

This chapter presents an open source package containing the approaches presented in previous chapters. Additionally, experimental results of a one-year field test are presented. The field test was designed to validate the charge scheduling heuristic.

In practice, the output of the charge scheduling heuristic presented in section 3.2.2 is an individual charge plan for each vehicle. The charge point operator (CPO) system transfers the vehicles' charge plans to the individual charging stations via standard protocols such as the Open Charge Point Protocol (OCPP).

With respect to CPO systems there is an evolving market with offerings from different industry segments including service providers, utilities and charging hardware manufacturers. Commercial offerings increasingly feature smart charging functions. However, proprietary smart charging solutions are typically limited with respect to analysis, modification and integration in other charging systems.

In this chapter we address the following research question:

How can a charge scheduling heuristic be implemented which is open and interoperable with other systems?

In this chapter we present an open source package containing the charge scheduling heuristic presented in section 3.2.2 together with experimental results from applying the heuristic in a one-year field test. The heuristic is flexible with regard to aspects such as EV fleet composition, charging station setup or hardware used. We refer to section 3.2.2 for a detailed discussion of the charge scheduling heuristic and in this chapter focus on interoperability and the validation of the heuristic.

The main contributions of this chapter are

- an open source package containing a real-time charge scheduling heuristic for heterogeneous EV fleets,
- a REST API for interoperability which encapsulates the charge scheduling heuristic and
- validation of the charge scheduling heuristic in a one-year field test.

The chapter is organized as follows. Sections 7.2.1 to 7.2.3 introduce the data model and the charge scheduling heuristic which are published in the open source repository. Section 7.2.4 describes the integration of the open source heuristic into CPO systems. The experimental setup of the one-year field test is described in section 7.3 and results are listed in section 7.4. Finally, sections 7.5 and 7.6 discuss relevance and limitations of the approach and conclude with an outlook.

7.2 Method

7.2.1 Data model

This section describes the data model used by the charge scheduling heuristic and implemented in the open source package. The data model is used to reflect complex charging infrastructures, EVs and charging processes.

Charging infrastructure. In the following, we create a model of the charging infrastructure concepts presented in section 2.3. The charging infrastructure is modelled as a tree of fuses (or circuit breakers). Each node in the tree contains a fuse that may have a charging station and other nodes as children. In practice, large charging infrastructure consist of multiple levels of hierarchical fuses. For example, in chapter 3 we consider a real charging infrastructure with a fuse tree with three levels of fuses (4000 A, 1250 A, 800 A). This particular charging infrastructure allows smart charging for hundreds of charging stations.

Additionally, an important electrical engineering constraint in practice is the consideration of multiple alternating current (AC) phases during charging. AC in the electrical grid is transmitted using a three-phase, four-wire system [153] where the fourth wire carries the neutral current.

The data model must reflect how charging stations are connected to the grid in practice. The connection includes the number of connected phases as well as how the phases are connected. For example, charging stations may be installed with rotating phases in order to allow minimizing load imbalance. Load imbalance is caused by single-phase EVs such as PHEVs charging on the first phase. Figure 7.1

shows an example of three charging stations where phases are rotated. In this example, three single-phase EVs would not cause load imbalance because the first phase of each charging station is connected to a different phase of the grid.

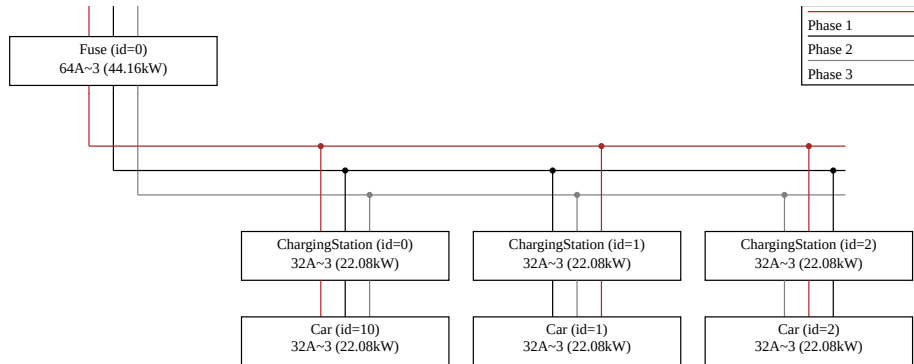


Figure 7.1: Charging stations connected to the grid with rotating phases

Electric vehicles. In this chapter we consider a heterogeneous fleet of EVs consisting of different EV models. The data model of an EV thus has many attributes. We refer to the documentation of the open source package for an exhaustive list of each attribute. Most importantly, the attributes include

- which phases the EV is able to use for charging,
- the maximum charging power of the EV and
- the starting capacity, minimum required capacity and the maximum capacity.

Energy prices. The charge scheduling heuristic is able to follow different objectives. If the set of objectives includes energy cost minimization an energy price per 15 minute time slot is required.

7.2.2 Charge scheduling heuristic

The open source charge scheduling heuristic is an implementation of the schedule guided heuristic presented in section 3.2.2.

To recap, the heuristic aims to maximize driver satisfaction in the sense that limited charging power is shared fairly among EVs with charging needs. Secondary objectives include energy cost minimization, load imbalance minimization and peak minimization. At the same time the heuristic takes into account practical engineering constraints such as EV model specific charging power, single phase

versus three phase charging and phase rotation between charging stations. Chapter 3 contains a detailed discussion of the individual constraints. Considering such practical constraints directly during charge scheduling avoids post-processing steps to make charge plans feasible for practical use.

The heuristic consists of three main steps: greedy charging, saturation adjustment and conflict resolution. First, the heuristic starts by creating a greedy charge plan for each EV in the sense that it plans to fill up the state of charge as soon as possible. For the greedy plan, the heuristic assigns the maximum charging current during all time slots directly after arrival of the EV. Second, the heuristic adjusts the planned charging current by accounting for charging saturation effects. Charging saturation occurs towards high SoC. Battery management system inside EVs manage saturation by decreasing the current drawn for charging. Constant voltage constant power (CPCV) charging is a common implementation of charging saturation in EVs [134]. The open source charge scheduling heuristic contains a simple saturation adjustment. The implementation linearly scales down the charging current during the last 15-minute time slot of the charging session. Regression techniques which allow more precise prediction of charging behavior during saturation are described in chapter 6. The regression techniques were not used during the field test, however.

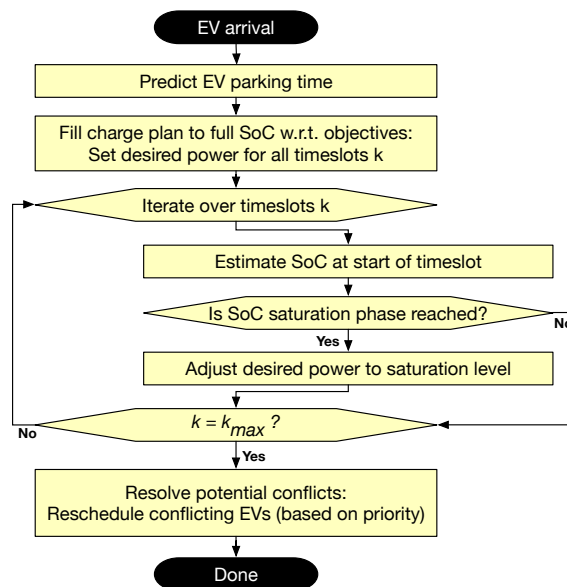


Figure 7.2: Flowchart of the charge scheduling heuristic: Program flow for creating charge plans upon arrival of an EV.

The third and last step of the heuristic is to resolve conflicts between the charge plans and the charge plans of all previously scheduled EVs. Due to the greedy charging in the first step the situation can arise that during some time slots the scheduled charging capacity exceeds the actual capacity of the charging infrastructure. In this case, priority based rescheduling is triggered where the EVs with the lowest priority are rescheduled to charge during other time slots.

7.2.3 Open source repository

This section discusses the open source package for smart charging¹. The repository is published under the Apache License 2.0. Benefits of open sourcing include:

- Ensuring reproducibility: It is simple to download and execute the code, particularly due to the provided Docker image.
- Facilitating collaboration: The community can directly suggest improvements, new features and bug fixes.
- Guarantee transparency: The open implementation of an heuristic is particularly important for commercial use which must adhere to security and data protection regulations.

REST API. Representational state transfer (REST) is an architectural style for communication in distributed systems [50]. The open source algorithm implements a REST API using the programming language Java. The REST API encapsulates the charge scheduling heuristic in order to allow access by other systems such as CPO backends.

The most important call to the REST API is a request to the service:

```
/api/v1/OptimizeChargingProfiles
```

The input to the REST API is the current state of the charging infrastructure with regard to EVs and available charging stations. The output of the REST API is one charge plan per EV.

Using a REST API for communication makes the smart charging approach protocol agnostic and interoperable with other systems. In other words, the charge scheduling heuristic can be used by CPOs in combination with high-level protocols such as OCPP or OSCP but also low-level protocols designed for use without a centralized CPO backend such as EEBUS. Additionally, other systems do not have to be implemented in the same programming language.

¹github.com/SAP/emobility-smart-charging

Web application. A secondary component in the open source package is an interactive web application. The web application is designed to visually communicate to stakeholders the motivation for smart charging and to show the internal data model of the charge scheduling heuristic. The web application allows users to interact with the REST API and thus enables learning how to use the API.

The web application presents both API input data and the charge plan output in a visual way. The inputs of the REST API are presented as a circuit diagram (figure 7.1) and as a fuse tree. Figure 7.3 shows a fuse tree with three charging stations and three EVs.

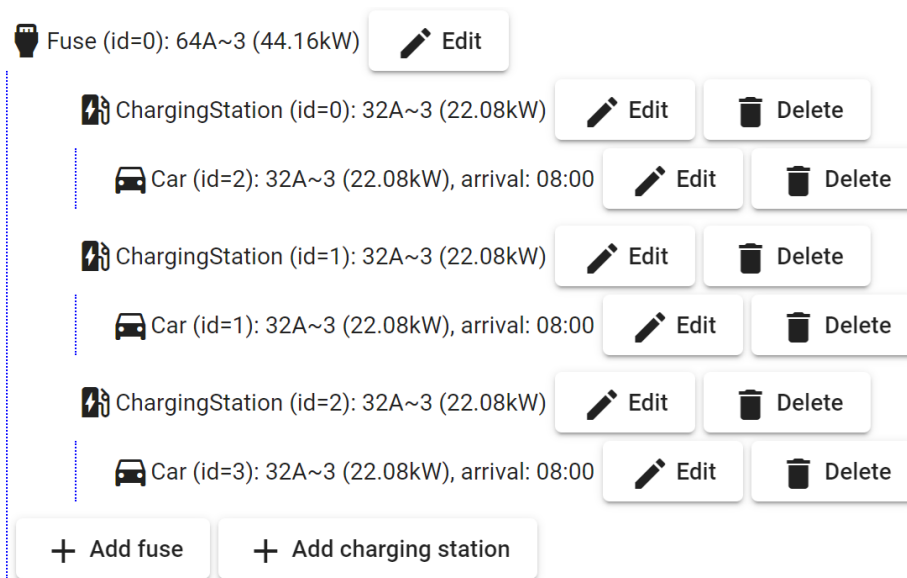


Figure 7.3: Screenshot: Visualization of a simple charging infrastructure with three charging stations and three EVs. The web application allows the user to configure a three-phase charging infrastructure with arbitrary inputs.

The output of the REST API is visualized as a stacked graph with individual charge plans. The graph shows how EV charging is distributed over time. Figure 7.4 presents the corresponding output for the input from the example in figure 7.3. In the example, only two EVs can charge concurrently to ensure the connection to the grid (44 kW) is not overloaded. The third EV is thus scheduled to charge later.

Figure 7.5 shows the visualization of a more complex charging infrastructure. The infrastructure contains four charging stations and four EVs. This specific hierarchical infrastructure is used for the simulations in chapter 3.

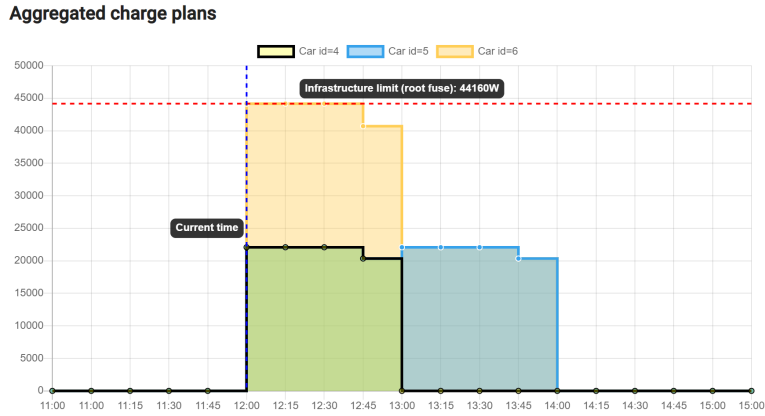


Figure 7.4: Screenshot: Visualization of individual EV charge plans

The screenshot shows a configuration interface for a charging infrastructure. It features a hierarchical list of components, each with an "Edit" (pencil icon) and "Delete" (trash icon) button. The components are:

- Fuse (id=0): 4000A~3 (2760kW)
- Fuse (id=1): 1250A~3 (862.5kW)
 - ChargingStation (id=3): 32A~3 (22.08kW)
 - Car (id=5): 32A~3 (22.08kW), arrival: 08:00
 - ChargingStation (id=4): 32A~3 (22.08kW)
 - Car (id=4): 32A~3 (22.08kW), arrival: 08:00
- Fuse (id=3): 800A~3 (552kW)
 - ChargingStation (id=5): 32A~3 (22.08kW)
 - Car (id=7): 32A~3 (22.08kW), arrival: 08:00
 - ChargingStation (id=6): 32A~3 (22.08kW)
 - Car (id=6): 32A~3 (22.08kW), arrival: 08:00

At the bottom, there are buttons to "+ Add fuse" and "+ Add charging station".

Figure 7.5: Screenshot: Visualization of a more complex charging infrastructure

7.2.4 Integration concept

This section discusses how the presented open source package may be integrated with other systems. Figure 7.6 shows the components required for a centralized smart charging approach. The charge scheduling heuristic may be combined with other open source software for the charging station controller and a CPO backend using OCPP. The charge scheduling heuristic can also be accessed directly without the REST API if the CPO backend is also implemented in Java. Smart charging approaches are typically categorized as centralized or decentralized [89]. Figure 7.6 describes a centralized approach where a central CPO backend is used. However, the server containing the charge scheduling heuristic can also be run in a decentralized manner in the commonly used Master-Slave configuration.

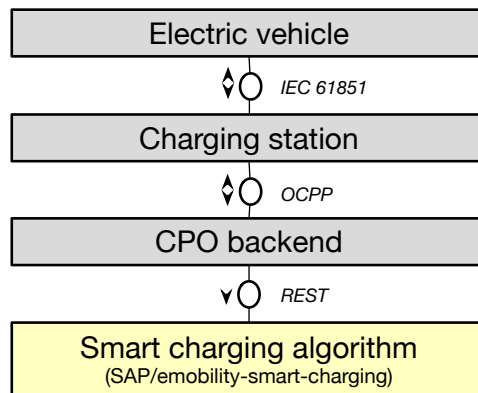


Figure 7.6: Components involved in smart charging and standardized communication protocols. Arrows indicate direction of requests.

Figure 7.7 shows a sequence diagram of the requests triggered by the arrival of an EV. This sequence was used in the experimental setup detailed in section 7.3 and roughly follows the sequence of steps when using OCPP 1.6. After an EV has connected, the station requests a new charging session. The CPO backend creates the session and sends a request for reoptimization to the charge scheduling heuristic. The charge scheduling heuristic responds with one charge plan per EV. The CPO backend confirms the new charging session and sends the charge plan to the charging station.

With regard to enhancing features of the open source package, the open source package offers interfaces for regression models to predict EV departures (chapter 4) as well as interfaces for models to simulate EV batteries to reflect charging saturation (chapters 5 and 6).

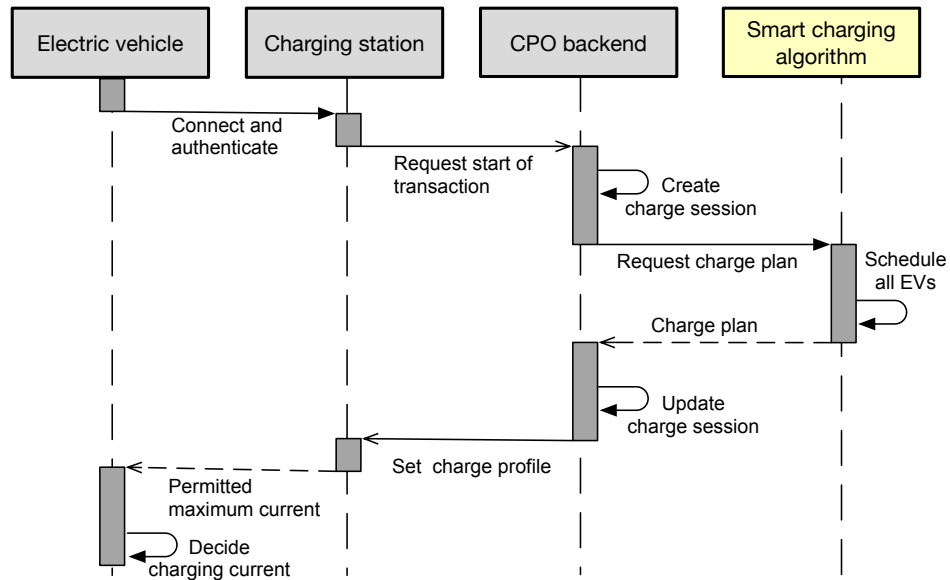


Figure 7.7: Sequence of requests triggered by arrival of an EV at a charging station.

7.3 Experimental setup

7.3.1 Physical charging infrastructure and field test

The charge scheduling heuristic underwent a field test in a real charging installation during the year of 2019. The physical installation consisted of six charging stations connected to a three-phase infrastructure. Figures 7.8 to 7.10 show photos of the installations. Each charging station was able to charge up to 32 A on 3 phases (corresponding to a charging power of 22 kW). The line section with all six stations together was protected by a three-phase 64 A fuse (44 kW). That is, only two EVs were able to charge at full power concurrently without triggering the fuse. Charging stations were connected to the grid with rotating phases (see figure 7.1).

Each charging station was equipped with an RFID card reader for user authentication and an Internet of Things (IoT) SIM card for internet connectivity via the cellular network. The endpoint of the connection was a proprietary CPO backend system. The overall software system setup is visualized in figure 7.11. The field test involved the two user roles of charge point operator and driver. The CPO interacted directly with the monitoring and control applications in the CPO backend system. The drivers interacted with a mobile app which included functions for starting and stopping the charge session as well as viewing the charge plan and monitoring the charge session. The apps used a central data store in the CPO system.

Regarding the participants of the field test, eight commuters were chosen with an average daily commute of 34 km. The fleet of the participants' vehicles contained both plug-in hybrid as well as fully electric vehicles with battery capacities ranging from 9 kWh to 85 kWh. Each participant was assigned an RFID card for authentication at the charging station. In the CPO backend system, each RFID code was linked with the charging characteristics of the associated vehicle. This way, EV attributes such as battery capacity and maximum charging current were sourced for the smart charging heuristic.



Figure 7.8: Station exterior

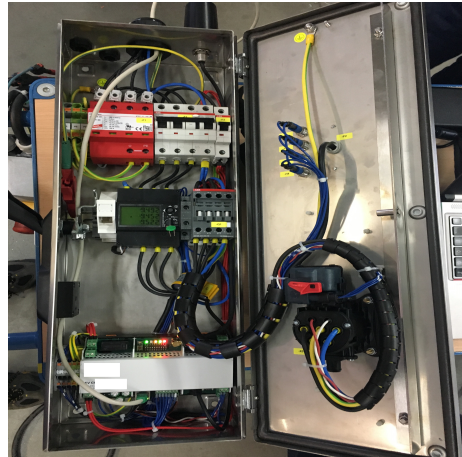


Figure 7.9: Station interior



Figure 7.10: Charging infrastructure in field test operations

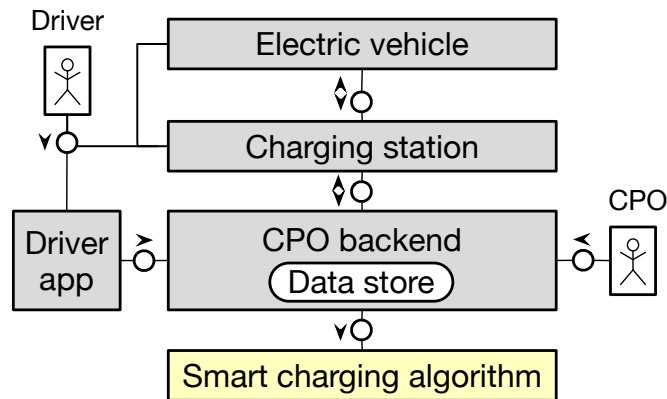


Figure 7.11: User roles and system components used in field test operations.

7.3.2 Open Charge Point Protocol (OCPP)

For the purpose of the one-year field test, Open Charge Point Protocol (OCPP) [124] was chosen to communicate charge plans to charging stations. OCPP is a protocol independent of charging station manufacturer. Messages are communicated to charging stations in a JSON format via WebSocket in a ping pong exchange with each message consisting of a request and a response. A charge plan is communicated as a certain type of OCPP message (`SetChargingProfile`).

A full example of a charge plan is shown in the appendix in section A.5. With regard to timing, each `ChargingProfile` consists of a `ChargingSchedule`. A `ChargingSchedule` has a starting time (`startSchedule`) The algorithm always assigns charging schedules based on full 15-minute timeslots. As such, the `startSchedule` is always chosen rounded up to the beginning of the current 15-minute timeslot. For example, 09:35 is rounded up to 09:30 and 17:13 is rounded up to 17:00. A `ChargingSchedule` consists of several unordered `ChargingSchedulePeriod` objects. Each period is chosen with the corresponding output of the algorithm (attribute `limit`) and a time offset (attribute `startPeriod`) of the timeslot multiplied by 900 seconds.

7.3.3 Field test assumptions

There are three parameters required for the charge scheduling heuristic which have uncertain values. For the purpose of the field test, a mobile application was developed which allows EV drivers to supply values for each parameter. However, a value must be assumed for each parameter if the EV driver does not supply a value.

Arrival SoC. There are protocols such as ISO 15118 which allow the charging

station to read the EV's SoC upon arrival. However, at the time of writing current charging stations and EVs seldomly implement the protocol [141], making it difficult to reliably acquire a value for the arrival SoC.

In the field test we assume an arrival SoC of 0 to allow all EVs a chance to fully charge. This value works in conjunction with an additional feedback loop to detect EVs at full charge: If an EV was scheduled to draw power via charge plan but did not draw power, we assume the EV is fully charged.

Minimum SoC. The minimum SoC allows the heuristic to prioritize EVs according to a user-specific minimum required SoC. If the EV driver does not supply a value we assume a minimum SoC of 0.5.

Departure time. The departure time is an important component of the priority function in the charge scheduling heuristic. If the EV driver does not supply a value we use a regression model to predict departure time based on historical data as described in chapter 4.

7.4 Experimental results

This section describes the experimental results gathered during the TRADE EVs project. Table 7.1 provides an overview of the experimental results.

Number of participants	17
Number of charge sessions	1,247
Number of charge schedules computed	358,779
Total power consumed	6.534 MWh
Average power consumed per session	5.2 kWh
Energy price forecast	Daily update

Table 7.1: Experimental results overview (TRADE EVs)

7.4.1 Field test of the charge scheduling heuristic

The purpose of the one-year field test was to validate the charge scheduling heuristic for practical application. The role of the heuristic was to supply charge plans which were used to control charging processes of EVs.

During the field test 468 charging sessions were recorded in total. Altogether 6118 kWh were charged, averaging 13.1 kWh per session. The average duration of the charging sessions was 8.3 h. Figure 7.12 shows the number of charging processes per EV model.

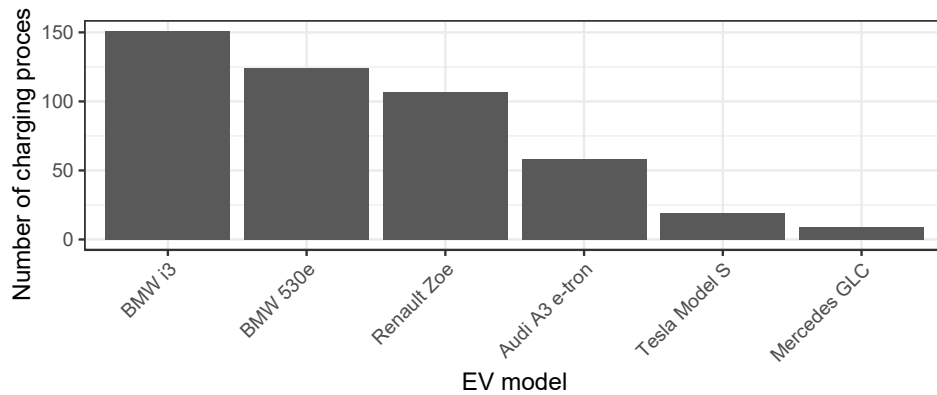


Figure 7.12: Number of charging processes per EV model

Overall, the field test was successful from both the drivers' and the CPO's perspective. For drivers, EVs were always fully charged at the end of the charge session. For the CPO, the power limit of 44 kW for the line section was always adhered to and the fuse was never triggered. However, there were multiple incidents with software errors in charge sessions requiring the CPO's intervention. Without the intervention, the EV would not have charged in the worst case.

Out of the 468 charging sessions, 97 sessions (or 20.7%) involved an error with the execution of the session and required intervention by the CPO. The overall high error rate is explained by the complex system setup with various software and hardware components from different manufacturers. There was a decreasing error rate over time due to continuous bug fixes in the CPO backend system and improved charge point configuration.

Troubleshooting by the CPO involved analysis of log files of the charging station, of the CPO backend application and of the cloud platform hosting the CPO application. Log files within the individual EVs are not available due to lack of standardized interfaces. The most common detected root causes were issues with the cloud infrastructure (16%) followed by software bugs in the OCPP communication of the CPO backend (14%). The charge scheduling heuristic rarely accounted for errors (4%).

Two sample charging sessions governed by charge plans are depicted in figure 7.13. Charge plans were computed by the charge scheduling heuristic. The charging station interprets the charge plan sent by the CPO backend and communicates a maximum current to the EV (the blue line). The EV's BMS then controls the current accordingly (the red line). For the depicted charge sessions the BMS achieves a tight compliance with the charge plans.

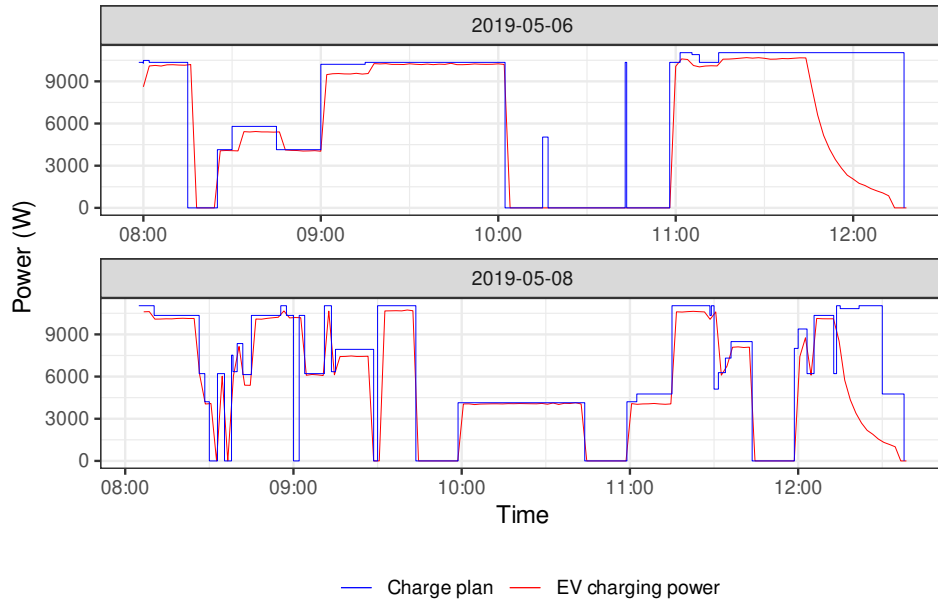


Figure 7.13: Two sample charging processes of a BMW i3

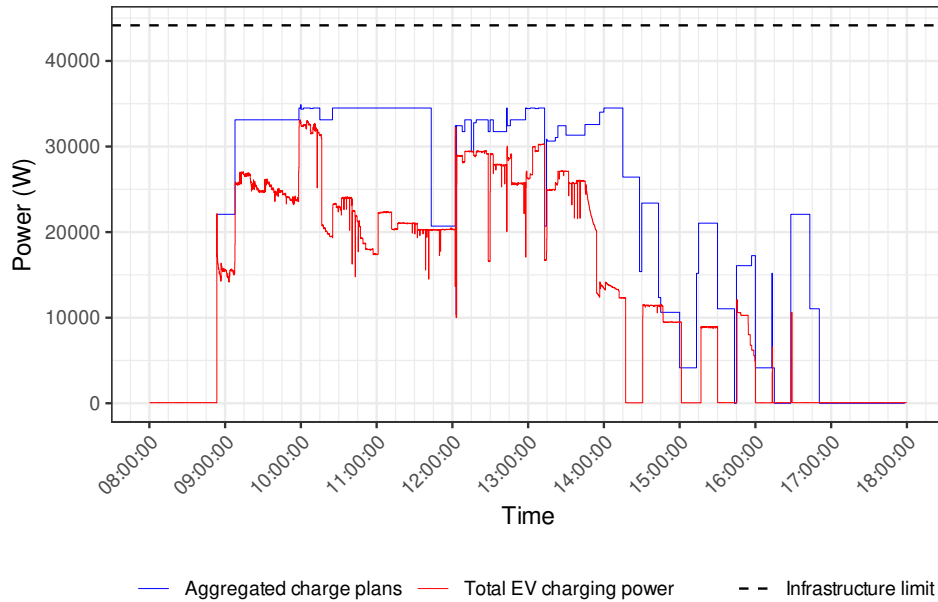


Figure 7.14: Total planned and drawn power on 2019-05-06 with four EVs connected at the same time

Figure 7.14 shows the total planned power and actual EV charging power during a typical day in May, with four EVs connected to the charging infrastructure. The main constraint of the heuristic is to schedule all EVs for charging such that the infrastructure limit (44 kW) is never exceeded.

Figure 7.14 also demonstrates that there can be gaps between planned power and actual EV charging power. For example, at 11:00 the heuristic planned for 35 kW in total but the actual power draw was only 22.5 kW. The gap occurs because the heuristic models saturation charging inaccurately. Saturation charging occurs towards high SoC and leads to decreasing charging power. The gap between planned and actual power is addressed in chapters 5 and 6 but the approaches were not applied in the field test.

To summarize, the open source charge scheduling heuristic was applied during the one-year field test for validation. The experimental results show the heuristic can be applied in a charging infrastructure with a limited connection to the grid.

7.4.2 Runtime of the REST API

This section discusses the runtime measurements of the REST API with varying inputs. We use the testing tool *artillery*² to record the runtime of the REST endpoint `/api/v1/OptimizeChargingProfiles`. The runtime includes overhead such as using Docker network interfaces and the server's REST API mapping. Each request is sent once per second for 60 seconds.

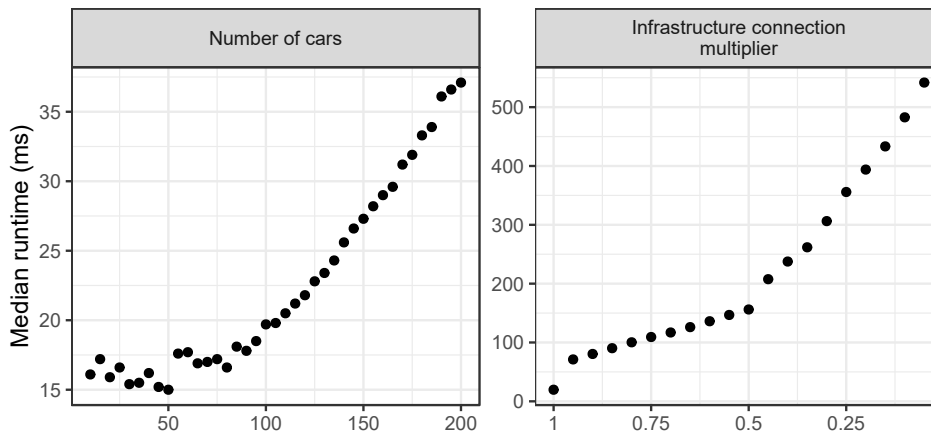


Figure 7.15: Median runtime of the REST API

²<https://artillery.io/>

We use the term infrastructure connection multiplier to refer to the size of the grid connection relative to the number of EVs. A multiplier of 1 allows all EVs to charge concurrently. In the following, EVs are assumed to charge with up to 22 kW. For example, in a fleet of ten EVs and a multiplier of 1 we set the infrastructure connection to 220 kW. A multiplier of 0.5 allows half of all EVs to charge concurrently. In a fleet of ten EVs the infrastructure connection is then set to 110 kW. A lower multiplier makes the scheduling process more computationally intensive because EVs must be rescheduled more often. In the field test, the multiplier would be 0.33.

Figure 7.15 shows the recorded median runtime for each request. For the left graph we vary the number of EVs from 10 to 200 while keeping the infrastructure connection multiplier at 1. The runtime per request behaves linearly and remains below 40 ms.

For the right graph we vary the infrastructure connection multiplier from 1 to 0.1 while keeping the number of EVs constant at 100. The runtime measurements remain sub-second which implies that the charge scheduling heuristic is able to be used in real-time with large EV fleets and very limited charging infrastructures.

7.5 Discussion

The open source charge scheduling heuristic presents an openly accessible option for CPOs to control charging operations with charge plans. Due to the fast computation times the heuristic can manage fleets of arbitrary sizes in real-time. For interoperability, the encapsulation of the heuristic into REST services enables integrating the heuristic with any CPO system thus bridging potential technology barriers. In contrast to commercial offerings, the open source heuristic is not limited to specific charging hardware or specific EV models but can be applied in any infrastructure.

Installations for charge point operations are complex and error-prone as the field test has shown. Smart charging adds another level of complexity to the layered system with components ranging from the vehicle to the charging station with its software and finally to the CPO backend system in its cloud environment. Each layer lies in the responsibility of potentially separate entities with their own business interests. Integrating the detailed log outputs from the open source package with other software layers would keep the system manageable for a CPO and would serve as input for automated error support systems.

In terms of future functional enhancements such as vehicle-to-grid enablement the open source package is easily extendable. The software design caters for code

inheritance and code changes can be contributed and shared via the open source repository. From the software engineering perspective a CI/CD pipeline is automatically executed upon each code change to ensure software quality through unit tests.

7.6 Conclusion

In this chapter we present an open source charge scheduling heuristic for EV fleets. We validated the heuristic during a one-year field test with a real charging infrastructure. We address the research question of how to implement a charge scheduling heuristic which is interoperable with other systems such as CPO backends.

The presented charge scheduling heuristic is accessible via REST API, is designed to be used in real-time and is open to individual requirements and preferences. Additionally, the open source package contains a web application which can be used to demonstrate the motivation for smart charging to stakeholders and to experiment with inputs and outputs to the REST API. Experimental results during the one-year field test show the charge scheduling heuristic can be applied in a charging infrastructure with a limited connection to the grid.

Future work includes extending the heuristic to be customizable with regard to attributes such as the voltage of the grid and to propose integrations with open source packages containing other systems required for a smart charging approach.

Chapter 8

Conclusion

8.1 Summary

This section recaps the research questions listed in section 1.2 and summarizes the approaches and results presented throughout the thesis.

How can EV charging be coordinated in a three-phase charging infrastructure during different times of planning?

Chapter 3 presents a smart charging approach which combines day-ahead planning with real-time planning [52]. A MIP model is used to precompute optimal schedules ahead of time. Schedules are optimal with regard to one or more objective function components: Maximizing fair share, minimizing peak demand, minimizing energy costs and minimizing load imbalance. Schedules are computed taking into constraints such as the available three-phase charging infrastructure and EV charging characteristics. The forecasting approaches in chapter 4 and section A.3 can be used to generate input data for the MIP model.

In practice, EVs do not arrive exactly as originally planned. We thus present a schedule guided heuristic which is used to adapt precomputed schedules in real-time. For example, if the EV arrives later than planned the schedule is adapted to allow the EV to reach a full SoC independent of its late arrival.

Simulations show a consistently higher mean final SoC when applying the presented methods over uncoordinated charging (table 3.6). The schedule guided heuristic on its own shows up to 58% more energy charged (526kWh vs 332kWh) while the combination of the MIP model and the schedule guided heuristic shows up to 123% more energy charged (741kWh vs 332kWh). At the same time, average energy costs are reduced by up to 27% with the schedule guide heuristic and by up to 28% with the combination of the MIP model and heuristic.

One of the main contributions of this approach is the consideration of single-phase and three-phase charging. In practice, EVs typically charge either on a single phase or on three phases. However, to the best of our knowledge this constraint is not modelled in related work on smart charging. A limitation of this approach is the assumption that EVs are able to charge at a constant power during the complete charging process. In practice, power falls off towards high SoC thus potentially making EV schedules inaccurate. This limitation is addressed in chapters 5 and 6.

How can we address the uncertainty of EV availability in smart charging and quantify a solution's impact on charge schedule quality?

Chapter 4 describes an approach aiming to address the uncertainty of EV availability in smart charging [54]. A regression model is trained on historical data and is used to predict each EV's departure time. The predicted EV departure time is used in the prioritization function of the heuristic presented in chapter 3. The main contribution of this approach is the direct integration of predictions in a smart charging approach.

The most accurate regression model (XGBoost) shows an MAE of 4911 seconds which is a 21% improvement compared to the baseline of using the historical median (MAE of 6245). Integrating the regression model in the charge scheduling heuristic leads to a comparatively small improvement of 3.2% more energy charged over using the historical median for unplanned EVs (6163kWh vs 5974kWh). However, there is potential for further gains when using more accurate regression models: Using a perfect predictor (oracle) shows an improvement of 9.2% (6524kWh vs 5974kWh).

Furthermore, we compare different regression models with varying levels of prediction accuracy. Different levels of prediction accuracy allows quantifying the impact of prediction accuracy on smart charging quality. Simulations show a higher prediction accuracy consistently leads to improved smart charging quality quantified by a correlation of -0.968 between the MAE and the mean fraction of minimum SoC.

How do integrated predictions of battery charge profiles affect smart charging?

Chapters 5 and 6 address one of the limitations of the smart charging heuristic, namely the assumption that EVs are able to charge at a constant power throughout the charging process. In practice, the power declines towards high SoC. Each of the two chapters presents a different approach to modelling the EV's power over time.

Chapter 5 uses a traditional battery modelling approach of using an equivalent circuit model (ECM) to describe the EV's charging power in relation to its SoC. An ECM is modelled based on parameters of battery cells used in two popular BEV models (Tesla Model S and Renault Zoe). The ECM is then directly integrated in the smart charging heuristic to allow simulating EV power and thus to compute more accurate charge plans. Simulations show how using the ECM over the linear version of the heuristic leads to EVs charging up to 8.7% more energy because the infrastructure is used more efficiently.

The main limitation of using an ECM is the availability of the parameters required by the ECM. For example, in practice, the CPO applying smart charging would likely be unable to access the EV's battery voltage.

Chapter 6 describes a more practical approach [55] to allow the smart charging heuristic to take into account battery behavior. Historical data is used to train a regression model to directly predict EV charging power depending on its SoC. Using a gradient tree boosting algorithm (XGBoost) as a regression model showed the highest prediction accuracy (MAE of 126W), a 94% improvement over the baseline of assuming the maximum power (MAE of 2077W).

The model of the EV's charging power is then directly integrated into the smart charging heuristic which allows the heuristic to produce more accurate charge plans. Experimental results show how in a limited charging infrastructure, EVs charge up to 21% more energy (259kWh vs 213kWh) when using the regression model over the baseline.

How can a charge scheduling heuristic be implemented which is open and interoperable with other systems?

Chapter 7 presents an open source package containing the smart charging heuristic. The heuristic is encapsulated in a server and is accessed via REST API. Additionally, the open source package contains an interactive web application. The web application uses the REST API to visualize the motivation of smart charging and to show the internal data model of the heuristic.

The chapter also describes experimental results from applying the smart charging heuristic in a physical installation during a field test in 2019. The infrastructure represented a limited charging infrastructure as described in the scenario (section 2.1). The infrastructure consisted of six charging stations and was limited to 44kW. Each charging station was rated to charge at 22kW. Consequently, only two charging stations could be used concurrently at full power. The smart charging heuristic was successfully applied in the field test to schedule EVs for charging. The infrastructure limit of 44kW was never exceeded.

8.2 Outlook

Alternative optimization methods. In chapter 3 we use a MIP model for day-ahead planning together with the schedule guided heuristic for real-time planning. In later chapters, we do not use the MIP model because of we focus on nonlinear aspects of the scenario. For example, the decline in EV charging power towards the end of charging processes is nonlinear. The MIP model is unable to take into account such nonlinear constraints. Chapter 5 uses an ECM to model the charging power as a differential equation. Approaches optimizing differential equations could be used to compute optimal schedules while taking into account nonlinear charging processes.

Smart charging in practice. From the perspective of implementing smart charging in practice, evolving standards such as OCPP and ISO 15118 facilitate several aspects of smart charging. For example, ISO 15118 was not available during the field test discussed in chapter 7. The protocol would allow continuously retrieving data from the EV such as its SoC.

Open source package. At the time of writing, the open source package offers a REST API to allow access to the smart charging heuristic. However, the integration of regression models for EV departure time prediction (chapter 4) is not implemented in a standardized manner. Similarly, allowing users to integrate models which predict EV charging power in advance (chapter 6) is another topic for future work.

Bibliography

- [1] I. Aghabali, J. Bauman, and A. Emadi, “Analysis of Auxiliary Power Unit and Charging for an 800V Electric Vehicle,” in *2019 IEEE Transportation Electrification Conference and Expo (ITEC)*, Jun. 2019, pp. 1–6.
- [2] E. Akhavan-Rezai, M. F. Shaaban, E. F. El-Saadany, and F. Karray, “Priority-based charging coordination of plug-in electric vehicles in smart parking lots,” in *ISGT 2014*, Feb. 2014, pp. 1–5.
- [3] A. T. Al-Awami and E. Sortomme, “Coordinating Vehicle-to-Grid Services With Energy Trading,” *IEEE Transactions on Smart Grid*, vol. 3, no. 1, pp. 453–462, Mar. 2012.
- [4] B. Albeg, S. Carter, D. Ettelson, M. Julian, and T. Paschos, “SmartCharge,” University of California, Santa Barbara, May 2019, <https://github.com/mjulian55/SmartCharge>.
- [5] B. Alinia, M. H. Hajiesmaili, and N. Crespi, “Online EV Charging Scheduling With On-Arrival Commitment,” *IEEE Transactions on Intelligent Transportation Systems*, pp. 1–14, 2019.
- [6] M. H. Amini, A. Kargarian, and O. Karabasoglu, “ARIMA-based decoupled time series forecasting of electric vehicle charging demand for stochastic power system operation,” *Electric Power Systems Research*, vol. 140, pp. 378–390, Nov. 2016.
- [7] E. Apostolaki-Iosifidou, P. Codani, and W. Kempton, “Measurement of power loss during electric vehicle charging and discharging,” *Energy*, vol. 127, pp. 730–742, May 2017.
- [8] M. F. M. Arani and Y. A. I. Mohamed, “Cooperative Control of Wind Power Generator and Electric Vehicles for Microgrid Primary Frequency Regulation,” *IEEE Transactions on Smart Grid*, vol. 9, no. 6, pp. 5677–5686, Nov. 2018.

- [9] M. B. Arias and S. Bae, “Electric vehicle charging demand forecasting model based on big data technologies,” *Applied Energy*, vol. 183, pp. 327–339, Dec. 2016.
- [10] A. Ashtari, E. Bibeau, S. Shahidinejad, and T. Molinski, “PEV Charging Profile Prediction and Analysis Based on Vehicle Usage Data,” *IEEE Transactions on Smart Grid*, vol. 3, no. 1, pp. 341–350, Mar. 2012.
- [11] P. Bach Andersen, J. Hu, and K. Heussen, “Coordination strategies for distribution grid congestion management in a multi-actor, multi-objective setting,” in *2012 3rd IEEE PES Innovative Smart Grid Technologies Europe (ISGT Europe)*, Oct. 2012, pp. 1–8.
- [12] P. Balram, T. Le Anh, and L. Bertling Tjernberg, “Effects of plug-in electric vehicle charge scheduling on the day-ahead electricity market price,” in *2012 3rd IEEE PES Innovative Smart Grid Technologies Europe (ISGT Europe)*, Oct. 2012, pp. 1–8.
- [13] X. Bi and W. K. S. Tang, “Logistical Planning for Electric Vehicles Under Time-Dependent Stochastic Traffic,” *IEEE Transactions on Intelligent Transportation Systems*, pp. 1–11, 2018.
- [14] A. Bilh, K. Naik, and R. El-Shatshat, “A Novel Online Charging Algorithm for Electric Vehicles Under Stochastic Net-Load,” *IEEE Transactions on Smart Grid*, vol. 9, no. 3, pp. 1787–1799, May 2018.
- [15] B. Bischl, M. Lang, L. Kotthoff, J. Schiffner, J. Richter, E. Studerus, G. Casalicchio, and Z. M. Jones, “Mlr: Machine Learning in R,” *Journal of Machine Learning Research*, vol. 17, no. 170, pp. 1–5, 2016.
- [16] E. Blasius and Z. Wang, “Effects of charging battery electric vehicles on local grid regarding standardized load profile in administration sector,” *Applied Energy*, vol. 224, pp. 330–339, Aug. 2018.
- [17] BMWi, “Bundesnetzagentur verbessert die Bedingungen zur Teilnahme an den Regelenergiemärkten Strom,” https://www.bundesnetzagentur.de/SharedDocs/Pressemitteilungen/DE/2017/28062017_Regelenergie.html?nn=265778, Jun. 2017, last accessed 23 Jan. 2020.
- [18] BMWi, “Innovationen für die Elektromobilität,” ”Bundesministerium für Wirtschaft und Energie”, Germany, Tech. Rep. ELEKTRO POWER II, Sep. 2018.

- [19] G. Box, G. Jenkins, and G. Reinsel, *Time Series Analysis, Fourth Edition*, fourth edition ed. John Wiley & Sons, Inc, Jun. 2008.
- [20] Y. Cao, S. Tang, C. Li, P. Zhang, Y. Tan, Z. Zhang, and J. Li, “An Optimized EV Charging Model Considering TOU Price and SOC Curve,” *IEEE Transactions on Smart Grid*, vol. 3, no. 1, pp. 388–393, Mar. 2012.
- [21] D. Caprino, M. L. Della Vedova, and T. Facchinetti, “Peak shaving through real-time scheduling of household appliances,” *Energy and Buildings*, vol. 75, pp. 133–148, Jun. 2014.
- [22] F. V. Cerna, M. Pourakbari-Kasmaei, R. A. Romero, and M. J. Rider, “Optimal Delivery Scheduling and Charging of EVs in the Navigation of a City Map,” *IEEE Transactions on Smart Grid*, vol. 9, no. 5, pp. 4815–4827, Sep. 2018.
- [23] E. Chemali, P. J. Kollmeyer, M. Preindl, and A. Emadi, “State-of-charge estimation of Li-ion batteries using deep neural networks: A machine learning approach,” *Journal of Power Sources*, vol. 400, pp. 242–255, Oct. 2018.
- [24] T. Chen and C. Guestrin, “XGBoost: A Scalable Tree Boosting System,” in *Proceedings of the 22nd ACM SIGKDD International Conference on Knowledge Discovery and Data Mining*, ser. KDD ’16. San Francisco, California, USA: Association for Computing Machinery, Aug. 2016, pp. 785–794.
- [25] F. Chollet, “Keras,” <https://keras.io>, 2015.
- [26] M. Clemente, M. P. Fanti, and W. Ukovich, “Smart Management of Electric Vehicles Charging Operations: The Vehicle-to-Charging Station Assignment Problem,” *IFAC Proceedings Volumes*, vol. 47, no. 3, pp. 918–923, Jan. 2014.
- [27] J. E. Contreras-Ocaña, M. R. Sarker, and M. A. Ortega-Vazquez, “Decentralized Coordination of a Building Manager and an Electric Vehicle Aggregator,” *IEEE Transactions on Smart Grid*, vol. 9, no. 4, pp. 2625–2637, Jul. 2018.
- [28] B. D’Andrade, *The Power Grid: Smart, Secure, Green and Reliable*. Academic Press, Mar. 2017.
- [29] Z. Darabi, P. Fajri, and M. Ferdowsi, “Intelligent Charge Rate Optimization of PHEVs Incorporating Driver Satisfaction and Grid Constraints,” *IEEE Transactions on Intelligent Transportation Systems*, vol. 18, no. 5, pp. 1325–1332, May 2017.

- [30] Datasheet, “Product Specification of LG E63,” <http://queenbattery.com.cn/our-products/677-1g-e63-376v-63ah-li-polymer-battery-cell.html>, Feb. 2018, last accessed 17 Dec. 2019.
- [31] M. de Weerd, M. Albert, and V. Conitzer, “Complexity of Scheduling Charging in the Smart Grid,” *arXiv:1709.07480 [cs]*, Sep. 2017.
- [32] S. Deilami, A. S. Masoum, P. S. Moses, and M. A. S. Masoum, “Real-Time Coordination of Plug-In Electric Vehicle Charging in Smart Grids to Minimize Power Losses and Improve Voltage Profile,” *IEEE Transactions on Smart Grid*, vol. 2, no. 3, pp. 456–467, Sep. 2011.
- [33] R. R. Desai, R. B. Chen, and W. Armington, “A Pattern Analysis of Daily Electric Vehicle Charging Profiles: Operational Efficiency and Environmental Impacts,” *Journal of Advanced Transportation*, vol. 2018, p. e6930932, 2018.
- [34] S. Detzler, “Lademanagement für Elektrofahrzeuge,” Ph.D. dissertation, KIT, Karlsruhe, May 2016.
- [35] Deutscher Wetterdienst, “Klimadaten Deutschland - Stundenwerte (Archiv),” <https://www.dwd.de/DE/leistungen/klimadatendeutschland/klarchivstunden.html>, 2020, last accessed 23 Apr. 2020.
- [36] A. Di Giorgio, F. Liberati, and S. Canale, “Electric vehicles charging control in a smart grid: A model predictive control approach,” *Control Engineering Practice*, vol. 22, pp. 147–162, Jan. 2014.
- [37] J. Dixon, W. Bukhsh, C. Edmunds, and K. Bell, “Keeping the car clean : Smart EV charging to support renewables,” in *ETP 8th Annual Conference 2019*, GBR, Nov. 2019, p. 1.
- [38] R. Donato and G. Quiles, “Machine learning systems based on xgBoost and MLP neural network applied in satellite lithium-ion battery sets impedance estimation,” *Adv. Comput. Intell. Int. J.*, vol. 5, pp. 1–20, 2018.
- [39] J. Dong, C. Liu, and Z. Lin, “Charging infrastructure planning for promoting battery electric vehicles: An activity-based approach using multiday travel data,” *Transportation Research Part C: Emerging Technologies*, vol. 38, pp. 44–55, Jan. 2014.
- [40] M. Dronia and M. Gallet, “CoFAT 2016 - Field test of charging management system for electric vehicle - State of the art charging management using

- ISO 61851 with EV from different OEMs,” in *5th Conference on Future Automotive Technology*, 2016.
- [41] J. Druitt and W.-G. Früh, “Simulation of demand management and grid balancing with electric vehicles,” *Journal of Power Sources*, vol. 216, pp. 104–116, Oct. 2012.
- [42] M. Duan, A. Darvishan, R. Mohammaditab, K. Wakil, and O. Abedinia, “A novel hybrid prediction model for aggregated loads of buildings by considering the electric vehicles,” *Sustainable Cities and Society*, vol. 41, pp. 205–219, Aug. 2018.
- [43] D. Dujic, “Presentation: Electric Vehicles Charging: An Ultrafast Overview (PCIM Asia 2019),” https://infoscience.epfl.ch/record/267807/files/Dujic_PCIM-Asia-2019-Keynote.pdf, 2019, last accessed 05 Feb. 2020.
- [44] C. Z. El-Bayeh, I. Mougharbel, M. Saad, A. Chandra, D. Asber, and S. Lefebvre, “Impact of Considering Variable Battery Power Profile of Electric Vehicles on the Distribution Network,” in *2018 4th International Conference on Renewable Energies for Developing Countries (REDEC)*, Nov. 2018, pp. 1–8.
- [45] D. C. Erb, O. C. Onar, and A. Khaligh, “Bi-directional charging topologies for plug-in hybrid electric vehicles,” in *2010 Twenty-Fifth Annual IEEE Applied Power Electronics Conference and Exposition (APEC)*, Feb. 2010, pp. 2066–2072.
- [46] European Commission, “Green eMotion,” Tech. Rep. FP7-TRANSPORT-2010-TREN-1, Feb. 2015.
- [47] S. Faddel, A. T. Al-Awami, and O. A. Mohammed, “Charge Control and Operation of Electric Vehicles in Power Grids: A Review,” *Energies*, vol. 11, no. 4, p. 701, Apr. 2018.
- [48] S. Falahati, S. A. Taher, and M. Shahidehpour, “Grid Secondary Frequency Control by Optimized Fuzzy Control of Electric Vehicles,” *IEEE Transactions on Smart Grid*, vol. 9, no. 6, pp. 5613–5621, Nov. 2018.
- [49] C. Fest and O. Franz, “Open ECOSPhERE,” RWE Effizienz GmbH, Dortmund, Tech. Rep. 01ME12085A, 2015.

- [50] R. Fielding, “REST : Architectural Styles and the Design of Network-based Software Architectures,” Ph.D. dissertation, University of California, California, 2000.
- [51] M. G. Flammini, G. Pretticco, A. Julea, G. Fulli, A. Mazza, and G. Chicco, “Statistical characterisation of the real transaction data gathered from electric vehicle charging stations,” *Electric Power Systems Research*, vol. 166, pp. 136–150, Jan. 2019.
- [52] O. Frendo, N. Gaertner, and H. Stuckenschmidt, “Real-Time Smart Charging Based on Precomputed Schedules,” *IEEE Transactions on Smart Grid*, vol. 10, no. 6, pp. 6921–6932, 2019, © 2020 IEEE. Reprinted, with permission.
- [53] O. Frendo, S. Karnouskos, N. Gaertner, O. Kipouridis, K. Rehman, and N. Verzano, “Charging Strategies and Implications for Corporate Electric Vehicle Fleets,” in *2018 IEEE 16th International Conference on Industrial Informatics (INDIN)*, Jul. 2018, pp. 466–471.
- [54] O. Frendo, N. Gaertner, and H. Stuckenschmidt, “Improving Smart Charging Prioritization by Predicting Electric Vehicle Departure Time,” *IEEE Transactions on Intelligent Transportation Systems*, pp. 1–8, 2020, © 2020 IEEE. Reprinted, with permission.
- [55] O. Frendo, J. Graf, N. Gaertner, and H. Stuckenschmidt, “Data-driven smart charging for heterogeneous electric vehicle fleets,” *Energy and AI*, vol. 1, Aug. 2020.
- [56] Y. Gao, X. Zhang, Q. Cheng, B. Guo, and J. Yang, “Classification and Review of the Charging Strategies for Commercial Lithium-Ion Batteries,” *IEEE Access*, vol. 7, pp. 43 511–43 524, 2019.
- [57] J. García-Villalobos, I. Zamora, K. Knezović, and M. Marinelli, “Multi-objective optimization control of plug-in electric vehicles in low voltage distribution networks,” *Applied Energy*, vol. 180, pp. 155–168, Oct. 2016.
- [58] M. Ghofrani, A. Arabali, and M. Ghayekhloo, “Optimal charging/discharging of grid-enabled electric vehicles for predictability enhancement of PV generation,” *Electric Power Systems Research*, vol. 117, pp. 134–142, Dec. 2014.
- [59] C. Goebel and M. Voß, “Forecasting driving behavior to enable efficient grid integration of plug-in electric vehicles,” in *2012 IEEE Online Conference on Green Communications (GreenCom)*, Sep. 2012, pp. 74–79.

- [60] M. González Vayá and G. Andersson, “Optimal Bidding Strategy of a Plug-In Electric Vehicle Aggregator in Day-Ahead Electricity Markets Under Uncertainty,” *IEEE Transactions on Power Systems*, vol. 30, no. 5, pp. 2375–2385, Sep. 2015.
- [61] ———, “Self Scheduling of Plug-In Electric Vehicle Aggregator to Provide Balancing Services for Wind Power,” *IEEE Transactions on Sustainable Energy*, vol. 7, no. 2, pp. 886–899, Apr. 2016.
- [62] K. Grave, M. Hazrat, S. Boeve, and e. al, *Electricity Costs of Energy Intensive Industries*. Berlin: Ecofys Germany GmbH, 2015.
- [63] Y. Gu, J. Xu, D. Chen, Z. Wang, and Q. Li, “Overall review of peak shaving for coal-fired power units in China,” *Renewable and Sustainable Energy Reviews*, vol. 54, pp. 723–731, Feb. 2016.
- [64] Y. Guo, J. Xiong, S. Xu, and W. Su, “Two-Stage Economic Operation of Microgrid-Like Electric Vehicle Parking Deck,” *IEEE Transactions on Smart Grid*, vol. 7, no. 3, pp. 1703–1712, May 2016.
- [65] H. V. Haghi and Z. Qu, “A Kernel-Based Predictive Model of EV Capacity for Distributed Voltage Control and Demand Response,” *IEEE Transactions on Smart Grid*, vol. 9, no. 4, pp. 3180–3190, Jul. 2018.
- [66] R. Halvgaard, N. K. Poulsen, H. Madsen, J. B. Jørgensen, F. Marra, and D. E. M. Bondy, “Electric vehicle charge planning using Economic Model Predictive Control,” in *2012 IEEE International Electric Vehicle Conference*, Mar. 2012, pp. 1–6.
- [67] L. Hirth and I. Ziegenhagen, “Balancing power and variable renewables: Three links,” *Renewable and Sustainable Energy Reviews*, vol. 50, pp. 1035–1051, Oct. 2015.
- [68] Y. Huang, “A Day-Ahead Optimal Control of PEV Battery Storage Devices Taking into Account the Voltage Regulation of the Residential Power Grid,” *IEEE Transactions on Power Systems*, pp. 1–1, 2019.
- [69] IBM, “CPLEX User’s Manual (Version 12 Release 7),” 889 Alder Avenue, Suite 200, Incline Village, NV 89451, USA, 2016.
- [70] H. Jahangir, H. Tayarani, A. Ahmadian, M. A. Golkar, J. Miret Tomàs, M. Tayarani, and H. O. Gao, “Charging demand of Plug-in Electric Vehicles:

- Forecasting travel behavior based on a novel Rough Artificial Neural Network approach,” *Journal of cleaner production*, vol. 229, pp. 1029–1044, Aug. 2019.
- [71] John Snow Labs, “Electric Vehicle Charging Network,” <https://datahub.io/JohnSnowLabs/electric-vehicle-charging-network>, 2018, last accessed 11 Mar. 2020.
- [72] M. Jun and A. Meintz, “Workplace Charge Management with Aggregated Building Loads,” in *2018 IEEE Transportation Electrification Conference and Expo (ITEC)*, Jun. 2018, pp. 315–319.
- [73] A. Junid, E. Yap, and P. Ng, “Electric Vehicle Charging at Telco Base Station and Bidirectional Charging at Hillslope Descent Technical-Commercial Cost-Benefit Study and Scheduling-Reservation System,” in *2018 International Conference on Smart Grid and Clean Energy Technologies (ICSGCE)*, May 2018, pp. 137–144.
- [74] V. Kaminski, *Energy Markets*. London: Risk Books, 2012.
- [75] Q. Kang, S. Feng, M. Zhou, A. C. Ammari, and K. Sedraoui, “Optimal Load Scheduling of Plug-In Hybrid Electric Vehicles via Weight-Aggregation Multi-Objective Evolutionary Algorithms,” *IEEE Transactions on Intelligent Transportation Systems*, vol. 18, no. 9, pp. 2557–2568, Sep. 2017.
- [76] E. C. Kara, J. S. Macdonald, D. Black, M. Bérges, G. Hug, and S. Kiliccote, “Estimating the benefits of electric vehicle smart charging at non-residential locations: A data-driven approach,” *Applied Energy*, vol. 155, pp. 515–525, Oct. 2015.
- [77] S. Karapostolakis, E. S. Rigas, N. Bassiliades, and S. D. Ramchurn, “EVLlib: A Library for the Management of the Electric Vehicles in the Smart Grid,” in *Proceedings of the 9th Hellenic Conference on Artificial Intelligence*, ser. SETN ’16. Thessaloniki, Greece: Association for Computing Machinery, May 2016, pp. 1–4, <https://github.com/skarapost/EVLlib>.
- [78] Karlsruhe Institute of Technology, “MeRegioMobil: Electric Mobility in the Future Energy System,” Tech. Rep., Nov. 2011.
- [79] S. Karnouskos, P. G. Da Silva, and D. Ilic, “Energy services for the smart grid city,” in *2012 6th IEEE International Conference on Digital Ecosystems and Technologies (DEST)*, Jun. 2012, pp. 1–6.

- [80] I. Kasikci, *Elektrotechnik Für Architekten, Bauingenue Und Gebäudetechniker: Grundlagen Und Anwendung in Der Gebäudeplanung*, 2nd ed. Weinheim: Springer Vieweg, 2018.
- [81] J. Kester, L. Noel, X. Lin, G. Zarazua de Rubens, and B. K. Sovacool, “The coproduction of electric mobility: Selectivity, conformity and fragmentation in the sociotechnical acceptance of vehicle-to-grid (V2G) standards,” *Journal of Cleaner Production*, vol. 207, pp. 400–410, Jan. 2019, 00002.
- [82] D. Kettles, “Electric Vehicle Charging Technology Analysis And Standards,” Electric Vehicle Transportation Center, Cocoa, Florida, Tech. Rep. FSEC-CR-1996-15, Feb. 2015.
- [83] A. Khurana, A. Sundaramoorthy, and I. A. Karimi, “Improving Mixed Integer Linear Programming Formulations,” in *Proc. of the AIChE Annual Meeting*, OH, 2005.
- [84] A. Kieldsen, A. Thingvad, S. Martinenas, and T. M. Sørensen, “Efficiency Test Method for Electric Vehicle Chargers,” in *Proceedings of EVS29 - International Battery, Hybrid and Fuel Cell Electric Vehicle Symposium*, 2016.
- [85] M. C. Kisacikoglu, F. Erden, and N. Erdogan, “Distributed Control of PEV Charging Based on Energy Demand Forecast,” *IEEE Transactions on Industrial Informatics*, vol. 14, no. 1, pp. 332–341, Jan. 2018.
- [86] S. L. Koh and Y. S. Lim, “Evaluating the economic benefits of peak load shifting for building owners and grid operator,” in *2015 International Conference on Smart Grid and Clean Energy Technologies (ICSGCE)*, Oct. 2015, pp. 30–34.
- [87] K. Kok, S. Karnouskos, J. Ringelstein, A. Dimeas, A. Weidlich, C. Warmer, S. Drenkard, N. Hatziaargyriou, and V. Lioliou, “Field-testing smart houses for a smart grid,” in *21st International Conference and Exhibition on Electricity Distribution (CIRED 2011)*, Frankfurt, Germany, 2011, pp. 6–9.
- [88] C. Kong, R. Jovanovic, I. S. Bayram, and M. Devetsikiotis, “A Hierarchical Optimization Model for a Network of Electric Vehicle Charging Stations,” *Energies*, vol. 10, no. 5, p. 675, May 2017.
- [89] P. Kong and G. K. Karagiannidis, “Charging Schemes for Plug-In Hybrid Electric Vehicles in Smart Grid: A Survey,” *IEEE Access*, vol. 4, pp. 6846–6875, 2016.

- [90] E. Kontou, Y. Yin, and Y.-E. Ge, “Cost-Effective and Ecofriendly Plug-In Hybrid Electric Vehicle Charging Management,” *Transportation Research Record*, vol. 2628, no. 1, pp. 87–98, Jan. 2017.
- [91] D. Kroeger, “Smart Charging Algorithms for Electric Vehicles considering Voltage and Thermal Constraints,” Technical University Dortmund, Feb. 2019, <https://github.com/regeork/smart-charging>.
- [92] K. N. Kumar, B. Sivaneasan, and P. L. So, “Impact of Priority Criteria on Electric Vehicle Charge Scheduling,” *IEEE Transactions on Transportation Electrification*, vol. 1, no. 3, pp. 200–210, Oct. 2015.
- [93] Z. J. Lee, D. Chang, C. Jin, G. S. Lee, R. Lee, T. Lee, and S. H. Low, “Large-Scale Adaptive Electric Vehicle Charging,” in *2018 IEEE Global Conference on Signal and Information Processing (GlobalSIP)*, Nov. 2018, pp. 863–864.
- [94] Z. J. Lee, T. Li, and S. H. Low, “ACN-Data: Analysis and Applications of an Open EV Charging Dataset,” in *Proceedings of the Tenth ACM International Conference on Future Energy Systems*, ser. E-Energy '19. Phoenix, AZ, USA: Association for Computing Machinery, Jun. 2019, pp. 139–149.
- [95] M. Lefrancois, “CNR-SmartChargingProvider,” MINES Saint-Étienne, Sep. 2016, <https://github.com/thSMARTENERGY/CNR-SmartChargingProvider>.
- [96] M. Lelie, T. Braun, M. Knips, H. Nordmann, F. Ringbeck, H. Zappen, and D. U. Sauer, “Battery Management System Hardware Concepts: An Overview,” *Applied Sciences*, vol. 8, no. 4, p. 534, Apr. 2018.
- [97] C. Li, C. Liu, K. Deng, X. Yu, and T. Huang, “Data-Driven Charging Strategy of PEVs Under Transformer Aging Risk,” *IEEE Transactions on Control Systems Technology*, vol. 26, no. 4, pp. 1386–1399, Jul. 2018.
- [98] W. Li, T. Zhang, and R. Wang, “Energy Management Model of Charging Station Micro-Grid Considering Random Arrival of Electric Vehicles,” in *2018 IEEE International Conference on Energy Internet (ICEI)*, May 2018, pp. 29–34.
- [99] F. Lidstrom, “Smartcharge-dev,” Stockholm, May 2020, <https://github.com/fredli74/smartcharge-dev>.
- [100] Q. Lin, J. Wang, R. Xiong, W. Shen, and H. He, “Towards a smarter battery management system: A critical review on optimal charging methods of lithium ion batteries,” *Energy*, vol. 183, pp. 220–234, Sep. 2019.

- [101] S. Liu and A. H. Etemadi, "A Dynamic Stochastic Optimization for Recharging Plug-In Electric Vehicles," *IEEE Transactions on Smart Grid*, vol. 9, no. 5, pp. 4154–4161, Sep. 2018.
- [102] Y.-H. Liu, C.-H. Hsieh, and Y.-F. Luo, "Search for an Optimal Five-Step Charging Pattern for Li-Ion Batteries Using Consecutive Orthogonal Arrays," *IEEE Transactions on Energy Conversion*, vol. 26, no. 2, pp. 654–661, Jun. 2011.
- [103] Z. Liu, Q. Wu, S. Huang, L. Wang, M. Shahidehpour, and Y. Xue, "Optimal Day-Ahead Charging Scheduling of Electric Vehicles Through an Aggregative Game Model," *IEEE Transactions on Smart Grid*, vol. 9, no. 5, pp. 5173–5184, Sep. 2018.
- [104] Z. Liu, Q. Wu, S. S. Oren, S. Huang, R. Li, and L. Cheng, "Distribution Locational Marginal Pricing for Optimal Electric Vehicle Charging Through Chance Constrained Mixed-Integer Programming," *IEEE Transactions on Smart Grid*, vol. 9, no. 2, pp. 644–654, Mar. 2018.
- [105] Z. Liu, Q. Wu, K. Ma, M. Shahidehpour, Y. Xue, and S. Huang, "Two-Stage Optimal Scheduling of Electric Vehicle Charging Based on Transactive Control," *IEEE Transactions on Smart Grid*, vol. 10, no. 3, pp. 2948–2958, May 2019.
- [106] C. Madina, I. Zamora, and E. Zabala, "Methodology for assessing electric vehicle charging infrastructure business models," *Energy Policy*, vol. 89, pp. 284–293, Feb. 2016.
- [107] S. J. Maher, T. Fischer, T. Gally, G. Gamrath, A. Gleixner, R. L. Gottwald, G. Hendel, T. Koch, M. E. Lübbecke, M. Miltenberger, B. Müller, M. E. Pfetsch, C. Puchert, D. Rehfeldt, S. Schenker, R. Schwarz, F. Serrano, Y. Shinano, D. Weninger, J. T. Witt, and J. Witzig, "The SCIP Optimization Suite 4.0," Aug. 2017.
- [108] L. K. K. Maia, L. Drünert, F. La Mantia, and E. Zondervan, "Expanding the lifetime of Li-ion batteries through optimization of charging profiles," *Journal of Cleaner Production*, vol. 225, pp. 928–938, Jul. 2019.
- [109] M. Majidpour, C. Qiu, P. Chu, R. Gadh, and H. R. Pota, "Fast Prediction for Sparse Time Series: Demand Forecast of EV Charging Stations for Cell Phone Applications," *IEEE Transactions on Industrial Informatics*, vol. 11, no. 1, pp. 242–250, Feb. 2015.

- [110] S. S. Mansouri, P. Karvelis, G. Georgoulas, and G. Nikolakopoulos, "Remaining Useful Battery Life Prediction for UAVs based on Machine Learning," *IFAC-PapersOnLine*, vol. 50, no. 1, pp. 4727–4732, Jul. 2017.
- [111] L. Markram, "Electric Vehicle Charging Stations: Energy Consumption & Savings," <https://boulder.colorado.gov/open-data/electric-vehicle-charging-stations>, Feb. 2020, last accessed 11 Mar. 2020.
- [112] F. Marra, G. Y. Yang, C. Træholt, E. Larsen, C. N. Rasmussen, and S. You, "Demand profile study of battery electric vehicle under different charging options," in *2012 IEEE Power and Energy Society General Meeting*, Jul. 2012, pp. 1–7.
- [113] E. Mashhour and S. M. Moghaddas-Tafreshi, "Bidding Strategy of Virtual Power Plant for Participating in Energy and Spinning Reserve Markets - Part I: Problem Formulation," *IEEE Transactions on Power Systems*, vol. 26, no. 2, pp. 949–956, May 2011.
- [114] R. Mehta, D. Srinivasan, A. M. Khambadkone, J. Yang, and A. Trivedi, "Smart Charging Strategies for Optimal Integration of Plug-In Electric Vehicles Within Existing Distribution System Infrastructure," *IEEE Transactions on Smart Grid*, vol. 9, no. 1, pp. 299–312, Jan. 2018.
- [115] I. Momber, A. Siddiqui, T. G. S. Román, and L. Söder, "Risk Averse Scheduling by a PEV Aggregator Under Uncertainty," *IEEE Transactions on Power Systems*, vol. 30, no. 2, pp. 882–891, Mar. 2015.
- [116] S. Mousavian, M. Erol-Kantarci, L. Wu, and T. Ortmeier, "A Risk-Based Optimization Model for Electric Vehicle Infrastructure Response to Cyber Attacks," *IEEE Transactions on Smart Grid*, vol. 9, no. 6, pp. 6160–6169, Nov. 2018.
- [117] J. C. Mukherjee and A. Gupta, "A Review of Charge Scheduling of Electric Vehicles in Smart Grid," *IEEE Systems Journal*, vol. 9, no. 4, pp. 1541–1553, Dec. 2015.
- [118] M. Mültin, F. Allering, and H. Schmeck, "Integration of electric vehicles in smart homes - an ICT-based solution for V2G scenarios," in *2012 IEEE PES Innovative Smart Grid Technologies (ISGT)*, Jan. 2012, pp. 1–8.
- [119] M. Muratori, "Impact of uncoordinated plug-in electric vehicle charging on residential power demand," *Nature Energy*, vol. 3, no. 3, p. 193, Mar. 2018.

- [120] K. Nandha, P. H. Cheah, B. Sivaneasan, P. L. So, and D. Z. W. Wang, “Electric vehicle charging profile prediction for efficient energy management in buildings,” in *2012 10th International Power Energy Conference (IPEC)*, Dec. 2012, pp. 480–485.
- [121] Nationale Platform Elektromobilitaet, “Technischer Leitfaden Ladeinfrastruktur,” p. 34, Aug. 2013.
- [122] C. Neiger, “Why do electric vehicles use so many batteries?” <http://www.bbc.com/autos/story/20140204-a-false-charge>, Nov. 2014, BBC, last accessed 5 Feb. 2020.
- [123] M.-F. Ng, J. Zhao, Q. Yan, G. J. Conduit, and Z. W. Seh, “Predicting the state of charge and health of batteries using data-driven machine learning,” *Nature Machine Intelligence*, pp. 1–10, Mar. 2020.
- [124] Open Charge Alliance, “Open Charge Point Protocol 1.6,” Oct. 2015.
- [125] M. Origuchi, “Presentation: EV/HEV Batteries (World Mobility Summit 2015),” <https://youtu.be/N6sRWGjFx5w>, Oct. 2015, last accessed 19 Dec. 2019.
- [126] S. Ø. Ottesen, A. Tomasgard, and S.-E. Fleten, “Prosumer bidding and scheduling in electricity markets,” *Energy*, vol. 94, pp. 828–843, Jan. 2016.
- [127] D. Panahi, S. Deilami, M. A. S. Masoum, and S. M. Islam, “Forecasting plug-in electric vehicles load profile using artificial neural networks,” in *2015 Australasian Universities Power Engineering Conference (AUPEC)*, Sep. 2015, pp. 1–6.
- [128] R. Passey, N. Haghdam, A. Bruce, and I. MacGill, “Designing more cost reflective electricity network tariffs with demand charges,” *Energy Policy*, vol. 109, pp. 642–649, Oct. 2017.
- [129] S. Pelletier, O. Jabali, and G. Laporte, “Charge scheduling for electric freight vehicles,” *Transportation Research Part B: Methodological*, vol. 115, pp. 246–269, Sep. 2018.
- [130] M. Pilát, “Controlling the Charging of Electric Vehicles with Neural Networks,” *arXiv:1804.05978 [cs]*, Apr. 2018.
- [131] M. Pinedo, *Scheduling*. Springer, 2012, vol. 5.

- [132] S. Pirouzi, J. Aghaei, T. Niknam, M. Shafie-khah, V. Vahidinasab, and J. P. S. Catalão, “Two alternative robust optimization models for flexible power management of electric vehicles in distribution networks,” *Energy*, vol. 141, no. Supplement C, pp. 635–651, Dec. 2017.
- [133] G. L. Plett, *Battery Management Systems, Volume I: Battery Modeling*. Artech House, Sep. 2015.
- [134] ———, *Battery Management Systems, Volume II: Equivalent-Circuit Methods*. Artech House, Dec. 2015.
- [135] Y. Pochet and L. A. Wolsey, *Production Planning by Mixed Integer Programming*. Springer Science & Business Media, Apr. 2006.
- [136] K. Qian, C. Zhou, M. Allan, and Y. Yuan, “Load model for prediction of electric vehicle charging demand,” in *2010 International Conference on Power System Technology*, Oct. 2010, pp. 1–6.
- [137] N. G. Reich, J. Lessler, K. Sakrejda, S. A. Lauer, S. Iamsirithaworn, and D. A. T. Cummings, “Case study in evaluating time series prediction models using the relative mean absolute error,” *The American statistician*, vol. 70, no. 3, pp. 285–292, 2016.
- [138] T. Rui, C. Hu, G. Li, J. Tao, and W. Shen, “A distributed charging strategy based on day ahead price model for PV-powered electric vehicle charging station,” *Applied Soft Computing*, vol. 76, pp. 638–648, Mar. 2019.
- [139] J. Savitz, *Dynamic Systems Modeling of Lithium Ion Battery Systems in MATLAB Inclusive of Temperature Dependency*. Thesis, Schreyer Honors College, May 2017.
- [140] H. Schmolke, *DIN VDE 0100*, 4th ed. VDE Verlag, 2018.
- [141] J. Schmutzler, C. A. Andersen, and C. Wietfeld, “Evaluation of OCPP and IEC 61850 for smart charging electric vehicles,” in *2013 World Electric Vehicle Symposium and Exhibition (EVS27)*, Nov. 2013, pp. 1–12.
- [142] P. Schnabel, *Elektronik-Fibel*, 7th ed. Elektronik-Kompandium, Sep. 2017.
- [143] M. Schneider, A. Stenger, and D. Goeke, “The Electric Vehicle-Routing Problem with Time Windows and Recharging Stations,” *Transportation Science*, vol. 48, no. 4, pp. 500–520, Mar. 2014.

- [144] C. Schober, “iZEUS - intelligent Zero Emission Urban System,” Baden-Württemberg, Tech. Rep. <http://www.izeus.de/projekt/beschreibung-ziele.html>, Jun. 2014.
- [145] J. Sears, D. Roberts, and K. Glitman, “A comparison of electric vehicle Level 1 and Level 2 charging efficiency,” in *2014 IEEE Conference on Technologies for Sustainability (SusTech)*, Jul. 2014, pp. 255–258.
- [146] M. F. Shaaban, M. Ismail, E. F. El-Saadany, and W. Zhuang, “Real-Time PEV Charging/Discharging Coordination in Smart Distribution Systems,” *IEEE Transactions on Smart Grid*, vol. 5, no. 4, pp. 1797–1807, Jul. 2014.
- [147] Y. A. Sha’aban, A. Ikpehai, B. Adebisi, and K. M. Rabie, “Bi-Directional Coordination of Plug-In Electric Vehicles with Economic Model Predictive Control,” *Energies*, vol. 10, no. 10, p. 1507, Oct. 2017.
- [148] Siemens AG, “Integration of renewable energies and e-mobility (IRENE),” Wildpolsried (Germany), Tech. Rep., Dec. 2014.
- [149] J. Smart and S. Schey, “Battery Electric Vehicle Driving and Charging Behavior Observed Early in The EV Project,” *SAE International Journal of Alternative Powertrains*, vol. 1, no. 1, pp. 27–33, 2012.
- [150] J. Soares, M. A. Fotouhi Ghazvini, Z. Vale, and P. B. de Moura Oliveira, “A multi-objective model for the day-ahead energy resource scheduling of a smart grid with high penetration of sensitive loads,” *Applied Energy*, vol. 162, pp. 1074–1088, Jan. 2016.
- [151] Z. Song, X. Wu, X. Li, J. Sun, H. F. Hofmann, and J. Hou, “Current Profile Optimization for Combined State of Charge and State of Health Estimation of Lithium Ion Battery Based on Cramer–Rao Bound Analysis,” *IEEE Transactions on Power Electronics*, vol. 34, no. 7, pp. 7067–7078, Jul. 2019.
- [152] E. SPOT, “Intraday Continuous,” <https://www.epexspot.com/en/market-data/intradaycontinuous/intraday-table/2017-10-17/DE>, Oct. 2017.
- [153] D. Sreenivasarao, P. Agarwal, and B. Das, “Neutral current compensation in three-phase, four-wire systems: A review,” *Electric Power Systems Research*, vol. 86, pp. 170–180, May 2012.
- [154] I. Stadler and M. Sterner, “2.3 - Urban Energy Storage and Sector Coupling,” in *Urban Energy Transition (Second Edition)*, P. Droege, Ed. Elsevier, Jan. 2018, pp. 225–244.

- [155] M. Stegen and W. den Hollander, “SmartEVSE,” Jan. 2020, <https://github.com/SmartEVSE/smarte vse>.
- [156] M. Straka, P. De Falco, G. Ferruzzi, D. Proto, G. van der Poel, S. Khormali, and Ľ. Buzna, “Predicting popularity of EV charging infrastructure from GIS data,” *arXiv:1910.02498 [cs, econ, stat]*, Oct. 2019.
- [157] B. Sun, Z. Huang, X. Tan, and D. H. K. Tsang, “Optimal Scheduling for Electric Vehicle Charging With Discrete Charging Levels in Distribution Grid,” *IEEE Transactions on Smart Grid*, vol. 9, no. 2, pp. 624–634, Mar. 2018.
- [158] J. Timpner and L. Wolf, “Design and Evaluation of Charging Station Scheduling Strategies for Electric Vehicles,” *IEEE Transactions on Intelligent Transportation Systems*, vol. 15, no. 2, pp. 579–588, Apr. 2014.
- [159] R. Torabikalaki and A. Gomes, “Optimizing the Coordinated Charging of a Group of Electric Vehicles,” in *2014 IEEE Vehicle Power and Propulsion Conference (VPPC)*, Oct. 2014, pp. 1–6.
- [160] O. Tremblay, L. Dessaint, and A. Dekkiche, “A Generic Battery Model for the Dynamic Simulation of Hybrid Electric Vehicles,” in *2007 IEEE Vehicle Power and Propulsion Conference*, Sep. 2007, pp. 284–289.
- [161] A. E. Trippe, R. Arunachala, T. Massier, A. Jossen, and T. Hamacher, “Charging optimization of battery electric vehicles including cycle battery aging,” in *IEEE PES Innovative Smart Grid Technologies, Europe*, Oct. 2014, pp. 1–6.
- [162] M. Uddin, M. F. Romlie, M. F. Abdullah, S. Abd Halim, A. H. Abu Bakar, and T. Chia Kwang, “A review on peak load shaving strategies,” *Renewable and Sustainable Energy Reviews*, vol. 82, pp. 3323–3332, Feb. 2018.
- [163] D. van der Meer, G. R. C. Mouli, G. M.-E. Mouli, L. R. Elizondo, and P. Bauer, “Energy Management System With PV Power Forecast to Optimally Charge EVs at the Workplace,” *IEEE Transactions on Industrial Informatics*, vol. 14, no. 1, pp. 311–320, Jan. 2018.
- [164] M. G. Vayá and G. Andersson, “Integrating renewable energy forecast uncertainty in smart-charging approaches for plug-in electric vehicles,” in *2013 IEEE Grenoble Conference*, Jun. 2013, pp. 1–6.

- [165] G. Wang, Z. Xu, F. Wen, and K. P. Wong, "Traffic-Constrained Multiobjective Planning of Electric-Vehicle Charging Stations," *IEEE Transactions on Power Delivery*, vol. 28, no. 4, pp. 2363–2372, Oct. 2013.
- [166] M. Wang, M. Ismail, X. Shen, E. Serpedin, and K. Qaraqe, "Spatial and temporal online charging/discharging coordination for mobile PEVs," *IEEE Wireless Communications*, vol. 22, no. 1, pp. 112–121, Feb. 2015.
- [167] M. Wang, M. Ismail, R. Zhang, X. Shen, E. Serpedin, and K. Qaraqe, "Spatio-Temporal Coordinated V2V Energy Swapping Strategy for Mobile PEVs," *IEEE Transactions on Smart Grid*, vol. 9, no. 3, pp. 1566–1579, May 2018.
- [168] Q. Wang, X. Liu, J. Du, and F. Kong, "Smart Charging for Electric Vehicles: A Survey From the Algorithmic Perspective," *IEEE Communications Surveys Tutorials*, vol. 18, no. 2, pp. 1500–1517, Secondquarter 2016.
- [169] Z. Wang and S. Wang, "Grid Power Peak Shaving and Valley Filling Using Vehicle-to-Grid Systems," *IEEE Transactions on Power Delivery*, vol. 28, no. 3, pp. 1822–1829, Jul. 2013.
- [170] Y. Wi, J. Lee, and S. Joo, "Electric vehicle charging method for smart homes/buildings with a photovoltaic system," *IEEE Transactions on Consumer Electronics*, vol. 59, no. 2, pp. 323–328, May 2013.
- [171] D. Wu, H. Zeng, C. Lu, and B. Boulet, "Two-Stage Energy Management for Office Buildings With Workplace EV Charging and Renewable Energy," *IEEE Transactions on Transportation Electrification*, vol. 3, no. 1, pp. 225–237, Mar. 2017.
- [172] Z. Xu, "Forecasting Electric Vehicle Arrival & Departure Time On UCSD Campus using Support Vector Machines," Ph.D. dissertation, UC San Diego, 2017.
- [173] E. Xydas, C. Marmaras, L. Cipcigan, A. Sani Hassan, and N. Jenkins, "Forecasting Electric Vehicle charging demand using Support Vector Machines," in *Proceedings of the Universities Power Engineering Conference*, Sep. 2013, pp. 1–6.
- [174] E. Xydas, C. Marmaras, L. M. Cipcigan, N. Jenkins, S. Carroll, and M. Barker, "A data-driven approach for characterising the charging demand of electric vehicles: A UK case study," *Applied Energy*, vol. 162, pp. 763–771, Jan. 2016.

- [175] Y. Yang, Q. Jia, X. Guan, X. Zhang, Z. Qiu, and G. Deconinck, "Decentralized EV-Based Charging Optimization With Building Integrated Wind Energy," *IEEE Transactions on Automation Science and Engineering*, vol. 16, no. 3, pp. 1002–1017, Jul. 2019.
- [176] W. Yao, J. Zhao, F. Wen, Z. Dong, Y. Xue, Y. Xu, and K. Meng, "A Multi-Objective Collaborative Planning Strategy for Integrated Power Distribution and Electric Vehicle Charging Systems," *IEEE Transactions on Power Systems*, vol. 29, no. 4, pp. 1811–1821, Jul. 2014.
- [177] Z. Yi and M. Shirk, "Data-driven optimal charging decision making for connected and automated electric vehicles: A personal usage scenario," *Transportation Research Part C: Emerging Technologies*, vol. 86, pp. 37–58, Jan. 2018.
- [178] A. Yoza, A. M. Howlader, K. Uchida, A. Yona, and T. Senjyu, "Optimal scheduling method of controllable loads in smart house considering forecast error," in *2013 IEEE 10th International Conference on Power Electronics and Drive Systems (PEDS)*, Apr. 2013, pp. 84–89.
- [179] Z. Yu, S. Chen, and L. Tong, "An intelligent energy management system for large-scale charging of electric vehicles," *CSEE Journal of Power and Energy Systems*, vol. 2, no. 1, pp. 47–53, Mar. 2016.
- [180] T. Zahid, K. Xu, W. Li, C. Li, and H. Li, "State of charge estimation for electric vehicle power battery using advanced machine learning algorithm under diversified drive cycles," *Energy*, vol. 162, pp. 871–882, Nov. 2018.
- [181] A. Zakariazadeh, S. Jadid, and P. Siano, "Multi-objective scheduling of electric vehicles in smart distribution system," *Energy Conversion and Management*, vol. 79, pp. 43–53, Mar. 2014.
- [182] F. Zhang, J. Xi, and R. Langari, "Real-Time Energy Management Strategy Based on Velocity Forecasts Using V2V and V2I Communications," *IEEE Transactions on Intelligent Transportation Systems*, vol. 18, no. 2, pp. 416–430, Feb. 2017.
- [183] G. Zhang, S. T. Tan, and G. G. Wang, "Real-Time Smart Charging of Electric Vehicles for Demand Charge Reduction at Non-Residential Sites," *IEEE Transactions on Smart Grid*, vol. 9, no. 5, pp. 4027–4037, Sep. 2018.
- [184] K. Zhang, Y. Mao, S. Leng, Y. He, S. Maharjan, S. Gjessing, Y. Zhang, and D. H. K. Tsang, "Optimal Charging Schemes for Electric Vehicles in Smart

- Grid: A Contract Theoretic Approach,” *IEEE Transactions on Intelligent Transportation Systems*, vol. 19, no. 9, pp. 3046–3058, Sep. 2018.
- [185] Y. Zhang, C. Wang, and H. Wei, “Parking Reservation Auction for Parked Vehicle Assistance in Vehicular Fog Computing,” *IEEE Transactions on Vehicular Technology*, vol. 68, no. 4, pp. 3126–3139, Apr. 2019.
- [186] Y. Zhang, P. You, and L. Cai, “Optimal Charging Scheduling by Pricing for EV Charging Station With Dual Charging Modes,” *IEEE Transactions on Intelligent Transportation Systems*, pp. 1–11, 2018.
- [187] T. Zhao, Y. Li, X. Pan, P. Wang, and J. Zhang, “Real-Time Optimal Energy and Reserve Management of Electric Vehicle Fast Charging Station: Hierarchical Game Approach,” *IEEE Transactions on Smart Grid*, vol. 9, no. 5, pp. 5357–5370, Sep. 2018.
- [188] D. Zhou, F. Gao, A. Ravey, A. Al-Durra, and M. G. Simões, “Online energy management strategy of fuel cell hybrid electric vehicles based on time series prediction,” in *2017 IEEE Transportation Electrification Conference and Expo (ITEC)*, Jun. 2017, pp. 113–118.
- [189] Y. Zhou, D. K. Y. Yau, P. You, and P. Cheng, “Optimal-Cost Scheduling of Electrical Vehicle Charging Under Uncertainty,” *IEEE Transactions on Smart Grid*, vol. 9, no. 5, pp. 4547–4554, Sep. 2018.

Appendix A

Appendix

A.1 Nomenclature: MIP model

This section contains the nomenclature for the MIP model and the heuristic presented in chapter 3.

Indices

i	Charging station
j	Phase
k	15 minute timeslot
l	Fuse

Decision variables

$I_{i,j,k} \in \mathbb{R}$	Charging current
$X_{i,n} \in \{0, 1\}$	Car assignment

Utility variables

$D_{k,i,i'}^+, D_{k,i,i'}^- \in \mathbb{R}^+$	Load imbalance differences
$E_k^+, E_k^- \in \mathbb{R}^+$	Deviation of total current from previous timeslot
$Q_{i,k,n} \in \mathbb{R}^+$	Sum previously loaded

$Q'_{n,below} \in [0, 1],$	Missing SoC fraction towards b'_n
$Q'_{n,above} \in [0, 1],$	Missing SoC fraction towards b_n
$U_{k,n} \in \{0, 1\}$	Is car n below max SoC at k ?
$U'_{k,n} \in \{0, 1\}$	Is car n below b'_n at k ?
$V_{k,n} \in \{0, 1\}$	Is car n charging at k ?
$Y_{k,n} \in \{0, 1\}$	Does car n start charging after k ?

Parameters

$a_{j,n} \in [0, 1]$	Proportion n charges on j , $a_{1,n} \geq a_{2,n} \geq a_{3,n}$ (w.l.o.g.)
$b_n \in \mathbb{R}, b_n \geq 0$	Charging needs per car n (in Ah)
$b'_n \in \mathbb{R}, b'_n \geq 0$	Min charging needs per car n (in Ah)
$b''_n \in \mathbb{R}, b''_n \geq 0$	Start capacity per car n (in Ah)
$c_k \in \mathbb{R}$	Energy price for k (in €/MWh)
$d_{k,n} \in \{0, 1\}$	Is car n available at k ?
$e_{i,j} \in \mathbb{R}, e_{i,j} \geq 0$	Fuse at i on j (in A)
$f_{j,n} \in \mathbb{R}, f_{j,n} \geq 0$	Max current for n on j (in A)
$g_{j,n} \in \mathbb{R}, g_{j,n} \geq 0$	Min current for n on j (in A)
$h_{l,j} \in \mathbb{R}, h_{l,j} \geq 0$	Fuse l on phase j (in A)
$o_n \in \{0, 1\}$	Is car n a BEV?
$o'_n \in \{0, 1\}$	Is car n a PHEV?
$o''_i \in \{0, 1\}$	Are BEVs allowed at charging station i ?
$o'''_i \in \{0, 1\}$	Are PHEVs allowed at charging station i ?
$r_n \in \{0, 1\}$	Must n start charging upon arrival?
$s_n \in \{0, 1\}$	Is charging for car n suspendable?
$t_n \in \{0, 1\}$	Can car n charge with variable current?
$w_n \in [0, 1]$	Car n charging efficiency
$M = 10^5$	Constant used for the big-M method

$PhaseMap_{i,j} \in \{1, 2, 3\}$	Charging station grid connection: Map for i from j to j'
----------------------------------	---

A.2 Nomenclature: ECM

This section contains the nomenclature for the ECM used in chapter 5.

η	$\in [0, 1]$	Charging efficiency
t	$\in \mathbb{R}^+$	Time
$z(t)$	$\in [0, 1]$	State of charge
z_{min}	$\in [0, 1]$	Minimum required state of charge
$C_1(z(t))$	$\in \mathbb{R}^+$	Battery's RC circuit capacitance (F)
$I(t)$	$\in \mathbb{R}$	Battery current (A)
$I_{R_1}(t)$	$\in \mathbb{R}$	Current in RC circuit (A)
N_p	$\in \mathbb{N}$	Number of battery cells in parallel
N_s	$\in \mathbb{N}$	Number of battery modules in series
$P_{CS}(t)$	$\in \mathbb{R}$	Maximum power allowed by charge schedules (W)
$P_{CS}(t_1, t_2)$	$\in \mathbb{R}$	Maximum power allowed in interval $[t_1, t_2]$ (W)
P_{CP}	$\in \mathbb{R}$	Maximum power during constant-power (CP) phase (W)
$P(t)$	$\in \mathbb{R}$	Power drawn by EV (W)
\hat{P}_{t_1, t_2}	$\in \mathbb{R}^+$	Desired energy to be charged in interval $[t_1, t_2]$ (kWh)
Q	$\in \mathbb{R}^+$	Battery capacity (Ah)
$R_0(z(t))$	$\in \mathbb{R}^+$	Battery's equivalent series resistance (Ω)
$R_1(z(t))$	$\in \mathbb{R}^+$	Battery's RC circuit resistance (Ω)
$V_{OC}(z(t))$	$\in \mathbb{R}^+$	Open circuit voltage (V)
$V(t)$	$\in \mathbb{R}^+$	Battery voltage (V)
$V_{terminal}$	$\in \mathbb{R}^+$	Terminal voltage (V)

A.3 Addendum: Predicting arrival SoC

The main topic in chapter 4 is the prediction of EV departures. Predicting EV departures improves smart charging once EVs are assigned. However, BEVs which are used for typical commutes do not require charging every single day. A charging process every few days may be more realistic. The experiments in chapter 3 show how if there are not enough charging stations for each EV to charge at every single day, a first-come, first-serve assignment approach performs badly. Additionally, in a workplace setting a first-come, first-serve scheduling approach incentivizes employees to arrive early.

Alternatively, a system of reservations could be introduced, where employees reserve a charging spot for the next day. This would be a more effective assignment approach, assuming employees use such a system responsibly. The goal of maximizing the minimum required SoC (represented by *adequately charged* EVs) remains the same. However, a system of reservations also creates additional effort for the employee to reserve a spot during every charging process. Forecasting may be used to automate the process of reservations, thus avoiding the additional effort.

This section focuses on predicting the SoC upon arrival to reserve charging stations fairly. EVs may then be prioritized during the process of charging station allocation using the predicted SoC.

Dataset characteristics

In this section, an earlier version of the historical dataset in section 4.2 is used. The dataset contains 58,000 charging processes from a period of roughly 22 months.

Figure A.1 shows the distribution of hours until the next charging process, from the end of one process to the end of the next process. The time difference is subtracted by 48 hours if there is a weekend in between and thus only shows working days. The highest peak far is around 24 hours, which means EVs (BEVs as well as PHEVs) are overwhelmingly charged again the next day.

Note that the data was gathered at a time when no smart charging system or system of reservations was implemented. This means employees, especially those with PHEVs, charge daily if given the chance. Additionally, there is no data available related to EVs that are unable to charge due to a lack of charging stations.

Forecasting features

The features listed in Table A.1 are used to create a dataset to train regression models. Categorical features are one-hot encoded.

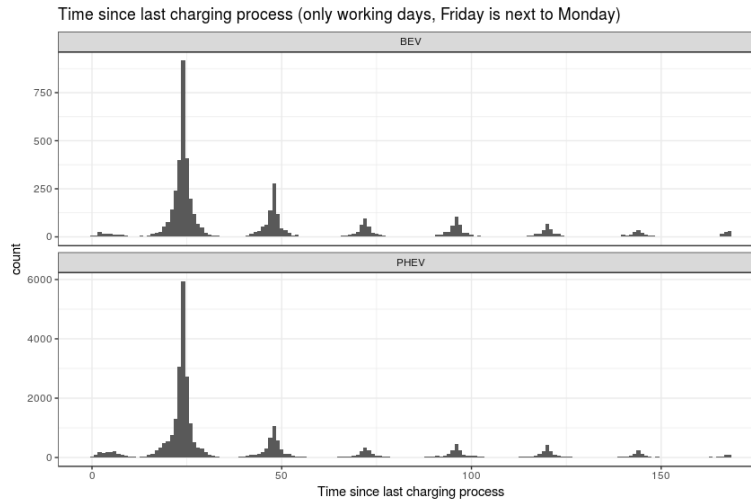


Figure A.1: Distribution of time between charging processes (weekend days are ignored and not counted). The most common time difference by far is 24 hours. BEVs (the top graph) and PHEVs (the bottom graph) show roughly the same behavior, with differences in how high the peak after 48h is relative to the 24h peak.

Feature name	Description
Last known arrival SoC	The relative SoC of the EV on arrival of the previous day
Last known arrival SoC (absolute)	The absolute SoC (in Ah) of the EV on arrival of the previous day
Last known departure SoC	The relative SoC of the EV on departure on the previous day. For forecasting, this is more useful than the arrival SoC since it contains information whether the EV was charged on that day
Last known departure SoC (absolute)	The absolute SoC (in Ah) of the EV on departure on the previous day
Last weekday	Weekday of the previous day (categorical)
Number of days since last process	How many days have passed since the last charging process? This contains information about whether there was a weekend since the last charging process
Car type	Is the car a BEV or PHEV? (categorical)
Car model name	Model name of the car (categorical)
Car maximum capacity	Maximum capacity of the EV (in Ah)
Current weekday	Weekday of current day (categorical)

Table A.1: Features for predicting arrival SoC: Categorical features are one-hot encoded.

Experimental setup

In the following, we discuss the experimental setup for predicting arrival SoC. The capacity of the grid connection is set such that all cars can safely charge at the same time. We set the number of EVs to 100 and the number of charging stations to 50. Each EV is assumed to arrive on company premises daily. The daily arrival is based on the historical data in figure A.1 showing that the most common time between charging processes is roughly 24 hours.

Furthermore, each EV is used daily. In the simulation, an amount is subtracted each day from the EV’s current SoC. The amount is sampled from discrete distributions generated from historical data, categorized by EV type (BEV/PHEV) and week day. For example, the amount of energy used during charging processes on Mondays (roughly an average of 16kWh) is higher than other weekdays (roughly an average of 12kWh). For PHEVs, the difference is not as large (6.5kWh vs 6.3kWh). Additionally, only charging processes that also have a charging processes less than 36 hours ago are used. In other words, each charging process is only used if the EV was also charged less than 36h ago.

To create charging schedules, the schedule guided heuristic from section 3.2.2 is applied without day-ahead planning. The approaches in Table A.2 are compared to assign EVs to charging stations.

Assignment strategy	Description
Baseline	A first-come-first-serve system representing the status quo
Round robin	Each EV is assigned every $\frac{nCars}{nChargingStations}$ days
Oracle	Predict arrival SoC perfectly. EVs are prioritized by relative SoC
Forecasting	Prioritize and assign EVs by forecasted (relative and absolute) SoC. Forecasting is implemented via different regression methods for predicting arrival SoC

Table A.2: Strategies for assigning EVs to charging stations

Experimental results

Regression methods

In this section we train and compare regression models for predicting the absolute SoC (in Ah) as well as the relative SoC. The final mean absolute error (MAE) on

the dataset is shown in Table A.3. XGBoost shows only slight improvements over using a simple linear regression. XGBoost hyperparameters are tuned using 10-fold cross validation. The average prediction error in the right column is relatively small (e.g. 15Ah corresponds to 3.45kWh).

Method	MAE (relative SoC)	MAE (absolute SoC)
Median	0.2997	78.700
Linear regression	0.1311	17.486
XGBoost	0.1197	15.705

Table A.3: Mean absolute error (MAE) per regression model predicting arrival SoC

Figure A.2 shows the feature importance of the trained XGBoost model. XGBoost weighs the absolute last known departure SoC highest.

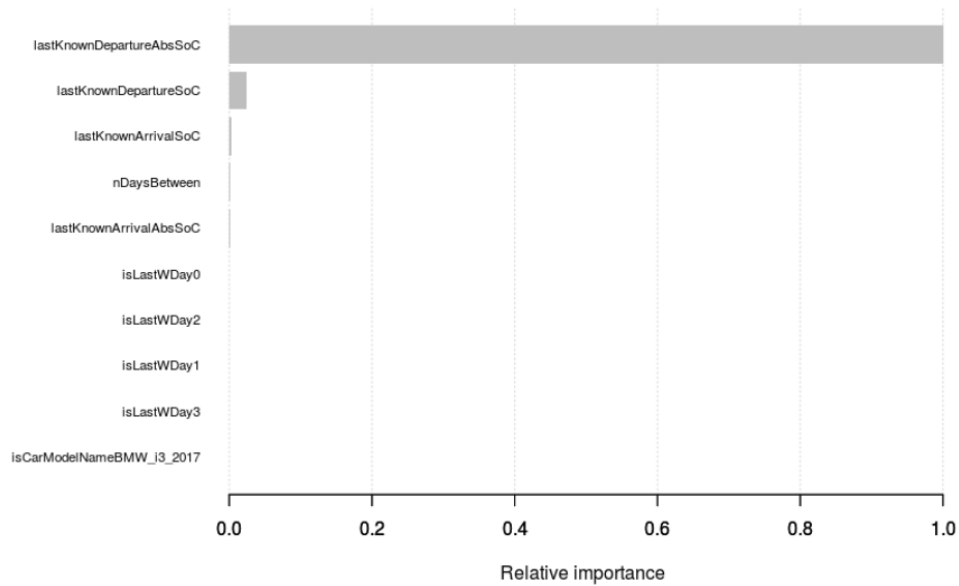


Figure A.2: Feature importance of the trained XGBoost model for predicting arrival SoC

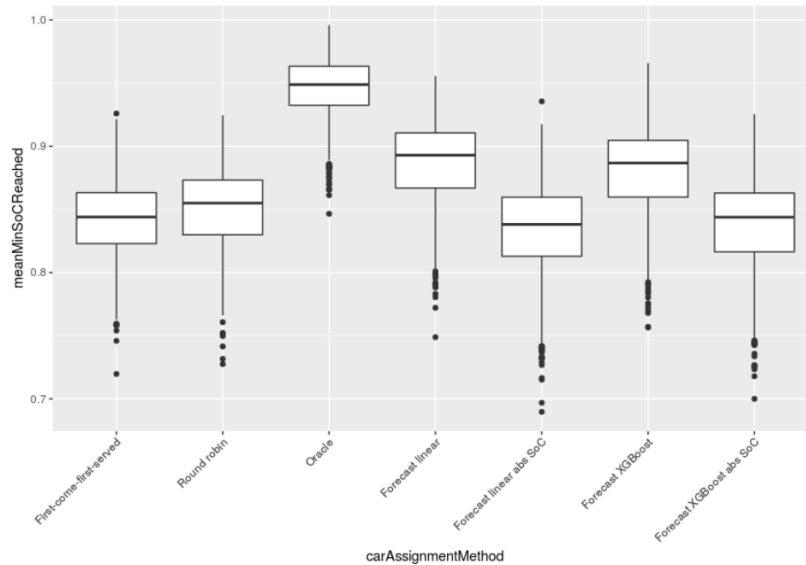


Figure A.3: Influence of regression method and assignment approach on the fraction of minimum SoC

Scheduling using predicted arrival SoC

In total, 1,400 days are simulated sequentially for each approach with 100 cars and 50 charging stations. The quality measure is defined by the fraction of the minimum SoC reached to represent the goal of maximizing fair share. Figure A.3 shows a box plot per scheduling approach.

The first-come-first-serve baseline shows the worst performance, even though car arrival times are randomized each day. A round robin approach giving an equal number of charging opportunities to each EV is only slightly better, which is likely due to the set of 5 different EV models implemented. Each EV model has a different battery maximum capacity. The oracle prioritizes EVs by the target variable and shows significantly better performance compared to other approaches.

Prioritizing by the predicted absolute SoC shows a low fraction of the minimum SoC reached for both the simple linear regression and XGBoost. Both models predicting the relative SoC show better performance. The performance of the regression methods lies between the two naive approaches and the oracle. This indicates that the accuracy of the linear regression may be sufficient in practice. Overall, using any method of prediction shows significant improvements in how EVs are prioritized over the naive approaches.

A.4 Addendum: Predicting EV charging profiles

External temperature as a feature

Chapter 6 describes how a charging profile per EV may be predicted in order to improve smart charging. However, in practice, *internal* as well as *external* (ambient) temperature affects EV charging processes and thus how well EVs adhere to charge plans. Internal EV battery temperature is not part of our dataset. It is unlikely that EVs will report their internal temperature to charging stations (and thus to the CPO) in future. Different EV models with active and passive cooling additionally complicate the issue of temperature.

Regarding external temperature, in our dataset EVs charge in different parking houses. In the following, we present additional experiments to study whether including temperature as a feature improves regression model accuracy.

First, we enrich the dataset with an external temperature feature. The temperature includes hourly measurements [35] from a weather station close ($< 50\text{km}$) to most of the parking houses. Second, we retrain the regression models with the additional temperature feature.

Table A.4 shows the mean absolute error (MAE) per regression model with and without the new temperature feature. There is no significant increase to prediction accuracy since the MAE is similar independent of whether temperature is added.

Method	MAE without temperature feature	MAE with temperature feature
Linear regression	656.13	655.89
Linear regression (on log-power)	765.97	765.75
Neural Network	151.28	190.80
XGBoost	126.21	126.87

Table A.4: Predicting EV charging profiles: MAE per regression model, with and without ambient temperature feature

Sensitivity study on charging efficiency

In the following we discuss the results of a sensitivity study on the value of the charging efficiency assumed in chapter 6. First, the SoC feature in the dataset was recomputed based on varying efficiency values ($\eta = \{0.80, 0.85, 0.90\}$). The results shown in chapter 6 are based on assuming an efficiency value of $\eta = 0.85$. Second, the regression models were retrained on each dataset. Table A.5 shows the results.

There is no significant difference in prediction accuracy since the MAE is similar independent of which efficiency value is used. For example, XGBoost shows very similar MAE across the different efficiency values (125.05 for $\eta = 0.80$, 126.21 for $\eta = 0.85$, 126.37 for $\eta = 0.90$).

Method	MAE ($\eta = 0.80$)	MAE ($\eta = 0.85$)	MAE ($\eta = 0.90$)
Baseline	2072.74	2077.63	2095.68
Linear regression	655.24	656.13	659.20
Linear regr. (log)	765.13	765.97	768.85
Neural Network	155.50	151.28	174.54
XGBoost	125.05	126.21	126.37

Table A.5: Predicting EV charging profile: Sensitivity study on charging efficiency

Comparing simulated and predicted charging profiles

Chapter 5 focuses on simulating charging profiles by using an ECM. Chapter 6 uses regression models to predict charging profiles based on historical data. This section compares the output from both approaches to examples of historical charging processes. The comparison is performed for the EV models Tesla Model S and Renault Zoe because the battery pack composition is known and ECM parameters are available for the used battery cells.

Figure A.4 shows a comparison of a historical, a simulated and a predicted charging profile for both EV models. The predicted charging profile is accurate and shows behaviour similar to the historical charging profile. However, for both EV models the simulated charging profile shows a difference in the length of the CV phase. For the Zoe, the simulated CV phase is shorter compared to the historical CV phase while the opposite holds for Tesla.

The main reason for the difference in the length of the CV phase is the ECM's parameters. Additionally, the initial SoC is required for the ECM. In this work, the initial SoC is an estimate based on an assumed efficiency of 0.85.

Comparison of a historical, simulated and predicted charging profile

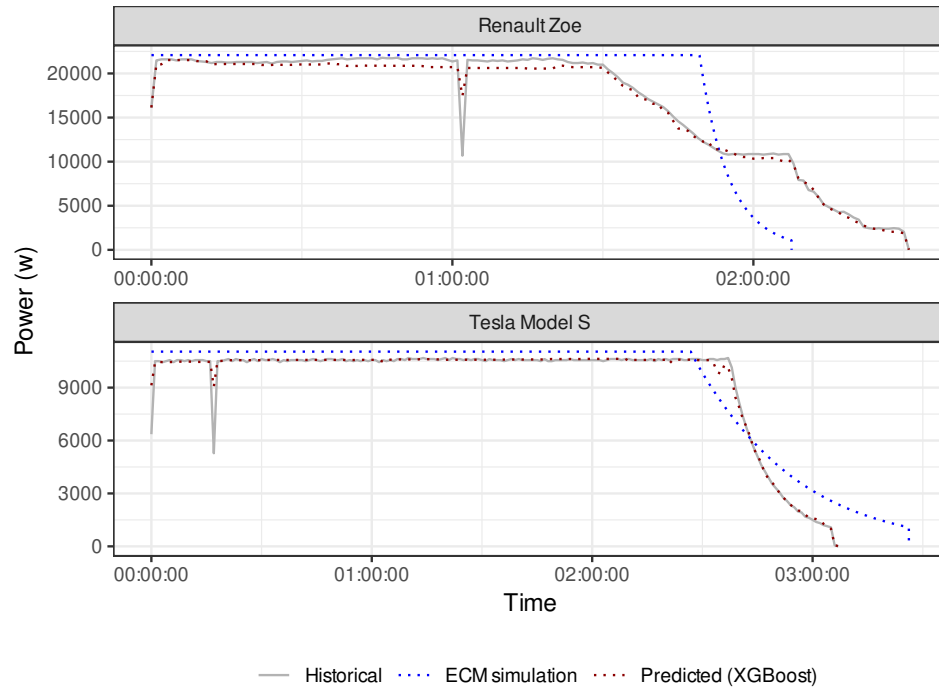


Figure A.4: Comparing simulated with predicted charging profiles

A.5 OCPP Charge Profile example

```
{
  "chargingProfileId" : 123,
  "transactionId" : 1,
  "stackLevel" : 0,
  "chargingProfilePurpose" : "TxProfile",
  "chargingProfileKind" : "Absolute",
  "chargingSchedule" : {
    "startSchedule" : 1582106181954,
    "chargingRateUnit" : "A",
    "chargingSchedulePeriod" : [ {
      "startPeriod" : 0,
      "limit" : 32.0
    }
  ]
}
```

```
    }, {
      "startPeriod" : 900,
      "limit" : 0.0
    }, {
      "startPeriod" : 1800,
      "limit" : 16.0
    }, {
      "startPeriod" : 2700,
      "limit" : 6.0
    }
  ]
}
```